



**GEOLOGICAL SURVEY OF CANADA  
OPEN FILE 7078**

**Shear Wave Velocity Measurement Guidelines  
for Canadian Seismic Site Characterization  
in Soil and Rock**

J.A. Hunter and H.L. Crow  
(Editors)

With Technical Contributions From:

J.-L. Arsenault, U. Atukorala, M.E. Best, D. Campos, C. Candy,  
L. Chouinard, M. Claprod, H.L. Crow, H. Dutrisac, J. Fleming, J.B. Harris,  
R. Hillman, J.A. Hunter, M. Karray, G. Lefebvre, M. Maxwell, S. Molnar,  
R. Paul, D. Perret, C. Phillips, S.E. Pullan, A.J.-M. Pugin, P. Rosset,  
J. Schmok, J.-J. Sincennes, S. Sol, I. Weemees, and D. Woeller

**2012**



Natural Resources  
Canada

Ressources naturelles  
Canada

**Canada**



**GEOLOGICAL SURVEY OF CANADA  
OPEN FILE 7078**

# **Shear Wave Velocity Measurement Guidelines for Canadian Seismic Site Characterization in Soil and Rock**

**2012**

©Her Majesty the Queen in Right of Canada 2012

doi:10.4095/291753

This publication can be downloaded free of charge from GEOSCAN (<http://geoscan.ess.nrcan.gc.ca/>).

**Recommended citation:**

Hunter, J.A. and Crow, H.L. (ed.), 2012. Shear Wave Velocity Measurement Guidelines for Canadian Seismic Site Characterization in Soil and Rock; Geological Survey of Canada, Open File 7078, 227 p.  
doi:10.4095/291753

Publications in this series have not been edited; they are released as submitted by the author.

## **Acknowledgement**

The GSC editors and contributors would like to acknowledge the encouragement and support of Dr. W.D.L. (Liam) Finn, currently emeritus professor at the University of British Columbia. Although near-surface seismic research at the GSC had previously addressed some issues of geotechnical applications using shear wave velocity measurements during the 1960's and 1970's, it was only through Liam's urging that we began our program of shear wave measurements in the soft soils of Canada in the 1980's, focused on earthquake shaking hazards. Subsequently, shear wave velocity measurements have become an integral part of hazard assessments, as given in the Canadian, U.S., and many other building codes worldwide. We deeply appreciate Liam's long-range vision.

# Table of Contents

<b>CONTRIBUTORS.....</b>	<b>6</b>
<b>REFERENCE TERMINOLOGY.....</b>	<b>7</b>
<b>CHAPTER 1.0 INTRODUCTION.....</b>	<b>9</b>
1.1 PURPOSE, SCOPE, AND LIMITATIONS OF THE GUIDELINES .....	10
1.2 IMPORTANCE OF SHEAR WAVE VELOCITY PROFILING IN THE PROFESSIONAL PRACTICE.....	11
1.3 TECHNICAL BACKGROUND .....	12
1.3.1 <i>Basic Earthquake Shaking Phenomena</i> .....	12
1.3.2 <i>Site Provisions in the National Building Code of Canada</i> .....	14
1.4.3 <i>Early Experience in Shear Wave Velocity Measurement at the GSC</i> .....	16
<b>CHAPTER 2.0 NON-INVASIVE SEISMIC TECHNIQUES.....</b>	<b>19</b>
2.1 SHEAR WAVES .....	23
2.1.1 <i>Shear Wave Refraction Technique for Hazard Studies</i> .....	23
2.1.2 <i>Shear Wave Reflection Techniques for Hazard Studies</i> .....	35
2.2 SURFACE WAVES.....	49
2.2.1 <i>Continuous Surface Wave (CSW) Technique for Hazard Studies</i> .....	49
2.2.2 <i>Spectral Analysis of Surface Waves (SASW) Technique for Hazard Studies</i> .....	56
2.2.3 <i>Multichannel Analysis of Surface Waves (MASW) Technique for Hazard Studies</i> .....	62
2.2.4 <i>Modal Analysis of Surface Waves (MMASW) Technique for Hazard Studies</i> .....	67
2.3 AMBIENT NOISE .....	77
2.3.1 <i>Single Station H/V Technique</i> .....	78
<i>On the Use of Single Station Ambient Noise Techniques for Microzonation</i> <i>Purposes: The Case of Montreal</i> .....	85
2.3.2 <i>Spatially Averaged Coherency Spectrum (SPAC) Ambient Noise Array Method</i> .....	94
2.3.3 <i>Frequency-wavenumber (f-k) Ambient Noise Array Method</i> .....	103
<b>CHAPTER 3.0 INVASIVE SEISMIC TECHNIQUES.....</b>	<b>111</b>
3.1 SEISMIC CONE PENETROMETER (SCPT) TECHNIQUE FOR HAZARD STUDIES .....	113
3.2 BOREHOLE METHODS .....	123
3.2.1 <i>Shear Wave Velocity Logs from Vertical Seismic Profiles (VSP)</i> .....	123
3.2.2 <i>Full Waveform Sonic Logging for Shear Wave Velocity</i> .....	139
3.2.3 <i>Crosshole Logging for Shear Wave Velocity</i> .....	150
3.2.4 <i>Multichannel Crosshole Shear Wave Surveys</i> .....	160
<b>CHAPTER 4.0 COMPLEMENTARY GEOPHYSICAL TECHNIQUES FOR SITE GEOMETRY ASSESSMENT .....</b>	<b>170</b>
4.1 <i>Electromagnetic (EM) Methods</i> .....	171
4.2 <i>Resistivity Methods</i> .....	182
4.3 <i>Ground Penetrating Radar (GPR) Methods</i> .....	191
4.4 <i>Borehole Logging Techniques in Unconsolidated Sediments for Hazard Studies</i> .....	198
4.5 <i>Microgravity Technique for Hazard Studies</i> .....	206

<b>CHAPTER 5.0</b>	<b>SHEAR WAVE GUIDELINES FOR NON-TECHNICAL USERS .....</b>	<b>211</b>
5.1	<i>Seismic Waves .....</i>	211
5.2	<i>Shear Waves and Ground Amplification.....</i>	211
5.3	<i>What is <math>V_{s30}</math>?.....</i>	212
5.4	<i>Seismic Site Classes and Shear Waves in Near Surface Materials.....</i>	213
5.5	<i>Site Classes and Amplification Factors .....</i>	214
5.6	<i>Measuring Shear Wave Velocity.....</i>	215
5.7	<i>Invasive vs. Non-invasive Shear Wave Methods .....</i>	215
5.8	<i>What to Expect: Reporting Guidelines.....</i>	216
5.9	<i>When to Question or Request More Information .....</i>	220
<b>CHAPTER 6.0</b>	<b>SUMMARY.....</b>	<b>224</b>

## Contributors

The Geological Survey of Canada gratefully acknowledges the technical contributions of the following authors and chapter leaders who shared their time and expertise in the development of these guidelines:

*Jean-Luc Arsenault, Géophysique GPR International, Longueuil, QC.*

*Upul Atukorala, Golder Associates Ltd, Burnaby, BC.*

*Melvyn Best, Bemex Consulting International, Victoria, BC.*

*Daniel Campos, Géophysique GPR International, Longueuil, QC.*

*Cliff Candy, Frontier Geosciences Ltd., North Vancouver, BC.*

*Hélène Dutrisac, Cement Canada, Ottawa, ON*

*Luc Chouinard, McGill University, Department of Civil Engineering, Montréal, QC.*

*Maxime Clapood, Institut National de la Recherche Scientifique, Québec, QC*

*Heather Crow, Geological Survey of Canada, Ottawa, ON.*

*Jeff Fleming, Golder Associates Ltd., Mississauga, ON.*

*Jamie Harris, Millsaps College, Department of Geology, Jackson, MS*

*Russell Hillman, Frontier Geosciences Ltd., North Vancouver, BC.*

*Jim Hunter, Geological Survey of Canada, Ottawa, ON.*

*Mourad Karray, Université Sherbrooke, Department of Civil Engineering, Sherbrooke, QC.*

*Guy Lefebvre, Université Sherbrooke, Department of Civil Engineering, Sherbrooke, QC.*

*Michael Maxwell, Golder Associates Ltd, Burnaby, BC.*

*Sheri Molnar, Geological Survey of Canada, Victoria, BC.*

*Réjean Paul, Géophysique GPR International, Longueuil, QC.*

*Didier Perret, Commission Géologique du Canada, Québec, QC.*

*Christopher Phillips, Golder Associates Ltd., Mississauga, ON.*

*Susan Pullan, Geological Survey of Canada, Ottawa, ON.*

*André Pugin, Geological Survey of Canada, Ottawa, ON.*

*Philippe Rosset, McGill University, Department of Civil Engineering, Montréal, QC.*

*Jeffrey Schmok, Golder Associates Ltd, Burnaby, BC.*

*Jean-Jacques Sincennes, Géophysique SIGMA, St. Bruno, QC.*

*Stéphane Sol, Golder Associates Ltd., Mississauga, ON.*

*Ilmar Weemees, ConeTec Investigations Ltd, Vancouver, BC.*

*David Woeller, ConeTec Investigations Ltd, Vancouver, BC.*

The GSC also gratefully acknowledges the guidance of the advisory panel, who provided feedback and direction throughout the course of the project.

*Gail Atkinson, University of Western Ontario, Department of Earth Sciences, London, ON.*

*Michael Bleakney, Public Works and Government Services Canada, Ottawa, ON*

*Hélène Dutrisac, Cement Canada, Ottawa, ON*

*K. Tim Law, National Research Council of Canada & Carleton University (ret'd), Ottawa, ON*

*Garry Stevenson, Klohn Crippen Berger, Vancouver, BC*

*Edward Woolery, University of Kentucky, Lexington, KY*

Funding for this document was provided through Natural Resources Canada's Public Safety Geosciences Program.

*Peter Bobrowsky, Guidelines Project Leader, Geological Survey of Canada, Ottawa, ON.*

## Reference Terminology

All terms expressed in SI units.

A	broad-band amplification
$A_{res}$	resonance amplification
c	phase velocity (expressed in metres/second)
$f$	frequency (expressed in Hertz)
$f_0$	fundamental site frequency (expressed in Hertz)
$f_n$	$n^{\text{th}}$ harmonic of the fundamental site frequency (expressed in Hertz)
$E_{max}$	small strain elastic modulus (expressed in kPa)
$F_a$	acceleration-based site coefficient (Table 4.1.8.4.B. – 2010 NBCC)
$F_v$	velocity-based site coefficient (Table 4.1.8.4.C. – 2010 NBCC)
G	shear modulus (expressed in kPa)
$G_{max}$	small strain shear modulus (expressed in kPa)
k	wavenumber
K	bulk modulus (expressed in kPa)
$N_1$	penetration index normalized for a vertical effective stress of 100 kPa (expressed in counts)
$N_{60}$	average standard penetration resistance corrected to a rod energy efficiency of 60% of the theoretical maximum (expressed in counts)
$q_c$	piezocone point resistance (expressed in kPa)
$q_{c1}$	piezocone point resistance normalized for a vertical effective stress of 100 kPa (expressed in kPa)
Q	soil-specific attenuation factor ( $Q=1/2*\zeta$ )
Sa(x)	spectral acceleration (5% damped) at a period (T) of x seconds
$S_u$	undrained shear strength (expressed in kPa)
t	traveltime (expressed in seconds)
T	period (expressed in seconds)
$V_p$	interval compressional wave velocity (expressed in metres/second)
$V_s$	interval shear wave velocity (expressed in metres/second)
$V_{sav}$	average shear wave velocity (expressed in metres/second)
$V_{s30}$	traveltime-weighted average shear wave velocity to 30 m depth (expressed in metres/second)
$V_{s1}$	$V_s$ normalized for a vertical effective stress of 100 kPa (expressed in metres/second)
$V_R$	Rayleigh wave phase velocity (expressed in metres/second)
$\nu$	Poisson's ratio
z	depth (expressed in metres)
Z	acoustic impedance ( $\rho * V_s$ )
$\phi$	phase angle (expressed in radians)
$\lambda$	wavelength (expressed in metres)
$\rho$	material density (expressed in $g/cm^3$ )
$\sigma_v$	total vertical stress (expressed in kPa)
$\sigma'_v$	vertical effective stress (expressed in kPa)
$\zeta$	material damping ratio (expressed in %)

## Common Acronyms

CDP	common depth point
CMP	common midpoint
CPT	cone penetrometer test
CSW	continuous surface wave
EM	electromagnetic
GPR	ground penetrating radar
H/V	ratio of the horizontal to the vertical Fourier spectra of ambient noise recorded at a single site by a three-component sensor
MASW	multi-channel analysis of surface waves
MMASW	multimodal analysis of surface waves
NBCC (...)	National Building Code of Canada (year in brackets)
NEHRP	National Earthquake Hazard Reduction Program (US)
RMS	root mean square
SH	shear wave – horizontal component
SCPT	seismic cone penetrometer
SPAC	spatially averaged coherency spectrum
SPT	standard penetration test
S/N	signal-to-noise ratio
SV	shear wave – vertical component
VSP	vertical seismic profile

# Chapter 1.0 Introduction

Jim Hunter  
Geological Survey of Canada, Ottawa, ON

Upul Atukorala  
Golder Associates Ltd. Vancouver, BC

An important option for seismic site category definition in the Seismic Provisions of the 2010 National Building Code of Canada (2010 NBCC) is the measurement of average shear wave velocities to a depth of 30 meters ( $V_{s30}$ ). This approach is the most versatile of the three recommended geotechnical seismic site assessment techniques. To support consistent near surface shear wave velocity classification, this reference document on methods for determining shear wave velocities has been developed by members of the Geological Survey of Canada with technical participants representing industry, government, and academia.

Figure 1.0-1 after Adams and Atkinson (2003) shows the major high earthquake hazard zones in Canada. The surficial geological histories of these hazard zones present unique geotechnical challenges. Most areas were glaciated during the Quaternary Era, resulting in minimal mechanically weathered bedrock; hence, the boundary between unconsolidated overburden and bedrock generally constitutes a large change in stiffness or seismic impedance. Glaciation also produced deposits of glacial till or glacially-derived unconsolidated Pleistocene materials of variable stiffness. In addition, widespread thick, soft, highly-porous, Holocene marine, fluvial and lacustrine sediments commonly occur within high hazard zones in both Eastern and Western Canada (e.g. the Fraser River Delta of the lower mainland BC, the Champlain Sea sediments of the Ottawa and St. Lawrence River valleys). As well, in many areas, site conditions can change markedly over short lateral intervals; hence it is important that these variable site conditions be addressed through typical Canadian geophysical case histories.

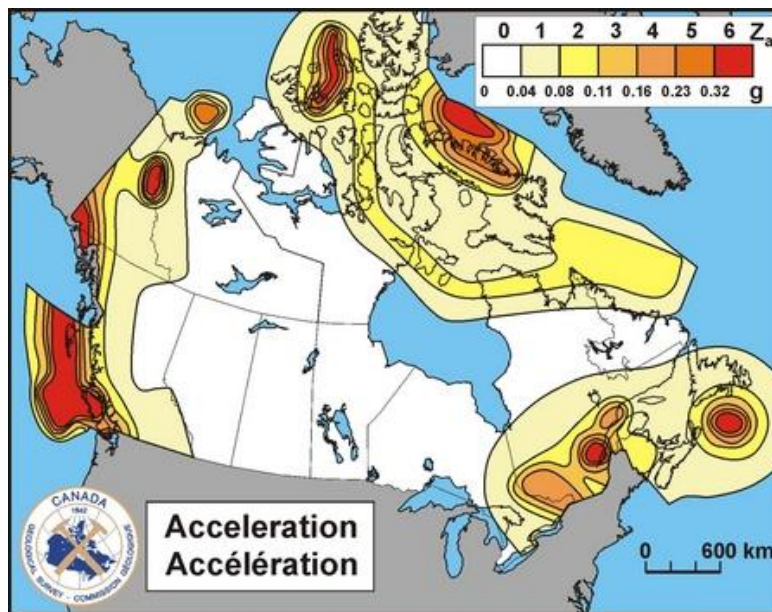


Figure 1.0-1 Probabilistic ground motion acceleration hazard estimates in Canada for a 1:2500 yr return period earthquake event for NERHP zone classification C.

### Recommended citation:

Hunter, J.A. and Atukorala, U., 2012. Chapter 1.0: Introduction; *in* Shear Wave Velocity Measurement Guidelines for Canadian Seismic Site Characterization in Soil and Rock, (ed.) J.A. Hunter and H.L. Crow; Geological Survey of Canada, Open File 7078, p. 9-18.

This report includes two technical chapters contributed by experienced Canadian practitioners describing various shear velocity measurement methods that are currently employed in near-surface soil and rock geotechnical site evaluations in Canadian settings. A third technical chapter has been included to describe other complementary geophysical techniques which can be used in support of site category definition, particularly important at large sites. A technical summary table of all the shear wave methods can be found in the concluding chapter (Table 6-1).

**Chapter 5 has been included for non-technical professionals who are required to review seismic site classification reports (using shear wave velocities) for municipal applications or engineering investigations. However, it also provides a useful review of seismic waves, amplification, and NBCC (2010) seismic site classification provisions for technical and non-technical professionals alike.** It contains a non-technical summary table of the shear wave methods described in the report (Table 5-1), and offers some guidance on the various types of information that may be contained, or asked for, in a seismic site classification report.

## ***1.1 Purpose, Scope, and Limitations of the Guidelines***

We anticipate that the Guidelines will be utilized by geophysicists, geotechnical engineers, and those concerned with municipal building codes requiring seismic site classification following the 2005 or 2010 NBCC. The guide is meant to assist geo-professionals who are not familiar with the specific methodologies, yet who have a general knowledge of the seismic provisions of the NBCC. Goals of the Guidelines project include:

- Development of a comprehensive guide to the types of seismic site characterization methods used in current practice,
- Compilation of example case histories in Canadian settings,
- Creation of an extensive 'go-to' reference resource of publications for current state-of-practice in seismic site characterization in Canada and abroad, and
- Presentation of a document in a form that allows for modifications and additions as seismic techniques evolve and as NBCC guidelines are altered or changed.

These guidelines represent an overview of the current body of knowledge in Canada of shear wave velocity measurement techniques in soil and rock from the combined experience of practitioners from industry, universities, and government research groups. It is intended to address established field acquisition and data processing techniques, yet introduce emerging technologies. The case history examples given herein come from current areas of application throughout Canada, and it is hoped that these guidelines offer sufficient breadth and depth of experience to aid the practitioner in making survey design decisions. The Guidelines are also offered for use by municipal authorities who are responsible for reviewing building permit applications; recommended reporting requirements are suggested for most applications.

It should be noted that the Guidelines document has the following limitations:

- It is not a legislated document;
- It is not an exhaustive treatment of all Vs measurement techniques;
- It is not an endorsement of any particular equipment, trademark, or processing method;
- It is not a standard;
- It should not be used directly to predict seismic hazard at any given location; and
- It is limited to terrestrial, non-permafrost, environments.

## **1.2 Importance of Shear Wave Velocity Profiling in the Professional Practice**

Local soil/site conditions play a key role in establishing the damage caused by seismic waves generated by earthquakes. Incorporating the local soil/site conditions in seismic design and building codes such as NBCC has been a challenge. The focus has been to incorporate them without overly/unduly complicating the design process.

The effects of local soil/site conditions on propagating seismic waves can be understood by studying the response of an elastic soil layer resting on bedrock. The thickness and shear stiffness (which is in turn related to the shear wave velocity) of the elastic soil layer, the impedance ratio between bedrock and the soil layer, and the critical damping ratio of the elastic soil layer are key inputs required to assess the seismic response. Quantifying the effects of local soil/site conditions over a range of ground shaking is complicated by the inherently non-linear, inelastic, and hysteretic response of soil. With increased level of seismic shaking, soil stiffness decreases and soil damping increases, thus changing the site period and the impedance ratio.

Prior to 2005 NBCC, the building codes incorporated the effects of seismic wave propagation resulting from local soil/site conditions by specifying a "Foundation Factor" that varied between 1.0 and 2.0. For soft soil sites, a larger Foundation Factor closer to 2.0 was assigned, whereas for stiff soil and rock sites, the assigned factor was closer to 1.0. The Foundation Factor was specified for several different typical soil profiles based on a qualitative description of site soils, ignoring the effects of site period and shaking intensity. In some published documents, the site response was characterized using curves showing the anticipated ground surface acceleration against the bedrock acceleration (Idriss, 1990), developed based on a combination of field measurements and theoretical ground response analyses.

Following the pioneering work completed by Borchardt of United States Geological Survey (USGS) in the early 1990s, a quantitative procedure for establishing the effects of local soil/site conditions was developed, where the sites were categorized into classes or categories in terms of the in-situ time-averaged shear wave velocity of the upper 30 m. Some approximate correlations of shear wave velocity with other commonly used in-situ measurements, such as the standard penetration resistance and undrained shear strength, are also provided for sites where direct measurement of shear wave velocity are not available. This procedure has been adopted in the 2005 and 2010 NBCC and by other codes and standards in the USA. It is now common practice to undertake in-situ measurements of shear wave velocity for important projects.

The building codes and standards that have adopted classifications based on the shear wave velocity of the top 30 m of the site, however, are silent on the specific testing techniques to be followed for measuring the shear wave velocity with depth. The technique to be used (i.e. downhole/crosshole measurements, vs. surface methods, such as multichannel analysis of surface waves (MASW), etc.) is left to the sole discretion of the geotechnical engineer, who in turn would consult a geophysicist to confirm the applicable testing technique(s) during planning of the field investigation. In some cases, more than one technique is used to collect the required data and to assess effects of soil structure anisotropy. The geotechnical engineer's familiarity with the testing techniques, accuracy of measurements, zone of influence, and affordability, etc. are key drivers in selecting the particular technique to be used for a given project. It is important to recognize that techniques such as downhole logging would influence a smaller zone of the medium and therefore result in highly variable shear wave velocity profile. Downhole velocity measurements taken inside grouted casings, however, rely on good soil-grout-geophone contact for wave transmission. Non-intrusive techniques, such as MASW, generally require waves to travel through a larger volume of material, and are subject to influence from buried man-made features. An understanding and appreciation of the accuracies and limitations of each test method, both by the geotechnical engineer and the owner, are critical to successfully executing the field program.

Shear wave velocities of the geological media are required not only to characterize the site in accordance with the building codes, but also to collect the data necessary for dynamic ground response analyses and

assessment of the liquefaction potential of soils when subjected to seismic waves. Both vertical and lateral variations in shear wave velocity are often used in 1D and 2D analyses of soil deposits and stress-deformation analyses that provide key input for seismic design.

It is common to encounter gas in the pore spaces of soil. Depending on how the gas bubbles are distributed in the soil, the presence of gas leads to either a homogeneous-partial-saturation (HPS) or a non-homogenous-partial-saturation (NHPS) condition (Naesgaard, 2012). While the shear wave velocity measurements are generally unaffected by the presence of a small amount of gas regardless of how the bubbles are distributed in the pore spaces, the compression wave velocity is significantly affected depending on whether the gas bubbles are present as scattered pockets throughout the medium (HPS) or as a few large pockets (NHPS).

These Guidelines are applicable to terrestrial sites only; however, it is important to note that the techniques of in-situ measurement of shear wave velocity with depth are not as well-established for offshore sites as for land-based sites. Considering the difficult test environments that exist for offshore site investigations, engineers commonly rely on specialist testing companies for data acquisition, processing, and interpretation in the form of shear wave velocity profiles.

### 1.3 Technical Background

#### 1.3.1 Basic Earthquake Shaking Phenomena

The nature of earthquake seismic waves radiating through the earth is strongly dependent on the source mechanism, the source location at depth, and the character of the rock types along the travel path to a particular surface site. The character of the shaking at the ground surface (amplitude, frequency and duration), however, is strongly affected by the materials through which the waves travel over the last few hundred meters (or less). For example, it has long been known that damage from earthquake shaking tends to be concentrated at locations where soft soils are present (e.g. damage from such earthquake events as the 1964 Niigata Japan, 1964 Alaska, 1976 Tangshan China; more recently 1985 Mexico City, 1989 Loma Prieta (San Francisco area), 1994 Northridge California, and 1995 Kobe (Anderson et al., 1986; Holzer., 1994, Choi and Stewart, 2003).

There is a clearly established link between ground motion amplification and the shear wave velocity structure of the subsurface soil(s) and bedrock (Kramer, 1996). Where shear wave velocities within a soil unit are much lower than in the immediately underlying material (another soil unit or bedrock), the velocity (and density) contrast results in a significant impedance boundary that causes both a shortening of shear wave wavelengths and an increase in shear wave amplitudes over a wide frequency band of earthquake shaking as the seismic energy passes from one medium to the other (Shearer and Orcutt, 1987). In the absence of significant attenuation within the soil, the **broad-band amplification** effect is:

$$A \sim (\rho_{\text{rock}} V_{\text{srock}} / \rho_{\text{soil}} V_{\text{ssoil}})^{1/2} \dots\dots\dots[1.3.1]$$

where,

- $\rho_{\text{rock}}$  = average density of bedrock
- $\rho_{\text{soil}}$  = average density of soil
- $V_{\text{srock}}$  = shear wave velocity of bedrock at the overburden-bedrock interface
- $V_{\text{ssoil}}$  = shear wave velocity of soil at the ground surface

An additional amplification effect also occurs in association with large seismic impedance boundaries. Known as **resonance amplification**, it results from seismic shear waves that have travelled up through the crust, and then reflect back and forth between the free surface of the ground and the underlying

impedance boundary at the soil-bedrock interface. This can result in shear wave energy being effectively trapped in the low velocity soil zone as manifested by ‘ringing’ at the fundamental frequency until the energy eventually dissipates by spherical divergence and anelastic attenuation. The fundamental resonant frequency ( $f_0$ ) and harmonics ( $f_1, f_2, \dots$  etc) are given by (Kramer, 1996):

$$f_n = (V_{s_{av}}/4H) * (1+2n) \text{ for } n = 0,1,2,3,4, \dots [1.3.2]$$

where,

$V_{s_{av}}$  = the average shear wave velocity of the soil (m/s)  
 $H$  = thickness of the soil column (m)

Commonly the largest spectral peak of the resonance transfer function is associated with the fundamental resonance frequency  $f_0$ ; the amplitude of this peak varies directly as:

$$A_{res} \sim (\rho_{rock} * V_{s_{rock}}) / (\rho_{avsoil} * V_{s_{avsoil}}) \dots [1.3.3]$$

where,

$\rho_{avsoil}$  = average density of the soil column  
 $V_{s_{avsoil}}$  = travel-time-weighted average shear wave velocity of the soil column

From a comparison of equations (1.3.1) and (1.3.3), it can be seen that the resonance amplification effect at the fundamental and harmonics can be significantly larger than broad-band amplification effects. Both effects contribute to the spectral amplification at a soft soil site.

Additional “**buried valley focusing**” **amplification effects** can occur where thick sediments are deposited in narrow bedrock topographic lows (Bard and Bouchon, 1985). As well, upcoming seismic waves impinging on the edges of the buried bedrock valley may generate surface waves which can constructively interfere at various locations within the buried valley feature resulting in anomalously large amplitude horizontal and vertical motion (Lomnitz, 1999). This effect is called **basin-edge surface wave amplification**. Four of the major contributions to site amplification in soft soil are summarized in Figure 1.3.1.

The key to unlocking the complexities of such ground motion effects lies with detailed delineation of the shear wave properties of soils and the underlying bedrock. The current National Building Code of Canada utilizes traveltime-weighted layer shear wave velocities to a depth of 30 m to establish site classifications associated with amplification effects (of which the above mentioned examples are commonly the major contributors – note that other 3D basin effects as well as surface topographic effects could also be factors). On the other hand, these current Guidelines give examples that describe the measurement of shear wave velocity-depth functions of soils and rocks extending well beyond the current 30 m depth, in order to provide techniques and examples for use in 1D, 2D, or 3D ground response modeling, which may become the norm in future geotechnical evaluations.

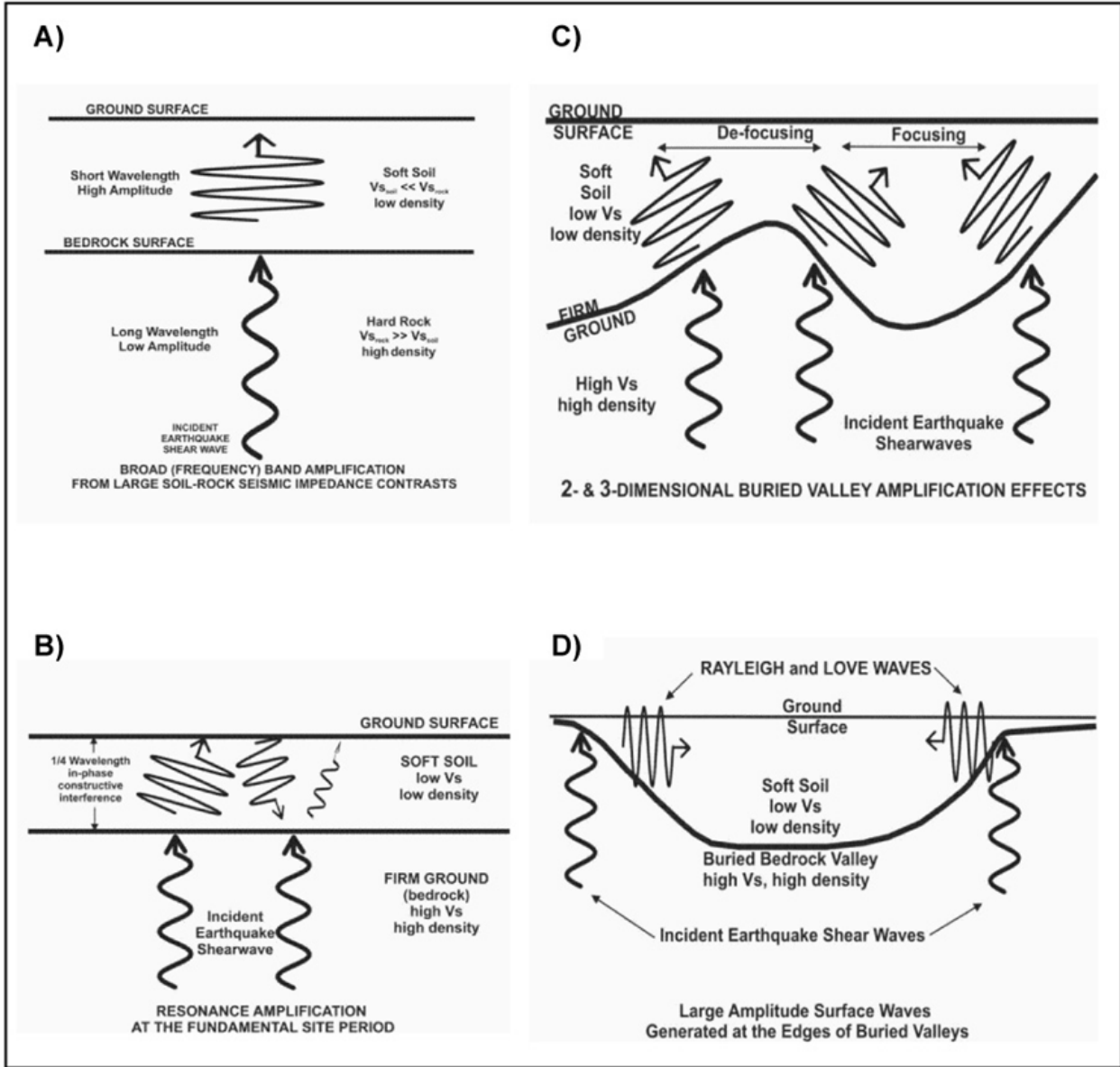


Figure 1.3.1 a), b), c) and d). Diagrammatic illustrations of the major amplification effects associated with soft soil overlying firm ground or bedrock.

### 1.3.2 Site Provisions in the National Building Code of Canada

The importance of seismic amplification for building design is recognized in the 2010 National Building Code of Canada (2010 NBCC) (see also 2005 NBCC, Finn and Wightman, 2003). This document offers a seismic site classification system that characterizes the underlying geological materials at a given location for the purpose of defining amplification factors that take into account impedance contrast amplification of the near-surface.

At any location in Canada, the 2010 NBCC (NRC, 2010) defines 5% damped spectral accelerations for four periods spanning the earthquake frequency range (0.5 Hz to 5 Hz) as determined for NEHRP (National Earthquake Hazard Reduction Program) Class C. For areas having other NEHRP site classes,

amplification factors given in “look-up” tables (NBCC 2010) must be applied to these values. The “design” ground motion represents the level of shaking with a 2% probability of exceedance in 50 years (or 1: 2475 years) although other probabilities can be utilized.

The site provisions follow the system developed by NEHRP in the 1990s for the United States (BSSC, 1994; BSSC, 1995). As shown in Table 1.1.1, five of the six site categories (or classes) correspond approximately to Hard Rock (Site Class A), Rock (Site Class B), Soft Rock or Very Dense Soil (Site Class C), Stiff Soil (Site Class D), and Soft Soil (Site Class E). The classes are defined based on the average geotechnical properties in the upper 30 m of the ground using either shear-wave velocity ( $V_s$ ), standard penetration resistance (blow counts), or undrained shear strength ( $S_u$ ). The sixth class (Site Class F) is a special case and is defined based on more site-specific characteristics, as listed in Table 1.3.1.

Since the use of combinations of these three techniques is **not** recommended for obtaining a  $V_{s30}$  by the NBCC (by combining local empirical relations between  $V_{s30}$ ,  $S_u$  or  $N$ ), it is apparent that the provisions of the 2010 NBCC with respect to NEHRP zones are strongly oriented towards shear wave velocity measurements of soils and rock as the primary assessment tool for site investigations.

Table 1.3.1 Seismic site categories as defined in the 2010 NBCC (NRC, 2010).

Site Class	Ground Profile Name	Average Properties in Top 30 m, as per Appendix A		
		Average Shear Wave Velocity, $\bar{V}_s$ (m/s)	Average Standard Penetration Resistance, $\bar{N}_{60}$	Soil Undrained Shear Strength, $s_u$
A	Hard rock	$\bar{V}_s > 1500$	n/a	n/a
B	Rock	$760 < \bar{V}_s \leq 1500$	n/a	n/a
C	Very dense soil and soft rock	$360 < \bar{V}_s < 760$	$\bar{N}_{60} > 50$	$s_u > 100$ kPa
D	Stiff soil	$180 < \bar{V}_s < 360$	$15 \leq \bar{N}_{60} \leq 50$	$50$ kPa $< s_u \leq 100$ kPa
E	Soft soil	$\bar{V}_s < 180$	$\bar{N}_{60} < 15$	$s_u < 50$ kPa
		Any profile with more than 3 m of soil with the following characteristics: <ul style="list-style-type: none"> <li>• plasticity index: <math>PI &gt; 20</math></li> <li>• moisture content: <math>w \geq 40\%</math>, and</li> <li>• undrained shear strength: <math>s_u &lt; 25</math> kPa</li> </ul>		
F	Other soils <sup>(1)</sup>	Site-specific evaluation required		

(1) Other soils include:

- (a) liquefiable soils, quick and highly sensitive clays, collapsible weakly cemented soils, and other soils susceptible to failure or collapse under seismic loading,
- (b) peat and/or highly organic clays greater than 3 m in thickness,
- (c) highly plastic clays ( $PI > 75$ ) more than 8 m thick, and
- (d) soft to medium stiff clays more than 30 m thick.

Commentary J of the 2005 NBCC (National Research Council, 2006) also addresses the resonance effect of a single low velocity layer (e.g. “Leda” clay overlying a high velocity bedrock surface). The fundamental site period is given by equation (1.1.2) for  $n=0$  for this model. Page J-17 of the NBCC Commentary J also gives the amplitude of the fundamental (or characteristic) resonance peak in terms of both seismic impedance contrast and soil damping ratio as:

$$A_{res} = 1/(K + \zeta_s \pi / 2) \dots\dots\dots[1.3.4]$$

where,

$$K = (\rho_{\text{rockl}} * V_{\text{srockl}}) / (\rho_{\text{avsoil}} * V_{\text{savsoil}})$$
$$\zeta_s = \text{critical damping ratio of the soil}$$
$$= 1/2Q$$

and

$$Q = \text{soil-specific attenuation factor}$$

Examples of significant resonance amplification at various fundamental site periods for thick soft soils are given by Hunter et al. (2010) for Champlain Sea sediments overlying competent bedrock. Amplifications in the range of 10 to 15 times are possible.

### 1.4.3 Early Experience in Shear Wave Velocity Measurement at the GSC

Since the 1960's, the Near Surface Geophysics section of the Geological Survey of Canada has been involved in surface and borehole measurements of shear wave velocities of soils and rock. Much of the early work was focused on either site-specific engineering problems (Hobson and Hunter, 1966 and 1969) or regional measurements on permafrost soils (Kurfurst and Hunter, 1977). In 1986, investigations of shear wave velocity structure of a 24 x 26 km<sup>2</sup> area of the Fraser Delta were initiated in order to provide basic information for 1D models of earthquake shaking response of the sediments. An overview of these investigations is given by Hunter et al. (1998a) and a compilation of data to 1998 is given by Hunter et al. (1998b). Approximately 40<sup>+</sup> deep boreholes were drilled in Holocene and Pleistocene sediments; these were cased with PVC casings and subsequently logged using vertical seismic profiling (VSP) shear wave techniques. In addition, approximately 425 non-invasive surface shear wave refraction/reflection sites were occupied, in order to obtain shear wave velocity-depth functions to 30 m depth. Reconnaissance maps of Vs<sub>30</sub> and resonance periods (to the top of the Pleistocene seismic impedance boundary) were published by Hunter et al. (2002). The early Fraser Delta work has served to indicate the lateral variability of soil lithology, stratigraphic structure and the resulting shear wave velocity structure. It has underlined the need to map such variations both at the regional scale as well as at the site-specific scale. Testing in the Fraser Delta has also included investigation of Multichannel Analyses of Surface Waves (MASW) (Xia et al., 2000) and preliminary investigations in high resolution Common Midpoint Profiling (CMP) shear wave reflection surveying (Hunter et al., 2002).

In recent years, the Geological Survey of Canada, in co-operation with Carleton University, completed a demonstration microzonation survey of the Ottawa and Gatineau areas which includes seismic site class and site resonance mapping (Hunter et al., 2010; Hunter et al., 2012). This work was based primarily on shear wave velocity estimates derived from direct shear wave velocity measurements at approximately 1000 sites within the city, as well as assignment of velocity-depth functions for approximately 21,000 borehole locations where subsurface lithology was known to at least 30 m depth. Velocity-depth measurements were done using both surface (refraction, reflection and MASW techniques) as well as downhole VSP methods. The resulting zonation map showed large horizontal variations throughout the cities. Mapping procedures and techniques developed for this survey have been described by Crow (2010).

The Ottawa Microzonation maps and associated data bases have been used in recent research in estimating shaking response to various earthquake models. Pal and Atkinson (2012) have shown that ground motion response to local significant crustal earthquakes is, to a great extent, modified by the seismic site designation; commonly those areas identified as class E (or F) experience higher shaking at most earthquake frequencies. The amount of shaking at any one site is also governed by the epicentral location within or circumjacent to the city.

Recently, an opportunity arose to "ground truth" the Ottawa site classification map with the occurrence of the June 23, 2010 M5.0 Val Des Bois earthquake event immediately to the NE of the city. A compilation of felt reports by Pal and Atkinson (2012) has shown a close correlation between intensity of shaking and NEHRP site classification.

Currently, continuing microzonation research is underway in Ottawa, Montreal and Vancouver as part of the Canadian Seismic Research Network (CSRN) Project (Motazedian et al., 2010). Shear wave seismic methods are being applied in all areas. Such basic regional information is required as input data for risk assessment modeling in Canadian cities where significant earthquake hazard has been delineated.

## References

Adams, J. and Atkinson, G., 2003. Development of seismic hazard maps for the proposed 2005 edition of the National Building Code of Canada; *in* Canadian Journal of Civil Engineering Special Issue, v. 30, Proposed Earthquake Design Requirements of the National Building Code of Canada, 2005 edition - National Research Council Canada Research Press.

Anderson, J.G., Bodin, P., Brune, J.N., Prince, J., Singh, S. K., Quass, R. and Onate, M., 1986. Strong Motion from the Michoacan, Mexico, Earthquake; *Science*, v. 233, p.1043-1049.

Bard, P. Y. and Bouchon, Michel, 1985. The two-dimensional resonance of sediment-filled valleys; *Bulletin of the Seismological Society of America*, v. 75, p. 519-541.

Building Seismic Safety Council (BSSC), 1994. NEHRP recommended provisions for seismic regulations of new buildings: part 1, provisions; Publication FEMA 222A, Federal Emergency Management Agency, Washington, D.C.

Building Seismic Safety Council (BSSC), 1995. A non-technical explanation of the 1994 NEHRP recommended provisions; Publication FEMA 99, Federal Emergency Management Agency, Washington, D.C.

Choi, Y. and Stewart, J.P., 2003. Nonlinear Site Amplification as Function of 30 m Shear Wave velocity; *Earthquake Spectra*, v. 21, p. 1-30.

Crow, H.L., 2010. Low Strain Shear Wave Damping ( $Q_s$ ) Measurements in Champlain Sea Deposits Using Downhole Geophysical and Lab Techniques, MSc. Thesis, Carleton University, Ottawa, ON, 222 p.

Finn, W.D.L. and Wightman, A., 2003. Ground motion amplification factors for the proposed 2005 edition of the National Building Code of Canada; *Canadian Journal of Civil Engineering*, 30, p. 272-278.

Hobson, G.D. and Hunter, J.A., 1966. Hammer Seismic Refraction Surveys, Suffield Alberta; *Geological Survey of Canada, Paper 66-1A*, p. 111.

Hobson, G.D. and Hunter J.A., 1969. In-situ Determination of Elastic Constants in Overburden Using a Hammer Seismograph; *Geo-exploration*, v. 7, p. 107-111.

Holzer, T.L., 1994. Loma Prieta damage largely attributed to enhanced ground shaking; *EOS, Trans. Am. Geophys. Union*, v. 75, p. 299-301.

Hunter, J.A., Douma, M., Burns, R.A., Good, R.L., Pullan, S.E., Harris, J.B., Luternauer, J.L. and Best, M. E., 1998a. Testing and application of near surface geophysical techniques for earthquake hazards studies, Fraser River Delta, British Columbia; *in* *Geology and Natural Hazards of the Fraser River Delta, British Columbia* (eds.) J. J. Clague, J. L. Luternauer, and D. C. Mosher, Geological Survey of Canada, Bulletin 525, p.123-145.

Hunter, J.A., Burns, R.A., Good, R.L. and Pelletier, C.F., 1998b. A compilation of shear wave velocities and borehole geophysics logs in unconsolidated sediments of the Fraser River Delta, British Columbia; Geological Survey of Canada, Open File 3622, 1 CD-ROM.

[ftp://ftp2.cits.mcan.gc.ca/pub/geott/ess\\_pubs/209/209974/of\\_3622.zip](ftp://ftp2.cits.mcan.gc.ca/pub/geott/ess_pubs/209/209974/of_3622.zip) [accessed: Jan 2012]

Hunter, J.A., Benjumea, B., Harris, J.B., Miller, R.D., Pullan, S.E., Burns, R.A. and Good, R.L., 2002. Surface and downhole shear wave seismic methods for thick soil site investigations; *Soil Dynamics and Earthquake Engineering*, vol. 22, p.931-941.

Hunter, J.A., Crow, H.L., Brooks, G.R., Pyne, M., Motazedian, D., Lamontagne, M., Pugin, A.J.-M., Pullan, S.E., Cartwright, T., Douma, M., Burns, R.A., Good, R.L., Kaheshi-Banab, K., Caron, R., Kolaj, M., Folahan, I., Dixon, L., Dion, K., Duxbury, A., Landriault, A., Ter-Emmanuil, V., Jones, A., Plastow, G. and Muir, D., 2010. Seismic Site Classification and Site Period Mapping in the Ottawa Area Using Geophysical Methods; Geological Survey of Canada, Open File 6273, 1 DVD.  
<[ftp://ftp2.cits.mcan.gc.ca/pub/geott/ess\\_pubs/286/286323/of\\_6273.zip](ftp://ftp2.cits.mcan.gc.ca/pub/geott/ess_pubs/286/286323/of_6273.zip)> [accessed: Jan 2012]

Hunter, J.A., Crow, H.L., Brooks, G.R., Pyne, M., Lamontagne, M., Pugin, A.J.-M., Pullan, S.E., Cartwright, T., Douma, M., Burns, R.A., Good, R.L., Motazedian, D., Kaheshi-Banab, K., Caron, R., Kolaj, M., Muir, D., Jones, A., Dixon, L., Plastow, G., Dion, K. and Duxbury, A., 2012. Ottawa-Gatineau seismic site classification map from combined geological/geophysical data; Geological Survey of Canada, Open File 7067, 1 sheet. <[ftp://ftp2.cits.mcan.gc.ca/pub/geott/ess\\_pubs/291/291440/of\\_7067.pdf](ftp://ftp2.cits.mcan.gc.ca/pub/geott/ess_pubs/291/291440/of_7067.pdf)> [accessed: Jul 2012]

Idriss, I.M., 1990. Response of Soft Soil Sites During Earthquakes; *in* Symposium to Honor Professor H. B. Seed, Berkeley, CA, p. 273-289.

Kramer, S.L., 1996. *Geotechnical Earthquake Engineering*, Prentice Hall, 653 p.

Kurfurst, P.J. and Hunter, J.A., 1977, Field and Laboratory Measurements of Seismic Properties of Permafrost, in National Research Council Technical Memorandum #177 (R. J. Brown ed), 16p.

Lomnitz, C., 1999. The End of Earthquake Hazard; *Seismological research Letters*, v. 70, p. 387-388.

Motazedian, D., Hunter, J.A., Belvaux, M., Sivathayalan, S., Pugin, A.J.-M., Chouinard, L., Kaheshi-Banab, K., Crow, H.L., Tremblay, M., Perret, D. and Rosset, P., 2010. Seismic Microzonation of Montreal and Ottawa, Canada; *in* proceedings, 10th Canadian & 9th US National Conference on Earthquake Engineering, Toronto, ON.

Naesgaard, E., 2012. A Combined Effective Stress - Total Stress Model for Analyzing Embankments Subjected to Potential Liquefaction and Flow; Ph.D. Dissertation, University of British Columbia.

National Research Council (NRC), 2010. National Building Code of Canada 2010, Volume 1, Division B, Part 4.

National Research Council (NRC), 2006. Commentary J, User's Guide – NBC 2005 Structural Commentaries (Part 4 of Division B), Canadian Commission on Buildings and Fire Codes, National Research Council of Canada.

Pal, J.D. and Atkinson, G.M., 2012. Scenario Shake Maps for Ottawa, Canada, *Bulletin of the Seismological Society of America*, v. 102, p. 650-660.

Shearer, P.M. and Orcutt, J.A., 1987. Surface and near-surface effects on seismic waves - theory and borehole seismometer results; *Bulletin of the Seismological. Soc. Am.*, v. 77, p. 1168-1196.

Xia, J., Miller, R.D., Park, C.B., Hunter, J.A. and Harris, J.B., 2000. Comparing shear wave velocity profiles from MASW with borehole measurements in unconsolidated sediments, Fraser River Delta, B.C., Canada; *Journal of Environmental and Engineering Geophysics*, v. 5, p. 1-13.

## Chapter 2.0 Non-invasive Seismic Techniques

### *Section Leaders:*

#### *2.1 Shear Waves:*

*Susan Pullan, Geological Survey of Canada, Ottawa, ON*

#### *2.2 Surface Waves:*

*Christopher Phillips, Golder Associates Ltd., Mississauga, ON*

#### *2.3 Ambient Noise:*

*Maxime Claprood, Institut National de la Recherche Scientifique (INRS), Québec, QC.*

This chapter presents various surface (non-invasive) seismic techniques which can be used as part of a seismic site investigation to measure shear wave velocity as a function of depth, as well as subsurface structure. The various methods are discussed below under three headings: Section 2.1 - shear waves (refraction and reflection), Section 2.2 - surface waves, and Section 2.3 - ambient noise measurements. It is important to note that under normal conditions, seismic testing generates a very low strain on the tested materials, and therefore it is low strain, dynamic, engineering properties that are estimated by seismic tests.

When energy is introduced to the subsurface by means of an applied force, it induces the propagation of seismic waves (or vibrations) in the subsurface. Two types of seismic waves are generated: body waves, which propagate spherically (in a homogeneous medium) from the energy source, and surface waves, which are confined to the near surface of the medium and propagate cylindrically from the source (Socco and Strobbia, 2004). As much as two thirds of the energy introduced into a medium from a circular footing converts to surface waves (Richart et al., 1970).

Wave motion generated by a disturbance within a medium can be described by two kinds of waves: compressional waves and shear waves. These are collectively called body waves as they travel within the body of the medium. In compressional waves, particles move in the same direction as the direction of wave propagation, forming zones of compression and extension (Fig. 2-1). Compressional (also called primary or P-) waves are the fastest form of seismic waves. Shear (secondary or S-) waves are characterized by particle motion in a direction perpendicular to the direction of wave propagation (Fig. 2-1).

Surface wave propagation is restricted to the near surface of a medium. Surface waves consist of Rayleigh waves (Rayleigh, 1885), in which ground motion is predominantly perpendicular to their wave front (Fig. 2-1), and Love waves, in which ground motion is predominantly in the horizontal plane. Rayleigh waves (also often referred to as ground roll) have a retrograde elliptical particle motion, with a depth of penetration of approximately three times their wavelength (Asten, 1976). Love waves are horizontally polarized shear waves that only exist in a layered media where they are channeled or guided within the surface layer. Love waves are formed by multiple total reflections of horizontally polarized shear waves from the subsurface layer interface. Both Rayleigh and Love waves are dispersive, meaning that different wavelengths can travel through the medium at different velocities, based on the velocity of the materials they encounter (Aki and Richards, 2003).

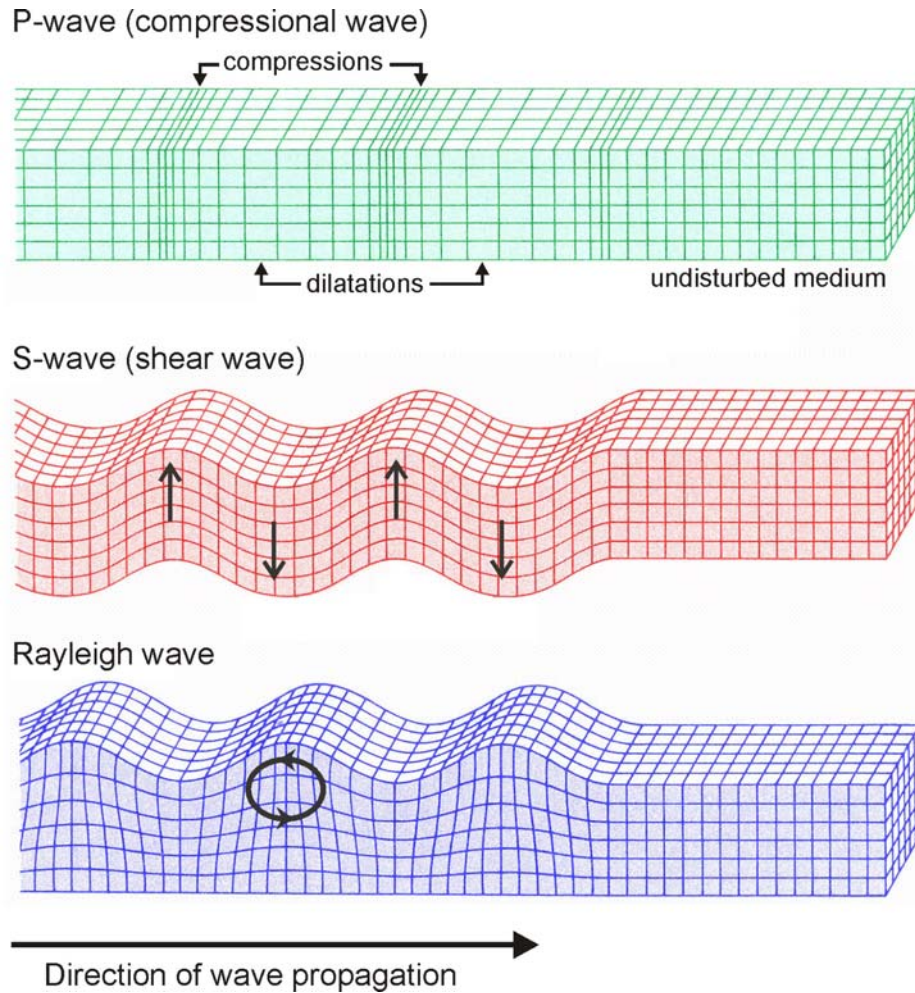


Figure 2-1. Particle displacements occurring with the passage of a harmonic plane P-wave (top), shear wave (centre) and Rayleigh wave (bottom). S-wave propagation is pure shear with no volume change, whereas P-wave involve alternating dilation and compression in the direction of wave propagation. Rayleigh waves contain both vertical and radial motion, and the wave amplitude decays strongly with depth. Strains are highly exaggerated compared to the actual seismic strains in the earth. Modified after Bolt (1993).

The velocity of seismic waves is a function of the elastic properties of the medium: the bulk modulus,  $K$ , the shear modulus,  $G$ , and material density,  $\rho$ . The velocity of shear waves ( $V_s$ ) and compressional waves ( $V_p$ ) are defined as (e.g. Bullen, 1965):

$$V_s = \sqrt{\frac{G}{\rho}} \quad [2-1]$$

$$V_p = \sqrt{\frac{K + \frac{4G}{3}}{\rho}} \quad [2-2]$$

The velocity of compressional waves and shear waves are related through Poisson's ratio,  $\nu$ , where:

$$\nu = \frac{\left(\frac{V_p}{V_s}\right)^2 - 2}{2\left(\frac{V_p}{V_s}\right)^2 - 1} \quad [2-3]$$

Equation 2-1 indicates that, with a known or estimated density of the ground, the shear wave velocity profile can be used to estimate the shear modulus,  $G$ . When  $G=0$ ,  $V_s$  is 0. Thus, shear waves are not transmitted through a substance of zero rigidity (i.e. fluid). Equations 2-2 and 2-3 further show that if both the P- and S-wave velocities of the subsurface are known, bulk modulus and Poisson's ratio can also be estimated.

Rayleigh wave velocity is also related to shear wave velocity through Poisson's ratio (see Sheriff, 1984; Sheriff and Geldart, 1995). The ratio between the velocity of Rayleigh waves and shear waves varies between 0.86 and 0.95 for Poisson's ratios between 0 and 0.5, respectively (Richart et al., 1970).

The equipment needed for conducting a seismic survey consists of three main components; a seismic source, to generate seismic waves in the subsurface; geophones (receivers) to measure ground vibration at specific locations; and a seismograph to digitally record the ground vibration with time. A specific category of seismic survey uses ambient background noise as source of seismic energy (Section 2.3) and does not require an anthropogenic seismic source.

There are several different types of seismic sources, including sledge hammers striking steel plates on the ground, weight drops, explosives, polarized shear wave sources, electrical 'sparker' sources, and controlled frequency vibrating sources. The choice of source type depends on many factors, including the type of seismic test, ground conditions, ambient seismic energy levels, and the required depth of investigation.

Geophones are very sensitive vibration detectors, which are typically planted into the ground or coupled to a borehole wall to measure ground velocity at a particular location. Geophones most commonly measure ground velocity in the vertical plane, but there are also geophones that can measure in the horizontal plane, and these are typically used in surveys designed to record shear waves. Modern seismographs are commonly digital acquisition systems, capable of simultaneously recording data from an array of geophones.

Seismic data are recorded for each receiver station as a function of time. Modern engineering seismographs are capable of 24, 48 or more channels with record lengths from a fraction of a second to several seconds at sample intervals from as small as 62.5 microseconds.

## References

- Aki, K. and Richards, P.G., 2002. Quantitative seismology; University Science Books, California, 704p. (second edition).
- Asten, M.W., 1976. The use of microseisms in geophysical exploration, PhD thesis, Macquarie University, Sydney, Australia.
- Bolt, B.A., 1993. Earthquakes, Newly revised and expanded; W.H. Freeman and Company, 331p.
- Bullen, K.E., 1963. An introduction to the theory of seismology; Cambridge University Press, New York, 381p. (third edition).

Rayleigh, J.W.S., 1885. On waves propagated along the plane surface of an elastic solid; Proceedings of the London Mathematical Society, v.17, p.4-11.

Richart, F.E., Hall, J.R. and Woods, R.D., 1970. Vibrations of Soils and Foundations; Prentice-Hall Inc., New Jersey, 414p.

Sheriff, R.E., 1984. Encyclopedic Dictionary of Exploration Geophysics; Society of Exploration Geophysicists, 232p.

Sheriff, R.E. and Geldart, L.P., 1995. Exploration seismology, Second Edition; Cambridge University Press, United Kingdom, 592p.

Socco, L. and Strobbia, C., 2004. Surface-wave method for near-surface characterization: a tutorial; Journal of Near Surface Geophysics, v.2, p.165-185.

## 2.1 Shear Waves

*Section Leader: Susan Pullan  
Geological Survey of Canada, Ottawa, ON*

Seismic methods such as refraction and reflection use measurements of the time taken for acoustic energy (seismic waves) to travel from a source on the surface through the subsurface and back to a series of receivers on the ground. Energy is refracted or reflected at boundaries where there is a change in acoustic impedance (the product of material density and seismic velocity). Because contrasts in acoustic impedance are generally associated with changes in material type (lithological boundaries), seismic techniques can be used to obtain subsurface structural information. This section presents two articles which deal specifically with the use of shear wave refraction (2.1.1) and reflection (2.1.2) methods for determining shear wave velocity as a function of depth and delineating subsurface structure.

### 2.1.1 Shear Wave Refraction Technique for Hazard Studies

*Jim Hunter & Heather Crow,  
Geological Survey of Canada, Ottawa, ON  
Jeffrey Schmok  
Golder Associates Ltd. Vancouver, BC*

#### Introduction

##### Principles of the Method

An elastic wavefront will be refracted according to Snell's Law when it impinges on a boundary between two materials with a seismic impedance ( $Z = \text{density} \times \text{velocity}$ ) contrast. For incident plane waves the amplitude partition between reflected and refracted waves is given by the Zoeppritz equations (1919). At the critical angle of incidence a non-planar wavefront (e.g. radiating from a point source) refracts along the boundary and radiates sufficient energy back to the surface (see Heelan, 1953; Brekhovskikh, 1960; Červený & Ravindra, 1971) yielding so-called "head-wave" refractions. Velocity of, and depth to, the refracting surface can be calculated by measuring the traveltimes of the seismic wave between the seismic source and the receivers (Figure 2.1.1-1).

##### Current State of Engineering Practice

Standard seismic refraction methodology for near-surface materials was developed over 50 years ago (Nettleton, 1940; Jakosky, 1950; Dobrin, 1960) and has been applied on a routine basis world-wide. ASTM standard D5777(2006) (Standard Guide for Using Seismic Refraction Method for Subsurface Investigation) describes the equipment and methodology of the refraction technique. Most early refraction applications employed compressional (P-wave) technology with vertical impact weight-drop or explosive sources and vertically-polarized geophones. Similar shear wave refraction procedures are discussed here, using polarized shear wave radiation from horizontal (SH) sources and horizontal geophones (Hunter et al., 1992, 1998, and 2002). This methodology is similar to that described in ASTM D5777 for P-waves.

##### **Recommended citation:**

Hunter, J.A., Crow, H.L. and Schmok, J., 2012. Shear Wave Refraction Technique for Hazard Studies; *in* Shear Wave Velocity Measurement Guidelines for Canadian Seismic Site Characterization in Soil and Rock, (ed.) J.A. Hunter and H.L. Crow; Geological Survey of Canada, Open File 7078, p.23-34.

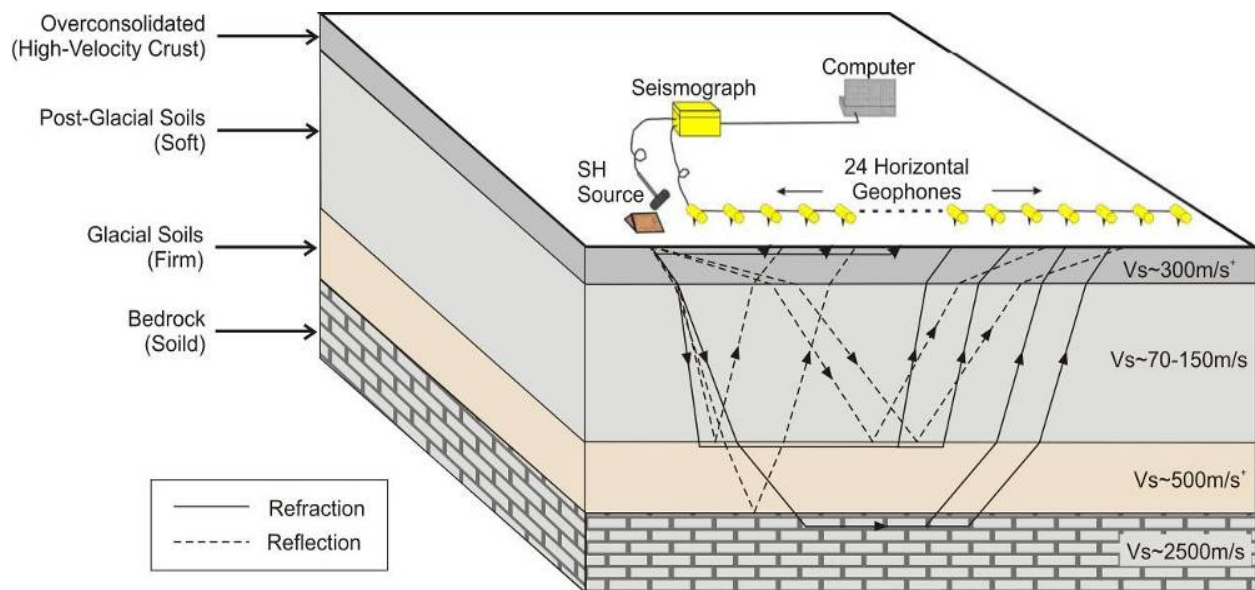


Figure 2.1.1-1. Schematic diagram of shear wave travel paths through soils and rock of the Ottawa region.

### **Limitations**

The refraction method relies on the fundamental assumptions of single-velocity layers and requires that velocities increase with depth; therefore, an important limitation of the approach is the inability to detect velocity reversals. In such an environment, other techniques (MASW, SCPT, Downhole shear) may be more appropriate. In addition, if shear wave velocity increases in step-wise fashion with depth, a velocity layer must have a certain minimum thickness to be detected (Xia et al., 2002); this phenomenon is often referred to as the 'hidden layer' or 'blind zone' problem and the potential scale of this limitation is discussed in the "3.2 Uncertainty Assessment" section below.

Refractions are low amplitude events, and in field environments where signal-to-noise ratios (S/N) are low, such events may be very difficult to observe. As well, significant velocity discontinuity layering may be dipping, and the downdip or updip apparent velocities may vary considerably for relatively low angles. Therefore, it is critical to collect records for forward and reverse shot positions for a geophone array. The measured up and down dip velocities can be averaged arithmetically to estimate refractor velocities for small dip angles (usually less than 20 degrees for common overburden-bedrock velocity contrasts – see Nettleton, 1940, page 270).

In general, geophone array length to refractor depth ratios must be quite large (~5 or more) in order for the refraction event from a high-velocity layer to be observable as a first arrival. Shorter arrays can be used where impedance contrasts between the layers are large ( $z > 20$ , i.e. soft soil over hard bedrock) however there is an increased possibility of hidden layer error.

## **Data Collection**

### **Required Equipment**

An array of low frequency horizontal geophones (e.g. 4.5Hz, 1 geophone per trace with direction transverse to the strike of the array) is recommended, along with a seismic cable, seismograph, laptop computer, seismic source and trigger wire, and a metal I-beam. Commonly engineering seismographs have at least 12 or 24 input channels, although some instruments offer 96 or more. For near surface refraction, a 16 lb hammer striking a horizontally imbedded I-beam plate is generally adequate, with the

direction of motion of the hammer at right angles to the linear geophone array imparting significant radiating SH polarized energy into the ground (Figure 2.1.1-2). The choice of SH polarized motion minimizes the possibility of converted wave (S to P) interference that is more likely to be present if the source and receivers are deployed radially (in-line).

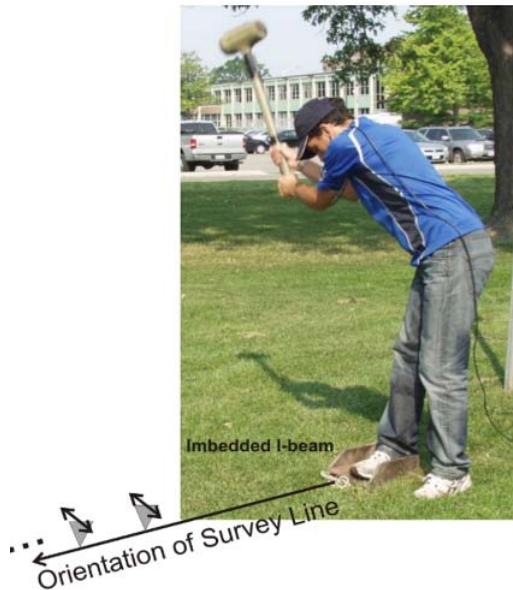


Figure 2.1.1-2. I-beam and 16lb hammer used as seismic source.

### **Data Collection Procedures**

Geophone spacing is chosen based on the anticipated depth to bedrock and velocity-depth distribution; in near surface applications, 1 to 5 metre separation is generally adequate; however multiple array positions may be used to obtain 24, 48 or 96 trace composite records. Shot locations are recommended at the center of the spread, at each end of the array in order to obtain a pseudo-reversed-refraction record suite. If time and cost allow, a true “reversed” refraction profile can be obtained wherein the geophone location at each end of the array is replaced by a source location; this approach minimizes unresolved statics. Additional shots offset from the end of the array can be used in place of moving the geophone spread if flat-lying subsurface layers can be assumed. Records from repeated sources may need to be digitally stacked in order to improve the signal-to-noise ratio and observe the low amplitude refractions from far source-geophone offsets. For shear wave refraction surveys, it is recommended at each shot position to record a shot(s) hammered in one polarizing direction, and then turn 180° to separately record a shot(s) hammered in the opposite direction.

### **Processing Techniques**

#### **Theory of Analysis**

The arrival time of shear wave energy at each geophone can be identified using display and processing software. Comparison of the records with opposite source polarity commonly can help in the presence of ambient noise. Travel times can be plotted against the distance between the source and the geophone, to create ‘time-distance’ plots (Figure 2.1.1-3). These can be interpreted in terms of refraction layers, with the velocities of the layers calculated from the arithmetic average of forward and reverse plots, using the reciprocal of the slope of each identified layer. From the velocities and intercept times of the slopes, layer thicknesses can be computed (the “intercept-time” method). Other layered interpretations can be made using the “critical distance” method. These, as well as several other methods, are well documented in literature by Nettleton (1940), Musgrave (1967), Palmer (1988), Telford et al. (1995) and others. Numerous inexpensive seismic software packages are readily available which can import seismic

records, perform gain adjustments and basic filtering if required, pick and export shear wave arrival times, and interpret velocities and depths to refracting horizons.

Different approaches using refraction tomography techniques have recently become more common (e.g. Sheehan et al., 2005). Tomographic methods do not assume laterally continuous, constant velocity layers and are better able to resolve velocity gradients and lateral variations where those are characteristic of the geological setting.

### **Uncertainty Assessment**

The results of a velocity analysis using refraction methods can be influenced by sources of uncertainty in geological setting (presence of dipping/irregular layers, velocity reversals, velocity gradients), environmental setting (background noise levels, sloping ground surface, practical limitations in array length, coupling of source to ground surface) and interpretation (hidden layers, low amplitude refractions, first arrival picking errors, interpreter variation/error in assigning slope segments). Subsurface inclined or irregular layering producing apparent velocities should be identified by performing forward and reverse shots in the field along with careful operator inspection of the field records. Identification of low amplitude refractions can be improved with careful signal stacking. Data should be acquired at times when noise levels are acceptable. Increasing the number of shots and receivers improves the definition of subsurface structure and can result in the use of more sophisticated analysis and interpretation routines which may permit lateral variations to be delineated. Williams et al. (2003) recommend a  $\pm 10\%$  error on all refraction velocity measurements.

The hidden layer problem must always be considered when interpreting first arrival data. Figure 2.1.1-3 illustrates the potential significance of this effect. In a geological setting where soft silty soils overlie a generally thin glacial layer and then bedrock, a substantial layer of intermediate high velocity material (e.g. till) can not be interpreted from first arrival times alone; although an experienced interpreter may identify the event from the presence of later arriving high amplitude (wide-angle) reflections. The very significant effect on the interpreted thicknesses of the layers and the calculated  $V_{s30}$  value is shown on the figure. In this case, a 600 m/s layer of up to 23 m thickness would not yield a first arrival.

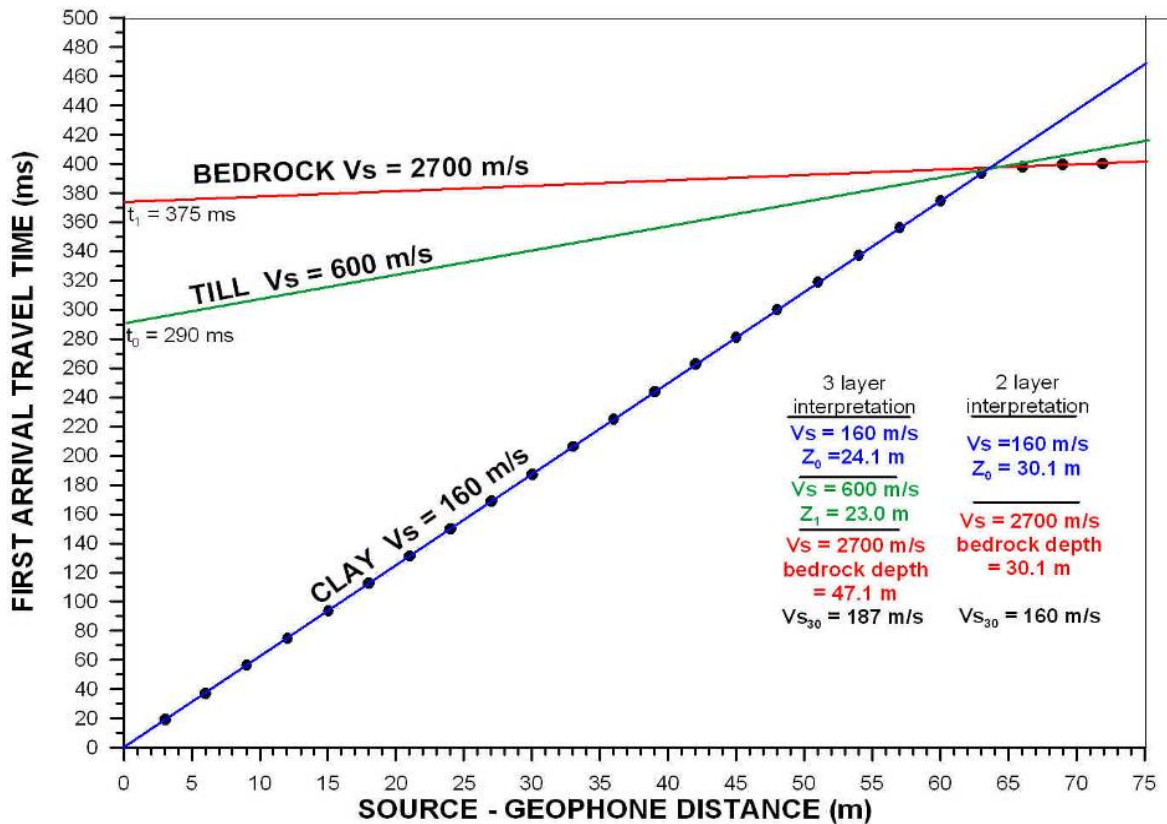


Figure 2.1.1-3. Interpreted single-end time-distance plot showing the effect of an intermediate layer of till which could be undetected as a “first” arrival. The variation in interpreted layer thicknesses is significant, and the resulting  $V_{S30}$  values are noted.

### Recommended Guidelines for Reporting

Minimum reporting requirements must describe survey components and configuration used. Survey impediments must also be outlined, such as line length limitations, noise levels at time of survey, and topography of the survey alignment. Other geological limitations must also be described (e.g. possibility of velocity reversals or of hidden layers based on analysis of available borehole data, etc). Seismic site classification reports must present sample seismic field records showing picked first arrivals of forward and reverse shots indicating data quality. Interpreted time-distance plots, and an error analysis of the slopes must also be presented.

Where applicable, calculation of the average shear wave velocity to the depth of interest ( $V_{S30}$  or other) should be clearly indicated along with a table showing the interpreted unit thicknesses ( $z$ ) and velocities ( $V_s$ ), and the calculated travel time in each unit. These travel times should be summed to the depth of interest and divided by this depth, as shown in Table 2.1.1-1.

Layer	Thickness (m)	Interval $V_s$ (m/s)	Calculated Travel Time (sec)	$V_{s30}$ ( $\Sigma z/\Sigma t$ )
1	10	200	0.050	
2	8	600	0.013	
3	12	2500	0.005	
Sum	30		0.068	440

Table 2.1.1-1. Sample  $V_{s30}$  calculation from interpreted refraction layer velocities and thicknesses. The travel time within a given layer is calculated (thickness divided by interval velocity) and then the total travel time to the depth of interest (30 m in this case) was used to determine  $V_{s30}$ .

## Hazard-Related Case Studies

### Ottawa area microzonation study – refraction example

A multi-year project was undertaken by the GSC and Carleton University to define the regional variation of soft soil thickness and shear wave velocity within the near surface across the City of Ottawa (2760 km<sup>2</sup>). During the field program, over 680 seismic test sites were occupied. At 508 sites, the bedrock and/or glacial (till) velocities were well defined by refraction measurements. An important product of the velocity surveys were two microzonation maps showing seismic site classes and fundamental site period (Hunter et al., 2010).

It was expected that the large contrast between soft soil and bedrock would yield excellent refraction (and reflection) records in most regions of the city, therefore this method was chosen for the survey. Prior to survey design and seismic site selection, surficial geology and overburden thickness maps derived from a large regional borehole database were consulted. The generalized stratigraphic sequence in the National Capital Region is composed of a Paleozoic (limestone, dolostone, shale) or Precambrian (granitic) bedrock, overlain by thin till deposits (averaging 6.8m), overlain by soft Champlain Sea muds (silts and clays). Where bedrock was within 25 – 30 m of surface, the refraction array design yielded accurate interval velocities down to, and into, the bedrock. Where bedrock was at a depth below approximately 30 m, the shear wave reflection data yielded average  $V_s$  velocities to the top of bedrock as well as throughout the overburden section. Typically, a 3m geophone separation was used, occasionally increasing to 5m in areas where thick soft soils ( $z > 100m$ ) were found to exist. Data were acquired for shot points at the centre of the array, and at off-end positions at one, one and a half, and 10 times the geophone spacing. As shown in Figure 2.1.1-2, the source was a loaded metal I-beam struck with a 16lb sledge hammer.

A high-velocity surface crust ( $V_s=250-400$  m/s) of either over-consolidated Champlain Sea sediments or surface fill materials was common and is interpreted on the near traces of Figure 2.1.1-4. This high-velocity layer is usually 1~5 m thick and it can be shown that neglecting this layer in the interpretation of  $V_{s30}$  and fundamental site period has only a limited effect. The interpreted post glacial, glacial (where visible), and bedrock refraction arrivals were exported from the picking software to produce traveltimes-distance plots for forward and reverse shot directions. The inverse of the slope was used to calculate the interval shear wave velocity for each stratigraphic unit. Standard layered refraction relationships were then used to calculate the thicknesses of the unit(s) above the bedrock.

A very common occurrence when interpreting time-distance plots was a difference in the forward and reverse bedrock velocities and time intercepts, indicating a dip in the bedrock surface. If the dip was less than ~20°, the bedrock velocities were averaged and considered representative of the bedrock conditions below the array (Figure 2.1.1-5). In rare cases where the dip was greater than 20° (e.g. a drop in bedrock surface of 32 m over an array length of 69 m), a corrected overburden thickness was calculated at either end of the array based on the traveltimes to the bedrock at the center of the array and the apparent

velocity calculated at the ends of the array. This tended to shallow the downdip and deepen the updip depths, reducing the severity of the sloping surface. In some cases, site classes were found to be different at either end of the array, and here, to be conservative, the lower of the two site classes was chosen.

The hidden layer case could occasionally be observed in the seismic records (Figure 2.1.1-6). Here, the refractions from the glacial materials (tills, sands and gravels, etc) never appear as first arrivals, although are visible in the record (see Figure 2.1.1-3). Varying the gains to bring forward faint refraction amplitudes was necessary, as the glacial features could often be quite subtle. Close attention to the reflections also assisted in the interpretation, as a glacial reflection could be more prominent in the record than the refraction. The surficial geology map and particularly the nearest boreholes were also helpful in knowing whether intermediate glacial layers of significant thickness (>10m) may be expected in the area.

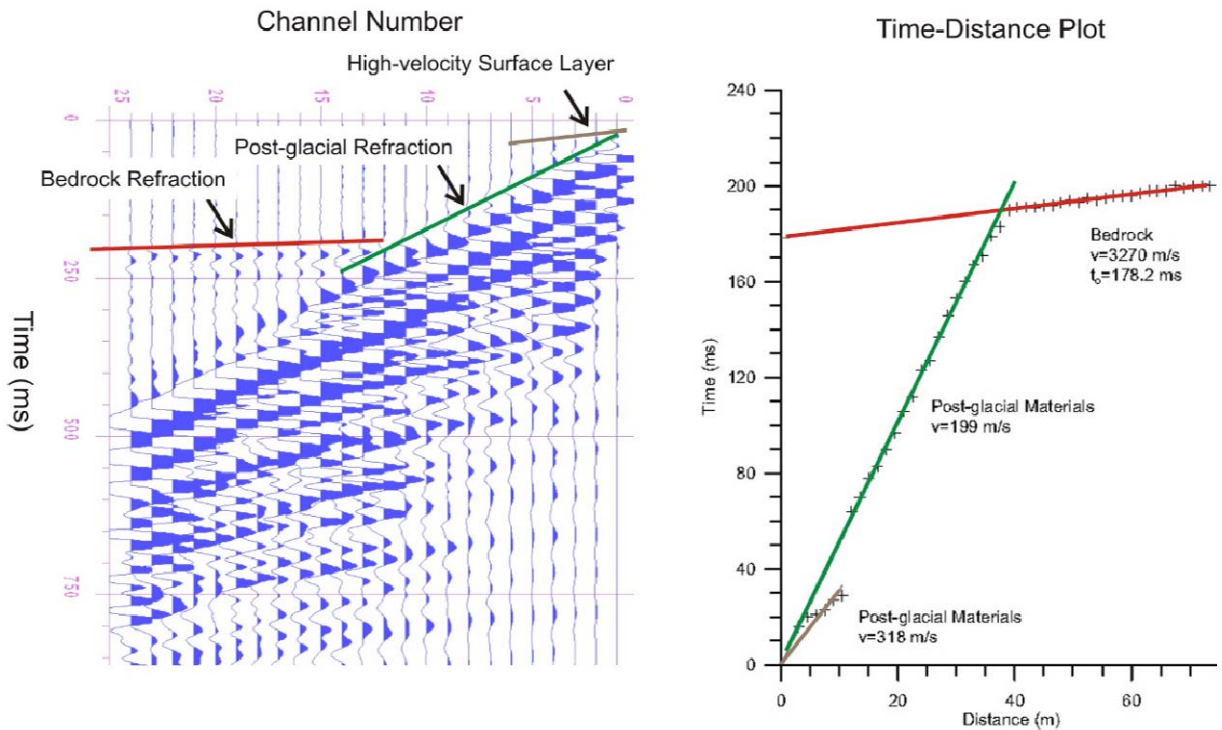


Figure 2.1.1-4. A single record showing a thin, high-velocity surface layer, the main overburden refraction event, the bedrock refraction, and the accompanying time-distance plot used to interpret the interval velocity of each unit.

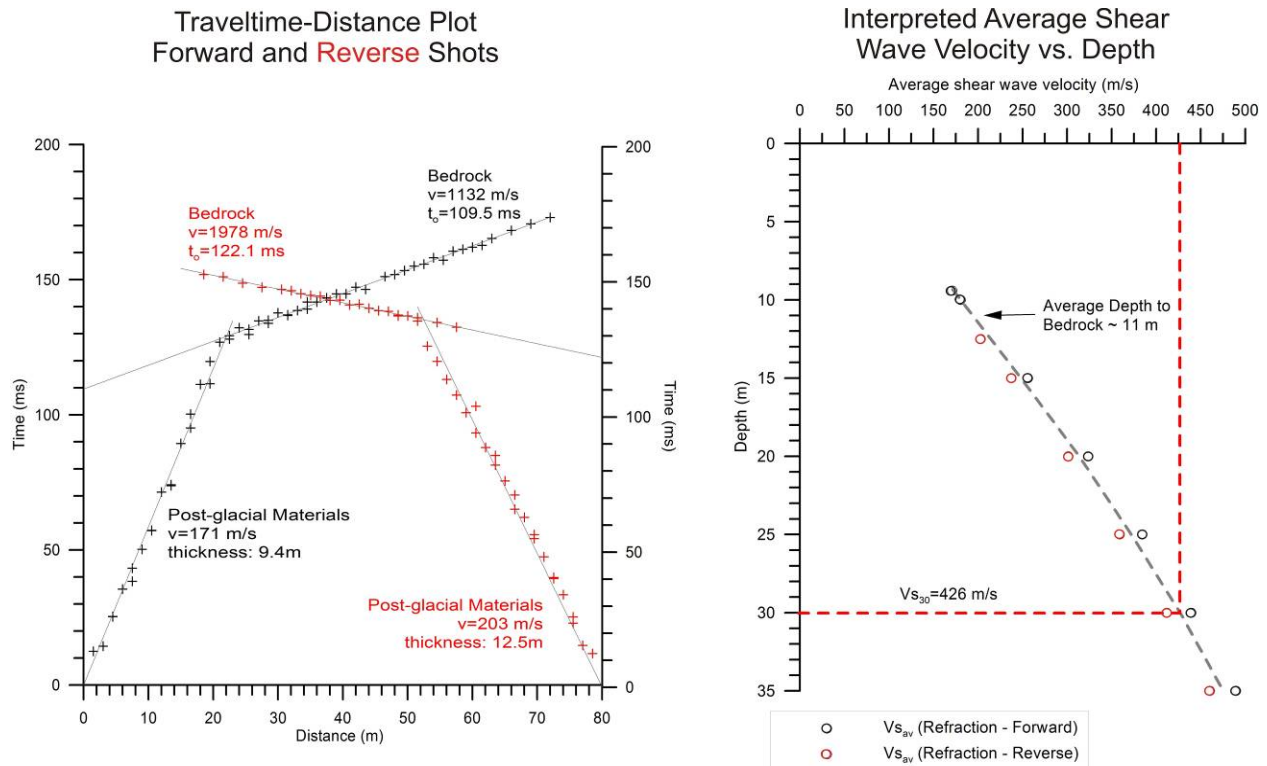


Figure 2.1.1-5. Interpreted refraction arrivals displayed on a time-distance plot showing intercept times, calculated velocities and post-glacial unit thicknesses. Results indicate a 3° downward dip (or 3m over 69m) from geophone 1 toward 24, and forward and reverse bedrock velocities were averaged for the site. These velocity and thickness results allow for the calculation of an average shear wave velocity down into the bedrock for seismic site class calculations. Open circles indicate the discrepancy between the forward and reverse interpretations due to the dipping bedrock surface.

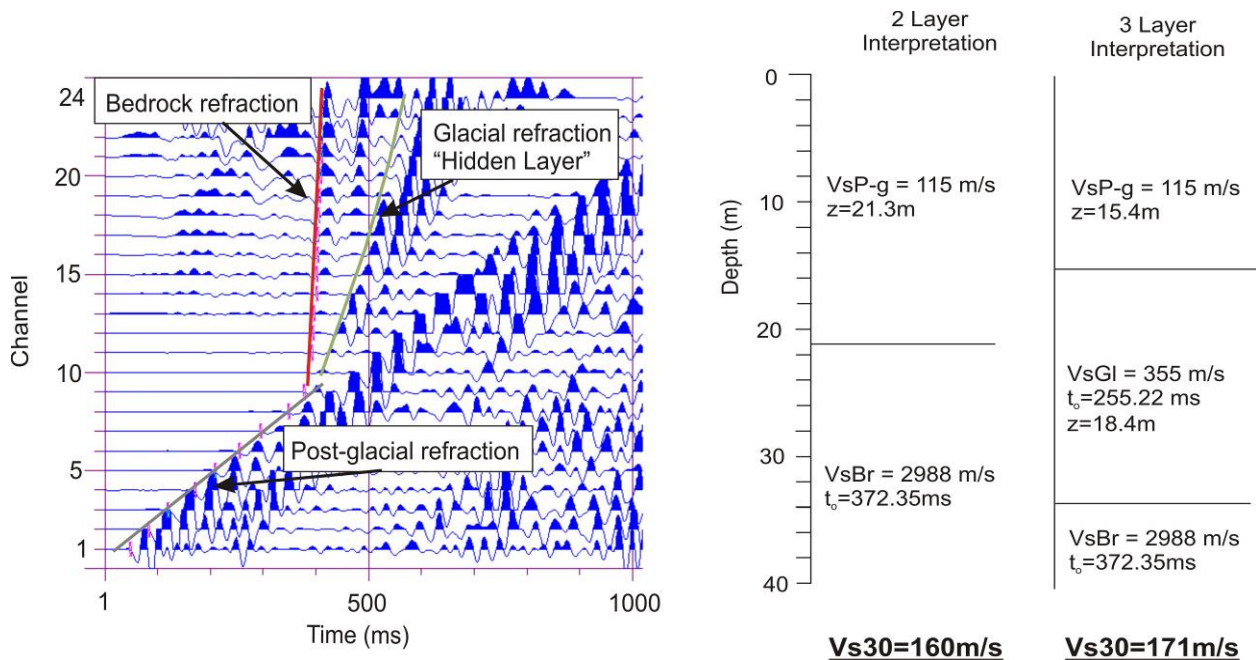


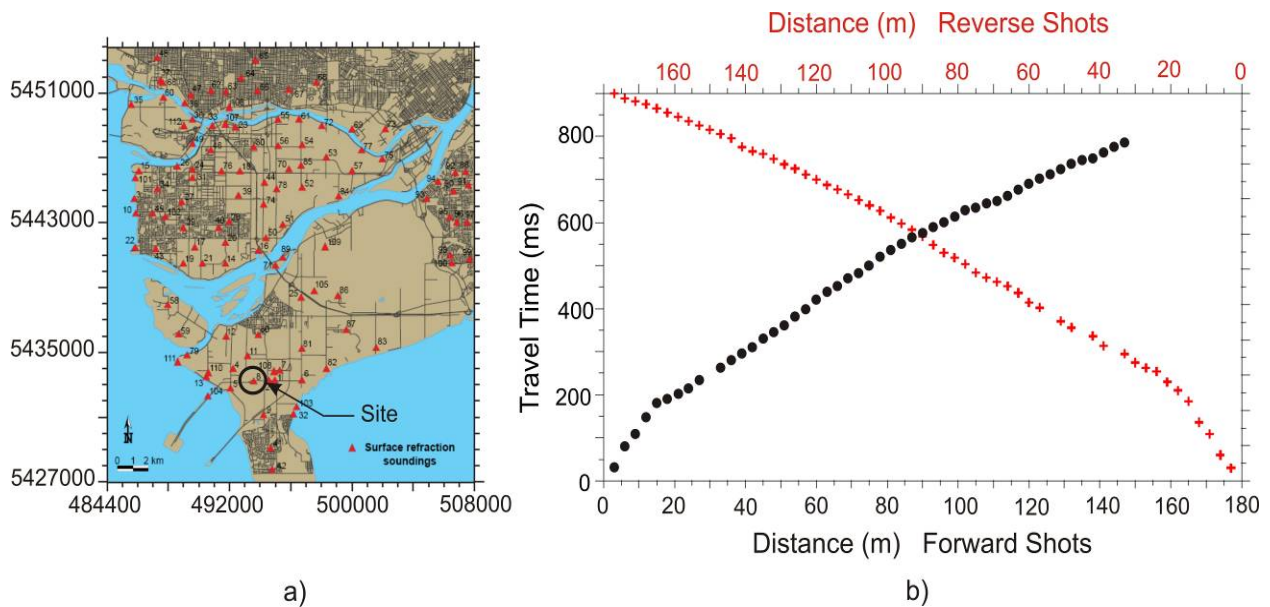
Figure 2.1.1-6. Sample refraction record from the Ottawa area where hidden layer (glacial refraction) is present. If unaccounted for, the stratigraphy and  $V_{s30}$  could be misinterpreted.

### **Fraser Delta hazard studies – refraction example**

As an aid to west coast regional earthquake hazard studies being carried out by federal, provincial, university, and industry organizations, the GSC began collecting surface and borehole seismic data in 1985 in the Fraser River Delta (Hunter et al., 1998, 1998b). It was recognized that broad-band and resonance amplification effects and seismic liquefaction all have a dependence on the variation of horizontal and vertical shear wave velocity structure within the Quaternary sediments of the Delta. As a result, shear wave refraction and reflection techniques were tested and used successfully at numerous sites within the study area, along with borehole geophysical logging.

Refraction surveys were carried out at 112 sites (Figure 2.1.1-7a). An array of 8Hz geophones (oriented in SH mode) was used, and shots originated from fixed locations on either end of the array. For shallow soundings of 40m or less, a loaded I-beam (see Figure 2.1.1-2) was sufficient, but in cases where overburden exceeded 100 m, an 8-gauge in-hole shot-gun was used.

First arrivals of the shear waves were interpreted by hand in both forward and reverse cases, and plotted as travel-time-distance curves (Figure 2.1.1-7b). Analysis was carried out using the traditional 'layer-case' method where the inverse of the slope of each straight line segment in the curve, along with the intercepts at zero-distance, provides a velocity and a thickness for each layer. A second method of analysis was the 'velocity-depth' routine. This automated routine (developed after Hunter, 1971), produces a running least-squares fit centered at each of the points on the curve, and removes the need to interpret straight line segments through the points, which can vary significantly between interpreters. As can be seen from Figures 2.1.1-7c and d, the two techniques show comparable results, but the 'velocity-depth' approach produces a more realistic gradual increase in velocity with depth, as opposed to sudden increases at interpreted layer boundaries. Data resulting from these velocity surveys are compiled in Hunter et al., 1998.



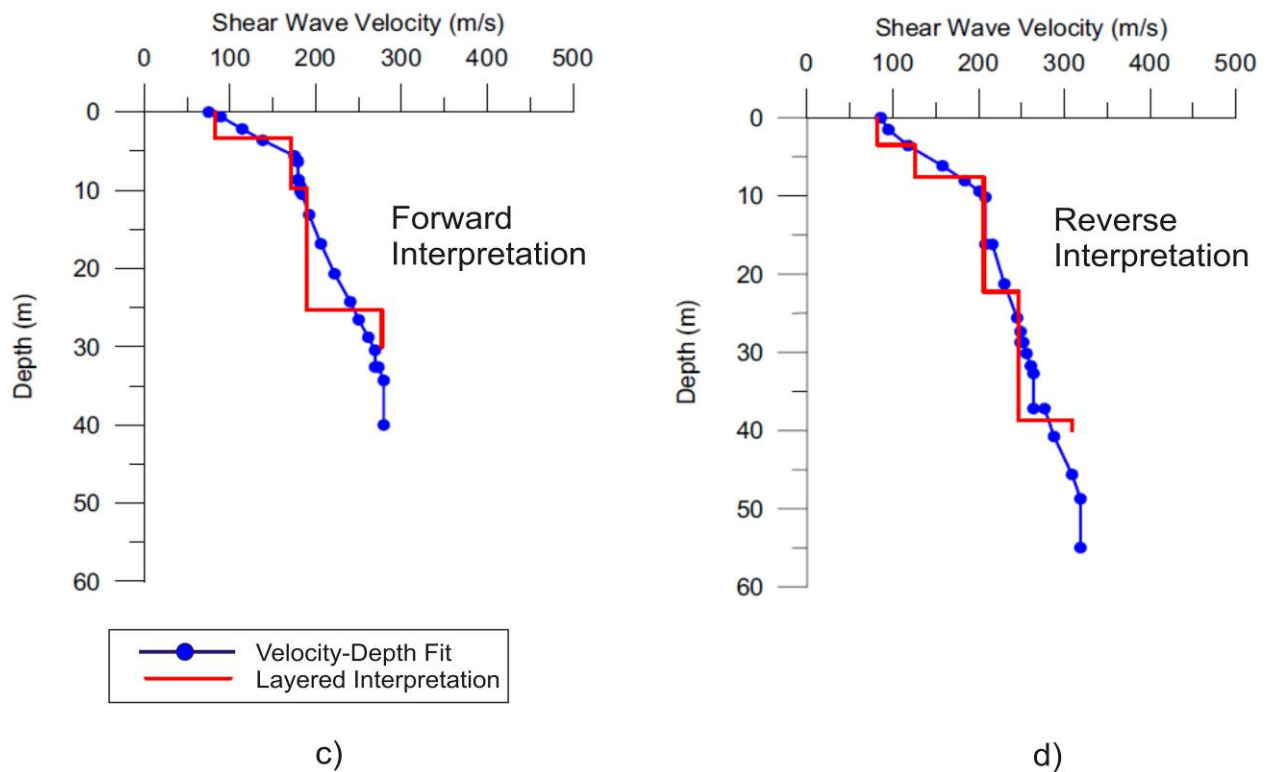


Figure 2.1.1-7. Refraction surveys carried out in the Fraser River Delta, BC, by Hunter et al. (1998, 1998b). a) Map indicating the locations of 112 refraction sites throughout the study area. The location of the interpreted site shown in this figure is outlined by the black circle. b) Sample travel-time-distance plot of the interpreted first shear wave arrivals of the forward and reverse shots. c) & d) Resulting velocity-depth profiles, presented as layered interpretations and as “velocity-depth” fits using a routine developed by Hunter (1971). Here, a 5-pt running least-squares fit is applied along the travel-time-distance curve, yielding a continually varying velocity profile rather than the single-velocity “layers” interpreted by traditional refraction methods.

#### **Vancouver Island subsurface delineation**

Refraction can also be used to profile the thickness of a near-surface low velocity layer(s) within a study area. The objective of the geophysical survey was to obtain cross-sections of a deltaic/fluvial silty sand unit overlying an overconsolidated till on Vancouver Island, prior to geotechnical design. Shear wave refraction surveys were selected as the survey method, as the velocity contrast was expected to yield clear refractions. The maximum depth of investigation over the entire site was estimated to be approximately 21m. Two 115 m-long perpendicular seismic lines were collected over the site (east-west profile is shown in Figure 2.1.1-8), using 4.5 Hz horizontal geophones spaced 5m apart. The source was a 16lb sledge hammer struck against a horizontal beam to produce SH waves. A borehole drilled just off the alignment was used to ground truth the interpretation.

Interpretation was carried out using a standard ray trace modeling method in the SIP (Seismic Imaging Processing) software. The shear waves in the seismic records are identified as the polarity reversed arrivals, and these are then picked in each record for each shotpoint. These arrival times are used to generate a time distance plot from which sub-surface layers are differentiated and their seismic velocities determined.

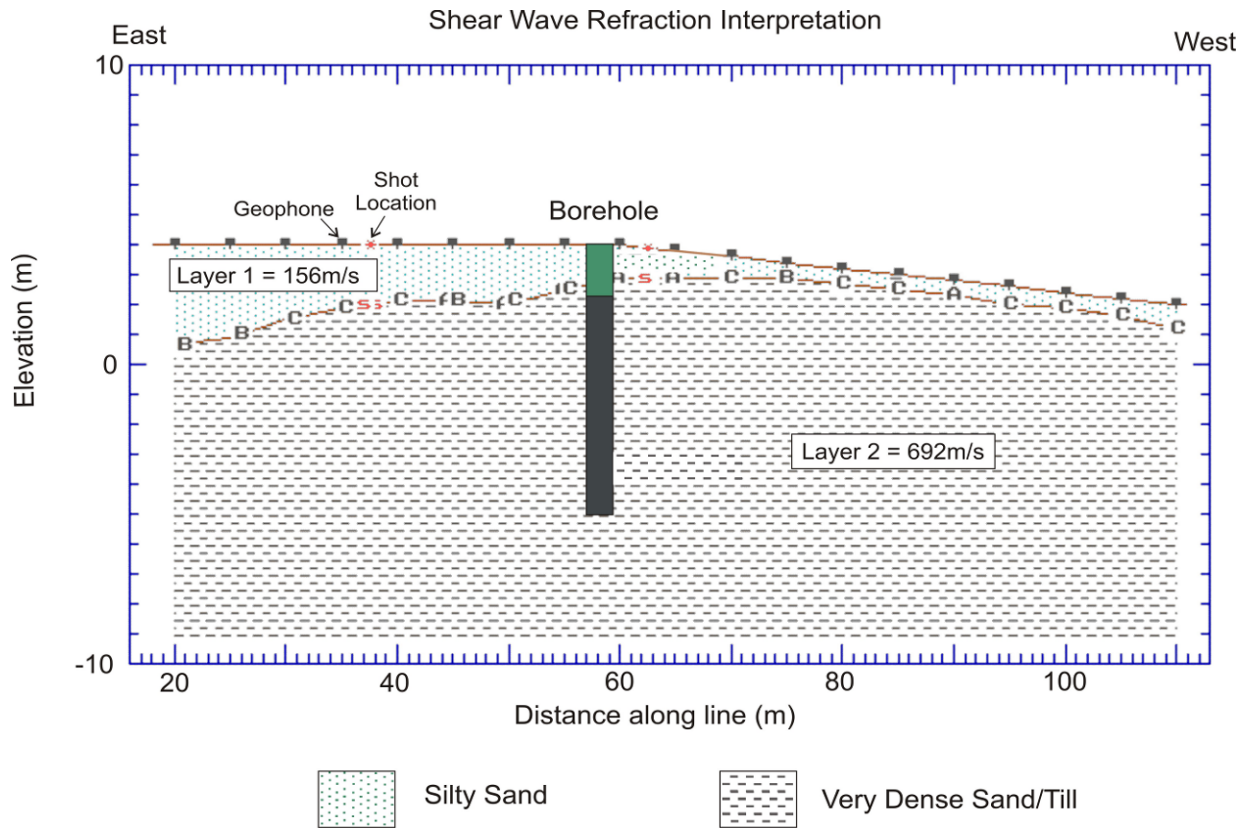


Figure 2.1.1-8. Sample layer interpretation from a shear wave refraction survey on Vancouver Island. A borehole along the alignment provides important ground truth for the profile.

## Acknowledgments

The authors would like to acknowledge funding support for the Ottawa work from Natural Resources Canada's Eastern Canada Geohazards Assessment Project and NSERC funding through Carleton University. Participants include Dariush Motazedian, Greg Brooks, Matt Pyne, Susan Pullan, Andre Pugin, Tim Cartwright, Ron Good, Rob Burns, and numerous student contributors.

## References

ASTM D5777-00 (Reapproved 2006). Standard Guide for Using the Seismic Refraction Method for Subsurface Investigation; *in* Annual Book of ASTM Standards 2008, Section Four: Construction, American Society for Testing and Materials International, Conshohocken, PA, v. 04.08, p.1574-1587.

Brekhovskikh, L.M., 1960. Waves in Layered Media; *in* Applied Mathematics and Mechanics, vol 6, (ed.) F.N. Frenkiel, G. Temple; Academic Press, New York.

Červeny, V. and Ravindra, R., 1971. Theory of seismic head waves; University of Toronto Press, Toronto, ON, 312p.

Dobrin, M.B., 1960. Introduction to Geophysical Prospecting; McGraw-Hill, New York, 446p.

Heelan, P.A., 1953. On the theory of headwaves; Geophysics, vol.18, p.871-893.

- Hunter J.A., 1971. A computer method to obtain the velocity–depth function from seismic refraction data. Report of Activities, Part B, Geological Survey of Canada Paper 71-1B; p.40–48.
- Hunter, J.A., Luternauer, J.L., Neave, K.G., Pullan, S.E., Good, R.L., Burns, R.A. and Douma, M., 1992. Shallow Shear Wave Velocity-Depth Data in the Fraser Delta From Surface Refraction Measurements, 1989, 1990, 1991; Geological Survey of Canada, Open File 2504, 271p. <[ftp://ftp2.cits.mcan.gc.ca/pub/geott/ess\\_pubs/133/133371/of\\_2504.pdf](ftp://ftp2.cits.mcan.gc.ca/pub/geott/ess_pubs/133/133371/of_2504.pdf)> [accessed: Jan 2012]
- Hunter, J.A., Burns, R.A., Good, R.L. and Pelletier, C.F., 1998. A compilation of shear wave velocities and borehole geophysics logs in unconsolidated sediments of the Fraser River Delta, British Columbia; Geological Survey of Canada, Open File 3622, 1 CD-ROM. <[ftp://ftp2.cits.mcan.gc.ca/pub/geott/ess\\_pubs/209/209974/of\\_3622.zip](ftp://ftp2.cits.mcan.gc.ca/pub/geott/ess_pubs/209/209974/of_3622.zip)> [accessed: Jan 2012]
- Hunter, J.A., Douma, M., Burns, R.A., Good, R.L., Pullan, S.E., Harris, J.B., Luternauer, J.L. and Best M. E., 1998b. Testing and application of near surface geophysical techniques for earthquake hazards studies, Fraser River Delta, British Columbia; *in* Geology and Natural Hazards of the Fraser River Delta, British Columbia; (ed.) J.J. Clague, J.L. Luternauer, and D.C. Mosher, Geological Survey of Canada, Bulletin 525, p.123-145.
- Hunter, J.A., Benjumea, B., Harris, J.B., Miller, R.D., Pullan, S.E., Burns, R.A. and Good, R.L., 2002. Surface and downhole shear wave seismic methods for thick soil site investigations; Soil Dynamics and Earthquake Engineering, vol. 22, p.931-941.
- Hunter, J.A., Crow, H.L., Brooks, G.R., Pyne, M., Motazedian, D., Lamontagne, M., Pugin, A. J.-M., Pullan, S.E., Cartwright, T., Douma, M., Burns, R.A., Good, R.L., Kaheshi-Banab, K., Caron, R., Kolaj, M., Folahan, I., Dixon, L., Dion, K., Duxbury, A., Landriault, A., Ter-Emmanuil, V., Jones, A., Plastow, G. and Muir, D., 2010. Seismic Site Classification and Site Period Mapping in the Ottawa Area Using Geophysical Methods; Geological Survey of Canada, Open File 6273, 1 DVD. <[ftp://ftp2.cits.mcan.gc.ca/pub/geott/ess\\_pubs/286/286323/of\\_6273.zip](ftp://ftp2.cits.mcan.gc.ca/pub/geott/ess_pubs/286/286323/of_6273.zip)> [accessed: Jan 2012]
- Jakosky, J.J., 1950. Exploration Geophysics; Trija Publishing Co., Los Angeles, CA., 1195p.
- Musgrave, A.W., 1967. Seismic refraction prospecting; Society of Exploration Geophysicists, Tulsa, OK, 604p.
- Nettleton, L.L., 1940. Geophysical Prospecting for Oil; New York, McGraw-Hill, 444p.
- Palmer, D., 1988. Refraction seismics: the lateral resolution of structure and seismic velocity; *in*: The handbook of geophysical exploration, Section 1: Seismic Exploration, vol. 13, (ed.) K. Helbig and S. Treitel; Geophysical Press, London, 296p.
- Sheehan, J.R., Doll, W.E. and Mandell, W.A. 2005. An evaluation of methods and available software for seismic refraction tomography analysis; Journal of Environmental and Engineering Geophysics 10, 21-34.
- Telford, W.M., Geldart, L.P. and Sheriff, R.E., 1995. Applied Geophysics; Cambridge University Press, New York, 770p. (second edition).
- Williams, R.A., Wood, S., Stephenson, W.J., Odum, J.K., Meremonte, M.E. and Street, R., 2003. Surface seismic refraction/reflection measurement determinations of potential site resonances and the areal uniformity of NEHRP site class D in Memphis, Tennessee; Earthquake Spectra, v. 19, p.159–189.
- Xia, J., Miller, R.D., Park, C.B., Wightman E. and Nigbor, R., 2002. A pitfall in shallow shear-wave refraction surveying; Journal of Applied Geophysics, v. 51, p.1-9.
- Zoeppritz, K., 1919. Erdbebenwellen VIII B, Uber Reflexion and Durchgang seismischer Wellen durch Unsteigkeitsflächen; Gottinger Nachr. I, p.66-84.

## 2.1.2 Shear Wave Reflection Techniques for Hazard Studies

*Susan Pullan, Jim Hunter, Heather Crow, and André Pugin*

*Geological Survey of Canada, Ottawa, ON*

*James B. Harris*

*Department of Geology, Millsaps College, Jackson, Mississippi, USA*

### Introduction

#### **Principles of the Method**

When seismic energy impinges on a boundary between two homogeneous materials with a seismic impedance ( $z = \text{density} \times \text{velocity}$ ) contrast, energy is partitioned between reflection and refraction according to Snell's law and the Zoeppritz equations (Fig. 2.1.2-1a; see e.g. Telford et al., 1995). Seismic reflection methods involve measurement of the time taken for seismic energy to travel from the source at or near the surface, down into the ground to an acoustical discontinuity, and back up to a receiver or series of receivers on the ground surface (Fig. 2.1.2-1). The travelttime curve of the reflection signal on a multi-channel record is hyperbolic (Fig. 2.1.2-2), and average velocity from the ground surface to the reflecting horizon can be calculated by the  $X^2-T^2$  method. In the simplest case of a flat-lying reflector (e.g. Fig. 2.1.2-1b), the slope of a plot of the reflection arrival time ( $T$ ) squared versus the distance between source and receiver ( $X$ ) squared is equal to the inverse of the velocity squared (e.g. Telford et al., 1995).

Reflection data can be acquired along with refraction data at a site using a single array of receivers (Fig. 2.1.2-1b, -2). Alternatively, data can be acquired continuously along a survey line, and processed to produce a seismic section which is a two-way travel time cross-section of the subsurface. The signal-to-noise ratio is improved by stacking data obtained with different source-receiver locations but the same common midpoint (CMP) (Fig. 2.1.2-3). Velocity-depth functions calculated from the data, or seismic logging of a nearby borehole(s), are used to translate the two-way travel time into depth.

#### **Current State of Engineering Practice**

Shallow seismic reflection methods offer a powerful non-invasive tool suitable for mapping the subsurface geological framework from the very near-surface to hundreds of metres below surface. These methods were developed in the 1980s (Doornenbal and Helbig, 1983; Hunter et al., 1984; Knapp and Steeples, 1986b), when technological advancements in engineering seismographs and computers allowed the adaptation of conventional oil-exploration seismic methods to the near-surface domain (Hunter et al., 1982; Knapp and Steeples, 1986a). Since that time, much experience and expertise in the application of shallow high-resolution reflection techniques have been gained. Today, these methods are accepted and proven shallow geophysical tools. Overviews of the application of seismic reflection methods to the shallow subsurface are given by Steeples and Miller (1990, 1998), Steeples (1998, 2005), Brouwer and Helbig (1998), Pullan and Hunter (1999), Brabham et al. (2005), and Rabbel (2006).

While most shallow or high-resolution seismic reflection surveys are conducted using compressional (P-) waves, there has also been an ongoing interest in shallow shear (S-) wave reflection methods, which potentially offer higher resolution of the near-surface because of the low shear wave velocities in unconsolidated sediments (Helbig and Mesdag, 1982; Stumpel et al., 1984; Carr et al., 1998; Pugin et al., 2006). Shallow shear wave reflection methods are particularly applicable to earthquake hazard studies (e.g. Woolery et al., 1993; Harris and Street, 1997; Benjumea et al., 2003; Motazedian and Hunter, 2008; Harris 2009, 2010; Hunter et al., 2010b). Shallow multi-component reflection surveying is now showing great potential (Pugin et al., 2009, 2010).

#### **Recommended citation:**

Pullan, S.E., Hunter, J.A., Harris, J.B., Crow, H.L. and Pugin, A.J.-M., 2012. Shear Wave Reflection Technique for Hazard Studies; *in* Shear Wave Velocity Measurement Guidelines for Canadian Seismic Site Characterization in Soil and Rock, (ed.) J.A. Hunter and H.L. Crow; Geological Survey of Canada, Open File 7078, p. 35-48.

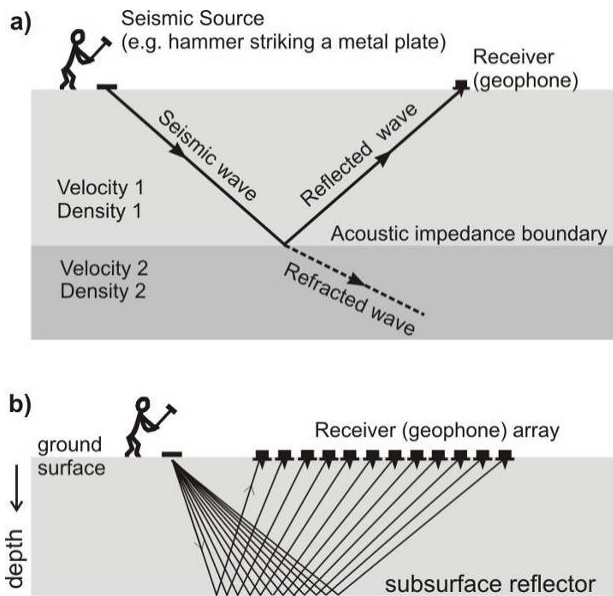


Figure 2.1.2-1: Basic premise of seismic reflection methods. a) Seismic energy produced on the ground surface travels from the source down to an acoustic impedance (product of density and velocity) boundary, where it is partially transmitted and partially reflected back towards the surface. b) Schematic diagrams showing the subsurface travel paths of reflections from a 12-channel field record.

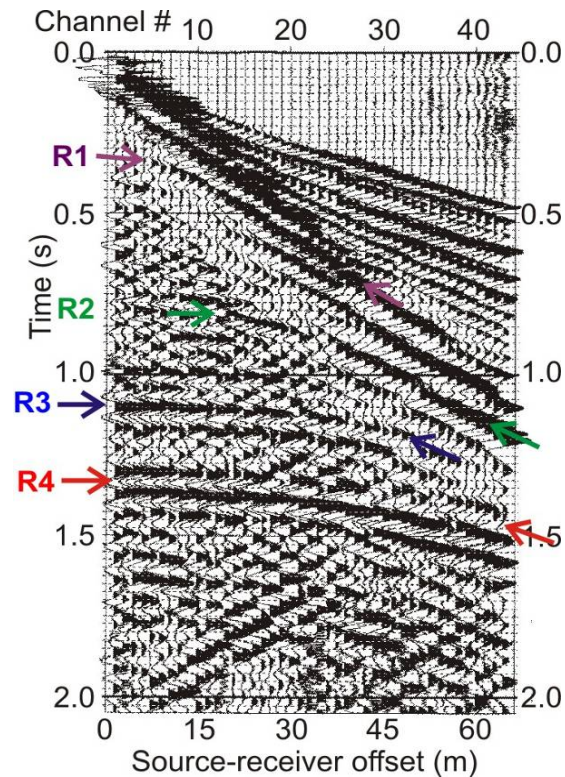


Figure 2.1.2-2. Example S-wave field record from the southern Fraser delta showing the hyperbolic nature of reflected arrivals (R1 to R4).  $X^2-T^2$  analysis of the arrival times from reflector 4 yields an average shear wave velocity of 155 m/s to this reflector and an estimated depth of ~100 m below ground surface ( $z=v*t/2$ ). These data were obtained using 8 Hz horizontal geophones and 3 stacks with the 7.3 kg hammer on a 15 kg I-beam.

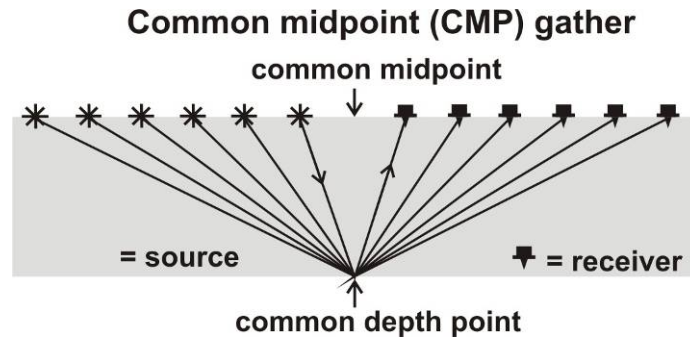


Figure 2.1.2-3. Schematic diagram showing the subsurface travel paths of 6 traces in a common midpoint gather which came from 6 different field records but will be processed together to produce 1 trace on the final seismic reflection section. The number of traces/cmp gather is referred to as the fold of the data (6-fold in this example).

### **Limitations**

Shallow reflection surveying depends on the detection of energy reflected from velocity and/or density discontinuities within the subsurface. The target of the survey must be large with respect to the wavelength of the seismic signal (where wavelength = velocity/frequency) to be successfully resolved. The ability to produce and record high-frequency energy depends on the ground conditions, the effectiveness of ground coupling for both receivers and source, the frequency and energy of the seismic source, source and receiver spacings, and the signal-to-noise (S/N) ratio of the recorded data. Noise sources include wind, traffic, and operating machinery. The quality of reflected events can also be compromised by interference with other types of seismic energy, including surface waves (ground roll) or airwaves.

Earth materials, and especially unconsolidated overburden materials, are strong attenuators of high-frequency energy. Thus, the ability of a particular site to transmit high-frequency energy is a major factor in determining the quality and the ultimate resolution of a shallow reflection survey. For P-wave surveys, velocity of unconsolidated materials is highly dependent on the degree of water saturation, and optimum conditions for reflection surveying are usually when the surface materials are fine-grained and water-saturated. Shear wave surveys are not sensitive to the presence of water. For the same frequency, because S-waves travel with lower velocities than P-waves, shear wavelengths are relatively short and resolution is often increased using S-wave techniques.

The quality of velocity estimates obtained from seismic reflection data depends on the signal-to-noise and frequency of the reflection data, the complexity of the subsurface structure, and the moveout (change in time of arrival across the array) of reflection events. In order for accurate velocities to be determined a reflection must be observed over a wide enough range of offsets that significant moveout can be measured. As moveout decreases with increasing depth (Fig. 2.1.2-2), the accuracy of velocity estimates also decreases with depth.

## **Data Collection**

### **Required Equipment**

In its most basic form, shallow seismic reflection surveying requires a seismograph, receivers or geophones, multi-channel cables to connect the array of receivers to the recording instrument, a seismic source and a highly accurate triggering unit to start the recording. Traditionally, individual geophones are manually planted in the ground and the survey progresses by continually picking up and transporting of cables and geophones along the line, recording data from a series of shot locations as the array is moved. This can be quite labour- and time-intensive. Landstreamers consist of towed arrays of geophones fixed on sleds and have been demonstrated to be an efficient means of recording reflection

data (e.g. Eiken et al., 1989; Van der Veen and Green, 1998; Van der Veen et al., 2001; Inazaki, 2004, Pugin et al., 2004).

The seismic source is an important factor in defining data quality, data acquisition rates and the costs of shallow seismic reflection surveys, and several controlled seismic source comparisons have been carried over the past two decades (Miller et al., 1992, 1994; Doll et al., 1998; van der Veen et al., 2000). Impulsive sources (e.g. sledge hammer, weight drops, shotgun sources, explosives) have traditionally been used for shallow seismic surveys. In comparison, vibrating sources are generally large, heavy and relatively expensive, but also non-destructive and highly repeatable, allow controlled input over a broad range of frequencies, and yield improved signal-to-noise ratios in many noisy environments (e.g. wind, traffic, etc.). Several efforts have been made over the last decade to design and build small and relatively inexpensive vibrators specifically for shallow seismic surveys (Ghose et al., 1998; Matsubara et al., 2002; Truskowski et al., 2004; Haines, 2006). Photos of a simple hammer source and a large vibrating source are shown in Figure 2.1.2-4.



Figure 2.1.2-4. Examples shear wave seismic sources. a) Sledgehammer hitting I-beam dug into the ground. b) Large vibrating source: IVI (Industrial Vehicles International, Inc) “Minivib” vibratory source.

### **Data Collection Procedures**

For site-specific reflection tests, a single array (12-, 24- or 48 channels) is laid out and data are acquired in the same manner as described above in the refraction write-up. Most shallow seismic reflection profiling data are collected and processed based on the common midpoint (CMP) method (often also referred to as the common-depth-point, or CDP, method) which is an adaptation of the methods used by the petroleum industry (Fig. 2.1.2-3). In CMP surveys, 12-, 24-, 48- (or more) channels of data are recorded for each shotpoint, usually with a consistent source-receiver geometry. Using the landstreamer, this is particularly easy – the source tows the receiver array, stopping at a regular interval to record data. For shallow reflection surveys, typical source spacings are on the order of a few metres while receiver spacings may range from sub-metre to metres.

### **Processing Techniques**

#### **Theory of Analysis**

Simple velocity and depth estimates can be made from individual seismic reflection records using the  $X^2-T^2$  method (assuming that the reflector is flat-lying and the reflection event is hyperbolic) (Fig. 2.1.2-2). There are several low-cost software programs that can be used for this purpose.

In contrast, producing a seismic reflection “section” or “profile” of equally spaced traces representing an image in two-way travel time of the ground beneath the survey line involves considerably more time and effort in processing. The aim of CMP technique is to improve the signal-to-noise ratio of reflection events by stacking many traces obtained with different source-receiver separations (Fig. 2.1.2-3). Reflection data are first sorted according to their common midpoints or common depth points, and each trace is corrected for offset (normal moveout, or NMO, corrections) according to a velocity-depth function determined from the data or from borehole information. A standard sequence of CMP data processing steps includes trace editing, static corrections, filtering, gain scaling, velocity analyses, normal moveout corrections and finally, stacking of the NMO-corrected traces in each CMP gather to create a single trace on the final section. Finally, corrections can be made to account for surface topography and the seismic section (in time) can be converted to depth using available velocity information. The processing of seismic reflection profiles requires fairly sophisticated software. The cost of reflection processing packages can vary considerably, from free open source code to packages costing many tens of thousands of dollars, depending on the complexity and features of the software.

### **Uncertainty Assessment**

The wavelength of the seismic energy recorded is the fundamental property affecting subsurface resolution and the uncertainty in velocity and depth estimates derived from reflection data. Wavelength is defined as the velocity of the material divided by the frequency of seismic energy. The best resolution is obtained in low velocity materials (soft soils). Under optimum conditions, seismic shear-wavelengths in near-surface (<30 m) soft soils may be less than 1 m; in general, equivalent compressional-wavelengths are on the order of several metres.

Secondly, the signal-to-noise ratio of the seismic data is a critical factor that must be considered in any uncertainty assessment. Uncertainty will always be significantly higher when dealing with noisy data. “Noise” can be cultural (e.g. traffic, machinery, etc), environmental (e.g. wind, rain etc) or geological (e.g. near-surface variations in material properties causing “statics”, rough or very steep reflecting horizons, etc).

Beyond these critical factors, the velocities and depths to reflectors determined from seismic reflection data are subject to uncertainties arising from (1) the picking of the time of arrival of reflected energy, (2) in the validity of the assumption of hyperbolic moveout across the receiver spread, and (3) phase shifts with offset. Arrival times will likely always be slightly overestimated (i.e. by picking peak or trough rather than exact onset) but careful picking or estimating the picking delay these uncertainties can be taken into account. The accuracy of a velocity estimate using the  $X^2-T^2$  method is strongly dependent of the “moveout” in arrival times measured across the receiver spread. Velocity estimates can be improved by using more receivers (improving definition of moveout) and longer spreads (producing greater moveout). The assumption of hyperbolic moveout is aided by the analysis of common midpoint gathers but interpreters must be aware of situations where this assumption may be violated (e.g. high-velocity surface layer). In general, estimates of velocity and depth to reflecting horizons will be less accurate as the target depths increase. Finally, as phase shifts in the reflected signal occur with changes in the source-receiver separation, this can result in errors in picking a consistent part of the reflection signal across the record which will then lead to errors in the velocity determination.

### **Recommended Guidelines for Reporting**

Archives of digital records must be supplemented by observer’s logs detailing all recording parameters, source characteristics, instrument used, line and environmental conditions. In addition, accurate records of source and receiver geometry, as well as elevation variations along the survey line are required. Example field record(s) should be included in any report to provide an indication of reflection data quality. The final processed section should be supplemented with information on the processing software used and details of the processing flow applied.

## Hazard-Related Case Studies

### Champlain Sea sediments in Eastern Canada

In areas of very soft soil (e.g. Champlain Sea sediments in Eastern Canada) we have had considerable success in acquiring excellent shear wave reflection data using only a lightweight (1 kg) hammer impacting a small triangular piece of wood (Hunter et al., 2002). This simple device is thought to preferentially transmit high frequency reflection energy because of the small mass of the hammer and plate. Figure 2.1.2-5a shows a 'split-spread' SH-polarized shear wave reflection record from a thick soft soil site in the Ottawa River valley using the light hammer/wood source. The receiver array consisted of 24 8-Hz horizontal geophones spaced 3 m apart, and records were acquired with the source in the centre of the array (as shown in upper panels of Figure 2.1.2-5) and at 3 and 30 m off each end of the array. The lower panels in Figure 2.1.2-5 are low fold CMP stacked reflection profiles obtained using all five field records showing the flat-lying nature of the subsurface reflectors. At this site similar P-wave reflection information was obtained using vertical geophones and a 12-gauge Buffalo gun seismic source (Fig. 2.1.2-5b). This is an example of simple test site data reflection data in both shear (SH-) and compressional (P-) mode being used to provide information on subsurface structure, including depth to major reflecting horizons.

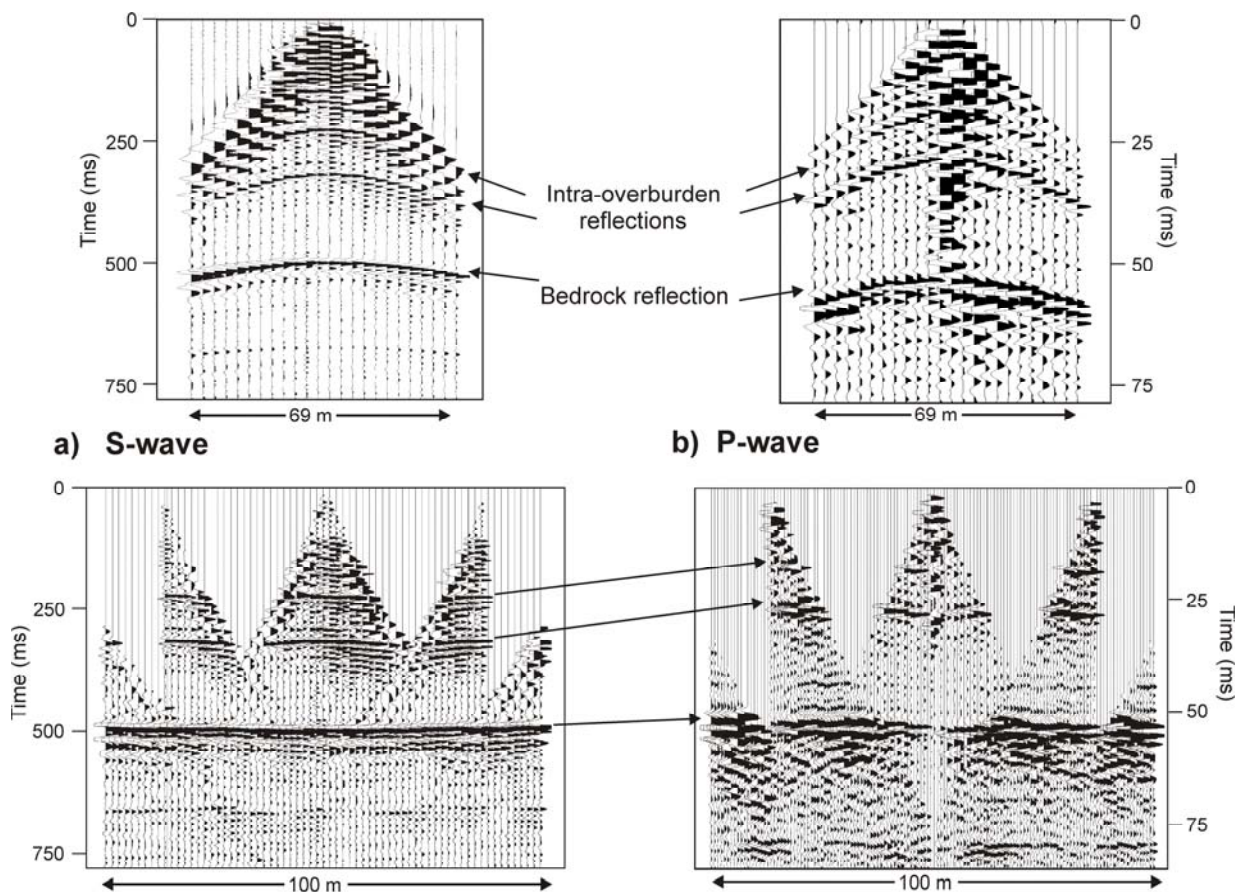


Figure 2.1.2-5: A high resolution SH and P wave reflection site in Holocene sediments of the Ottawa valley, Ontario. The upper panels show the centre shot field records; the lower panels are low fold CMP stacked reflection profiles obtained using all five field records obtained at the site. (a) High-resolution SH reflections obtained with a small 1 kg hammer and block of wood source. (b) P wave reflections obtained with a 12-gauge Buffalo gun source (from Hunter et al., 2002).

### Ottawa area microzonation study – reflection example

Between 2004 and 2008, the Geological Survey of Canada and Carleton University undertook a project to produce regional  $V_{s30}$  and fundamental site period maps of the Cities of Ottawa and Gatineau (Motazedian and Hunter, 2008; Hunter et al., 2010a,b, 2012). In the study area, thick deposits of Holocene-aged Champlain Sea sediments (“Leda Clays”) are known to overlie thin glacial deposits and bedrock. Throughout the city, 685 seismic reflection/refraction sites were occupied, producing thousands of traveltim records. These records were analysed to produce average traveltim-weighted shear wave velocity-depth profiles at each of the sites, from which a seismic site class could be assigned. Examples of refraction interpretation were included in Section 2.1.1; here we present an example of interpretation of reflection data.

At each site, a 24-channel array of 4.5-Hz horizontal axis geophones oriented in horizontal shear (SH) mode was laid out at either a 3 metre or 5 metre spacing. The seismic source consisted of a steel I-beam plate with one edge dug into the ground in SH orientation and a 10-lb hammer connected to a piezometric trigger system (Fig. 2.1.2-4a). Source points were chosen at 1 and 1½ geophone spacings off each end of the array, and one centre shot was taken between geophones 12 and 13. This configuration allowed for trace-to-trace correlation of wide angle reflections from the glacial or bedrock interface, while permitting sufficient source-geophone spacing to detect the bedrock refractor at depths up to 30 m.

In some parts of the City where the post-glacial sediments are very thick, the standard array geometry was unable to detect a bedrock refraction first arrival. In these cases, the glacial and/or bedrock reflection and intermediary reflections from within the overburden were used to produce the velocity-depth profile for the site (Figure 2.1.2-6). This is an example of surface test site reflection data being used to provide shear-wave velocity as a function of depth. See Williams et al. (1999, 2003b) and Harris and Street (1997) for additional examples of the application of these techniques. Williams et al. (2003a) showed that the velocity-depth profiles obtained using high-resolution seismic-reflection/refraction data compared well with near surface seismic-velocity downhole measurements.

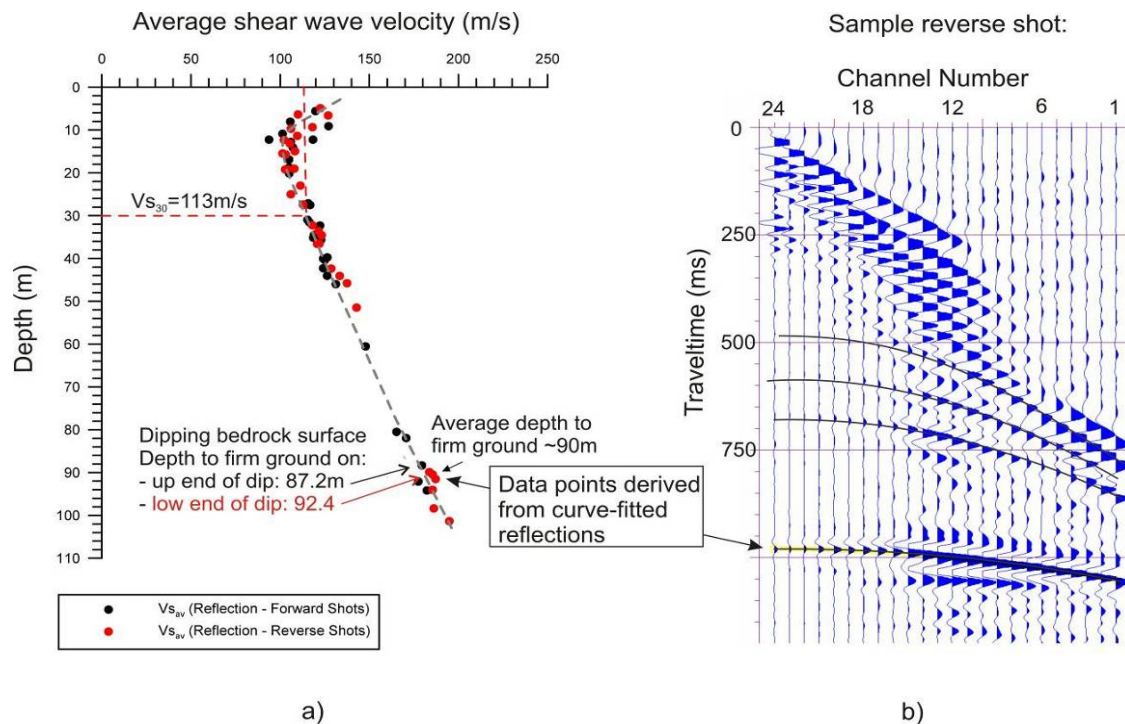


Figure 2.1.2-6: In the Ottawa area microzonation project, average velocity-depth profiles (a) are determined from several forward and reverse reflection records recorded at a site (b). Time-averaged shear wave velocities are derived from hyperbolic curves fit to the reflections using seismic processing software. The sample record shows a reverse shot from a deep (90m) bedrock site, with several intra-overburden reflectors.

### **Shear wave seismic profile – Fraser delta**

Regions underlain by thick deposits of unconsolidated sediments, such as the Fraser River delta in southwestern British Columbia, are known to experience greater levels of earthquake damage due to amplification of seismic waves. The delta's architecture, its location within the most seismically active region in Canada, and the rapid growth of communities situated on the delta have raised concerns about the area's seismic vulnerability. As part of a continuing effort to identify and help assess earthquake hazards of the Fraser delta, seismic reflection data were collected to image the subsurface structure of the delta (Pullan et al., 1989; Pullan and Hunter, 1987). The depth, shape and velocity contrast of the Holocene/Pleistocene boundary are important parameters for modeling ground motion amplification. The following section discusses the use of S-wave reflection profiling to investigate the structure of the Pleistocene surface and shows some example data. The locations for the reflection profiles collected as part of this study were chosen because of their proximity to boreholes that encountered Pleistocene sediments.

Four S-wave reflection profiles were shot beneath the Arthur Laing Bridge that connects Vancouver to Sea Island (location of the Vancouver International Airport). These data were recorded on a Geometrics S-24 using an array of 24 receivers (4.5 Hz horizontal geophones) at 3 m spacing. The source was a 4.5 kg hammer impacting a ribbed I-beam (provided by Frontier Geosciences) at an offset of 3 m from the receiver array. The Laing Bridge profiles are processed as 6-fold sections. Profile Laing 1, approximately 350 m in length is shown in Figure 2.1.2-7. The southeast end of this profile is adjacent to borehole 90-1, which encountered Pleistocene till at a depth of 35 m (Hunter, 1995). The top of Pleistocene interpreted on the reflection profiles correlates very well with the borehole shear-wave velocity data. The Pleistocene surface shows apparent dip ( $< 3$  degrees) to the northwest on this section.

Other examples of the use of shear wave reflection sections providing information on the depth to major acoustic impedance boundaries and near-surface faulting for earthquake studies can be found in Woolery et al. (1993, 1996), Woolery and Street (2002), and Wang et al. (2003).

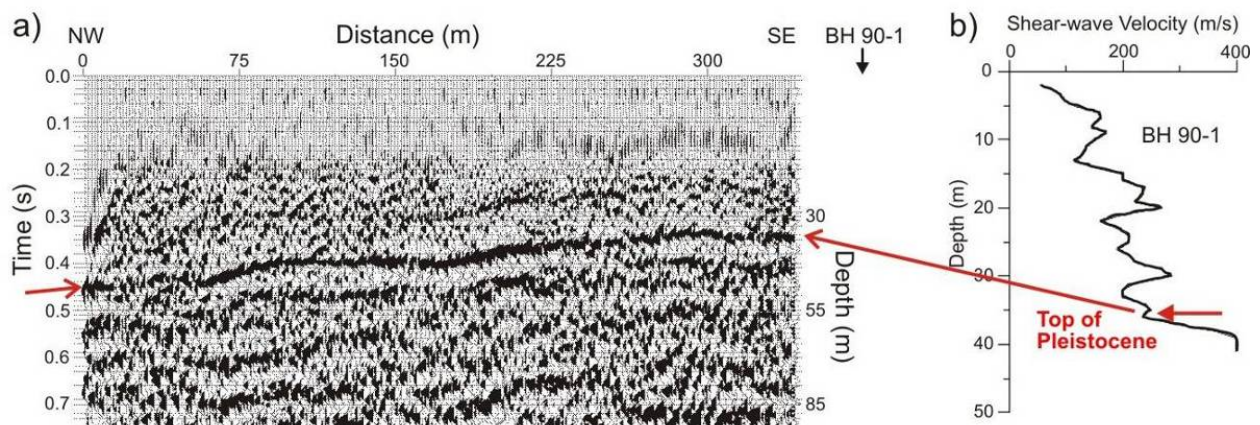


**Figure 2.1.2-7.** a) Shear-wave seismic reflection profile from the northern Fraser River delta (Laing 1) showing a strong reflection from the top of the Pleistocene surface. b) The velocity log from an adjacent borehole (90-1).

### **Shear wave seismic profiling using the minivib-landstreamer - Ottawa area**

The Geological Survey of Canada now routinely uses a vibrating source (e.g. the Industrial Vehicles International, Inc. minibuggy minivib source - <http://www.indvehicles.com> - and a landstreamer receiver array (Fig 2.1.2-8) to collect 3-component reflection data. The minivib source is a low-impact, vibrating seismic source which can be operated in both P- (vertical) and S- (horizontal) mode. The landstreamer can be fitted with either individual geophones or multi-component receiver arrays so that both P- and S-wave data can be collected at the same time (Pugin et al., 2009). With the vibrating source-landstreamer

data acquisition system, we are now able to routinely collect ~1000 multi-channel records/day. This is an improvement in data acquisition rates of many times over that possible with the traditional method of planted geophones. As well, use of a vibratory source means that the system can be used in urban settings as data are less susceptible to interference from traffic or wind noise.

Figure 2.1.2-9 shows an example shear wave reflection section obtained with this data acquisition system in the Orleans suburb of Ottawa (Hunter et al., 2007). This high-resolution section shows the Paleozoic bedrock surface just below ground surface at the south end of the line, then dropping abruptly in two steps to a depth of ~90 m at the base of the buried escarpment. The depth to bedrock has been confirmed by a near-by borehole. The bedrock surface is overlain by a thin (few metres) layer of glacial sediments (based on borehole logs and the high-amplitude reflection character) and a very thick Holocene (Champlain Sea deposits) marine sequence. This landstreamer section accurately delineates the southern portion of a significant buried bedrock valley. The thick soft soils in the valley are associated with significant ground motion amplification during earthquake events (Pugin et al., 2007). Careful velocity analyses of data such as these can provide detailed cross-sections of average and interval shear-wave velocity estimates (e.g. Pugin et al., 2010), and in some cases evidence of subsurface disturbance which is believed to have been caused by pre-historic earthquake shaking (Pugin et al., 2010).



Figure 2.1.2-8: Photo of the GSC Minivib/landstreamer system in operation, Ottawa area, 2010.

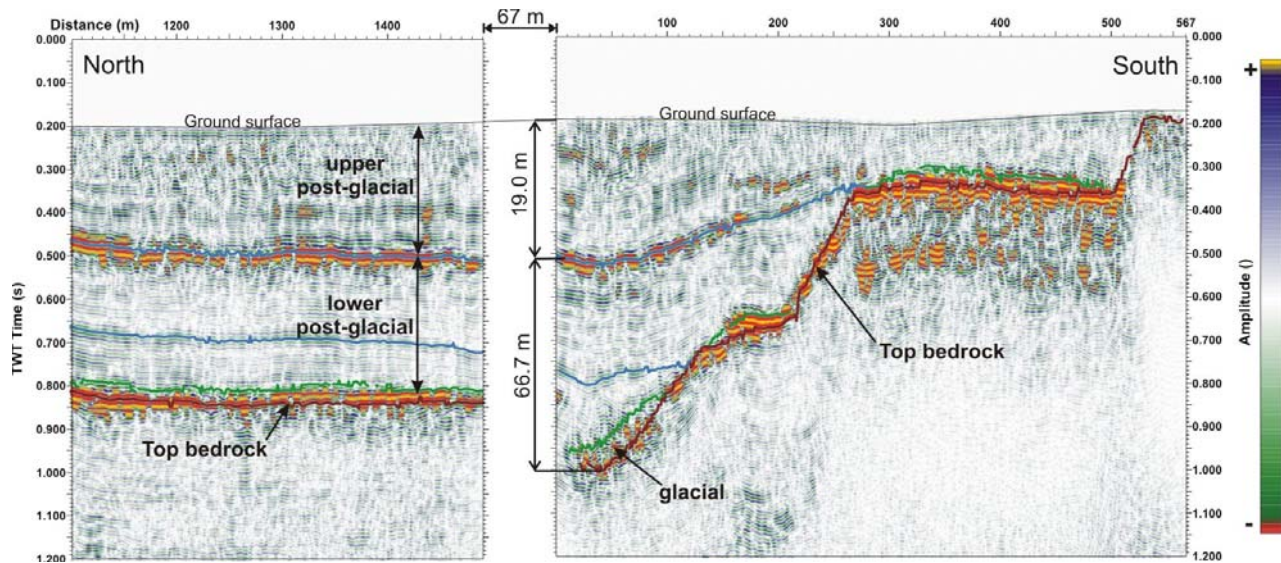


Figure 2.1.2-9: An interpreted high-resolution shear wave reflection section across a buried bedrock valley in Ottawa. The data were acquired along a busy paved urban street with a Mark I minivibe source and a towed landstreamer array consisting of 24 channels at 0.75 m spacing (from Hunter et al., 2007).

## Acknowledgments

The authors would like to acknowledge funding support from the Geological Survey of Canada (Natural Resources Canada) under the Public Safety Geoscience and Groundwater Geoscience Programs.

## References

- Benjumea, B., Hunter, J.A., Aylsworth, J.M. and Pullan S.E., 2003. Application of high-resolution seismic techniques in the evaluation of earthquake site response, Ottawa Valley, Canada. in *Contributions of High Resolution Geophysics to Understanding Neotectonic and Seismic Hazards*, (eds.) J. H. McBride and W. J. Stephenson; *Tectonophysics* (special issue), v. 368, p.193-209.
- Brabham, P.J., Thomas, J. and McDonald, R.J., 2005. The terrestrial shallow seismic reflection technique applied to the characterization and assessment of shallow sedimentary environments; *Quarterly Journal of Engineering Geology and Hydrogeology*, v. 38, p. 23-38.
- Brouwer, J. and Helbig, K., 1998. *Shallow high-resolution reflection seismics: Handbook of Geophysical Exploration*, (eds.) K. Helbig and S. Treitel; v. 19, Elsevier Science Ltd., Amsterdam, 391 p.
- Carr B. J., Hajnal Z. and Prugger A., 1998. Shear-wave studies in glacial till; *Geophysics* v. 63, p.1273-1284.
- Doll, W.E., Miller, R.D. and Xia, J., 1998. A noninvasive shallow seismic source comparison on the Oak Ridge Reservation, Tennessee; *Geophysics*, v. 63, p. 1318-1331.
- Doornenbal, J.C. and Helbig, K., 1983. High-resolution shallow seismics on a tidal flat in the Dutch Delta- acquisition, processing and interpretation; *First Break*, v.1, p. 9–20.
- Eiken, O., Degutsch, M., Riste, P. and Rød, K., 1989. Snowstreamer: an efficient tool in seismic acquisition; *First Break*, v. 7, p. 374-378.

- Ghose, R., Nijhof, V., Brouwer, J., Matsubara, Y., Kaida, Y. and Takahashi, T., 1998. Shallow to very shallow, high-resolution reflection seismic using a portable vibrator system; *Geophysics*, v. 63, p. 1295-1309.
- Harris, J.B., 2009. Hammer-impact, SH-wave seismic reflection methods in neotectonic investigations: General observations and case histories from the Mississippi Embayment, U.S.A; *Journal of Earth Science*, v. 20, p. 513-525.
- Harris, J.B., 2010. Application of shallow shear-wave seismic reflection methods in earthquake hazard studies; *The Leading Edge*, v. 29, p. 960-963.
- Harris, J.B. and Street, R.L., 1997. Seismic investigation of near-surface geological structure in the Paducah, Kentucky, area: Application to earthquake hazard evaluation; *Engineering Geology*, v. 46, p. 369-383.
- Haines, S.S., 2006. Design and application of an electromagnetic vibrator seismic source; *Journal of Environmental and Engineering Geophysics*, v. 11, p. 9-15.
- Helbig K. and Mesdag C. S., 1982. The potential of shear-wave observations; *Geophysical Prospecting* v. 30, p. 413-431.
- Hunter, J.A., 1995. Shear wave velocities of Holocene sediments, Fraser River delta, British Columbia; *Geological Survey of Canada, Current Research 1995-A*, p. 29-32.
- Hunter, J.A., Burns, R.A., Gagne, R.M., Good, R.L. and MacAulay, H.A., 1982. Mating the digital engineering seismograph with the small computer - some useful techniques; *in Current Research, Part B, Geological Survey of Canada, Paper 82-1B*, p. 131-139.
- Hunter, J.A., Pullan, S.E., Burns, R.A., Gagne, R.M. and Good, R.L., 1984. Shallow seismic reflection mapping of the overburden-bedrock interface with the engineering seismograph - some simple techniques; *Geophysics*, v. 49, p. 1381-1385.
- Hunter, J.A., Benjumea, B., Harris, J.B., Miller, R.D., Pullan, S.E., Burns, R.A. and Good R.L., 2002. Surface and downhole shear wave seismic methods for thick soils site investigations; *Soil Dynamics and Earthquake Engineering*, v. 22, p. 931-941.
- Hunter, J.A., Motazedian, D., Pugin, A.J.-M. and Khaheshi-Banab, K., 2007. Near surface geophysical techniques for mapping soft soil earthquake shaking response within the City of Ottawa, Canada., *Society of Exploration Geophysicists Annual Meeting, San Antonio, TX*, p. 1118-1122 (expanded abstract).
- Hunter, J.A., Crow, H., Brooks, G.R., Pyne, M., Lamontagne, M., Pugin, A.J.-M., Pullan, S.E., Cartwright, T., Douma, M., Burns, R.A., Good, R. L., Motazedian, D., Kaheshi-Banab, K., Caron, R., Kolaj, M., Folahan, I., Dixon, L., Dion, K., and Duxbury, A., 2010a. Seismic site classification and site period mapping in the Ottawa area using geophysical methods. *Geological Survey of Canada, Open File Report 6273*, 80 pages 1 DVD. <[ftp://ftp2.cits.mcan.gc.ca/pub/geott/ess\\_pubs/286/286323/of\\_6273.zip](ftp://ftp2.cits.mcan.gc.ca/pub/geott/ess_pubs/286/286323/of_6273.zip)> [accessed: Jan 2012]
- Hunter, J.A., Burns, R.A., Good, R.L., Pullan, S.E., Pugin, A.J.-M. and Crow, H., 2010b. Near-surface geophysical techniques for geohazard investigations: Some Canadian examples; *The Leading Edge*, v. 29, p. 936-947.

Hunter, J.A., Crow, H.L., Brooks, G.R., Pyne, M., Lamontagne, M., Pugin, A.J.-M., Pullan, S.E., Cartwright, T., Douma, M., Burns, R.A., Good, R.L., Motazedian, D., Kaheshi-Banab, K., Caron, R., Kolaj, M., Muir, D., Jones, A., Dixon, L., Plastow, G., Dion, K. and Duxbury, A., 2012. Ottawa-Gatineau seismic site classification map from combined geological/geophysical data; Geological Survey of Canada, Open File 7067, 1 sheet. < [ftp://ftp2.cits.mcan.gc.ca/pub/geoft/ess\\_pubs/291/291440/of\\_7067.pdf](ftp://ftp2.cits.mcan.gc.ca/pub/geoft/ess_pubs/291/291440/of_7067.pdf)> [accessed: Jul 2012]

Inazaki, T., 2004. High resolution reflection surveying at paved areas using S-wave type land streamer. *Exploration Geophysics*, v. 35, p. 1-6

Knapp, R.W. and Steeples, D.W., 1986a. High-resolution common-depth-point reflection profiling; instrumentation; *Geophysics*, v. 51, p. 276-282.

Knapp, R.W. and Steeples, D.W., 1986b. High-resolution common-depth-point reflection profiling, Field acquisition parameter design; *Geophysics*, v. 51, p. 283-294, *Geophysics*, v. 51, p. 1519 (Errata) and *Geophysics*, v. 51, 2011 (Discussion) and 2012 (Reply).

Matsubara, Y., Yamamoto, M., Nobuoka, D. and Kaida, Y., 2002. High-resolution shallow seismic reflection using a portable S-wave vibrator; Society of Exploration Geophysicists Annual Meeting; Expanded Technical Program Abstracts with Biographies, v. 21, p. 1618-1621.

Miller, R.D., Pullan, S.E., Steeples, D.W. and Hunter, J.A., 1992. Field comparison of shallow seismic sources near Chino, California; *Geophysics*, v. 57, p. 693-709.

Miller, R.D., Pullan, S.E., Steeples, D.W. and Hunter, J.A., 1994. Field comparison of shallow P-wave seismic sources near Houston, Texas; *Geophysics*, v. 59, p. 1713-1728.

Motazedian, D. and Hunter J.A., 2008. Development of an NEHRP map for the Orleans suburb of Ottawa, Ontario; *Canadian Geotechnical Journal*, v. 45, p. 1180-1188.

Pugin, A.J.-M., Larson, T.H., Sargent, S.L., McBride, J.H. and Bexfield, C.E., 2004. Near-surface mapping using SH-wave and P-wave seismic land-streamer data acquisition in Illinois, U.S; *Leading Edge (Tulsa, OK)*, v. 23, p. 677-682.

Pugin, A.J.-M., Sargent, S.L. and Hunt, L., 2006. SH and P-wave seismic reflection using landstreamers to map shallow features and porosity characteristics in Illinois; *in Proceedings, Symposium on the Application of Geophysics to Engineering and Environmental Problems*, Seattle, WA, Environmental and Engineering Geophysical Society, p. 1094-1109.

Pugin, A.J.-M., Hunter, J.A., Motazedian, D., Brooks, G.R. and Kaheshi-Banab, K., 2007. An application of shear wave reflection landstreamer technology to soil response of earthquake shaking in an urban area, Ottawa, Ontario; *in Proceedings, Symposium on the Application of Geophysics to Engineering and Environmental Problems*, Denver, CO, Environmental and Engineering Geophysical Society, p. 885-896.

Pugin, A.J.-M., Pullan, S.E. and Hunter, J.A., 2009. Multicomponent high-resolution seismic reflection profiling; *The Leading Edge*, v. 28, p. 1248-1261.

Pugin, A.J.-M., Pullan, S.E. and Hunter, J.A., 2010. Update on recent observations in multi-component seismic reflection profiling; *in Proceedings, Symposium on the Application of Geophysics to Environmental and Engineering Problems*, Keystone, CO, Environmental and Engineering Geophysical Society, p. 607-614.

Pullan, S.E., and Hunter, J.A., 1987. Application of the "optimum offset" shallow reflection technique in the Fraser delta, British Columbia; 57th Annual Meeting of the Society of Exploration Geophysicists, New Orleans, LA, p. 244-246.

- Pullan, S.E., Jol, H.M., Gagné, R.M. and Hunter, J.A., 1989. Compilation of high resolution "optimum offset" shallow seismic reflection profiles from the southern Fraser River delta, British Columbia; Geological Survey of Canada, Open File 1992.
- Pullan, S.E. and Hunter, J.A., 1999. Land-based shallow seismic methods; *in* A handbook of geophysical techniques for geomorphic and environmental research (Chapter 3), (ed.) Gilbert, R; Geological Survey of Canada, Open File 3731, p. 31-55.
- Rabbel, W., 2006. Seismic methods; *in* Groundwater Geophysics: A Tool for Hydrogeology, (ed.) Kirsch, R.; Springer Heidelberg, Germany, p. 23-83.
- Steeple, D.W., 1998. Special Issue: Shallow seismic reflection section – Introduction; *Geophysics*, v. 63, p. 1210-1212.
- Steeple, D.W., 2005. Shallow Seismic Methods; *in* HydroGeophysics, (ed.) Y. Rubin and S.S. Hubbard; Water Science and Technology Library, v. 50, p. 215-251.
- Steeple D.W. and Miller R.D., 1990. Seismic reflection methods applied to engineering, environmental and groundwater problems; *in* Geotechnical and Environmental Geophysics, v. 1, (ed.) S. A. Ward; Society of Exploration Geophysics, p. 1-29.
- Steeple D.W. and Miller R.D., 1998. Avoiding pitfalls in shallow seismic reflection surveys; *Geophysics*, v. 63, p. 1213–1224.
- Stumpel H., Kahler S., Meissner R. and Milkereit B., 1984. The use of seismic shear waves and compressional waves for lithological problems of shallow sediments; *Geophysical Prospecting*, v. 32, p. 662-675.
- Telford, W.M., Geldart, L.P. and Sherriff, R.E., 1995. *Applied Geophysics*; Cambridge University Press, New York, 770 p. (second edition).
- Truskowski, M., Warner, J., Clark, J. and Tisoncik, D., 2004. Fault and fracture system delineation of bedrock aquifer; *Society of Exploration Geophysicists*, v. 23, p. 1393-1396. (extended abstract)
- van der Veen, M. and Green, A.G., 1998. Landstreamer for shallow seismic data acquisition: Evaluation of gimbal-mounted geophones; *Geophysics*, v. 63, p. 1408-1413.
- van der Veen, M., Bunes, H.A., Bueker, F. and Green, A.G., 2000. Field comparison of high-frequency seismic sources for imaging shallow (10-250 m) structures; *Journal of Environmental and Engineering Geophysics*, v. 5, p. 39-56.
- van der Veen, M., Spitzer, R., Green, A.G. and Wild, P., 2001. Design and application of a towed landstreamer for cost-effective 2D and pseudo-3D shallow seismic data acquisition; *Geophysics*, v. 66, p. 482-500.
- Wang, Z., Madin, I.P. and Woolery, E.W., 2003. Shallow SH-wave seismic investigation of the Mt. Angel Fault, Northwest Oregon, USA; *in* Contributions of High Resolution Geophysics to Understanding Neotectonic and Seismic Hazards, (eds.) J. H. McBride and W. J. Stephenson; *Tectonophysics (special issue)*, v. 368, p. 105-117.
- Williams, R.A., Stephenson, W.J., Frankel, A.D. and Odum, J.K., 1999. Surface Seismic Measurements of Near-Surface P- and S-Wave Seismic Velocities at Earthquake Recording Stations, Seattle, Washington; *Earthquake Spectra*, v. 15, p. 565-584.

Williams, R.A., Stephenson W.J., Odum J.K. and Worley, D.M., 2003a. Comparison of P- and S-wave velocity profiles from surface seismic refraction/reflection and downhole data; *in* Contributions of High Resolution Geophysics to Understanding Neotectonic and Seismic Hazards, (ed.) J. H. McBride and W. J. Stephenson; Tectonophysics (special issue), v. 368, p. 71-88.

Williams, R.A., Wood, S., Stephenson, W.J., Odum, J.K. Meremonte, M.E., Street, R. and Worley, D.M., 2003b. Surface Seismic Refraction/Reflection Measurement Determinations of Potential Site Resonances and the Areal Uniformity of NEHRP Site Class D in Memphis, Tennessee; Earthquake Spectra, v. 19, p. 159-189.

Woolery, E.W., Street, R.L., Wang, Z. and Harris, J.B., 1993. Near-surface deformation in the New Madrid seismic zone as imaged by high resolution SH-wave seismic methods; Geophysical Research Letters, v. 20, p. 1615-1618.

Woolery, E.W., Wang, Z., Street, R.L. and Harris, J.B., 1996. A P- and SH-wave seismic reflection investigation of the Kentucky Bend Scarp in the New Madrid Seismic Zone; Seismological Research Letters, v. 67, p. 67-74.

Woolery, E.W. and Street, R.L., 2002. Quaternary fault reactivation in the Fluorspar Area Fault Complex of Western Kentucky: Evidence from shallow SH-wave reflection profiles; Seismological Research Letters, v. 73, p. 628-639.

## 2.2 Surface Waves

*Section Leader: Christopher Phillips  
Golder Associates Ltd., Mississauga, ON*

Surface wave methods measure variations in the propagation velocities of Rayleigh waves, with respect to frequency, to estimate the shear wave velocity profile at a site. The dispersive nature of Rayleigh waves is used to generate a dispersion curve, which is a plot of frequency versus Rayleigh wave velocity. This dispersion curve is then modeled using either forward or inverse modeling to obtain a Rayleigh wave velocity profile with depth. As Rayleigh wave velocity is very similar to shear wave velocity, and related through Poisson's ratio, the surface wave traveltime results can be used to obtain the shear wave velocity profile of the tested site. In this section, four articles discuss different surface wave methods and their application to hazard studies: 2.2.1 - Continuous Surface Wave (CSW) methods; 2.2.2 - Spectral Analysis of Surface Waves (SASW); 2.2.3 - Multichannel Analysis of Surface Waves (MASW); and 2.2.4 - Multimodal Analysis of Surface Waves (MMASW).

### 2.2.1 Continuous Surface Wave (CSW) Technique for Hazard Studies

*Ilmar Weemees & David Woeller,  
ConeTec Investigations Ltd, Vancouver, BC*

#### Introduction

##### Principles of the Method

The Continuous Surface Wave (CSW) technique is a surface wave testing method in which a frequency controlled vibrator generates continuous Rayleigh wave motion. In a homogeneous isotropic medium Rayleigh wave particle motion is retrograde elliptical, with the major axis of motion in the vertical direction (Sheriff and Geldart, 1982). The motion is measured on the ground surface with vertically oriented, low frequency geophones. Since the Rayleigh wave velocity is closely related to shear wave velocity, it is used as an indirect method of determining shear wave velocity. The bulk of the wave energy is limited to one wavelength in depth. In non-uniform media, Rayleigh waves are dispersive; hence the measurement of wave velocity at different frequencies (and wavelengths) will provide an indication of wave velocity versus depth. Waves of short wavelength travel along the ground surface to a shallow depth, while longer wavelengths are used to provide an indication of velocity from the surface to a greater depth.

##### Current State of Engineering Practice

An early application of CSW, referred to as the steady state technique, was made by Jones (1958). More recently the technique was improved by using a digitally controlled electromagnetic vibrator to generate surface waves recorded with two geophones (Tokimatsu et al., 1991). The current CSW technique specifies the use of a frequency controlled vibrator to generate steady state surface wave ground motion, and an array of geophones (usually 6) to record the surface wave motion (Menzies, 2001). The surface wave phase velocity is derived from the geophone records enabling the generation of a field dispersion curve, a plot of phase velocity versus wavelength. From the field dispersion curve forward modeling or direct inversion is used to derive the shear wave velocity profile that best fits the field measurements. Given that the testing surface required is relatively small, this technique is well suited for relatively shallow soil stiffness investigations.

##### **Recommended citation:**

Weemees, I. and Woeller, D., 2012. Continuous Surface Wave (CSW) Technique for Hazard Studies; *in* Shear Wave Velocity Measurement Guidelines for Canadian Seismic Site Characterization in Soil and Rock, (ed.) J.A. Hunter and H.L. Crow; Geological Survey of Canada, Open File 7078, p. 49-55.

### **Limitations**

The nature of the surface wave testing results in good velocity resolution at shallow depths, however resolution decreases with depth. Coupled with the fact that it is an indirect measure of shear wave velocity, the results will not be as detailed as an intrusive test.

The use of a portable vibratory source for the test does provide excellent control over the source frequency. With all vibratory sources, the energy delivered into the ground decreases substantially as the minimum rated frequency of the source is approached. To generate waves of very long wavelength to sample at depths required for the determination of  $V_{s30}$  requires an extremely large vibratory source that can deliver adequate energy in the range of 1 to 2 Hz. Most CSW portable systems have a minimum vibration frequency of 5 Hz.

Depth of investigation is limited by the energy delivered into the ground or by the velocity of the material being tested. For a uniform soil having a surface wave velocity of 150 m/s, using Equation 2.2.1-2 shows that the maximum wavelength that one could expect to generate at 5 Hz would be 30 m. This would roughly translate into a maximum depth of investigation of 10 metres based on Equation 2.2.1-3. In higher velocity material the depth of investigation will not be limited as much by the frequency of the vibrator; however in practice the typical depth limit using portable compact vibrators tends to be around 15 metres due to source energy limitations. As with all active source seismic tests, ambient noise can be a problem if it is being produced at the same frequencies that the active source is producing. The test can be limited by site geometry; generally the test should take place on level ground, and vertical discontinuities should be avoided as this will affect the propagation of the surface waves.

### **Data Collection**

#### **Required Equipment**

The most commonly used portable vibrator system produces surface waves with frequencies in the range 5 Hz to 600 Hz (Figure 2.2.1-1). A string of geophones of either 2 or 4.5 Hz resonant frequency are used to measure the vertical ground velocity generated by the source. A vibrator drive and control unit synchronizes data acquisition from the geophones and provides the sinusoidal output signals for the vibratory source.



Figure 2.2.1-1. CSW vibratory source.

### **Data Collection Procedures**

A row of six geophones is placed at equal spacing (typically ranging from 0.5 to 1.25m) on a line which is co-linear with the vibrator (Figure 2.2.1-2). The vibrator is stepped through an initial range of frequencies from 5 to 200 Hz such that surface waves over a wide wavelength range are generated. At each frequency the vibrator generates a steady state wave and the time domain data are collected and displayed for each geophone.

During the test, the time domain data are converted to the frequency domain so that the amplitude spectrum at each geophone can be assessed to ensure that it displays a clear spike at the vibrator frequency. The data are further processed to determine the phase velocity and the wavelength such that a dispersion curve, a plot of phase velocity versus wavelength, can be constructed during the test. After the initial set of measurements, additional data are collected at user selected frequencies such that the field dispersion curve can be completed with as few gaps as possible.

### **Processing Techniques**

#### **Theory of Analysis**

The signals received at the geophones are recorded digitally in the time domain and are then subjected to Fourier transform to convert the signals into the frequency domain. The frequency domain components are used to calculate the phase spectrum at each geophone. By using the phase data from the source frequency the phase is plotted versus the geophone distance. A linear regression analysis of the data determines the slope of the unwrapped phase versus distance plot (Figure 2.2.1-3). The regression analysis provides an indication of the quality of the data. The slope ( $d\phi/dx$ ) is then used to calculate the wavelength ( $\lambda$ ) at the source frequency ( $f$ ) in Equation 2.2.1-1, and then the Rayleigh wave phase velocity ( $V_R$ ) from Equation 2.2.1-2. The approximate depth ( $z$ ) sampled from a surface wave of a given wavelength can be estimated from Equation 2.2.1-3. Post processing the data entails checking that the phase is properly unwrapped, and that the regression analysis from each frequency provides a reasonable fit. Once vetted, the data are then used to establish the experimental dispersion curve.

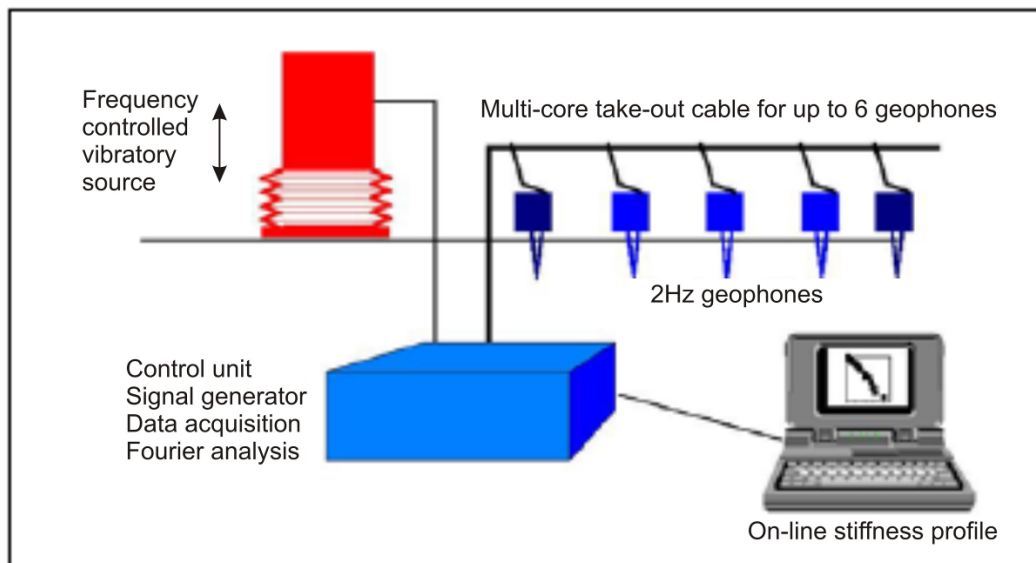


Figure 2.2.1-2. Schematic representation of the CSW test.

$$\lambda = \frac{360f}{\left(\frac{\partial\phi}{\partial x}\right)} \quad [2.2.1-1]$$

$$V_R = \lambda f \quad [2.2.1-2]$$

$$z = \frac{\lambda}{\text{scalingfactor}} \quad [2.2.1-3]$$

where  $f$  = source frequency,  $\lambda$  = wavelength,  $V_R$  = Rayleigh wave phase velocity, and  $z$  = depth.

The ratio between wavelength and depth (scaling factor) is commonly assumed to be between 2 to 3. For CSW testing, Menzies (2001) suggested using a scaling factor of 3. Equation 2.2.1-4 (Stokoe et al., 2004) provides a convenient approximation for shear wave velocity ( $V_s$ ) from Rayleigh wave velocity for a given Poisson's ratio ( $\nu$ ) in a homogeneous isotropic medium.

$$V_s \approx \frac{(1 + \nu)}{(0.874 + 1.117\nu)} V_R \quad [2.2.1-4]$$

The field dispersion curve can be quickly scaled using Equations 2.2.1-3 and 2.2.1-4 to provide a first estimate of shear wave velocity versus depth. However, a more rigorous solution based on modeling of the data using forward modeling or inversion techniques is preferred.

### **Uncertainty Assessment**

When producing the field dispersion curve, the quality of the data points can be assessed based on the goodness of the fit of the phase vs. distance plot for the geophones at each measured frequency. Once the data are collected there is usually an abundance of data at shallow depths and more sporadic data at greater depths, generally leading to more confidence in fitting the field dispersion curve at shallow depths.

For the field curve it must be recognized that the CSW method measures a composite dispersion curve that can be a combination of modes more (or other) than the assumed primary mode. This can lead to overestimations of shear wave velocity. Multiple modes are more prevalent in complex layer sequences.

The closeness of the fit of the theoretical dispersion curve compared to field dispersion curve provides an indication of the appropriateness of the model for the field data. When constructing the model, estimates of Poisson's ratio (or P wave velocity) and material density are required. Prior knowledge of the site geology can help in the selection of these parameters.

## **Recommended Guidelines for Reporting**

Reporting of the results must include a description of the recording equipment and survey layout, test coordinates, time of test, test identifier, field and theoretical dispersion curves, and the shear wave velocity tabular data and profile. Uncertainty in the results, as discussed above, must be addressed.

## **Hazard-Related Case Study**

### **CSW tests in Saanich, BC**

CSW testing was used to develop shear wave velocity profiles at a number of sites around the Greater Victoria region (Molnar et al., 2007). In their paper, the authors used shear wave velocity determinations from a number of sources to estimate site frequency (resonance) and then compared those values to

actual microtremor frequency response. Two CSW tests were conducted in Saanich, BC, in an area described as a drumlinoid ridge of dense Pleistocene materials. Non-intrusive CSW techniques were selected at this location because the material was not conducive to seismic cone penetration testing. To determine the most likely shear wave velocity profile, the program WinSASW (Joh, 1992) was used to generate theoretical dispersion curves that closely matched the field curve. The velocity model was perturbed until the theoretical curve closely matched the field curve (Figure 2.2.1-4a). The final shear wave velocity profile is shown in Figure 2.2.1-4b. The final layer is of indeterminate depth and is referred to as the half space. Given that the maximum wavelength measured was approximately 36 m, the depth of presented data was 12 m. The half space velocity of 450 m/s is in the expected range for till and preglacial overconsolidated sediments in the region. Calculating  $V_{s30}$  is done by using a travel time averaged velocity from the surface to a depth of 30 m. In this case the velocity of the final layer does not extend to a depth of 30m hence the velocity of the deepest measurement is assumed to carry down to 30m. This results in a  $V_{s30}$  value of 350 m/s, however it should be noted that the projection of traveltimes down to 30m is not the method outlined in the NBCC, and can result in an incorrect site class assignment.

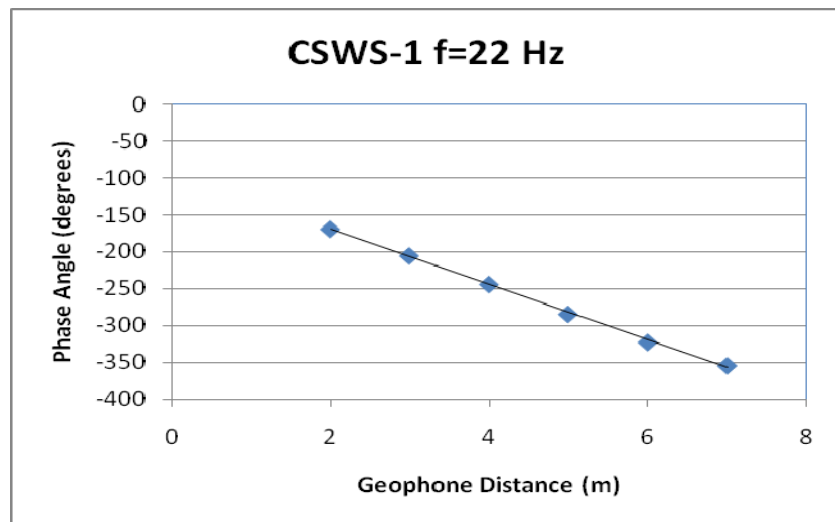


Figure 2.2.1-3. Phase versus geophone offset.

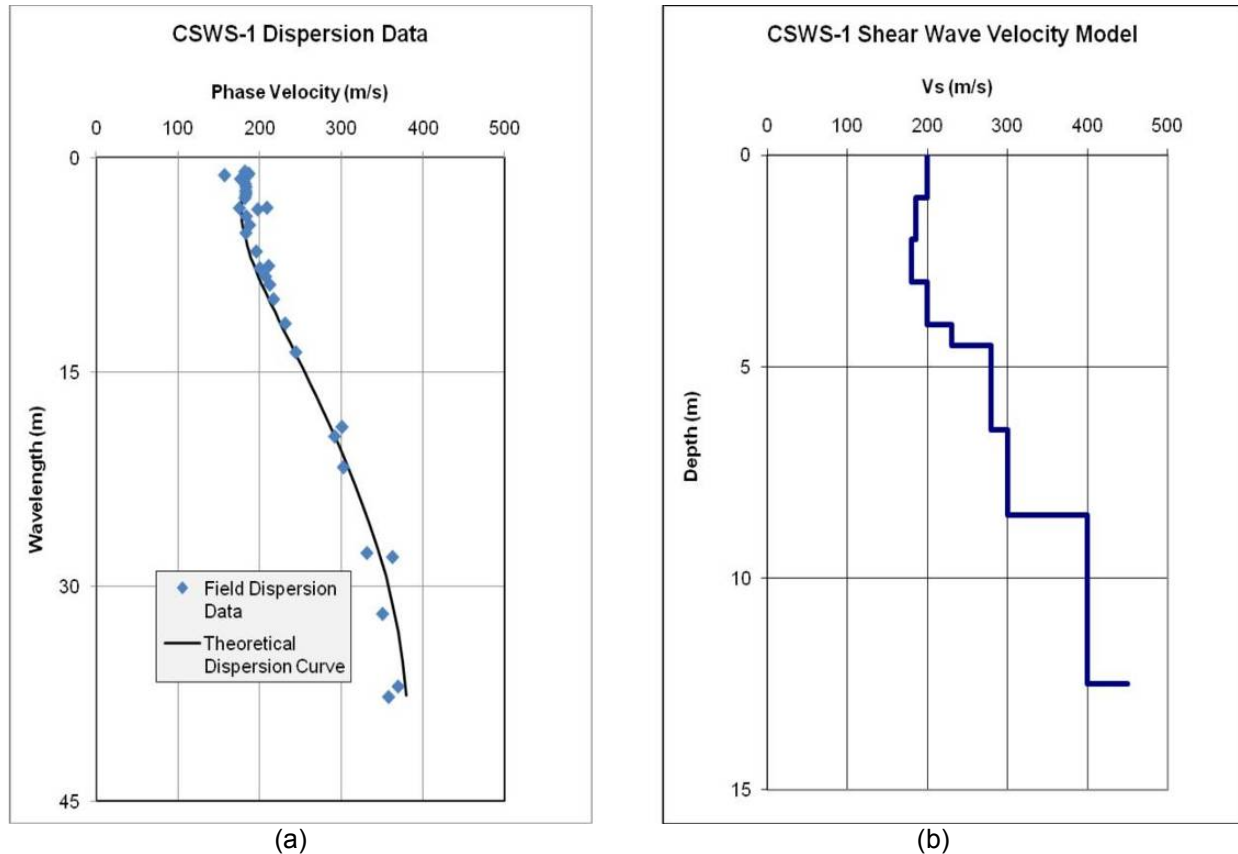


Figure 2.2.1-4. (a) Field dispersion and model dispersion curve. (b) Shear wave velocity model. The maximum wavelength measured was approximately 36 m, therefore, the depth of presented data is 12 metres.

## References

- Joh, S.H., 1992. User's guide to WinSASW, a program for data reduction and analysis of SASW measurements; The University of Texas at Austin.
- Jones, R., 1958. In situ measurement of the dynamic properties of soil by vibration methods; *Géotechnique*, v. 8, p. 1-21.
- Menzies, B.K., 2001. Near-surface site characterization by ground stiffness profiling using surface wave geophysics; *in* Instrumentation in Geotechnical Engineering, H.C.Verma Commemorative Volume, (eds.) K.R. Saxena and V.M. Sharma; Oxford & IBH Publishing Co. Pvt. Ltd., New Delhi, Calcutta, p. 43-71.
- Molnar, S., Cassidy, J.F., Monahan, P.A. and Dosso, S.E., 2007. Comparison of Geophysical Shear-Wave Velocity Methods; *in* 9<sup>th</sup> Canadian Conference on Earthquake Engineering, Ottawa, Ontario, Canada, BiTech Publishers Ltd, p. 390-400.
- Sheriff, R.E. and Geldart, L.P., 1982. Exploration seismology, vol 1: History, theory, & data acquisition; Cambridge Univ. Press, United Kingdom, 253p.

Stokoe, K.H., Joh, S.H. and Woods, R.D., 2004. Some Contributions on In Situ Geophysical Measurements to Solving Geotechnical Engineering Problems (Invited SOA Paper); *in* Proceedings, ISC-2 (2<sup>nd</sup> International Conference) on Geotechnical and Geophysical Site Characterization, September 19-22, 2004, Porto, Portugal, (eds.) V. da Fonseca, and P. W. Mayne; Millpress, Rotterdam, v. 1, p. 97-132.

Tokimatsu K., Kuwayama, S., Tamura, S. and Miyadera, Y., 1991. Vs determination from steady state Rayleigh wave method; *Soils and Foundations*, v. 31, p. 153-163.

### **Further Reading**

Lai, C.G. and Rix, G.J., 1998. Simultaneous Inversion of Rayleigh Phase Velocity and Attenuation for Near-Surface Site Characterization; Report No. GIT-CEE/GEO-98-2, School of Civil and Environmental Engineering, Georgia Institute of Technology, 258 pp.

## 2.2.2 Spectral Analysis of Surface Waves (SASW) Technique for Hazard Studies

*Ilmar Weemees & David Woeller,  
ConeTec Investigations Ltd, Vancouver, BC*

### Introduction

#### Principles of the Method

The Spectral Analysis of Surface Waves (SASW) test is a non-intrusive test that measures frequency dependant surface wave velocity to indirectly determine in-situ shear wave velocity. SASW testing is normally accomplished with mechanical sources that generate Rayleigh wave motion that is measured by two or more receivers. The size and energy delivered by the source governs the frequency content and the wavelength of the resulting waves, hence the range of investigation into the ground. The larger and more energetic is the source, the longer the wavelengths that are created and the greater the depth of investigation. For surface waves, the bulk of the wave energy is limited to one wavelength in depth. In non-uniform media, Rayleigh waves are dispersive; hence the measurement of wave velocity at different frequencies (and wavelengths) will provide an indication of wave velocity versus depth.

#### Current State of Engineering Practice

The use of SASW was introduced into the mainstream of geophysics for engineering applications by the University of Texas for pavement and soil shear wave velocity profiling (Stokoe and Nazarian, 1985). With large sources capable of generating energy down to 1 to 2 Hz and low frequency geophones, SASW is currently used for determining shear wave velocity for depths greater than 30 m.

#### Limitations

The frequency of the source will limit the depth of investigation. The types of impact sources used range from various sizes of sledge hammers to larger portable sources such as drop weights or accelerated masses. Using a bulldozer, such as the D8 CAT running back and forth over a small distance can allow depths of investigation from 30 to 60<sup>+</sup> m. Low frequency generating vibroseis units have the capability to profile to depths of 30 to 100<sup>+</sup> m (Stokoe et al., 2006).

Surface wave testing does not directly measure shear wave velocity. Modeling must be done to determine the most likely shear wave velocity profile based on the surface wave dispersion data. In surface wave testing it is recognized that in some circumstances, multiple modes of surface waves will be measured. These higher modes will appear as higher velocity data as compared to the fundamental mode. The SASW test is not able to discern between each of the modes, hence the test results are a combination of all surface wave modes. Surface wave testing velocity resolution decreases with depth. This should be kept in mind when modeling the data such that layered model does not imply more resolution than the technique is capable of, and that the possible contribution of higher modes to the field data should be recognized.

Site geometry can constrain the test. The testing should be done on level ground away from vertical discontinuities that will reflect waves that may cause erroneous results. The length of the testing area can be a limitation; it will be more than twice the target depth of the survey. For a 30 m target depth, the required length of the test line will be at least 60 m.

#### **Recommended citation:**

Weemees, I. and Woeller, D., 2012. Spectral Analysis of Surface Waves (SASW) Technique for Hazard Studies; *in* Shear Wave Velocity Measurement Guidelines for Canadian Seismic Site Characterization in Soil and Rock, (ed.) J.A. Hunter and H.L. Crow; Geological Survey of Canada, Open File 7078, p. 56-61.

## Data Collection

### Required Equipment

The sources usually used for shallow SASW are sledge hammer impacts, drop weights, or accelerated weight systems. For deeper testing heavy tracked equipment, such as a bulldozer, can be utilized, and are generally available in most areas.

Depending on the expected frequency content of the source the geophones used should have a low enough resonant frequency to respond to the ground motion. The geophones used should be calibrated and have near identical phase responses. Usually geophones with a resonant frequency of 1 or 2 Hertz are used for deeper testing, while higher frequency geophones or accelerometers can be used for shallow investigations. The recording system should collect and store time domain records, calculate and display amplitude and phase spectrum data during testing.

### Data Collection Procedures

The field setup involves two or more geophones with a centre point of that is maintained as the separation between the geophones is increased. The distance to the first receiver is usually equivalent to the anticipated depth of investigation. In a two-receiver set up, the source to first receiver and receiver spacing are usually kept equal (Figure 2.2.2-1). The distance from the source to the first receiver is referred to as the near offset ( $d$ ), and this distance is chosen according to Equation 2.2.2-1 to ensure that the Rayleigh wave is well developed before reaching the first receiver (Stokoe et al., 1994). Using the same value for the receiver separation allows for accurate determination of the phase difference compared to a small geophone separation, although a smaller separation will still give adequate results. Tokimatsu et al. (1991) recommended a minimum acceptable geophone separation as being  $1/16^{\text{th}}$  the maximum wavelength being measured.

$$d > \frac{\lambda_{\max}}{2} \quad [2.2.2-1]$$

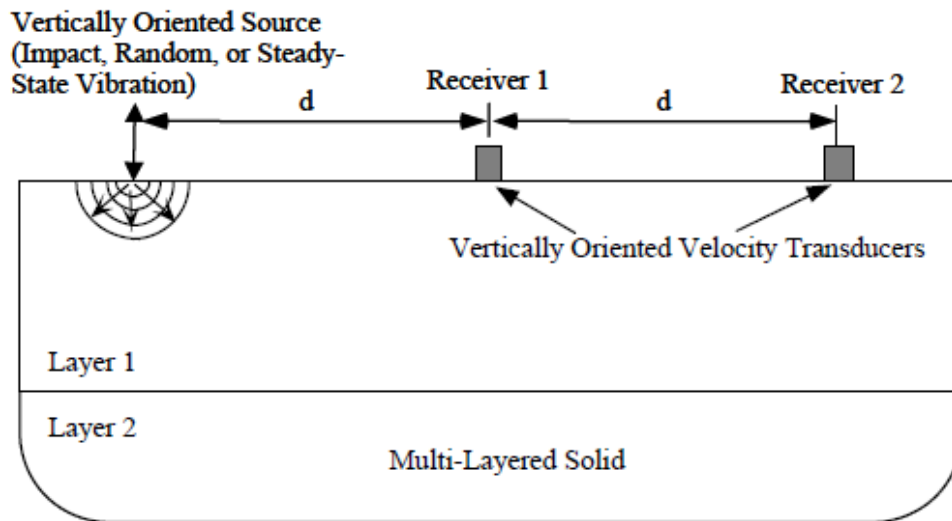


Figure 2.2.2-1. SASW two receiver test setup developed by Stokoe.

The near offset used is a function of the stiffness of the material and the depth of investigation. Typically the test begins with the use of a hammer source at small distances to establish the velocity of the short wavelength waves that travel along the near surface. Values of  $d$  used with a sledge hammer range from 1 to 6 metres. Once it is found that the signal from the hammer source can no longer generate the required wavelengths, larger sources are used. For a large source such as a bulldozer (Figure 2.2.2-2),

the near offset can start at 15 metres, and subsequently be increased in 15 metre increments. The final spacing used will tend to vary depending on the site conditions. The test is completed once adequate data have been collected over a range of wavelengths that cover the near surface to the target, or maximum attainable depth. The maximum depth of investigation is in the range of the maximum wavelength measured ( $\lambda_{max}$ ) divided by 2 to 3 (Andrus et al., 1998), hence a  $d$  value of 60 m would correspond to a maximum depth of investigation of 40 to 60 m.



When using 1 and 2 Hz geophones in a cylindrical case (Figure 2.2.2-3), the weight of the geophones alone is adequate for coupling the receivers to the ground. The geophones must be level and set flush to the ground surface. In some situations removing the top few centimetres of loose or organic material is necessary. Smaller, higher frequency geophones usually have spiked cases that are pressed into the ground, which can present a problem in very hard or frozen soils.

During testing, the time domain records are converted to the frequency domain and a net phase spectrum plot is generated. By stacking the data in the frequency domain the improvement to the quality of the phase data can be observed during testing. Testing at one spacing continues until the quality of the phase data remain relatively unchanged. For a sledge hammer source this is usually about 5 to 10 records, while for a source such as a bulldozer that has a low signal to noise ratio, around 20 or more records may be required. Once a spacing is complete, the phase difference data should be converted to dispersion curve points and added to the composite test location dispersion curve. The testing should be done at a number of spacings such that a complete, relatively gap free site experimental dispersion curve can be created.

Figure 2.2.2-2. SASW Testing using a bulldozer source.



Figure 2.2.2-3. SASW receiver (1 Hz geophone).

## Processing Techniques

### Theory of Analysis

The time domain data from each geophone is converted to the frequency domain to examine signal content and to calculate the phase difference,  $d\phi$ , given a distance  $x$  between a pair of geophones. The phase difference is used to calculate the wavelength ( $\lambda$ , Equation 2.2.2-2) and Rayleigh wave phase velocity ( $V_R$ , Equation 2.2.2-3) at each frequency ( $f$ ).

$$\lambda = \frac{2\pi x}{\partial\phi} \quad [2.2.2-2]$$

$$V_R = \lambda f \quad [2.2.2-3]$$

By calculating the velocity and frequency points for data in which there is sufficient amplitude and quality, a dispersion curve (a plot of phase velocity versus wavelength) is produced from the testing. A layered soil model is developed that generates the theoretical dispersion curve that best matches the field dispersion curve. Each layer in the soil model is described by its shear wave velocity, Poisson's ratio, density, and thickness.

### Uncertainty Analysis

The points in the dispersion curve are calculated from the phase of the cross spectrum. The quality of the cross spectrum data can be assessed from the coherence and power spectrum. Points used for the dispersion curve with high coherence and adequate power should produce a good quality dispersion curve.

The dispersion curve produced by SASW testing is an apparent dispersion curve that is a combination of all modes present. As such it can lead to higher apparent velocities in complex layer sequences. For this reason modeling using a 3D solution that takes into account all modes of surface and body wave motion should be used (Stokoe et al., 2004).

The closeness of the fit of the theoretical dispersion curve compared to field dispersion curve provides an indication of the appropriateness of the model for the field data. When constructing the model, estimates of Poisson's ratio (or P wave velocity) and material density are required. A detailed discussion of the effect of Poisson's ratio can be found in Karray and Lefebvre (2008). Prior knowledge of the site geology can help in the selection of these parameters. Comparisons of SASW results with intrusive shear wave velocity methods show good agreement (Joh, 1996; Stokoe et al., 2004).

## Recommended Guidelines for Reporting

Reporting of the results must include a description of the recording equipment and survey layout, including the test midpoint and boundaries of the test line. The test date and time, along with a unique identifier for the test name for the project should be noted. Test spacing should be noted along with the maximum wavelength measured. The final product should be a shear wave profile presented in tabular and graphical form for each location.

## Hazard-Related Case Study

### SASW test in British Columbia

A number of SASW tests were performed at a site in British Columbia to carry out a seismic site classification and assist in a risk assessment. A non-intrusive method was chosen for the testing as the surficial geology of the area was not conducive to cone pushing, being composed of alluvial sand and

gravel outwash deposits overlying glacial marine clay and glacial till. The water table was 3.6 m below ground level. The SASW test was carried out with a D8 CAT as the primary surface wave source. The maximum recorded wavelength was 65 metres, which would result in a maximum depth of investigation in the range of 33 metres based on the assumption that the depth is equivalent to the wavelength divided by two. Modeling using the data from this location provided the shear wave velocity profile shown in Figure 2.2.2-4. The velocity of the material in the first 15 metres is consistent with compact sand and gravel, while below 15m the modeled velocity would indicate glacial till. Converting the velocities to equivalent travel times in each layer led to a calculation of the travel time weighted velocity in the first 30 metres ( $V_{s30}$ ). The calculated  $V_{s30}$  was 362m/s, resulting in a class C NBCC 2010 seismic site classification.

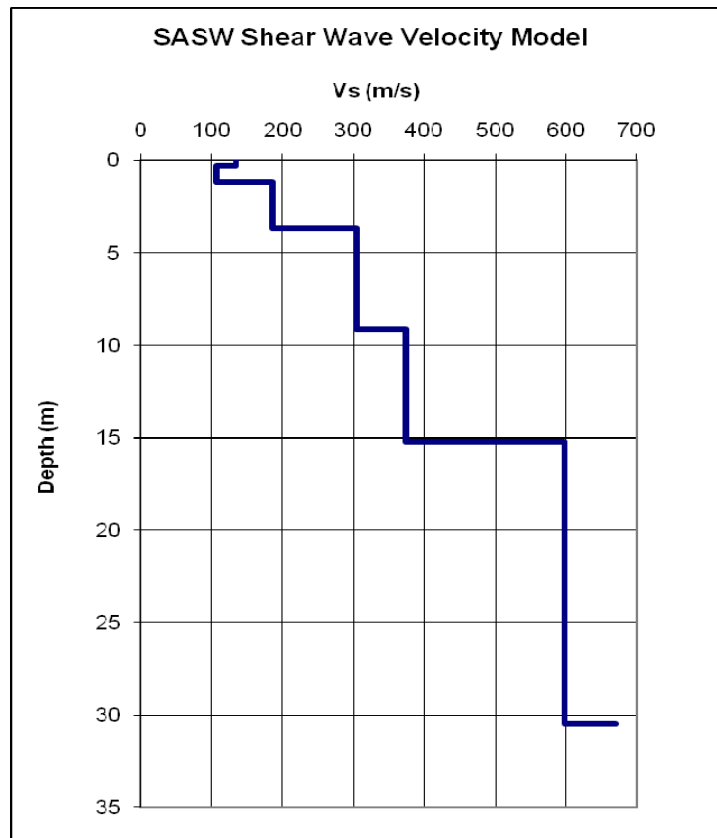


Figure 2.2.2-4. SASW Shear wave velocity profile.

## References

Andrus, R.D., Chung, R.M., Stokoe, K.H. and Bay, J.A., 1998. Delineation of densified sand at Treasure Island by SASW testing; *in* Proceedings, 1st International Conference on Site Characterization (ISC'98), Atlanta, GA., (eds.) P. K. Robertson and P. W. Mayne; Balkema, Rotterdam, v. 1, p.459-464.

Joh, S.H., 1996. Advances in interpretation and analysis techniques for spectral-analysis-of-surface-waves (SASW) measurements; Ph.D. thesis, University of Texas at Austin.

Karray, M. and Lefebvre, G., 2008. Significance and evaluation of Poisson's ratio in Rayleigh wave testing; Canadian Geotechnical Journal, v. 45, p. 624-635.

Stokoe, K.H. and Nazarian, S., 1985. Use of Rayleigh waves in liquefaction studies; *in* Measurement and Use of Shear Wave Velocity for Evaluating Dynamic Soil Properties, (ed.) R.D. Woods; A.S.C.E., New York, p.1-17

Stokoe, K.H., Wright, S.G., Bay, J.A. and Roesset, J.M., 1994. Characterization of geotechnical sites by SASW method; *in* Geophysical Characteristics of Sites, ISSMFE, Technical Committee 10 for XIII ICSMFE, Balkema Publishers, Netherlands, p. 785-816.

Stokoe, K.H., Joh, S.H. and Woods, R.D., 2004. Some Contributions of In Situ Geophysical Measurements to Solving Geotechnical Engineering Problems; *in* Proceedings, ISC-2 on Geotechnical and Geophysical Site Characterization, Porto, Portugal, (ed.) V. da Fonseca and P.W. Mayne; Millpress, Rotterdam, v. 1, p. 97-132.

Stokoe, K.H., Cox, B.R., Lin, Y.-C., Jung, M.J., Menq, F.-Y., Bay, J.A., Rosenblad, B. and Wong, I., 2006. Use of Intermediate to Large Vibrators as Surface Wave Sources to Evaluate Vs Profiles for Earthquake Studies; *in* Proceedings, 19th Symposium on the Application of Geophysics to Engineering and Environmental Problems (SAGEEP), Seattle, WA., p. 1241-1258.

Tokimatsu K., Kuwayama, S., Tamura, S. and Miyadera, Y., 1991. Vs determination from steady state Rayleigh wave method; *Soils and Foundations*; v. 31, p. 153-163.

## 2.2.3 Multichannel Analysis of Surface Waves (MASW) Technique for Hazard Studies

*Christopher Phillips and Stephane Sol  
Golder Associates Ltd., Mississauga, ON*

### Introduction

#### Principles of the Method

The multichannel analysis of surface waves technique, also referred to as MASW, is a method commonly used to indirectly measure the shear velocity profile of a site. MASW testing measures the velocity of Rayleigh waves, a surface wave with a depth of investigation proportional to the wavelength. By measuring the velocity of Rayleigh waves of increasing wavelengths along the ground surface, a shear wave velocity profile with depth can be determined using either forward modeling or inversion software. MASW testing is based on the same physical principles as the CWS and SASW testing methods. It differs in that it uses multiple geophones and is therefore able to use advanced processing methods to estimate Rayleigh wave velocity, compared to the CWS and SASW methods.

#### Current State of Engineering Practice

The MASW method was first proposed in the late 1990's (Park et al., 1998, 1999) as an extension of the SASW testing method. The MASW method was developed to take advantage of the multichannel capabilities of modern seismograph equipment to reduce testing time compared to SASW testing and to take advantage of advanced methods to generate a dispersion curve, a plot of Rayleigh wave velocity versus frequency (or wavelength) which is necessary to generate an accurate shear wave velocity profile. Since its introduction, there has been a lot of research into the effects of different seismic sources, source offset from the geophone array, geophone spacing, dispersion curve generation, and inversion techniques. There is currently no single standard describing the equipment and methodology of the MASW technique.

#### Limitations

The MASW method relies on the fundamental assumption that the medium being tested is laterally homogeneous. MASW, for example, is not applicable in an area where depth to bedrock is fluctuating across the site, or where there are lateral changes in overburden materials. MASW testing should be done on level ground, as significant changes in topography along a survey line affect the nature of propagation of the surface waves along the line.

Higher mode surface waves are generated in a layered earth and can have very strong energy, particularly in cases where there is a velocity reversal (higher velocity layer overlying lower velocity layer), such as an area which has been paved or has concrete present or where there is frost or frozen ground present in the near surface materials. The presence of higher mode surface waves can complicate the interpretation of the dispersion curve, and result in an erroneous shear wave velocity profile. In these cases other techniques, such as downhole shear wave testing, would be more appropriate.

#### **Recommended citation:**

Phillips, C. and Sol, S., 2012. Multichannel Analysis of Surface Waves (MASW) Technique for Hazard Studies; *in* Shear Wave Velocity Measurement Guidelines for Canadian Seismic Site Characterization in Soil and Rock, (ed.) J.A. Hunter and H.L. Crow; Geological Survey of Canada, Open File 7078, p. 62-66.

There are a few common geological settings where obtaining accurate shear wave velocity profiles to 30 metres depth using the MASW technique can be difficult. One case is where soft near-surface materials ( $V_s < 200$  m/s) are present in great thicknesses. In this case, MASW testing requires low frequency surface waves (less than 2 Hz) to image to 30 metres depth. However, generation and measurement of such low frequencies can be difficult with conventional MASW testing equipment.

Another example is where bedrock is present very close to the ground surface. In this case, using conventional MASW processing methods can significantly underestimate the shear wave velocity of the bedrock. In order to properly estimate the  $V_s$  in the bedrock, very long Rayleigh wave wavelengths (up to 400 metres) must be resolved (Casto et al., 2009). However, most conventional MASW setups are only able to resolve Rayleigh wave wavelengths typically up to 180 metres long.

## Data Collection

### Required Equipment

An array of 24 low frequency vertical geophones (e.g. 4.5 Hz) is recommended, along with a seismic cable, seismograph, laptop computer, seismic source and trigger wire. For near surface testing, within approximately 10 metres of ground surface, a 16-lb sledgehammer striking a metal plate is generally an adequate seismic source. To survey to greater depths a higher energy source, such a weight drop or accelerated weight drop or a controlled vibrating source can be used. In some cases ambient noise, such as traffic, construction noise, or microtremors are employed to survey to extend depth of investigation to greater than 60 metres.

### Data Collection Procedures

Selection of seismic source and geophone spacing is based on anticipated depth of investigation and velocity-depth distribution. For deep bedrock sites where anticipated depth of investigation is in the range of 30 metres, a geophone separation of 2 to 3 metres is generally adequate. The seismic source is located off the end, and co-linear, to the geophone array. Photos of an MASW setup are presented in Figure 2.2.3-1.



Figure 2.2.3-1: Typical setup of an MASW survey line in the field. Left side shows a seismic weight drop used as the source. Right side shows a series of geophones planted in the ground at regular spacings, and measurements are recorded with a seismograph attached to a laptop.

Offset of the seismic source is dependent on the soil type, but a generally accepted axiom is that the source offset should be equal to or greater than the desired depth of investigation (Park et al., 1999). This is because Rayleigh waves can only be considered to be horizontally travelling plane waves after they've propagated a certain distance. In practice several source offsets are usually collected, as the influence of higher mode surface waves can be reduced with different source offsets.

Data are collected with a sufficient time window to capture the entire surface wave train. The sample rate of the collected data needs to be sufficient to resolve the highest frequency desired to be interpreted, which is controlled by the Nyquist frequency, where the maximum resolvable frequency,  $f$ , is defined as

$$f = \frac{1}{2t} \quad [2.2.3-1]$$

where  $t$  is the sample rate of the seismic record.

If a trigger is used for the seismic source, data can be stacked to increase signal-to-noise, however even small errors in triggering times can lead to poor data quality so this practice is not commonly employed.

## Processing Techniques

### Theory of Analysis

The collected MASW data are first processed to remove any bad records, such as a geophone with poor response. Data can also be time filtered to remove any spurious noise on the seismic records at times before or after the source energy, to reduce their effect on the calculated phase velocities. The data are then processed in the frequency domain through analysis of the phase spectrum. There are two common methods to generate a dispersion curve, through swept-sine filtering (Park et al., 1999) or through frequency-wavenumber plots (Foti, 2000). The interpreted fundamental mode Rayleigh wave dispersion curve is picked based on either of these representations of the data which is then modeled to obtain a shear wave velocity profile of the ground, based either on forward or inverse modeling methods.

### Uncertainty Analysis

The dispersion curve produced by MASW testing can be calculated by several different methods, as discussed in the section above. However, it still requires manual interpretation to identify the fundamental mode dispersion curve. The dispersion curve plots provide the data processor with a measure of quality based on the strength and shape of the fundamental mode with respect to frequency.

Similar to the SASW method, the measured fitness of the theoretical dispersion curve compared to field dispersion curve provides an indication of the appropriateness of the model for the field data. When constructing the model, estimates of Poisson's ratio (or P wave velocity) and material density are required. Prior knowledge of the site geology can help in the selection of these parameters and to verify the MASW model results.

## Recommended Guidelines for Reporting

An MASW report should summarize the testing methodology, field procedures (including source type, geophone spacing, source offset, and sampling rate), and processing steps, including a discussion of the assumptions used in the inversion of the data. The report must also include sample seismic records collected at the site, dispersion curve picks, shear-wave velocity depth profiles, and a comparison of field vs. modeled data.

## Hazard-Related Case Studies

### MASW Tests in Southern Ontario

Two examples of MASW surveys, conducted by Golder Associates for the purpose of seismic site classification as required by the 2010 National Building Code of Canada (NBCC), are presented below. In both examples, MASW data were collected using a 24-channel seismograph and 4.5 Hz geophones, with a geophone spacing of 3 metres. A 45-kg weight drop was used as the seismic source, and was positioned at several offsets from the geophone array. The record length was adjusted to ensure the entire wave train was collected for each seismic record.

The first site was underlain by several hundred of metres of sediment. The source distance was 10m from the end of the geophone array. The resulting shear-wave velocity model indicated variations in shear-wave velocity within the overburden ranging from 150 to 500 m/s to an interpreted depth of 30 metres below ground surface (Figure 2.2.3-2). In this investigation, the NBCC  $V_{s30}$  was calculated to be 296 m/s, or a site class D (stiff soil).

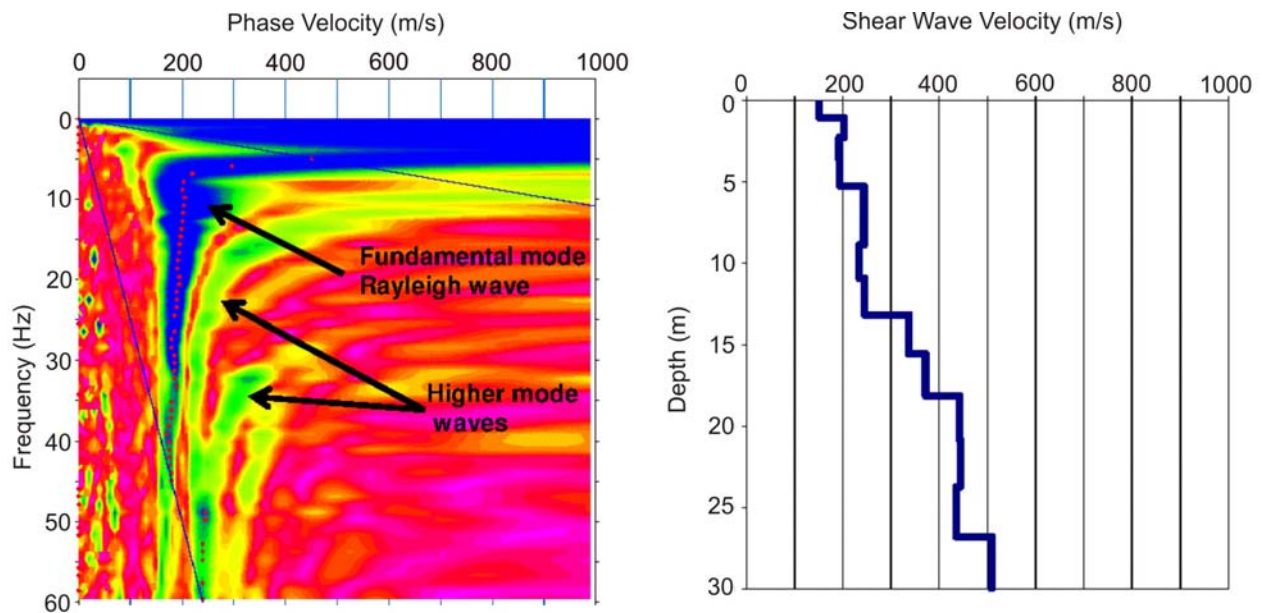


Figure 2.2.3-2: Field data example of a dispersion curve with identification of the fundamental mode (red dots) and the presence of higher modes (left) and resulting shear wave velocity profile (right).

The second site consisted of approximately 11 metres of silty clay on top of limestone bedrock. The source distance was 5m from the end of the geophone array. The resulting shear wave velocity model indicated the presence of a thin, low velocity layer near surface underlain by approximately 9 metres of sediments with a consistent shear wave velocity of approximately 500 m/s. Below 11 metres the shear wave velocity model indicates variations in  $V_s$  within the bedrock ranging from 1,100 to 1,700 m/s. This change in bedrock  $V_s$  is interpreted to indicate a change from weathered to fresh limestone bedrock (Figure 2.2.3-3). In the case of this investigation the NBCC  $V_{s30}$  was calculated to be 770 m/s, or a site class B (Rock) based on the shear wave velocity – however since there is more than 3 metres of overburden present above the rock the highest site class this site could be awarded is a site class C (Very Dense Soil and Soft Rock).

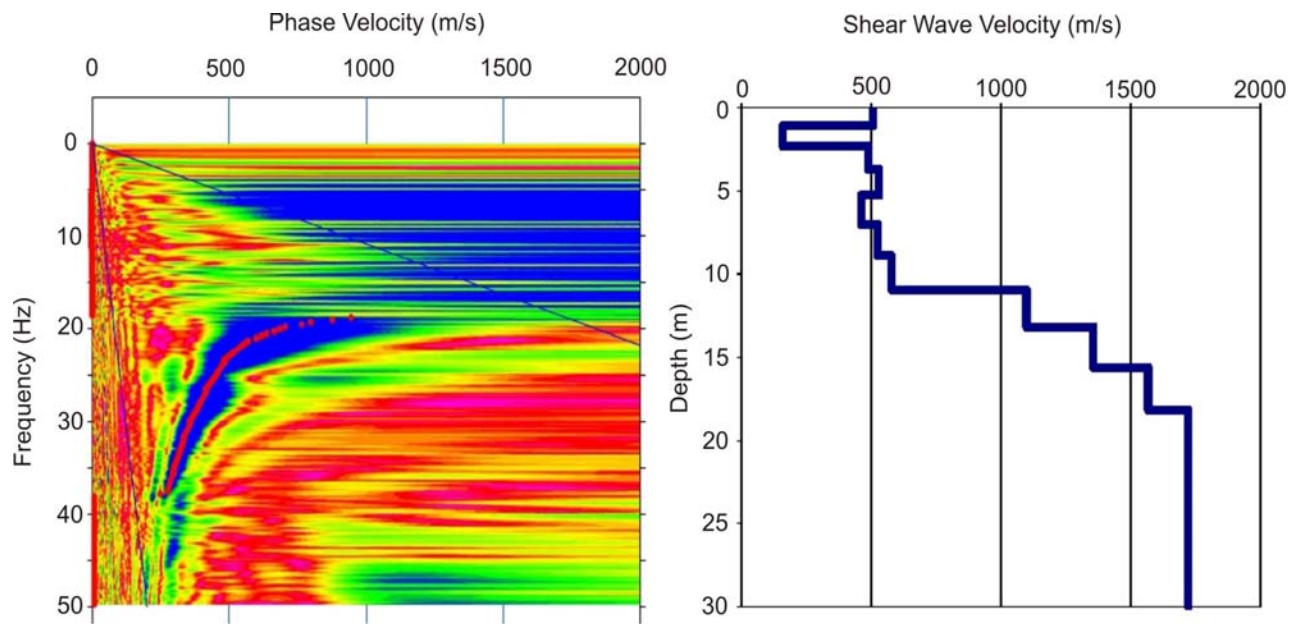


Figure 2.2.3-3: Field data example of a dispersion curve with identification of the fundamental mode (red dots) (left) and resulting shear wave velocity profile (right).

## References

Casto, D.W., Luke, B., Calderon-Macias, C. and Kaufmann, R., 2009. Interpreting Surface-wave Data for a Site with Shallow Bedrock; *Journal of Environmental & Engineering Geophysics*, v.14, p.115-127.

Foti, S., 2000. Multistation methods for geotechnical characterization using surface waves; PhD thesis, Politecnico di Torino, Italy.

Park, C.B., Miller, R.D. and Xia, J., 1998. Imaging dispersion curves of surface waves on multichannel record; *in Proceedings, Technical Program with biographies, 68<sup>th</sup> Annual Meeting of the Society of Exploration Geophysicists (SEG)*, New Orleans, Louisiana, p. 1377-1380.

Park, C.B., Miller, R.D. and Xia, J., 1999. Multichannel analysis of surface waves (MASW); *Geophysics*, v. 64, p. 800-808.

Park, C.B. and Miller, R.D., 2008. Roadside passive multichannel analysis of surface waves (MASW); *Journal of Environmental and Engineering Geophysics*, v. 13, p. 1-11.

## Additional Readings

Phillips, C., Cascante, G. and Hutchinson, J., 2004. Evaluation of lateral homogeneity with the distance analysis of surface waves; *Canadian Geotechnical Journal*, v. 41, p. 212-226.

Xia, J., Miller, R.D. and Park, C.B., 1999, Estimation of near-surface shear-wave velocity by inversion of Rayleigh waves; *Geophysics*, v. 64, p. 691-700.

## 2.2.4 Modal Analysis of Surface Waves (MMASW) Technique for Hazard Studies

*Guy Lefebvre and Mourad Karray*  
*Université de Sherbrooke, Sherbrooke, Québec*

### Introduction

#### Principles of the Method

A surface Rayleigh wave is generally generated by an impact at ground surface and its velocity is determined using sensors placed on the ground. The first step in the interpretation of a surface wave test is to analyze the signals recorded at each sensor to establish the relation between the wavelength and the phase velocity, designated as the dispersion curve. The transformation of the dispersion curve into a Vs profile by an inversion process is the second interpretation stage of a surface wave test. An inversion involves first the calculation of a theoretical dispersion curve corresponding to an assumed Vs profile and the comparison of the theoretical dispersion curve with the experimental dispersion curve. The assumed Vs profile is then adjusted until the calculated and the experimental dispersion curves coincide. The calculation of the dispersion curve corresponding to a Vs profile needs as an input the unit mass and the Poisson ratio or compression wave velocity.

The ground surface vibrates not only according to its fundamental mode, but also according to higher modes which travel faster than the fundamental mode. While the fundamental mode is generally dominant, it is often affected by higher modes and there are cases where the higher modes are dominant. The SASW method (Stokoe et al., 2004) proposes criteria to eliminate the higher modes since the method considers that only the fundamental mode contributes to the dispersion curve. Although the conditions that favor the contribution of higher modes are not yet fully understood, there is today a consensus that the eventual contribution of the higher modes must be considered in the interpretation of surface wave tests (Lefebvre and Karray, 1998; Foti, 2000; Karray, 1999; Stokoe et al., 2004; Karray and Lefebvre, 2008).

#### Current State of Engineering Practice

The method "Multi-modal Analysis of Surface Wave" (MMASW) was developed in the civil engineering department at the Université de Sherbrooke in the 1990s, in particular, to meet the needs for accuracy and reliability in engineering analyses by addressing the contribution of higher modes in the dispersion curve. The MMASW method (Lefebvre and Karray, 1998; Karray, 1999) has to be distinguished from the "Multi-Channel Analysis of Surface Waves" (MASW) method (Park et al., 1999). As implicitly expressed in its name, "Modal Analysis of Surface Wave" involves a formal separation of all the modes contributing to the signals recorded by the sensors. The design of the method was based on soil dynamic behavior observed in numerical modeling and verified in the field. Techniques for mode separation are described in Karray (1999) and Lefebvre and Karray (1998).

#### **Recommended citation:**

Lefebvre, G. and Karray, M., 2012. Modal Analysis of Surface Waves (MMASW) Technique for Hazard Studies; *in* Shear Wave Velocity Measurement Guidelines for Canadian Seismic Site Characterization in Soil and Rock, (ed.) J.A. Hunter and H.L. Crow; Geological Survey of Canada, Open File 7078, p. 67-76.

## Data Collection

### Required equipment

Typically vertical geophones with low natural frequency ( $\approx 4$  Hz) can be used to perform surface wave testing. However, for MMASW geophones can induce instrumental phase error at low frequencies (large wavelengths) depending on the natural frequency of the geophones and the depth of investigation. Thus, the sensors used to perform MMASW are highly sensitive PCB accelerometers with a natural frequency of 5 kHz. Depending on the depth of investigation, the excitation on the surface of the ground can be generated by a weight drop of 15 or 60 kg from a drop height of about 1 to 2 m. The use of a sledgehammer is generally not recommended because of the non-repetitivity of its blows. The MMASW tests are generally repeated at least three times to reduce noise.

### Data Collection Procedures

In routine MMASW testing, 16 sensors are placed 1 m apart (array length of 15 m) and the source (a 60 kg weight with a 2 m fall) is positioned at least 8 m from the nearest sensor. This arrangement allows one to record all the wave lengths necessary to have a detailed profile close to surface and to penetrate a soil deposit to  $\sim 50$  m deep. The  $V_s$  profile determined in such a test is located in the center of the sensor array and represents an average over the distance covered by the 16 sensors. MMASW tests are generally run one after the other displacing the source only every 2 or 3 tests. Different sets of 16 signals can then be selected as shown in Figure 2.2.4-1 and interpreted to determine closely spaced  $V_s$  profiles, typically every 2 m. This allows one to present the results as a tomography panel in terms of  $V_s$  or  $V_{s1}$  ( $V_{s1}$  is  $V_s$  normalized for a vertical effective stress of 100 kPa).

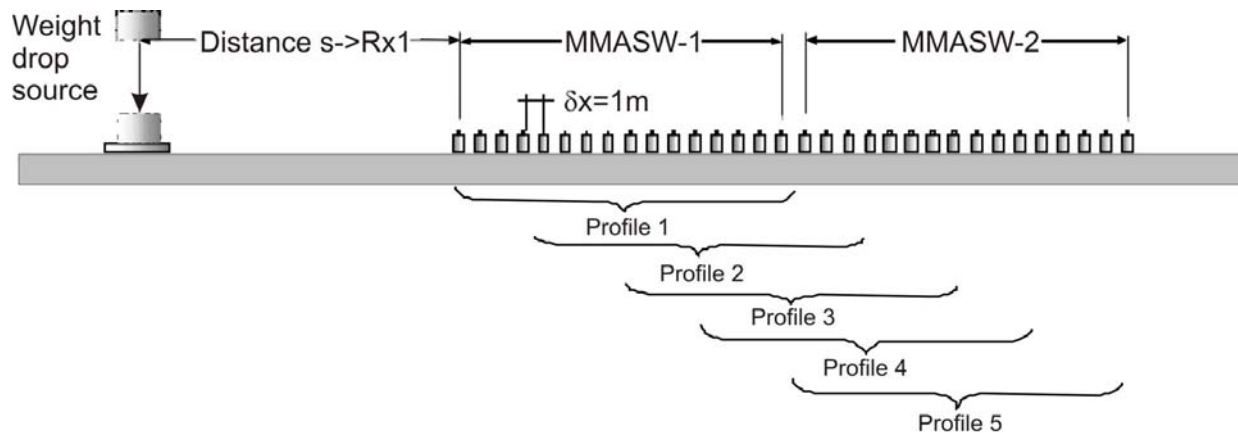


Figure 2.2.4-1. Typical arrangement for sequential MMASW tests.  $S \rightarrow Rx1$  is the distance between the source and the first receiver, and geophone separation is 1 m. MMASW-1 and MMASW-2 are the first and second 16-geophone spreads.

## Processing Techniques

### Theory of Analysis

Figure 2.2.4-2 illustrates the mode separation in the MMASW method. The dots on Figure 2.2.4-2 are the experimental points after mode separation, while the curves are the theoretical dispersion curves for the different modes corresponding to the final  $V_s$  profile at the end of the inversion process (Figure 2.2.4-2b). In most cases, the experimental points define the dispersion curves for at least two Rayleigh modes, including, but not always, the fundamental mode. As illustrated on this figure, the experimental points corresponding to higher modes are not rejected but are used in the inversion process. Traditionally, the inversion process consists of adjusting a  $V_s$  profile until its theoretical dispersion curve for the fundamental mode coincides with the experimental dispersion curve assumed to represent the fundamental mode. An inversion can however be made for the first higher mode or for any other mode.

As well, for a given  $V_s$  profile, inversion for different modes should lead to exactly the same  $V_s$  profile if the assumed Poisson's ratio or compression wave profile is correct. The mode separation in MMASW does not involve only the correct definition of the fundamental mode, but also a multi mode inversion leading to greater reliability and accuracy. A multi-mode inversion also allows for the determination of Poisson's ratio. Figures 2.2.4-3a and 2.2.4-4a present examples of sites where the fundamental Rayleigh mode was not dominant or almost absent. Even if the  $V_s$  profiles at those sites are not really unusual (Figures 2.2.4-3b and 2.2.4-4b), there is a high probability that methods using surface waves without formal mode separation would yield erroneous  $V_s$  profiles at such sites.

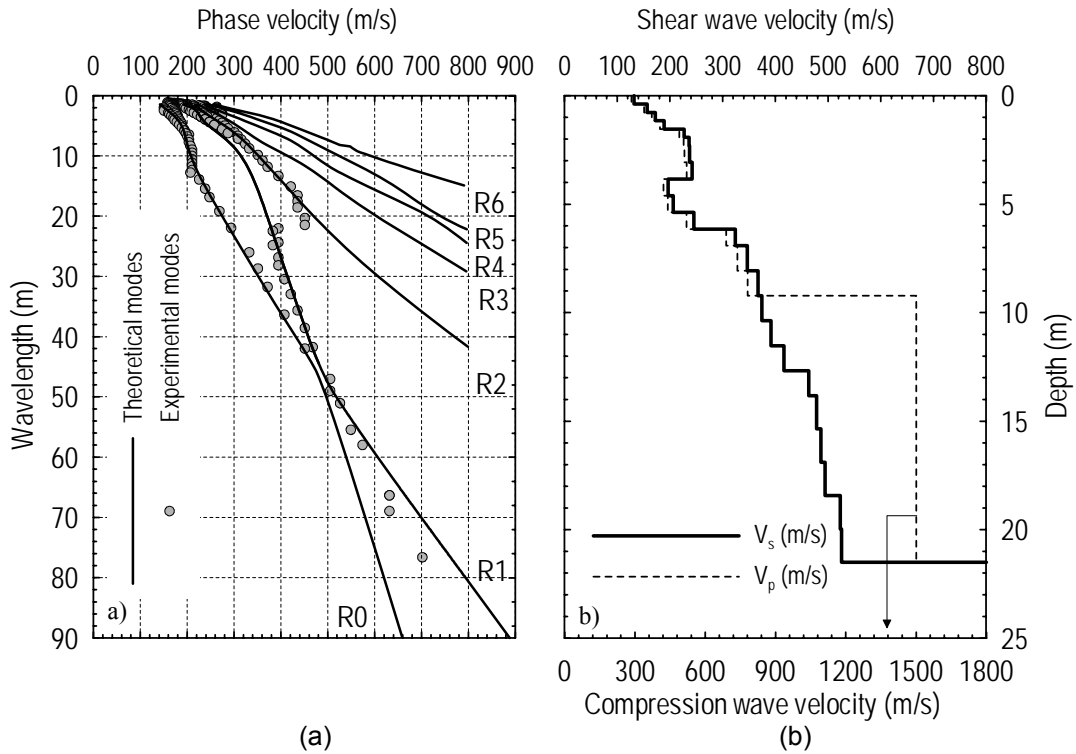


Figure 2.2.4-2. Example of mode separation a) experimental and theoretical dispersion curves, b)  $V_s$  and  $V_p$  profiles.  $R_n$ =Rayleigh wave mode  $n$ .

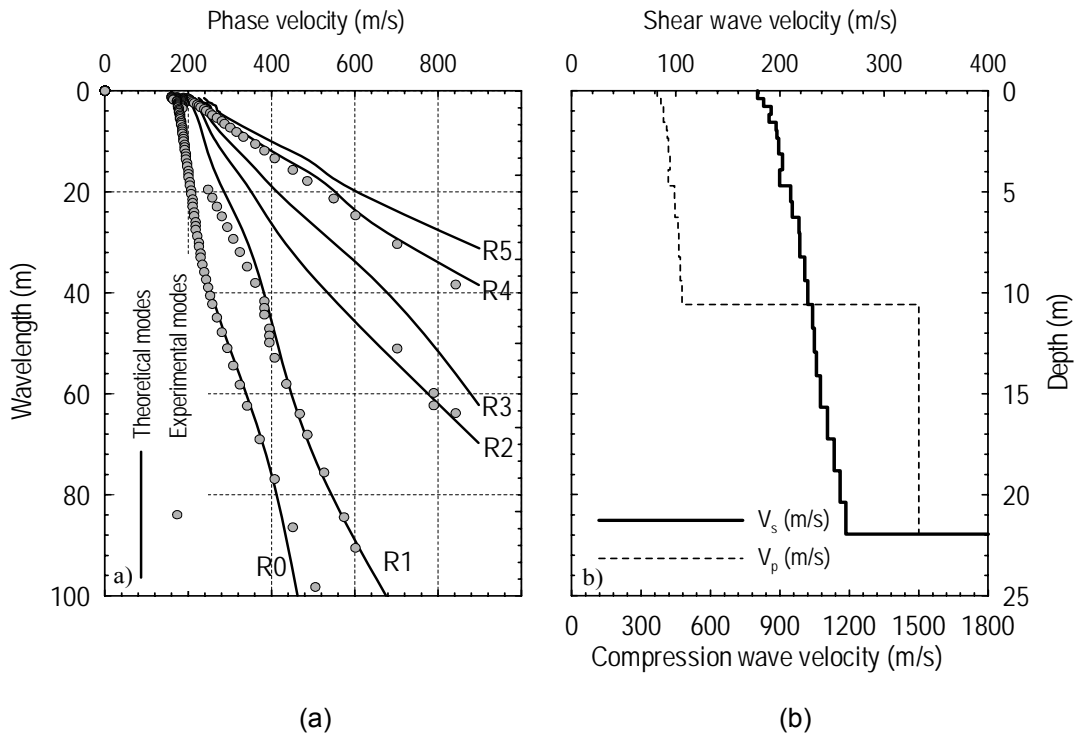


Figure 2.2.4-3. Example of dominant higher Rayleigh modes a) experimental and theoretical dispersion curves, b)  $V_s$  and  $V_p$  profiles.  $R_n$ =Rayleigh wave mode  $n$ .

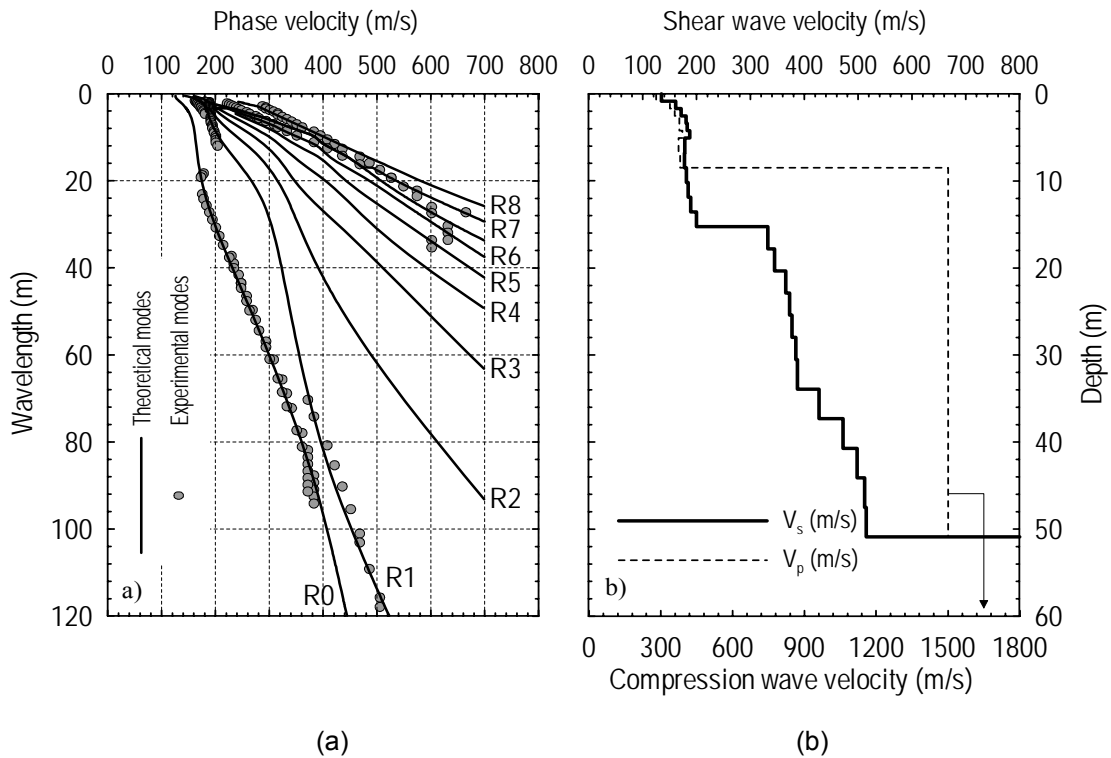


Figure 2.2.4-4. Example of absent fundamental Rayleigh mode at certain wavelengths. a) experimental and theoretical dispersion curves, b)  $V_s$  and  $V_p$  profiles.  $R_n$ =Rayleigh wave mode  $n$ .

### **Uncertainty Assessment**

The accuracy of the  $V_s$  profile determined by an inversion depends on how closely the theoretical and the experimental curves can be fit together. Traditionally the  $V_s$  profile is adjusted until the difference between the two curves becomes smaller than a certain criteria expressed in terms of phase velocity ( $\Delta c$ ). Experience has shown that the accuracy in an inversion process is related not only to  $\Delta c$  but also to the shape of the dispersion curve at any wavelength ( $\delta c/\delta \lambda$ ). In MMASW, the criterion for the fitting of the theoretical and experimental curves is expressed both in terms of  $\Delta c$  and ( $\delta c/\delta \lambda$ ). This is particularly important to detect weaker or stronger layers in a profile. The use of both  $\Delta c$  and  $\delta c/\delta \lambda$  increases the accuracy of the  $V_s$  profile and also results in a more rapid convergence of the inversion

It is important that geotechnical engineers make use of available tools to assess the accuracy of  $V_s$  profiles, often determined by subcontractors. One way to do this is to use relationships between  $V_s$  and the penetration Index,  $N$ , or piezocone point resistance,  $q_c$ . These quantities are routinely determined in geotechnical investigations and are related to soil rigidity and thus to  $V_s$ . Wride and colleagues have proposed  $V_s - N$  and  $V_s - q_c$  correlations based on six fine sand sites well-characterized in the CANLEX project (Wride et al., 2000). Karray et al. (2011) have extended these correlations to include medium and coarse sands using the investigation data from the Péribonka and La Romaine dam sites (Karray et al., 2010). These correlations use  $N_1$ ,  $q_{c1}$ , and  $V_{s1}$ , all normalized for a vertical effective stress of 100 kPa using:

$$N_1 = N \left( \frac{100}{\sigma'_v} \right)^{0.5} \quad [2.2.4-1]$$

$$q_{c1} = q_c \left( \frac{100}{\sigma'_v} \right)^{0.5} \quad [2.2.4-2]$$

$$V_{s1} = V_s \left( \frac{100}{\sigma'_v} \right)^{0.25} \quad [2.2.4-3]$$

As seen below, the relations between  $V_{s1}$  and  $N_1$  as well as between  $V_{s1}$  and  $q_{c1}$  are influenced by the particle size expressed as  $D_{50}$ , the median diameter of the grain size distribution:

$$V_{s1} = 125.5 (q_{c1}^{0.25}) (D_{50}^{0.115}) \quad [2.2.4-4]$$

$$V_{s1} = 107.8 (N_1^{0.25}) (D_{50}^{0.18}) \quad [2.2.4-5]$$

Such correlations between these relationships and measured  $V_s$  from MMASW are given in the second case study presented below.

### **Recommended Guidelines for Reporting**

The MMASW survey technique is currently proprietary, and at the time of the  $V_s$  Guidelines publication, the method is being carried out by only one organization. A report of this type would summarize the testing methodology, field procedures, and processing steps, including the selection of the fundamental and higher order Rayleigh wave modes, present a comparison of theoretical and experimental dispersion curves, and discuss the assumptions used in the inversion. The report would ultimately present the inverted shear-wave velocity depth profile, accompanied by any other available site data, including the penetration Index,  $N$ , or piezocone point resistance,  $q_c$ , as discussed above.

## Hazard-Related Case Studies

### Péribonka Dam, Québec

Figure 2.2.4-5 presents an example of tomography in terms of  $V_{s1}$  at the Péribonka Dam site in Québec where MMASW was used to control deep compaction by vibroflotation (Karray et al., 2010). Figures 2.2.4-5a and 2.2.4-5b present the  $V_{s1}$  before and after compaction respectively. Note that in the dense layer identified below a depth of 25 m, the  $V_{s1}$  determined before compaction and those determined after are identical, confirming the good reproducibility of the MMASW tests. The closely spaced borings made for bedrock injection below the cut-off wall confirmed the accuracy of the bedrock position determined with MMASW.

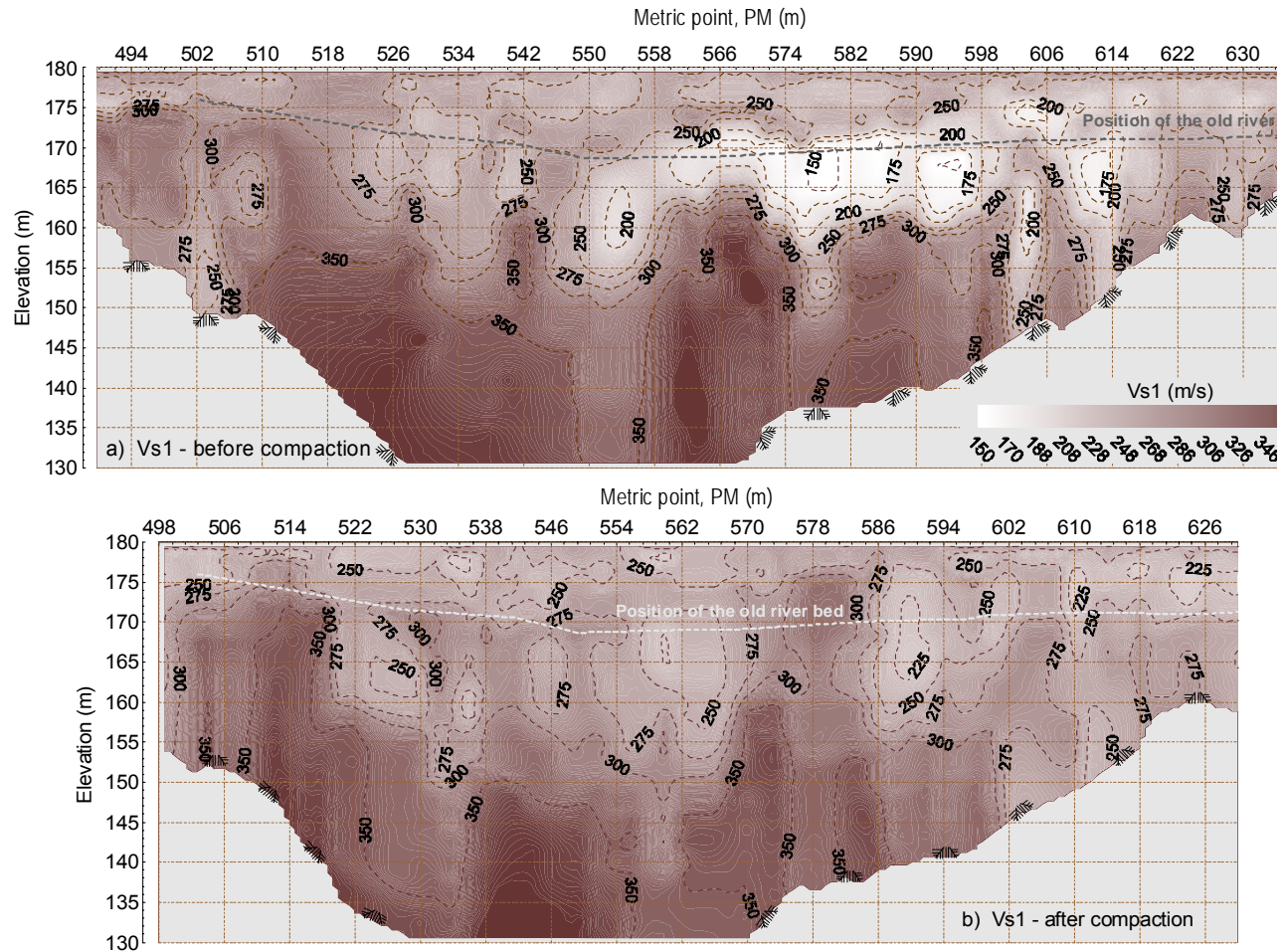


Figure 2.2.4-5. Example of tomographic presentation at the Péribonka Dam site a)  $V_{s1}$  before compaction; b)  $V_{s1}$  after compaction.

### **Vs Correlations with SPT and Piezocone**

Figure 2.2.4-6 presents an example where  $V_s$ , evaluated from  $N$  and  $q_c$  using these correlations, are compared with  $V_s$  measured using MMASW. The  $V_s$  obtained from  $N$  and  $q_c$  are within 10% of the measured values with a slightly higher difference in the silty clay layer since the correlation has been developed for granular soils. In granular soils, evaluation of  $V_s$  from  $N$  and  $q_c$  constitute an alternative when there is no  $V_s$  measurement at sites well characterized in terms of  $N$  and  $q_c$ . Such correlations should always be used to verify the reliability of the  $V_s$  measurement as well as the consistency of the results obtained by different types of test, namely Standard Penetration, piezocone and  $V_s$  measurements. Figure 2.2.4-7 presents a comparison between  $V_s$  profiles from the same site, determined with and without formal mode separation. The  $V_s$  determined without mode separation is in relatively good agreement from surface to 10 m depth. However, they diverge completely below 10 m from the profiles determined by MMASW and by correlations based on  $N$  and  $q_t$ , showing  $V_s$  values two times higher at about 25 m depth. As mentioned before, conditions favoring the contribution of higher Rayleigh modes are not well understood and energy from higher modes can exist and even dominate in different situations as shown by Figures 2.2.4-2, 2.2.4-3, and 2.2.4-4.

Many non intrusive methods are available today. It is important that the reliability and accuracy of the methods be demonstrated before being used in engineering analyses. Methods based on surface Rayleigh waves can be highly reliable and accurate, but it is the authors' (GL and MK) opinion that formal mode separation and multi mode inversion are required. Verifying the reliability of  $V_s$  measurement is difficult due to the lack of reference standards. Geotechnical engineers should however always establish reference profiles by published correlations based on geotechnical parameters they are familiar with: the penetration index,  $N$ , and the piezocone point resistance,  $q_c$ . Such  $V_s$  profiles should be used as verification or eventually as a replacement for  $V_s$  measurements.

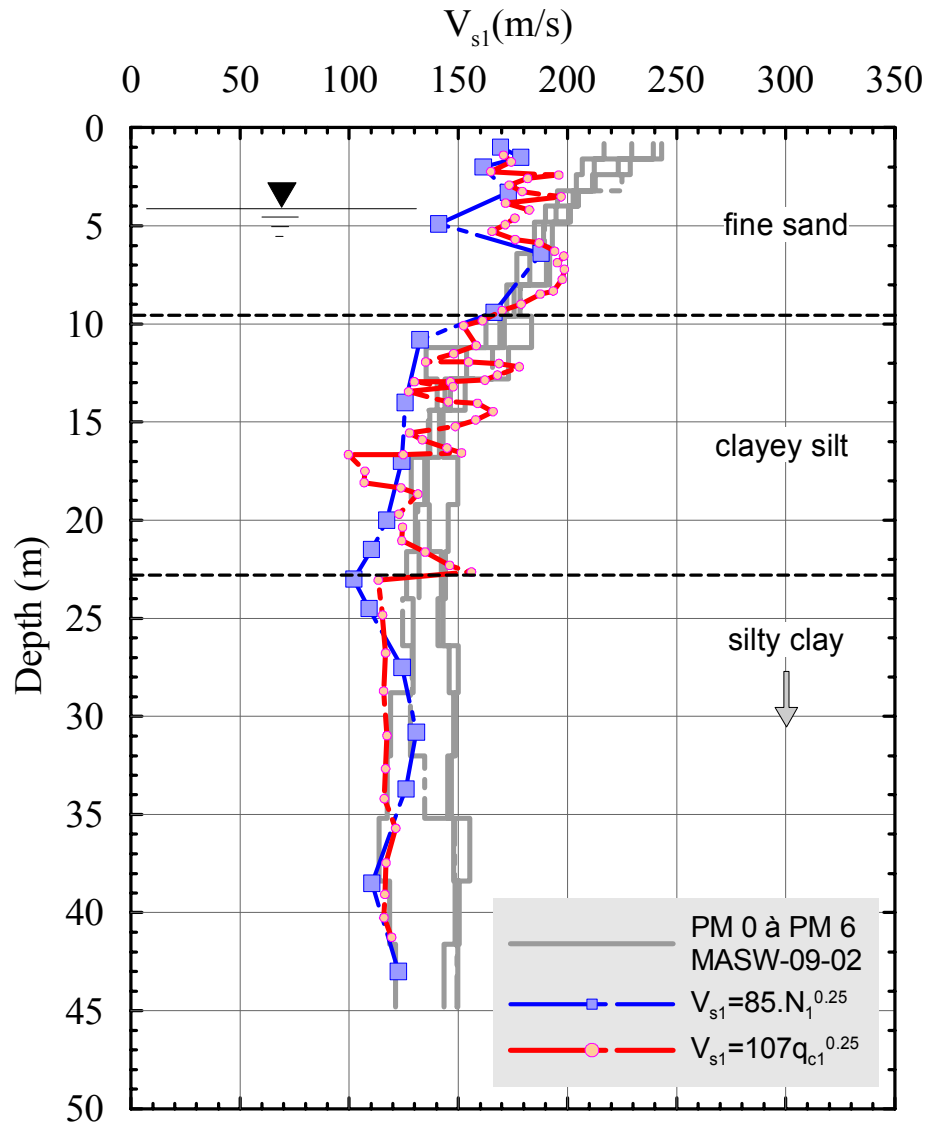


Figure 2.2.4-6. Comparison of Vs1 profiles evaluated from N and qc with MMASW profile.

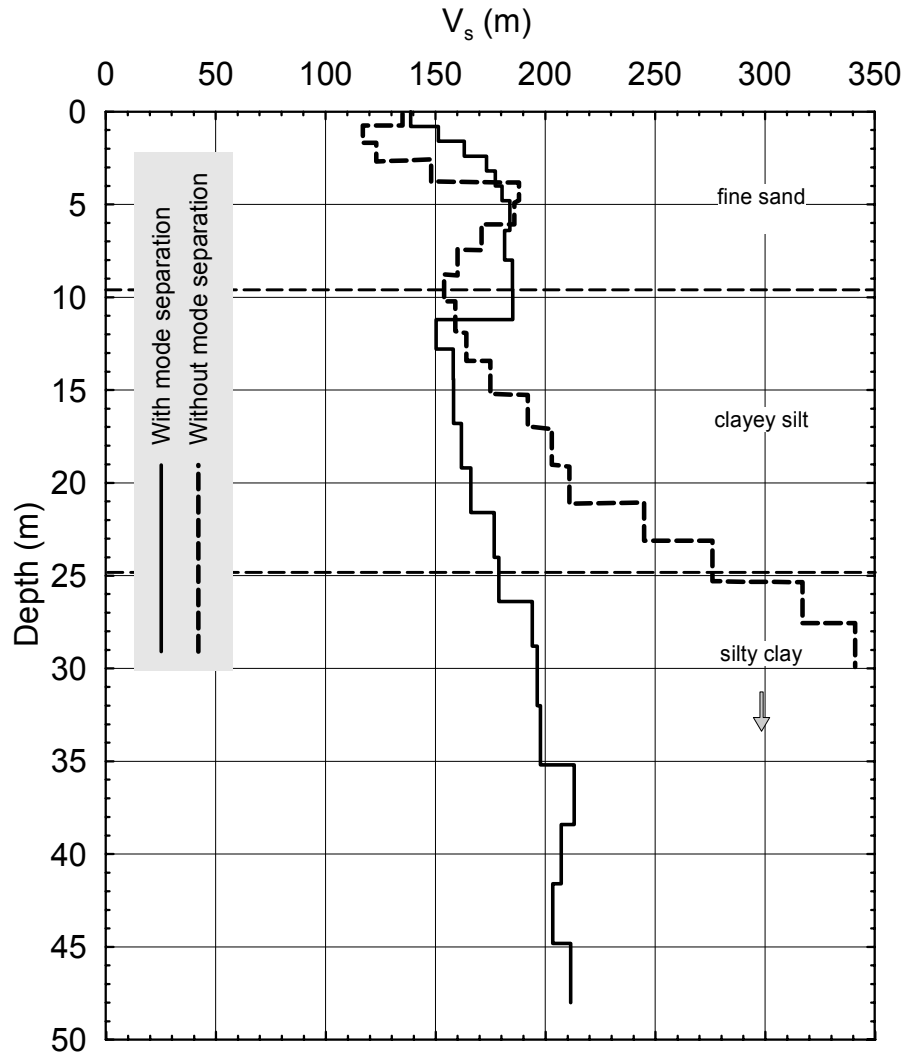


Figure 2.2.4-7. Example showing the importance of mode separation in surface wave testing.

## Acknowledgments

The authors thank the Natural Sciences and Engineering Research Council of Canada (NSERC) for their financial support, and Hydro-Québec who have given us the opportunity to carry out field testing and permission to publish the results.

## References

Foti, S., 2000. Multistation methods for geotechnical characterization using surface waves; Dottorato di Ricerca in Ingegneria Geotecnica, Università degli Studi di Genova, 106 p.

Karray, M., 1999. Utilisation de l'analyse modale des ondes de Rayleigh comme outil d'investigation géotechnique in-situ; Ph.D thesis, Université de Sherbrooke, Sherbrooke, Québec, 275 p.

Karray, M. and Lefebvre, G., 2008. Significance and evaluation of Poisson's ratio in Rayleigh wave testing; Canadian Geotechnical Journal, v. 45, p. 624-635.

Karray, M., Lefebvre G., Éthier, Y. and Bigras A., 2010. Assessment of deep compaction at the Péribonka dam using Modal-Analysis-of-Surface-Wave "MASW"; Canadian Geotechnical Journal, v. 47, p. 312-326.

Karray, M., Lefebvre G., Éthier, Y. and Bigras A., 2011. Influence of particle size on the correlation between shear wave velocity and cone tip resistance; Canadian Geotechnical Journal, v. 48, p. 599-615.

Lefebvre, G. and Karray, M., 1998. New development in in-situ characterization using Rayleigh waves; *in* Proceedings, 51<sup>st</sup> Canadian Geotechnical Conference, Edmonton, Alberta, BiTech Publishers Ltd., v. 2, p. 821-828.

Stokoe, K.H., Joh, S.H. and Woods, R.D., 2004. Some Contributions of In Situ Geophysical Measurements to Solving Geotechnical Engineering Problems; *in* Proceedings, ISC-2 on Geotechnical and Geophysical Site Characterization, Porto, Portugal, (eds.) V. da Fonseca and P. W. Mayne; Millpress, Rotterdam, v. 1, p. 97-132.

Park, C.B., Miller, R.D. and Xia, J., 1999. Multichannel analysis of surface waves; Geophysics, v. 64, p. 800-808.

Youd, T. L., Idriss, I. M., Andrus, R. D., Arango, I., Castro, G., Christian, J. T., Dobry, R., Finn, W. D. L., Harder, L. F., Hynes, M., E., Ishihara, K., Koester, J. P., Liao, S. S. C., Marcuson, W. F., Martin, G. R., Mitchell, J. K., Moriwaki, Y., Power, M. S., Robertson, P. K., Seed, R. B. and Stokoe, K. H., 2001. Liquefaction resistance of soils: summary report from the 1996 NCEER and 1998. NCEER/NSF workshops on evaluation of liquefaction resistance of soils; Journal of Geotechnical and Geoenvironmental Engineering, ASCE, v. 127.

Wride, C.E., Robertson, P.K., Biggar, R.G., Campanella, R.G., Hofmann, B.A., Hughes, J.M.O., Kupper, A. and Woeller, D.J., 2000. Interpretation of in situ test results from the CANLEX sites; Canadian Geotechnical Journal, v. 37, p. 505-529.

## 2.3 Ambient Noise

*Section Leader: Maxime Claprood*

*Institut National de la Recherche Scientifique (INRS), Québec, QC.*

Ambient noise methods measure background seismic noise to evaluate the mechanical properties of the earth's subsurface, using the dispersive properties of surface waves as a function of frequency to make predictions about the subsurface geology.

Ambient noise is defined as the constant vibration of the earth's surface, generated by low frequency (<~1 Hz) natural phenomena (earthquakes, wind, tides, rivers, rain, variations of atmospheric pressure) and high frequency (>~1 Hz) human activities (road traffic, machinery, pedestrians). This background noise is a mixture of body and surface waves, which contain information on the sources and transmission paths of waves, and subsurface structure. Most sources of ambient noise are located at the surface of the earth or at the bottom of the sea, releasing most of their energy as surface waves. Rayleigh waves become predominant at large distances from the sources because their geometric attenuation is much lower than that of body waves (Socco and Strobba, 2004). It is commonly assumed that Rayleigh and Love surface waves dominate an ambient noise record at more than one wavelength from the sources (Arai and Tokimatsu, 2004).

It is impossible to isolate every wave from an ambient noise record. Aki (1957) proposed to analyze ambient noise as a temporal and spatial stochastic process with reference to the nature of wave propagation. By recording the background noise over a long period of time with an array of sensors, the record is considered an assemblage of coherent waves travelling in various directions over an extended frequency interval, which typically includes frequencies between 0.5 to 20 Hz.

There exist two main classes of ambient noise techniques:

- Single station methods to evaluate the resonance frequencies of soft sediments over hard bedrock (article 2.3.1), and
- Array based methods to evaluate a  $V_s$  profile with depth (articles 2.3.2 and 2.3.3).

Single station methods (2.3.1) are now commonly used as a reconnaissance tool, but cannot be used to assign a seismic site class alone without significant background work (as exemplified by the Montreal case history by Chouinard and Rosset).

Array-based ambient vibration methods, using either SPatially Averaged Coherency (SPAC) spectrum (article 2.3.2), or Frequency-wavenumber ( $f-k$ ) processing (article 2.3.3) are best suited to evaluate  $V_s$  profiles above soft, low velocity sedimentary layers overlying hard bedrock. While these techniques are gaining in popularity, they are still under development. Used together, the two methods can reinforce interpretation and/or aid in distinguishing wave modes. The SPAC method is especially attractive in terrains where traditional methods of evaluating  $V_s$  profiles cannot be implemented and when noise sources are from a large range of azimuths. The  $f-k$  method is preferred in the presence of a dominant (uni-directional) noise source and/or when a non-symmetrical field array is required.

## References

Aki, K., 1957. Space and time spectra of stationary stochastic waves, with special reference to microtremors; Bulletin of the Earthquake Research Institute, v. 35, p. 415–456.

Arai, H. and Tokimatsu, K., 2004. S-wave velocity profiling by inversion of microtremor H/V spectrum; Bulletin of the Seismological Society of America, v. 94, p. 53-63.

Socco, L. and Strobba, C., 2004. Surface-wave method for near-surface characterization: a tutorial; Near Surface Geophysics, v. 2, p. 165-185.

## 2.3.1 Single Station H/V Technique

Didier Perret

Geological Survey of Canada, Quebec City, Québec

**With an expanded Hazard-Related Case Study:**

**“On the Use of Single Station Ambient Noise Techniques for Microzonation Purposes: The Case of Montreal”**

Luc Chouinard and Philippe Rosset

McGill University, Dept. of Civil Engineering, Montréal, QC

### Introduction

#### Principles of Method

The single station method was initially developed in Japan by Nogoshi and Igarashi (1971) for characterizing site response under seismic loading, and was later popularized and diffused to the Western world by Nakamura (1989). This method consists of the calculation of the ratio (typically noted as H/V) of the horizontal to the vertical Fourier spectra of ambient noise recorded at a single site by a three-component sensor. Empirical evidence, supported by numerical simulations, indicate that the maximum of the H/V spectral ratio generally occurs at, or close to, the fundamental resonance frequency of the site, provided that there is a sufficiently strong impedance contrast at depth (see e.g. Bonilla et al., 1997; Bour et al., 1998; Bard, 1999; Woolery and Street, 2002; Haghshenas et al., 2008).

Figure 2.3.1-1a shows an example of ambient noise recorded with a three-component seismometer in Gloucester, about 20 km south of Ottawa. The site features 18 m of soft to firm Champlain Sea clays underlain by 2 m of till resting on hard bedrock. The average shear wave velocity in the soil column is 110 m/s. The shear wave velocity of the bedrock has not been measured but is probably higher than 2,000 m/s according to values obtained for similar lithologies in the Ottawa region. The impedance contrast is thus very high. The Fourier spectrum for each of the three recording directions (East-West, North-South, Vertical), and the corresponding H/V spectral ratio, where H is the quadratic average of the two horizontal components, are also shown (Figures 2.3.1-1b and 2.3.1-1c, respectively). The spectral ratio displays a well defined peak at a frequency of 1.38 Hz. This peak is related to the maximum divergence of the Fourier spectra of the two horizontal and vertical components around the fundamental frequency of the site. For comparison, the 1-D transfer function calculated from a shear wave velocity profile obtained at the site is plotted on Figure 2.3.1-1c. The 1D assumption is thought to be valid as the bedrock topography is probably flat and sediment layers horizontal in the area. The first peak from the left of the transfer function shows that the theoretical fundamental frequency is 1.41 Hz, which is for all practical purposes, and given uncertainties, almost identical to the value determined from ambient noise measurement.

Due to the low cost of data acquisition and simplicity of processing, this method is widely used in seismic microzonation projects and for calibrating site response analyses. The method is especially recommended in areas of low to moderate seismicity where earthquake recordings are rare or even non-existent and the classical site-to-reference approach (Borcherdt, 1970) is not applicable. Since the fundamental frequency of a site is related to the average shear wave velocity of the soil profile and its thickness, the method is also frequently used as a geophysical exploration tool for estimating one of these two parameters, knowing the other one.

#### **Recommended citation:**

Perret, D., 2012. Single Station H/V Technique; *in* Shear Wave Velocity Measurement Guidelines for Canadian Seismic Site Characterization in Soil and Rock, (ed.) J.A. Hunter and H.L. Crow; Geological Survey of Canada, Open File 7078, p. 78-84; 90-93.

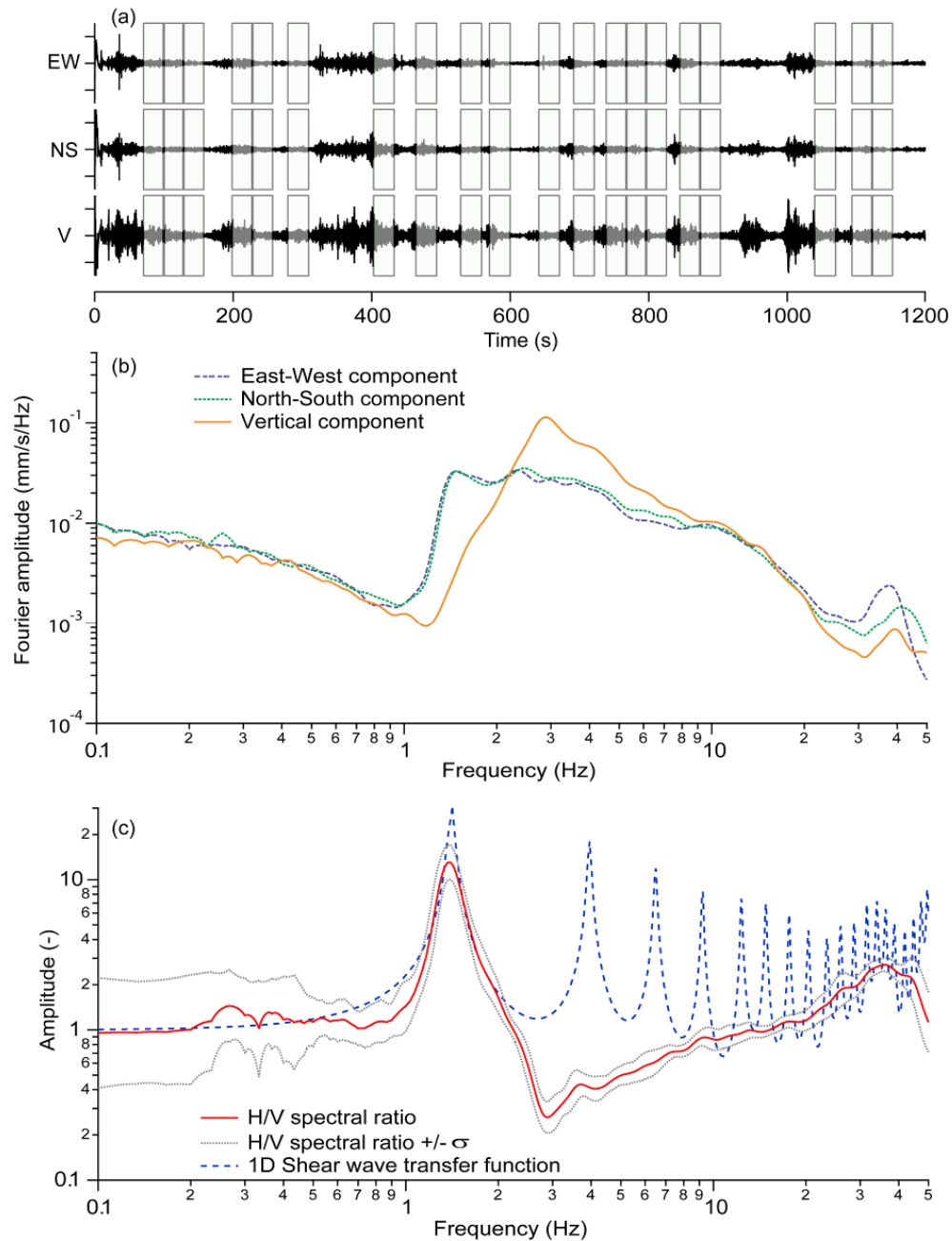


Figure 2.3.1-1. Example of a single station ambient noise record, Gloucester (Ontario); a) three-component time series, b) mean Fourier spectra for the three components, c) H/V spectral ratio with one standard deviation confidence interval, and 1D S-wave transfer function. Light green rectangles on (a) outline the windows selected for the analysis after main transients detection.

### **Current State of Engineering Practice**

Currently, there are no standards describing the H/V spectral ratio method, in Canada or abroad. As the method is still under active development, some significant differences may exist in the manner ambient noise records are acquired, processed and interpreted. However, guidelines formulated within the framework of a large European project (project SESAME, Site Effects Assessment Using Ambient Excitations) which has involved 14 research institutes and 85 scientists, are gaining wide acceptance.

These best practice guidelines have been published in a 62 pages report (Bard, 2004), and in a special issue of the Bulletin of Earthquake Engineering (Bard, 2008) where some aspects are further developed. Many publications have since supported the SESAME project findings (e.g. Maresca et al., 2011), although a few recommended analysis procedures have been questioned (e.g. Parolai et al., 2009, on the usefulness to exclude transients; Castellaro and Mulargia (2009a), on peak identification criteria and recording on stiff artificial ground; Cara et al. (2010), on the stability of H/V over time).

The reader is referred to the SESAME guidelines for a detailed description of the method. Only a brief overview is presented in the following sections, which highlight some still-debated points.

### **Limitations**

The H/V spectral ratio method is based on the fundamental assumption that the vertical component of the ambient noise record is not influenced by the soil overburden, whereas the horizontal components are. However, the theoretical framework that would justify this assumption is not yet fully established and the physical meaning of the H/V spectral ratio is still controversial (see e.g. Lunedei and Albarello (2010), and Sanchez-Sesma et al. (2011), for recent discussions). Bonnefoy-Claudet et al. (2006) have shown for example that, depending on the spatial distribution of the noise source and its nature, the soil/rock impedance contrast, and the thickness of the overburden, the shape of the H/V spectral ratio could be explained for horizontally layered media, either by shear wave resonance, the ellipticity of the fundamental mode of Rayleigh waves, or by the Airy phase of the fundamental mode of Love waves. This very complex and not well understood interaction between the noise wave-field and the geological structure limits the information that can be reliably retrieved from single station measurements.

The H/V spectral ratio alone cannot be confidently inverted into a shear wave velocity profile, unless additional information is provided such as the respective contribution of Rayleigh and Love waves, and the depth to the bedrock (e.g. Castellaro and Mulargia, 2009b; Hobiger et al., 2009, Foti et al., 2011). Another consequence of this complex interaction is that the amplitude of the peak(s) of the H/V ratio is not a reliable predictor of the amplification of ground motions (e.g. Bonilla et al., 1997; Bard, 1999). Except in some rare circumstances (Chavez-Garcia, 2009), the H/V spectral ratio is not equivalent to a shear wave transfer function.

The geological interface that relates to the peak on H/V curves, or of the lowest frequency peak in case of several, is not always the top of bedrock or the deepest large impedance contrast, but can be an interface within the soil deposit. In Eastern Canada for example, it has been shown that the top of Pleistocene sediments, often significantly stiffer than the overlying Holocene sediments, can be the controlling interface, and not the underlying bedrock, as depicted in Figure 2.3.1-2. This means that for some geological settings the H/V method is unable to retrieve information below the first strong impedance contrast and thus cannot be used as an exploration tool for mapping the bedrock topography. Similar behaviours have been documented by Lunedei and Albarello (2010).

In the case of deep and narrow buried valleys 2-D or 3-D effects can dominate the resonance pattern. Estimating the depth to the bedrock or average shear wave velocities with a 1-D model can lead to severe errors especially near steep basin edges, as warned by Cornou et al. (2007) and Gueguen et al. (2007). Moreover, H/V curves may not display a clear peak in these situations but rather a broad bump or a plateau which complicates the identification of the site fundamental frequency. The H/V method is also reported to be inefficient (i.e. no interpretable peak) for complex sedimentary structures where no single interface controls the impedance ratio, even if significant seismic wave amplification is known to occur during earthquakes (Chavez-Garcia, 2009).

Finally, it should be kept in mind that ambient noise vibrations are of very low amplitude compared to those generated by a strong earthquake. Consequently, the site fundamental frequency determined from the H/V curve may be not representative of the frequency (usually lower) controlling site effects during an earthquake due to the non-linear response of soils under strong shaking.

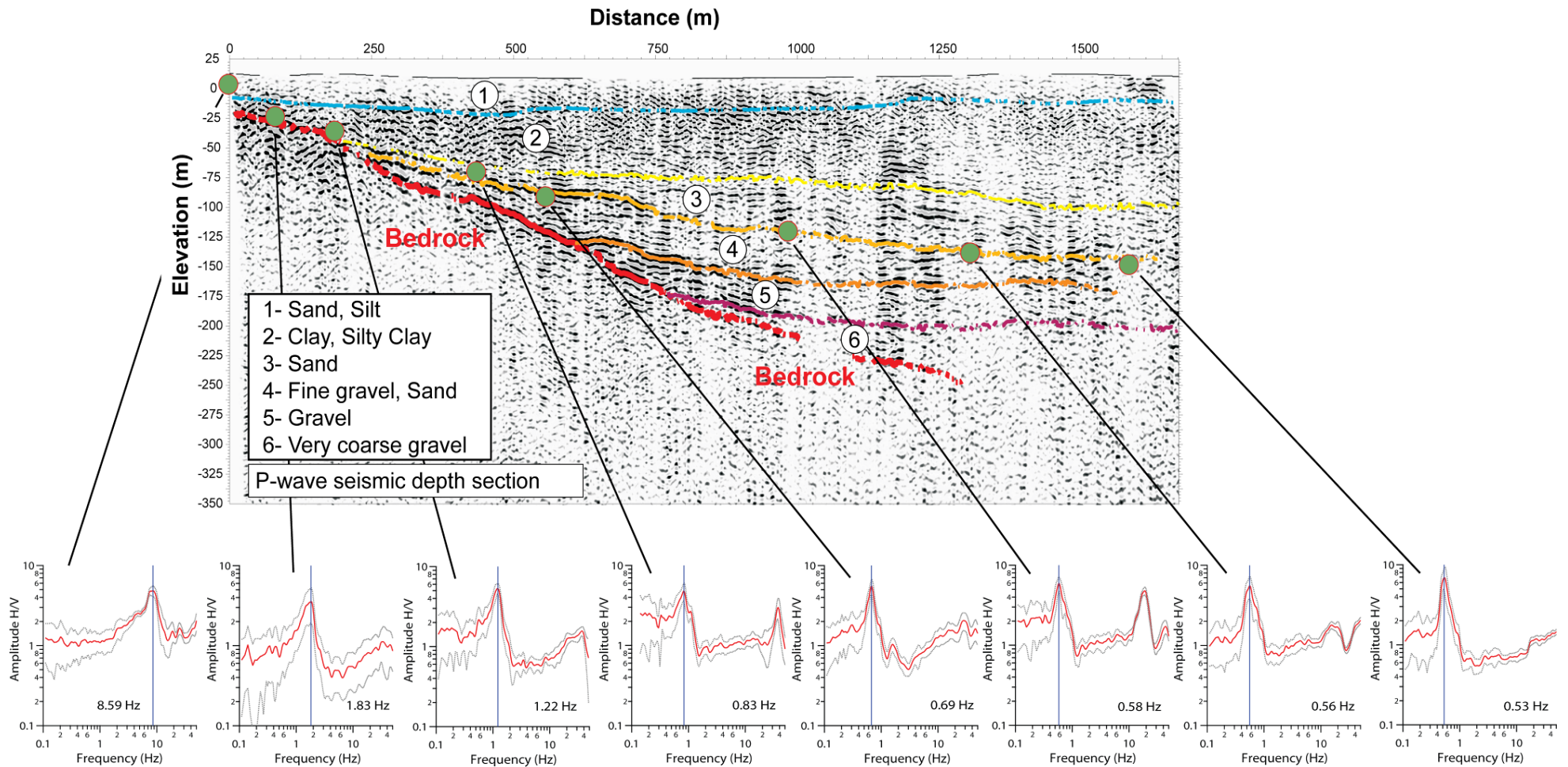


Figure 2.3.1-2. H/V spectral ratios obtained across part of a buried valley, Charlevoix region (Quebec). Depths corresponding to the peak of lowest frequency on H/V curves have been estimated from S-wave profiles (not shown here), and positioned (green circles) on a landstreamer P-wave seismic section. The interface controlling the H/V main peak is the top of bedrock for the three leftmost sites, and the top of sedimentary unit 4 for the other sites (landstreamer data processing and interpretation by A. Pugin, Geological Survey of Canada).

## Data Collection

### Required Equipment

Only one three-component sensor and a signal digitizer are required. As a general rule, it is recommended to use seismometers (velocimeters) that have their natural frequency below the lowest frequency of interest, which, for the purpose of the H/V method, should be the fundamental frequency of the site plus a margin for safety. Due to a relatively high intrinsic noise level, accelerometers should be avoided, although technological development may change this soon. According to the SESAME guidelines (Guiller et al., 2008), the most versatile sensor is a 5 s seismometer. Broad-band seismometers can be used, but take a longer time to stabilize and offer no advantages over a 5 s seismometer for the frequency range of interest in earthquake engineering. Depending on the manufacturer, digitizers can be integrated into all-in-one measurement systems but are more frequently independent of sensors. The sampling rate should be at least 50 Hz, i.e. twice the maximum frequency of engineering interest which is about 25 Hz. Other criteria to consider for the selection of digitizers are indicated in the SESAME guidelines. Whatever the equipment used, it is important to perform periodic calibrations to detect possible equipment malfunctions over time.

### Data Collection Procedures

The single most important recording parameter is the duration of acquisition. As a guiding concept, the lower the anticipated fundamental frequency and the “noisier” the environment (e.g. heavy road traffic nearby, foul weather conditions), the longer the recording duration should be. According to the SESAME guidelines, the minimum recommended duration should vary from 2 to 30 minutes for sites with a fundamental frequency comprised between 10 and 0.2 Hz respectively. We emphasize that these values are the minimum recommended: in doubt, it is preferable to record for a period longer than strictly required based on the anticipated fundamental frequency and on an estimation of signal contamination by transients. Ten more minutes in the field cost less than redoing a measurement after realizing in the office that the acquisition duration was too short.

For ground/sensor coupling, an installation on firm natural ground is always preferred. The ground surface must remain stable during the acquisition, and not deform. Otherwise, the sensor may tilt and the shape of the H/V curve could be altered. Measurements on very stiff artificial grounds (like pavement) overlaying softer soils should also be avoided whenever possible. In this case, the velocity inversion close to the surface may obliterate the peak on the H/V curve and render the analysis more problematic, as evidenced by Castellaro and Mulargia (2009a,b). The SESAME group however only reports slight perturbations when measurements are made on asphalt or concrete.

Some environmental conditions may perturb records. Measurements should be avoided during windy days, especially for sites having a fundamental frequency lower than about 1 to 2 Hz, as wind can strongly influence the H/V curve for frequencies in this range. Acceptable records can still be obtained if the sensor is buried in a hole and/or efficiently protected against direct wind. Close sources of noise, like car traffic or even footsteps, may generate strong transients (short-duration disturbances of the record). Transients have been reported to have possible detrimental impacts on the H/V curve (SESAME group, Castellaro and Mulargia, 2010) although Parolai et al. (2009) mention that they have no significant effects. Given these contradictory results, it is recommended to record ambient noise a few tens of metres away from a strong transient source. If not possible, transients may generally be eliminated by signal processing and this is not a major problem as long as the remaining stationary signal is of a sufficient duration for conducting a reliable analysis. Sustained vibrations generated by machinery are a more serious concern as spurious peaks unrelated to underground geological structures may considerably affect the shape of the H/V curve above 1 Hz (Chatelain et al., 2008; Cara et al., 2010). If these peaks are in the range of the resonance frequency of the site, filtering the record to remove them cannot be done without altering the signal to be preserved. The only solution is then to redo the measurement when the machinery is not in operation.

Unless soil-structure interaction assessment is sought, ambient noise should be recorded in free-field conditions. The distance at which ambient noise is no longer influenced by structures is still debated, but in the absence of other information, a minimal distance of about 15 m should be observed. This value is

based on the study by Castellaro and Mulargia (2010) who have shown that free-field conditions are met at about 12 m from the heavy or tall structures they considered, interestingly even if measurements were made under windy conditions.

For a single site response analysis, it is important not to rely on a single measurement. At least three records should be obtained, preferably at different moments of the day or at different days, to check the stability of the H/V curve. For microzonation studies, measurements should initially be made at a large spacing (i.e. 500 m), and later filled in with a denser spacing (i.e. 250 m or less) in areas where rapid spatial variations of the fundamental frequency are observed.

## **Processing Techniques**

### **Theory of Analysis**

There is no special theory behind the processing of ambient noise records but rather a recipe founded on statistical principles and validated by experience. The SESAME recommended processing procedure requires five main steps, as follows:

- a) Each of the three components of a record is split into several time windows of equal or varying length. The window length is chosen according to criteria based on the fundamental frequency of the site and on the statistical representativeness of the H/V curve to be determined. A few trials may thus be needed before obtaining an appropriate value. Transients may be removed either manually or by using an automatic “anti-trigger” algorithm.
- b) Fourier spectra are computed for every time window and are smoothed to eliminate spikes which may create artifacts on the H/V curve with a Konno-Ohmachi logarithmic filter (Konno and Ohmachi, 1998). It is common practice to fix the bandwidth parameter at a value of 40.
- c) The two horizontal Fourier spectra are merged with a quadratic mean for every window.
- d) The H/V spectral ratio is calculated for every window.
- e) H/V spectral ratios are averaged over all windows with a geometric mean to obtain a single H/V curve, and the standard deviation is calculated.

It is mandatory practice to systematically analyse H/V curves in conjunction with the Fourier spectra of the recorded ambient noise components to detect anomalies, for example spurious peaks of industrial origin.

### **Uncertainty Assessment**

Two sets of criteria are proposed in the SESAME guidelines to estimate whether the frequency of the main peak of an H/V curve can be safely considered as the fundamental frequency of the site (or the frequency related to the first strong impedance contrast at depth). The first set is aimed at assessing the reliability of the H/V curve and the quality of the record, while the second set is used for assessing the clearness of the peak. These criteria are adapted to most situations and have been designed for use without any a priori information on geological conditions at the recording site. As pointed out by Haghshenas et al. (2008), the threshold value of some criteria, like the minimum amplitude at which a peak is considered to correspond to the fundamental frequency of the site, may be lowered if other data indicate that some characteristics of the H/V curve or the Fourier spectra occur at the expected frequency.

## **Recommended Guidelines for Reporting**

It is good practice to systematically specify the type of equipment used and document the conditions under which ambient noise is recorded. The report should present the mean Fourier spectra calculated for the three components of the record, and the mean H/V curve with a one standard deviation confidence interval. In addition, the frequency of the main peak, if any, and the values of the reliability and clearness criteria should also be provided. Figure 2.3.1-3 shows an example of a field form (Bard, 2004) which can be adapted to meet specific needs or equipment.

DATE		HOUR		PLACE	
OPERATOR			GPS TYPE and #		
LATITUDE		LONGITUDE		ALTITUDE	
STATION TYPE		SENSOR TYPE			
STATION #		SENSOR #		DISK #	
FILE NAME				POINT #	
GAIN		SAMPL. FREQ. Hz		REC. DURATION <span style="float:right">minutes seconds</span>	
WEATHER CONDITIONS		WIND <input type="checkbox"/> none <input type="checkbox"/> weak (5m/s) <input type="checkbox"/> medium <input type="checkbox"/> strong Measurement (if any): _____ RAIN <input type="checkbox"/> none <input type="checkbox"/> weak <input type="checkbox"/> medium <input type="checkbox"/> strong Measurement (if any): _____ Temperature (approx): _____ Remarks _____			
GROUND TYPE		<input type="checkbox"/> earth ( <input type="checkbox"/> hard <input type="checkbox"/> soft) <input type="checkbox"/> gravel <input type="checkbox"/> sand <input type="checkbox"/> rock <input type="checkbox"/> grass = ( <input type="checkbox"/> short <input type="checkbox"/> tall) <input type="checkbox"/> asphalt <input type="checkbox"/> cement <input type="checkbox"/> concrete <input type="checkbox"/> paved <input type="checkbox"/> other _____ <input type="checkbox"/> dry soil <input type="checkbox"/> wet soil Remarks _____			
ARTIFICIAL GROUND-SENSOR COUPLING <input type="checkbox"/> no <input type="checkbox"/> yes, type _____					
BUILDING DENSITY <input type="checkbox"/> none <input type="checkbox"/> scattered <input type="checkbox"/> dense <input type="checkbox"/> other, type _____					
TRANSIENTS		MONOCHROMATIC NOISE SOURCES (factories, works, pumps, rivers...)			
		<input type="checkbox"/> no <input type="checkbox"/> yes, type _____			
		NEARBY STRUCTURES (trees, polls, buildings, bridges, underground structures, ...)			
		(description, height, distance)			
	none	few	moderate	many	very dense
					distance
cars					
trucks					
pedestrians					
other					
OBSERVATIONS				FREQUENCY: _____ Hz (if computed in the field)	

Figure 2.3.1-3. Example of a field form for single station ambient noise recording (SESAME guidelines, Bard, 2004).

## Hazard-related Case Study

### ***On the Use of Single Station Ambient Noise Techniques for Microzonation Purposes: The Case of Montreal***

*Luc Chouinard and Philippe Rosset  
McGill University, Dept. of Civil Engineering, Montréal, QC*

#### **Introduction**

In Canada, seismic hazard is considered the primary concern among all natural and man-made catastrophes; it is prone to affect the largest proportion of a given territory, and it represents the most stringent test for the robustness of existing infrastructures and for the responsiveness of emergency management agencies. Based on exposed population and on the probability of earthquake occurrence, Montreal ranks second in Canada (around 20% of national risks) after Vancouver for seismic risk (Adams et al., 2002). The city is particularly vulnerable to seismic events for two main reasons: (1) most of its infrastructure is old and deteriorated or has been designed according to standards that predate modern seismic design codes, and (2) the amplification of seismic waves due to unconsolidated river and Champlain sea deposits.

Two microzonation approaches were investigated using the resonance frequency  $f_0$  of a soil deposit as a site characteristic. The first approach is based on the correlation between the frequency of resonance and the maximum amplification factor predicted from an equivalent linear seismic response analysis at the site. The second approach is based on the relationship between the shear wave velocity  $V_S$  and  $f_0$  for various types of soil deposits in the Montreal area.

#### **Data Collection**

The basement of Montreal Island is composed of igneous and metamorphic rocks of Precambrian age covered by Ordovician sedimentary rocks (Trenton Limestone and Utica Shale). The chronological sequence of glacial deposition is described as Malone Till, Middle Till Complex and Fort Covington Till during the Wisconsinian period (ca. 125 000 – 10 000 years BP). All superficial deposits (clay, sand and silt) originate from the Champlain Sea and subsequent wanderings of the St-Lawrence riverbed. The geological map of Figure 2.3.1-4 shows the spatial distribution of these various types of deposits across the island of Montreal.

Site characteristics in the Montreal metropolitan area were investigated with the single station ambient noise method at over 2 600 locations over the span of several years. Three different configurations of 24-bit digitizers coupled to a 3-component velocimeter were used. Field experience shows that recording sessions of 5–7 min at a sampling rate of 100 Hz is adequate to obtain stable and repeatable results for the sites investigated using all three equipment types. Records were analyzed to detect and reject those with an excessive number of transients. For the remaining records, a clear peak could be associated to the resonance frequency on the H/V ratios for two-thirds of the sites. The analysis for the other sites was more complex and required several assumptions (Rosset and Chouinard, 2009).

#### **Recommended citation:**

Chouinard, L. and Rosset, P., 2012. On the Use of Single Station Ambient Noise Techniques for Microzonation Purposes: the Case of Montreal; *in* Shear Wave Velocity Measurement Guidelines for Canadian Seismic Site Characterization in Soil and Rock, (ed.) J.A. Hunter and H.L. Crow; Geological Survey of Canada, Open File 7078, p. 85-93.

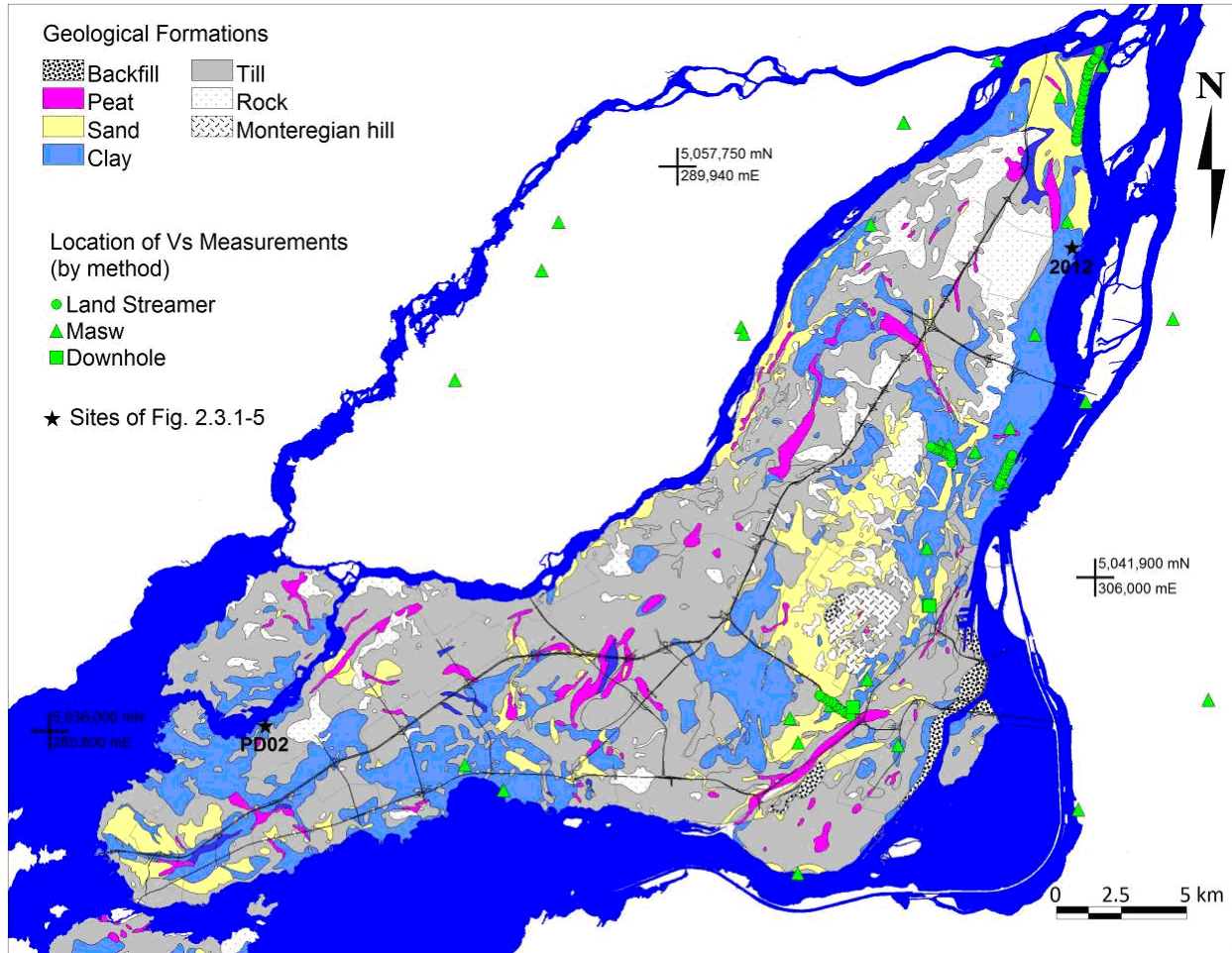


Figure 2.3.1-4. Surface geology map of Montreal showing post-glacial sediments (backfill, peat, sand and clay), glacial (tills) deposits and bedrock (adapted from Prest and Hode-Keyser, 1977). Black stars indicate the locations of the sites presented in Figure 2.3.1-5. Also shown are the locations of field measurement of  $V_s$ .

A dataset of more than 26 600 boreholes (courtesy of the City of Montreal) was compiled to develop a map for depth to bedrock. These boreholes are typically located in areas where roads, metro lines, and lifelines are built, and provide information either on the thickness and type of soils above bedrock, or the thickness and type of soil within the first few metres of the ground surface. A subset of 2500 boreholes provided detailed geological profiles that follow the sequence of the different episodes of deposition from base to top: till, clay, sand, and backfill corresponding to the glacial, marine, river, and man-made episodes respectively.

Shear wave velocity data were obtained from seismic surveys using both body and surface wave measurements: multichannel analyses of surface waves (MASW) at 29 sites, downhole seismic measurements in 3 boreholes, and high resolution multichannel seismic reflection records using a land streamer over a total distance of 7.5 km (Figure 2.3.1-4). The combined data set was used to derive a relationship for  $V_s$  as a function of depth and to obtain  $V_{s30}$ .

### Microzonation

Chouinard and Rosset (2007) and Rosset and Chouinard (2009) combine predominant frequencies of resonance ( $f_0$ ) derived from 750 ambient noise records with soil amplification factors obtained from 1D-SHAKE numerical analyses for 1287 sites (Figure 2.3.1-5).

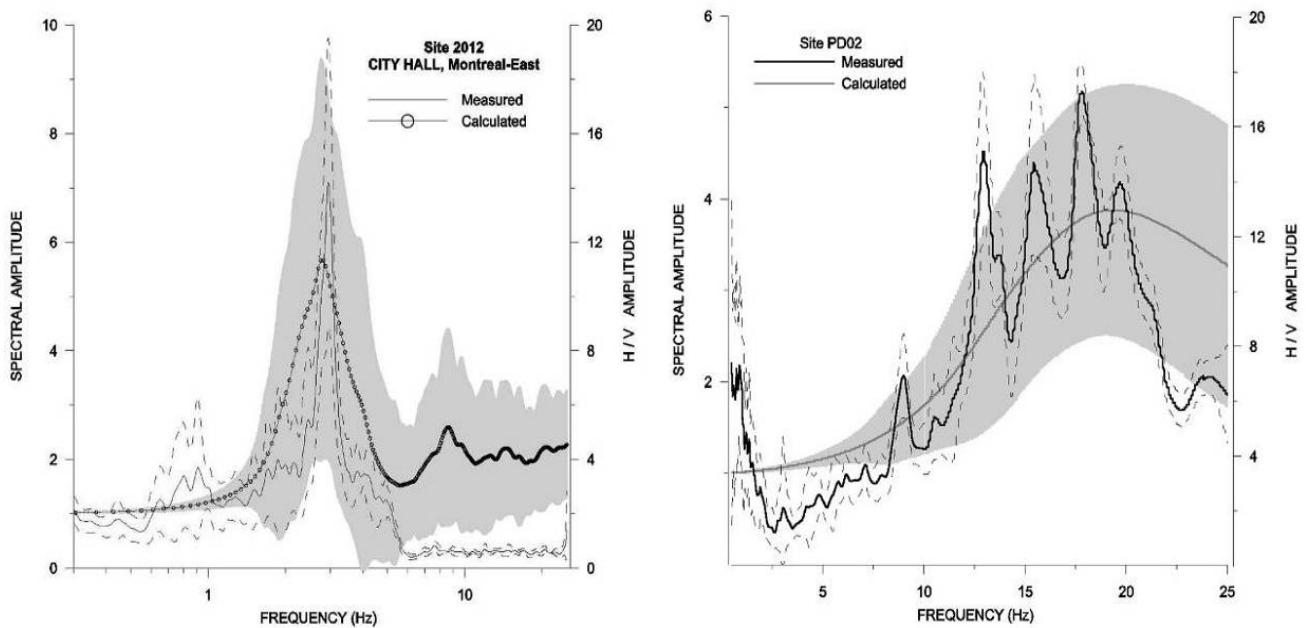


Figure 2.3.1-5. Comparison of H/V spectra (right vertical axis) and 1D modeling (left vertical axis) at two sites. The first site (site 2012) is characterized by a single clear peak while the second site (site PD02) exhibits a more complex response with several peaks. Both cases show good agreement between field measurements and calculated 1D results using borehole data. The grey shaded area corresponds to the margin of error on the calculated sites. Dashed lines relates to the upper and lower ranges of the measured sites.

The frequency-amplitude analysis was performed with a set of 17 input accelerograms from five earthquakes selected by considering the seismic context of Montreal and covering three frequency bands (low, intermediate and high). A relation between amplification factor and  $f_0$  was established showing four frequency ranges: Low amplification for values up to 13 Hz, intermediate amplification for ranges between 1-3 Hz and 7-13 Hz, and large amplification for the range 3-7 Hz. Figure 2.3.1-6 shows the interpolated map of  $f_0$  segregated into zones corresponding to the amplification ranges. The North Eastern tip of the island has the lowest resonance frequencies starting at 2 Hz close to the St-Lawrence River and increasing inland to more than 10 Hz for tills and rock outcrops. Low resonance frequencies are also observed along the Eastern shore of the island close to the St-Lawrence River with values increasing towards the centre of the island.

The frequency of resonance was also correlated with depth to bedrock using a subset of 2159 boreholes reaching basement, particularly in zones where clays are predominant. Figure 2.3.1-7a shows the data and relationship for a subset of 297 sites where clay overlies rock or till basement for boreholes that are within 50 m of an ambient noise measurement. As expected, the results indicate that frequency of resonance decreases with depth to bedrock. Assuming a uniform and homogeneous soil layer, an average shear wave velocity of 147 m/s is inferred for clay deposits with the relationship,  $f_0 = V_S / 4H$ . A significantly better coefficient of determination is obtained when depth is measured to top of till instead of top of bedrock.

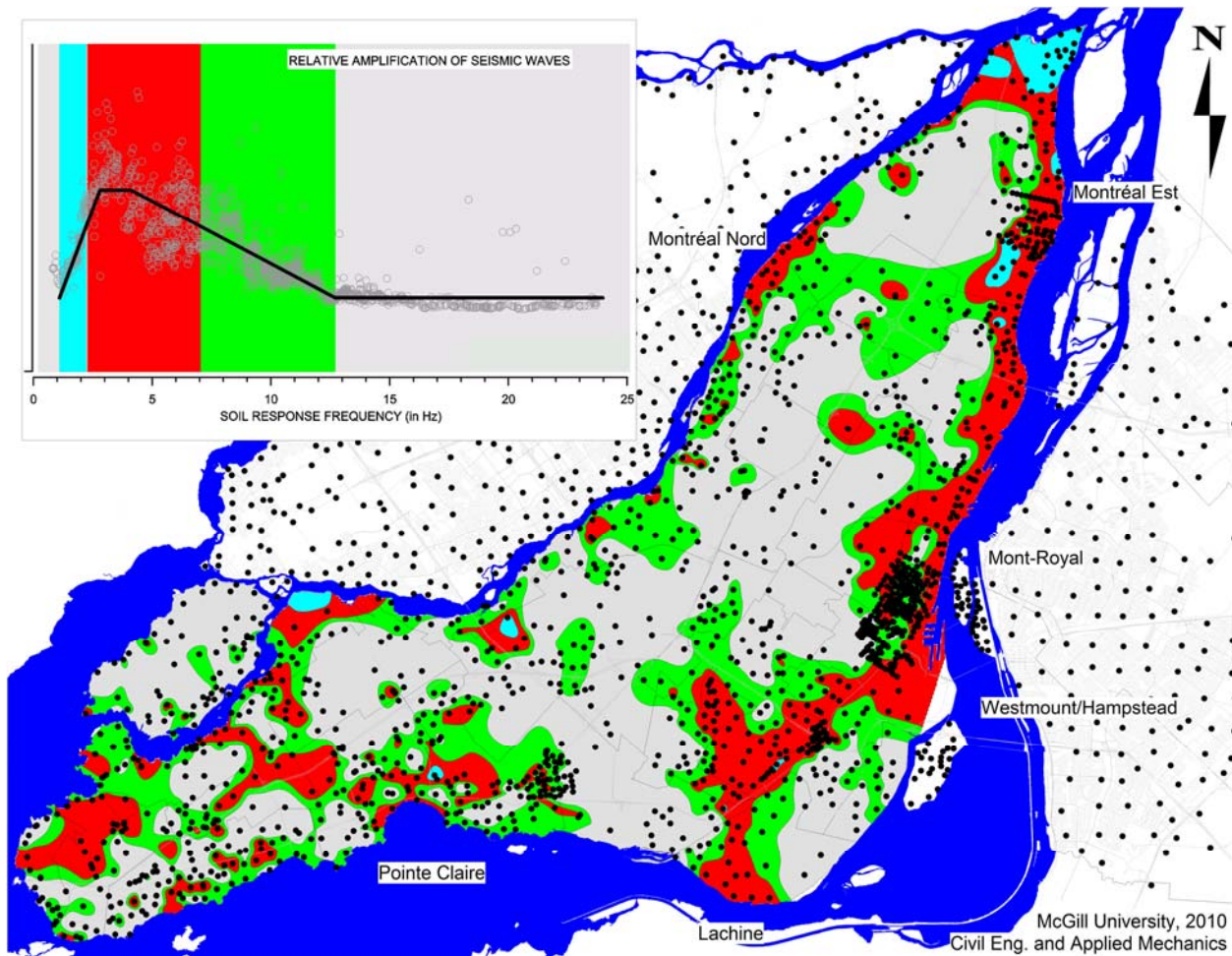


Figure 2.3.1-6. Microzonation map of Montreal based on the fundamental frequency of resonance  $f_0$  HVSR (black dots) and amplification factors derived from a 1D numerical model (top-left graph).

Estimates of  $f_0$  and  $V_{S30}$  at neighbouring locations were obtained from seismic data at 86 sites (Figure 2.3.1-7b). A weighted linear regression was used to derive a relationship between  $f_0$  and  $V_{S30}$  by assigning a lower weight (0.5) to data points when the spatial distance between the location of  $f_0$  and  $V_{S30}$  measurements is greater than 50m or when  $V_{S30}$  measurements were obtained with MASW. The resulting equation is as follows:

$$V_{S30} = 177 + 44.7 f_0 \quad [2.3.1-1]$$

where  $V_{S30}$  is in m/s, and 1 standard deviation is 89m/s.

The predominant period of resonance  $T_0$  obtained with ambient noise was compared to the one derived from the double travel time on 2D high resolution seismic profiles at 33 sites. A very good agreement was obtained between the two estimates up to 0.7 s (Figure 2.3.1-7c) which validates the accuracy of the ambient noise technique for deposits typical of Montreal.

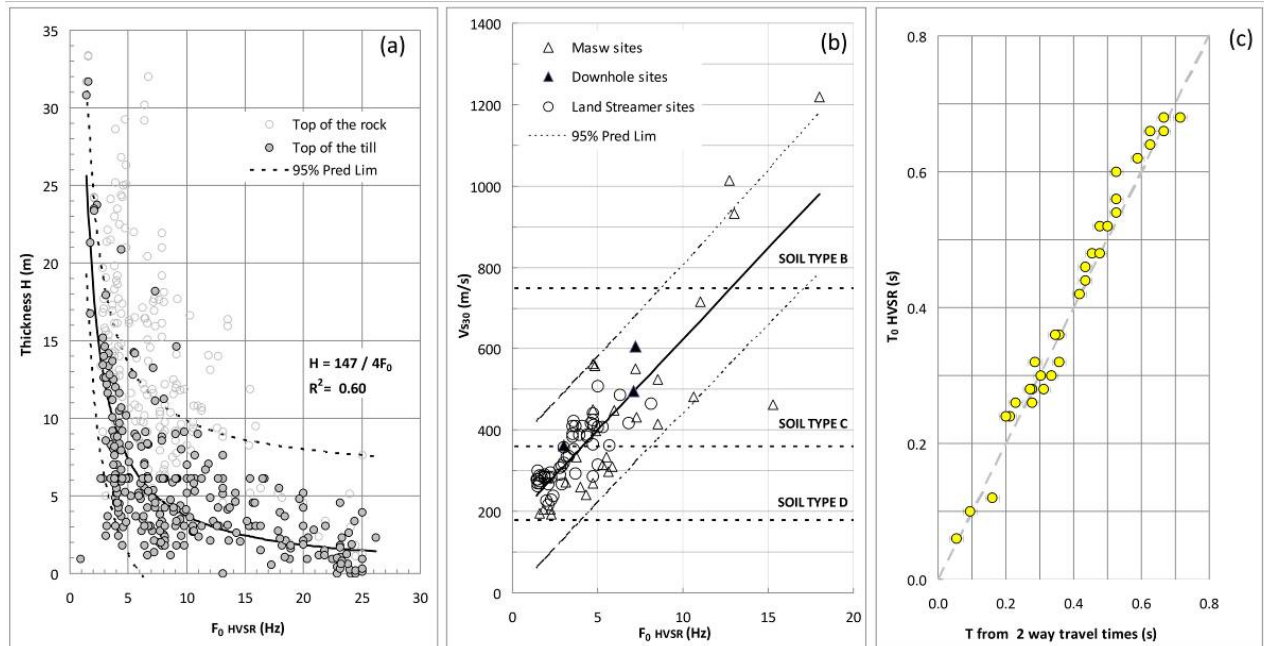


Figure 2.3.1-7. (a) Non-linear regressions between frequency of resonance and thickness of post-glacial layer. (b) Relation between  $V_{S30}$  derived from various seismic methods and the frequency of resonance estimated from ambient noise records. (c) Comparison between the periods of resonance estimated from ambient noise measurements and calculated from the double travel time on seismic reflection profiles.

Figure 2.3.1-8 shows estimates of  $V_{S30}$  obtained by applying Equation 2.3.1-1 with the frequency of resonance  $f_0$  obtained at 2413 locations. A natural weighted neighbourhood interpolation procedure is used to estimate  $V_{S30}$  on a regular grid of points with 50 m spacing. The contour lines are based on soil classes A to E defined in the NBCC 2005 according to  $V_{S30}$  ranges. Rosset et al. (2011) describe and compare in more detail various alternate procedures to obtain estimates of  $V_{S30}$  from field data.

## Conclusions

In urban areas, the frequency of resonance of a site  $f_0$  can be easily and quickly obtained with the single station ambient noise method. A comparison of frequencies derived from ambient noise measurements and from 2D high resolution seismic profiles showed good agreement for clay sites. Different means of integrating this information in producing microzonation maps were investigated. One approach is to correlate  $f_0$  with the frequency of the maximum amplification factor obtained from equivalent linear seismic response analyses for a set of input strong motion records. The second approach is to combine the information on the frequency with corresponding field measurements of the shear wave velocity. A function was derived between  $V_{S30}$  (obtained from  $V_S$  values of 86 sites) and  $f_0$  and applied at 2413 sites where  $f_0$  had been measured. The interpolated values of  $V_{S30}$  were then used to derive a soil classification map using the categories defined in the NBCC 2005.

Finally, a comparison of  $f_0$  with soil thickness and  $V_{S30}$  measurements shows that the classification procedure is accurate for clay and sand deposits. For locations predominantly with till or complex deposition history, the proposed classification procedures are less accurate. To correct for this limitation, Rosset et al. (2011) propose a more advanced classification procedure that incorporates additional information obtained from borehole data and geological information.

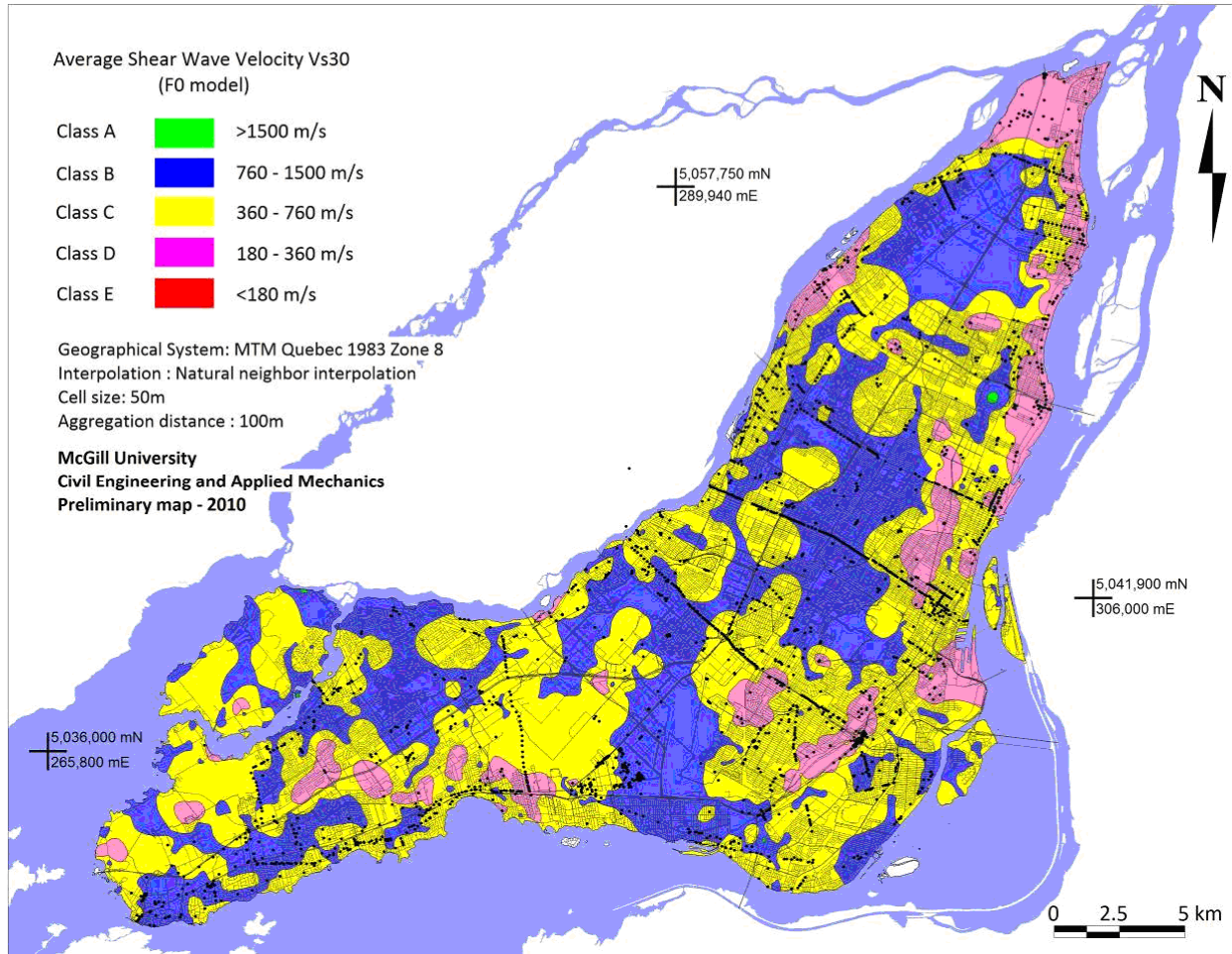


Figure 2.3.1-8. Microzonation map of soil classes (NBCC 2005) derived from ambient noise measurements of  $f_0$  at 2413 sites and Equation 2.3.1-1.

## Acknowledgements

Luc Chouinard and Philippe Rosset would like to acknowledge the financial support of NSERC and the financial support and collaboration of the City of Montreal and the Geological Survey of Canada.

## References

Adams, J., Rogers, G., Halchuk, S., McCormack, D. and Cassidy, J., 2002. The case for an advanced national earthquake monitoring system for Canada's cities at risk; *in* Proceedings, 7<sup>th</sup> U.S. National Conference on Earthquake Engineering, Boston, MA.

Bard, P.-Y., 1999. Microtremor measurements: a tool for site estimation?; *in* Proceedings, 2<sup>nd</sup> International Symposium on the Effects of Surface Geology on Seismic Motion, Yokohama, Balkema Publishers, Netherlands, v3, p.1252-1279.

Bard, P.-Y. (co-ordinator), 2004. Guidelines for the implementation of the H/V spectral ratio technique on ambient vibrations measurements, processing and interpretation; Final report: European Commission - Research General Directorate, Project No. EVG1-CT-2000-00026, SESAME, 62 p. <[http://sesame-fp5.obs.ujf-grenoble.fr/Papers/HV\\_User\\_Guidelines.pdf](http://sesame-fp5.obs.ujf-grenoble.fr/Papers/HV_User_Guidelines.pdf)> [accessed March 2012].

Bard, P.-Y., 2008. Forward - The H/V technique: capabilities and limitations based on the results of the SESAME project; *Bulletin of Earthquake Engineering*, v.6, p.1-2.

Bonilla, L.F., Steidl, J.H., Lindley, G.T., Tumarkin, A.G. and Archuleta, R.J., 1997. Site amplification in the San Fernando Valley, California: Variability of site-effect estimation using the S-Wave, coda, and H/V methods; *Bulletin of the Seismological Society of America*, v. 87, p.710-730.

Bonnefoy-Claudet, S., Cornou, C., Bard, P.-Y., Cotton, F., Moczo, P., Kristek, J. and Fäh, D., 2006. H/V ratio: a tool for site effects evaluation. Results from 1-D noise simulations; *Geophysical Journal International*, v. 167, p. 827-837.

Borcherdt, R.D., 1970. Effects of local geology on ground motion near San Francisco Bay; *Bulletin of the Seismological Society of America*, v. 60, p. 29-61.

Bour, M., Fouissac, D., Dominique, P. and Martin, C., 1998. On the use of microtremor recordings in seismic microzonation; *Soil Dynamics and Earthquake Engineering*, v. 17, p. 465-474.

Cara, F., Di Giulio, G., Milana, G., Bordoni, P., Haines, J. and Rovelli, A., 2010. On the stability and reproducibility of the horizontal-to-vertical spectral ratios on ambient noise: Case study of Cavola, Northern Italy; *Bulletin of the Seismological Society of America*, v. 100, p.1263-1275.

Castellaro, S. and Mulargia, F., 2009a. The effect of velocity inversions on H/V; *Pure and Applied Geophysics*, v. 166, p. 567-592.

Castellaro, S. and Mulargia, F., 2009b. Vs30 estimates using constrained H/V measurements; *Bulletin of the Seismological Society of America*, v. 99, p.761-773.

Castellaro, S. and Mulargia, F., 2010. How far from a building does the ground-motion free-field start? The Cases of three famous towers and a modern building; *Bulletin of the Seismological Society of America*, v. 100, p.2080-2094.

Chatelain, J.L., Guiller, B., Cara, F., Duval, A.-M., Atakan, K., Bard, P.-Y. and WP02 SESAME Team, 2008. Evaluation of the influence of experimental conditions on H/V results from ambient noise recordings; *Bulletin of Earthquake Engineering*, v. 6, p. 33-74.

Chavez-Garcia, F.J., 2009. Ambient noise and site response: From estimation of site effects to determination of the subsoil structure; *in Increasing Seismic Safety by Combining Engineering Technologies and Seismological Data*, NATO Science for Peace and Security, Series C, (eds.) M. Mucciarelli et al.; Springer Science, Chapter 1.4, p. 53-71.

Chouinard, L.E. and Rosset, P., 2007. Seismic site effects and seismic risk in the Montreal urban area. The influence of marine clays; *in Proceedings, 9<sup>th</sup> Canadian conference on earthquake engineering*, Ottawa, Ontario, Canada, p.26-29.

Cornou, C., Guiller, B., Boussoura, K., Selmi, K. and Renalier, F., 2007. Limite de la technique H/V comme outil d'exploration géophysique pour les structures 2D/3D; *in Proceedings, 7<sup>th</sup> Conference AFPS (Association Française de Génie Parasismique)*, p.1-8.

Foti, S., Parolai, S., Albarello, D. and Picozzi, M., 2011. Application of surface-wave methods for seismic site characterization; *Surveys in Geophysics*, v. 32, p. 777-825.

<<http://edoc.gfz-potsdam.de/gfz/get/17300/0/c1fe6ced83fd521c052dd55da80c233/17300.pdf>>

[accessed March 2012]

- Gueguen, P., Cornou, C., Garambois, S. and Banton, J., 2007. On the limitation of the H/V spectral ratio using seismic noise as an exploration tool: Application to the Grenoble Valley (France), a small apex ratio basin; *Pure and Applied Geophysics*, v. 164, p. 115-134.
- Guiller, B., Atakan, K., Chatelain, J.-L., Havskov, J., Ohrnberger, M., Cara, F., Duval, A.-M., Zacharopoulos, S., Teves-Costa, P. and SESAME Team, 2008. Influence of instruments on the H/V spectral ratios of ambient vibrations; *Bulletin of Earthquake Engineering*, v. 6, p. 3-31.
- Haghshenas, E., Bard, P.-Y., Theodulidi, N. and WP04 SESAME Team, 2008. Empirical evaluation of microtremor H/V spectral ratio; *Bulletin of Earthquake Engineering*, v. 6, p. 75-108.
- Hobiger, M., Le Bihan, N., Cornou, C. and Bard, P.-Y., 2009. Rayleigh wave ellipticity estimation from ambient seismic noise using single and multiple vector-sensor techniques; *in Proceedings, 17<sup>th</sup> European Signal Processing Conference (EUSIPCO 2009)*, Glasgow, Scotland, p.2037-2041. <<http://www.eurasip.org/Proceedings/Eusipco/Eusipco2009/contents/papers/1569190656.pdf>> [accessed March 2012]
- Konno, K. and Ohmachi, T., 1998. Ground-motion characteristics estimated from spectral ratio between horizontal and vertical components of microtremor; *Bulletin of the Seismological Society of America*, v. 88, p. 228-241.
- Lunedei, E. and Albarello, D., 2010. Theoretical HVSR curves from full wavefield modelling of ambient vibrations in a weakly dissipative layered Earth; *Geophysical Journal International*, v. 181, p. 1093-1108.
- Maresca, R., Nardone, L., Pasquale, G., Pinto, F. and Bianco, F., 2011. Effects of surface geology on seismic ground motion deduced from ambient-noise measurements in the town of Avellino, Irpinia region (Italy); *Pure and Applied Geophysics*, doi: 10.1007/s00024-011-0390-3.
- Nakamura, Y., 1989. A method for dynamic characteristics estimation of subsurface using microtremor on the ground surface; *Quarterly Report of Railway Technical Research Institute (RTRI)*, Japan, v. 30, p. 25–33.
- Nogoshi, M. and Igarashi, T., 1971. On the amplitude characteristics of microtremor (Part 2); *Journal of the Seismological Society of Japan*, v. 24, p. 26-40 (in Japanese, with English abstract).
- Parolai, S., Picozzi, M., Strollo, A., Pilz, M., Di Giacomo, D., Liss, B. and Bindi, D., 2009. Are transients carrying useful information for estimating H/V spectral ratios? *in Increasing Seismic Safety by Combining Engineering Technologies and Seismological Data*, NATO Science for Peace and Security, Series C, (eds.) M. Mucciarelli et al.; Springer Science, Chapter 1.2, p.17-31.
- Prest, V.K. and Hode-Keyser, J., 1977. Geology and engineering characteristics of surficial deposits, Montreal island and vicinity, Quebec; *Geological Survey of Canada*, Paper no.75–27, 28 p. and 2 maps.
- Rosset, P. and Chouinard, L.E., 2009. Characterization of site effects in Montreal, Canada; *Natural Hazards*, v. 48, p. 295-308.
- Rosset, P., Bour, M. and Chouinard, L.E., 2011.  $V_{s30}$  maps for Montreal. Variability of the contours (in preparation).
- Sanchez-Sesma, F. J., Rodriguez, M., Iturraran-Viveros, U., Luzon, F., Campillo, M., Margerin, L., Garcia-Jerez, A., Suarez, M., Santoyo, M.A. and Rodriguez-Castellanos, A., 2011. A theory for microtremor H/V spectral ratio: application for a layered medium; *Geophysical Journal International*, v. 186, p. 221-225.
- Woolery, E.W. and Street, R., 2002. 3D near-surface soil response from H/V ambient-noise ratios; *Soil Dynamics and Earthquake Engineering*, v. 22, p. 865-876.

## Additional Readings

Bonnefoy-Claudet, S., Köhler, A., Cornou, C., Wathelet, M. and Bard, P.-Y., 2008. Effects of Love waves on microtremor H/V ratio; *Bulletin of the Seismological Society of America*, v. 98, p. 288-300.

Finn, W.D. L. and Wightman, A., 2003. Ground motion amplification factors for the proposed 2005 edition of the National Building Code of Canada; *Canadian Journal of Civil Engineering*, v. 30, p. 272–278.

Lermo, J. and Chavez-Garcia, F.J., 1994. Are microtremors useful in site response evaluation?; *Bulletin of the Seismological Society of America*, v. 84, p. 1350–1364.

Nakamura, Y., 2000. Clear identification of fundamental idea of Nakamura's technique and its application; *in Proceedings, 12<sup>th</sup> World conference Earthquake Engineering, New Zealand, Paper no.2656.*

Rosset, P., 2002. SPCRATIO User's Manual: a tool to analyze ambient noise records; *Structural Engineering Series, University McGill, Montreal, Report no.2002-01, 20 p.*

Wathelet, M., 2006. Noise blind test: retrieving dispersion curves and inversion with the conditional neighbourhood algorithm; *in Proceedings, 3<sup>rd</sup> International Symposium on the Effect of Surface Geology on Seismic Motion, Grenoble, France.* <<http://marc.geopsy.org/publi/wathelet-esg2006.pdf>> [accessed March 2012].

A free **open-source software**, J-SESAME, has been developed by the SESAME group for processing and analysing ambient noise data. The functionalities of J-SESAME have since been ported to the H/V toolbox of the more comprehensive Sesarray/Geopsy application (Wathelet, 2006).

J-SESAME, 2004. User manual, Version 1.08:

FTP site: <ftp://ftp.geo.uib.no/pub/sesame/JSESAME/>

Journal summary: <http://dx.doi.org/10.1007/s10518-008-9059-4>

Sesarray/Geopsy (2011). Release 2.4.0. ([www.geopsy.org](http://www.geopsy.org)).

## 2.3.2 Spatially Averaged Coherency Spectrum (SPAC) Ambient Noise Array Method

Maxime Claprod

Institut National de la Recherche Scientifique (INRS), Québec, QC

### Introduction

#### Principles of the Method

Simultaneous ambient noise records (time series) are recorded by all sensors of a 2D array. The SPAC method considers ambient noise as a temporal and spatial stochastic process in order to evaluate coherency spectra between all pairs of sensors in the array. Coherency spectra are a measure of the similitude of ambient noise records from specific sensors for the frequency bandwidth investigated, and are mostly related to the  $V_s$  profile under the array of sensors. The coherency spectra generated between all pairs of sensors in the array are azimuthally averaged over several inter-station separations (Henstridge, 1979; Cho et al., 2004) to determine spatially averaged coherency spectra which have the shape of Bessel functions with respect to the  $V_s$  profile (Aki, 1957). The principles of the method are described in detail in Okada (2003).

#### Current State of Engineering Practice

The SPAC method is one of the traditional array-based ambient noise methods used to determine  $V_s$  profiles. It was developed by Aki (1957) under the name 'Spatial Autocorrelation' method. The name 'SPatially Averaged Coherency' method is now preferred because it better represents the actual data processing in the frequency domain (coherency spectra). Typical arrays used in practice are the centered triangular and hexagonal arrays (Figure 2.3.2-1).

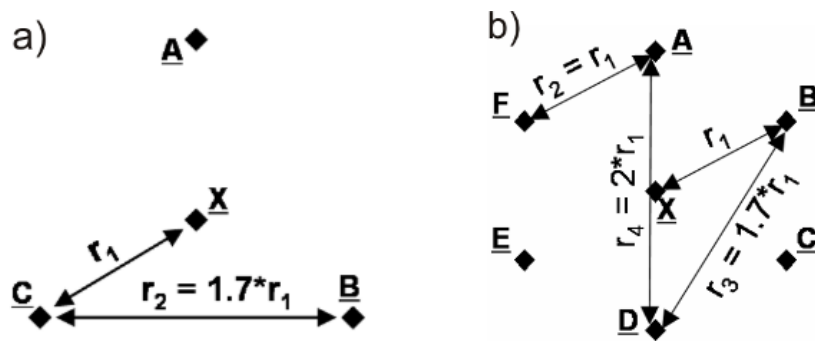


Figure 2.3.2-1. Conventional array geometries for SPAC observations. a) Centered triangular array (3 sensors – A,B,C, plus a center sensor - X) with two inter-station separations  $r_1$  and  $r_2$ . b) Centered hexagonal array (6 sensors – A-F, plus a center sensor - X) with four inter-station separations  $r_1$ ,  $r_2$ ,  $r_3$ , and  $r_4$ .

#### Recommended citation:

Claprod, M., 2012. Spatially Averaged Coherency Spectrum (SPAC) Ambient Noise Array Method; in Shear Wave Velocity Measurement Guidelines for Canadian Seismic Site Characterization in Soil and Rock, (ed.) J.A. Hunter and H.L. Crow; Geological Survey of Canada, Open File 7078, p. 94-102.

Successive use of arrays with increasing radii is common to widen the frequency range, and by doing so, to extend the depth of investigation. Arrays which deviate from the standard configurations have also provided excellent results (Bettig et al., 2001; Ohori et al., 2002; Cho et al., 2004). Traditional use of SPAC data considers only the vertical component of ambient vibrations, but adaptation to three-components (3c-SPAC) has proven efficient in resolving Rayleigh and Love wave dispersion curves, gaining further constraints on the  $V_S$  profile (Aki, 1957; Köhler et al., 2007). The SPAC method requires fewer sensors and smaller arrays to achieve similar resolution to the  $f-k$  method (Henstridge, 1979; Chavez-Garcia et al., 2005; Okada, 2003, 2006; Claprod and Asten, 2009a), making it the preferred method where urban logistics preclude the use of arrays with more complex geometry (Stephenson et al., 2009).

### **Limitations**

The most restricting limits are the need of a flat-layered earth and ground surface topography beneath the spatial extent of the array. A methodology was developed by Claprod et al. (2011) to evaluate  $V_S$  profiles above the deepest part of 2D valley, thereby extending the limits of the method. In contrast to the  $f-k$  method, the SPAC method requires a complete azimuthal distribution of ambient noise to provide unbiased  $V_S$  profiles (Asten, 2006). The interpretation of SPAC observations does not resolve fine layered structure and offers poor resolution of the bedrock velocity (Cornou et al., 2006; Molnar et al., 2010), consistent with surface wave methods in general. The depth of investigation is related to the frequency content of the ambient noise data obtained in the field, which is relatively unknown *a priori*; hence, there are no universal guidelines at this time.

## **Data Collection**

### **Required Equipment**

A centered triangular array of three circumferential vertical-component sensors (plus a center sensor) is a recommended minimum. The use of 3-component sensors is ideal because it allows the evaluation of horizontal to vertical spectral ratio (HVSR), which can be used to evaluate the frequencies of resonance at the site, and can also be used to check the required layered earth assumption of surface wave methods. Equipment includes a three-component broad-band sensor connected to a digitizer, an external GPS antenna for timing, a small external battery, and associated cables. Tape measure and/or a GPS for spatial measurement are required for positioning the geophones in the array. A compass is recommended to align all sensors to the same orientation if 3cSPAC is used.

### **Data Collection Procedures**

Similar data collection procedures are recommended for the array method as for the single-station method. Good sensor/ground coupling is required. Symmetric array geometries are ideal to gain redundancy in data for noise reduction and zeroing of imaginary component of the observed complex coherency spectra, which is used as quality control on data (Asten, 2006). The recording of long time series (20 minutes or more) is recommended to reduce uncorrelated statistical noise in the collected data. The length of the time series should be chosen proportionally to the expected frequency of interest (lower frequency = longer time series). To obtain dispersion characteristics over the widest frequency band possible, the array aperture is adjusted several times in the field to account for the trade-off between resolution and aliasing of the narrow target wavelength associated with each array aperture (Jongmans et al. 2005). The domain of validity of the frequency interval to interpret SPAC observations is still debated in the literature. Henstridge (1979) and Okada (2006) suggested restricting the upper frequency limit to the Nyquist frequency or to a frequency relative to the number of sensors used in the array. On the other hand, Asten (2006) and Claprod and Asten (2010) have demonstrated that the SPAC method can be reliable to much higher frequency when the ambient vibration wavefield has adequate azimuthal distribution, increasing resolution in shallow layers.

## Processing Techniques

### Theory of Analysis

Ambient noise from all sources and directions is observed with an array of sensors azimuthally distributed at a distance  $r$  from a center sensor. The integration of coherency spectra over azimuth leads to the spatially averaged coherency spectrum:

$$C(f) = J_0(rk) = J_0\left[\frac{2\pi fr}{V(f)}\right] \quad [2.3.2-1]$$

where  $f$  is the frequency and  $J_0$  is the Bessel function of first kind and zero order of variable  $rk$  ( $k$  is spatial wavenumber).  $V(f)$  is the  $V_s$  dispersion function of a layered earth model for which the  $V_s$  profile is evaluated. Observed time series of ambient noise are divided into time segments which are then fast-Fourier transformed in the frequency domain to obtain the raw spectra  $S_i(f)$  of ambient noise energy at every sensor  $i$ . The coherency spectrum between each pair of sensors ( $i,j$ ) is computed using the equation:

$$C_{i,j}(f) = \frac{S_i(f)S_j^*(f)}{\sqrt{S_i(f)S_i^*(f)S_j(f)S_j^*(f)}}, \quad [2.3.2-2]$$

where  $C_{i,j}(f)$  is the complex coherency spectra and  $*$  denotes the complex conjugate. Complex coherency spectra are averaged over time segments to yield the temporally averaged coherency spectrum at each pair of sensors, which are then averaged over azimuth for all  $n$  to obtain the observed spatially averaged coherency spectrum  $C(f)$  and recover  $V(f)$  from Equation 2.3.2-1.

### Uncertainty Assessment

An assessment of uncertainty is essential to evaluate the reliability of SPAC observations and the interpreted  $V_s$  profile. Asten (2006) proposed to use the imaginary component of complex coherency spectra to evaluate the ambient noise distribution and the level of uncorrelated statistical noise in the ambient vibration record with respect to frequency. This concept was applied with success in Clapgood and Asten (2010) and Clapgood et al. (2011) to describe the ambient noise azimuthal distribution, and identify possible 2D geological effects on SPAC observations. The evaluation of misfit criteria such as the sum of square of residuals (SSR) or mean square of residuals (MSR) between observed and theoretical coherency spectra is a minimum uncertainty assessment technique, while a complete search of the model parameterization space is preferred. While higher mode Rayleigh waves are not always included in the inversion process, it is suggested to plot the fundamental and 1st higher mode Rayleigh waves when comparing observed and theoretical dispersion curves (or coherency spectra), to identify possible jumps to higher modes of propagation.

## Recommended Guidelines for Reporting

The field procedure must be reported (array layout, number of sensors, inter-station separation, etc.), along with the level of noise at proximity to (or within) the array. SPAC processing is optimal when most of the ambient noise energy originates  $\geq 2$  radii from the array. Sources of noise within 2 radii (i.e. heavy traffic road, industries, etc.) should be noted to explain possible departure to the theoretical SPAC curves (Roberts and Asten, 2008). The processing procedures used to extract dispersion characteristics should be explained, with presentation of empirical dispersion curve and associated fit obtained by  $V_s$  profiles (models) from the inversion. Generally, non-linear optimization-based inversion procedures are applied with presentation of the best-fit  $V_s$  profile with/out all or a sub-set of models sampled during the inversion. Asten et al. (2004) suggested inverting the coherency spectrum and directly evaluating  $V_s$  profiles without the additional step of computing the dispersion curve, in order to optimize the information recovered from

the coherency spectra. Wathelet et al. (2003) successfully used a neighbourhood search algorithm to directly recover  $V_S$  profiles from inversion of the coherency spectra. Amplification spectra are usually predicted based on the  $V_S$  profiles and compared with empirical earthquake and/or ambient vibrations spectral ratios for evaluation of site response characterization.

## **Hazard-Related Case Studies**

To the author's knowledge, the SPAC method is yet to be applied in Canada. There are plans to acquire SPAC data to investigate the sedimentary successions of the St. Lawrence Lowlands in the near future. A case study from Tasmania, Australia is presented (Clapgood and Asten, 2009b).

### **Launceston, Tasmania, Australia**

Ambient vibrations were recorded at ten sites within the city centre of Launceston, Tasmania, Australia (Figure 2.3.2-2a) to evaluate the  $V_S$  structure and its variation in the Tamar Valley region. Rapid changes in surface geology occur within the city of Launceston, as shown in Figure 2.3.2-2b. The bedrock at Launceston is a dense, fractured and weathered dolerite of Jurassic age. Structures built on this outcropping bedrock tend to experience reduced seismic shaking when compared to structures built on accumulations of local unconsolidated deposits (Leaman, 1994). Tertiary sands and clays of low density fill an ancient valley system running beneath the city of Launceston, as outlined by the interpretation of two gravity profiles (Figure 2.3.2-2c). These deposits are overlain by poorly consolidated Quaternary alluvial sediments (silts, gravels, fills) deposited on the valley floor and in marshy areas near sea level.

SPAC observations were derived from microtremors recorded during two field surveys in 2006 and 2007. Centered hexagonal arrays of seven vertical component 4.5 Hz sensors were used in 2006, while centered triangular arrays of four three-component low-frequency (0.0167 or 0.033 Hz) geophones were used in 2007 to gain sensitivity at low frequency and depth. Arrays with radii varying between 15 m to 150 m were used during the two surveys. The observed coherency spectra are directly fit to the theoretical coherency spectrum by least-squares optimization to evaluate the  $V_S$  profile under each array (Figure 2.3.2-3). A complete search of the model parameterization space was not completed at Launceston, and confidence in the interpretation is expressed by the mean square of residuals between the observed and theoretical coherency spectra.

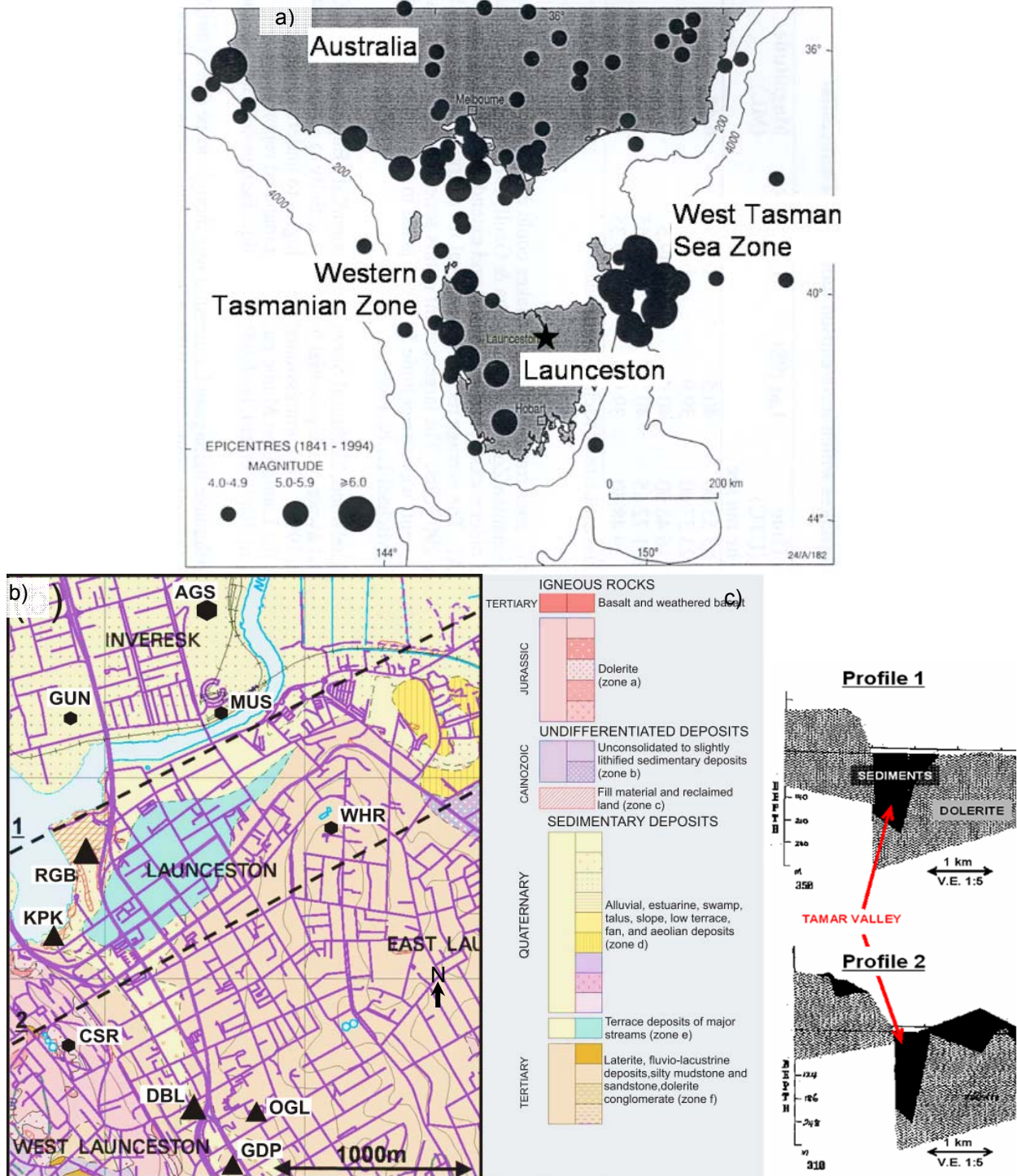


Figure 2.3.2-2. a) Location of Launceston, Tasmania, Australia. Epicentres of earthquakes with Richter magnitude of 4.0 or more from 1884-1994 (modified from Michael-Leiba, 1995). b) Surface geology map of Launceston (modified from Mineral Resources Tasmania), with location of SPAC microtremor observations during 2006 and 2007 field surveys. c) Geological profiles obtained from gravity survey 1 and 2 in geological map outlining the presence of the Tamar valley (modified from Leaman, 1994).

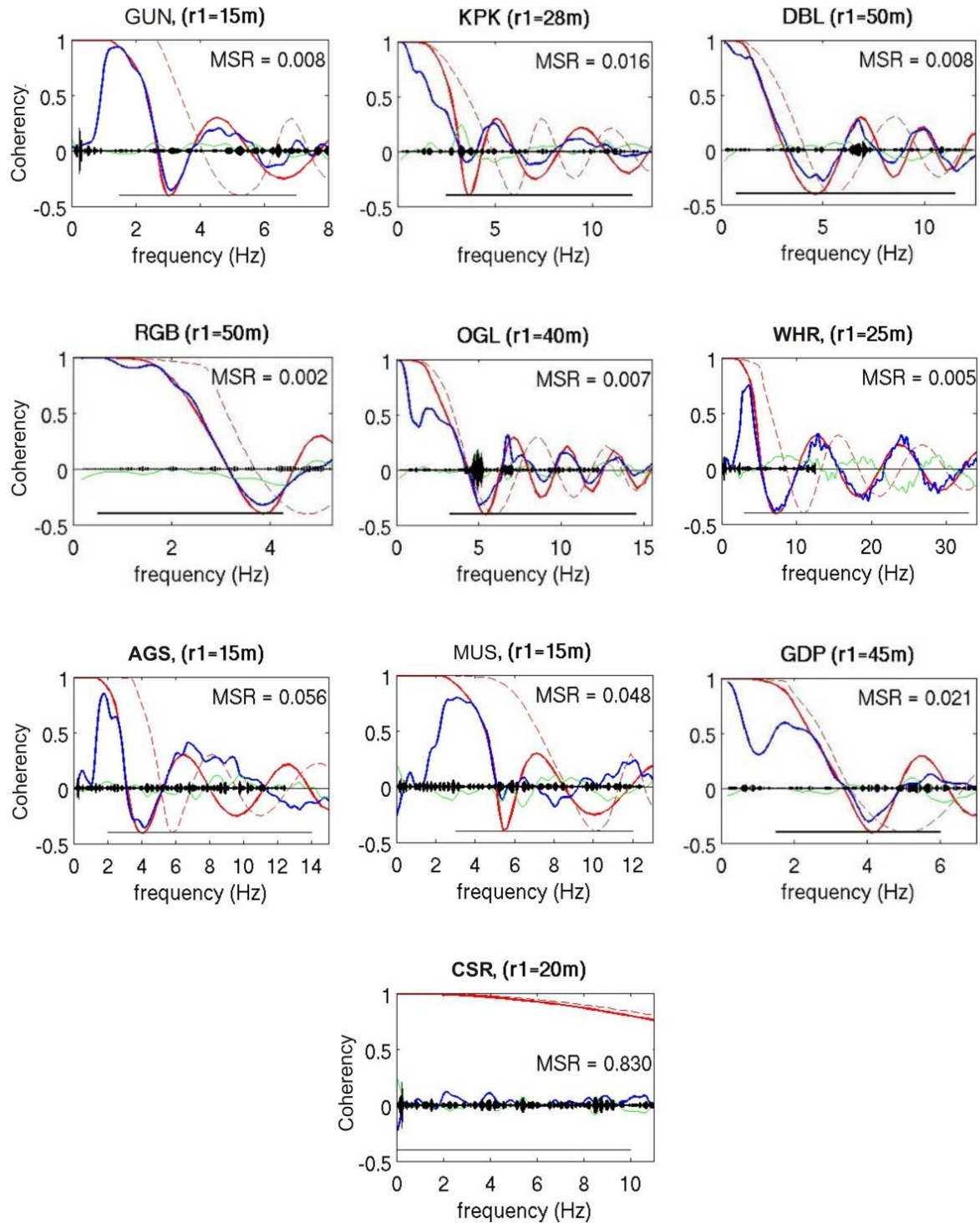


Figure 2.3.2-3. Selected observed coherency spectrum (COH) at sites (from top left to bottom right): GUN, MUS, AGS, KPK, DBL, RGB, OGL, GDP, WHR, and CSR. Location of sites is shown in Figure 2.3.2-2b. Blue lines: Observed spatially averaged COH at inter-sensor separation  $r_1$ . Solid and dashed red lines: Theoretical COH from preferred SWV profile, fundamental and 1<sup>st</sup> higher modes respectively. Green line and black bars: Imaginary components of COH to evaluate the ambient noise distribution and the level of uncorrelated statistical noise. Straight line at bottom of each graph is the frequency interval where theoretical COH is fit to observed COH.

Figure 2.3.2-4 shows the resulting best-fit  $V_S$  profile for each inverted COH spectra for the ten sites. The errors were evaluated directly on the coherency spectrum, and a complete error analysis on  $V_S$  profiles was not performed.  $V_S$  profiles interpreted in North Launceston (Inveresk, sites AGS, MUS, GUN) suggest the presence of very low velocity sediments over shallow dolerite bedrock; the  $V_S$  profiles agree well with the information interpreted from HVSr data recorded and calculated at all three sites.  $V_S$  profiles evaluated at two sites located above the deepest point of the Tamar Valley in Launceston City Centre suggests the SPAC method may be applied in a 2D valley environment (i.e. sites DBL, KPK). SPAC observations recorded over the eastern flank of the Tamar Valley (i.e. sites OGL, RGB) suggest a rapidly varying bedrock surface and, as expected, low quality coherency spectra. SPAC observations recorded on top of the hill in West Launceston (site CSR) show low level of microtremor energy, poor coherency spectra, and absence of peak on HVSr observations, suggesting the presence of dolerite bedrock at the surface.

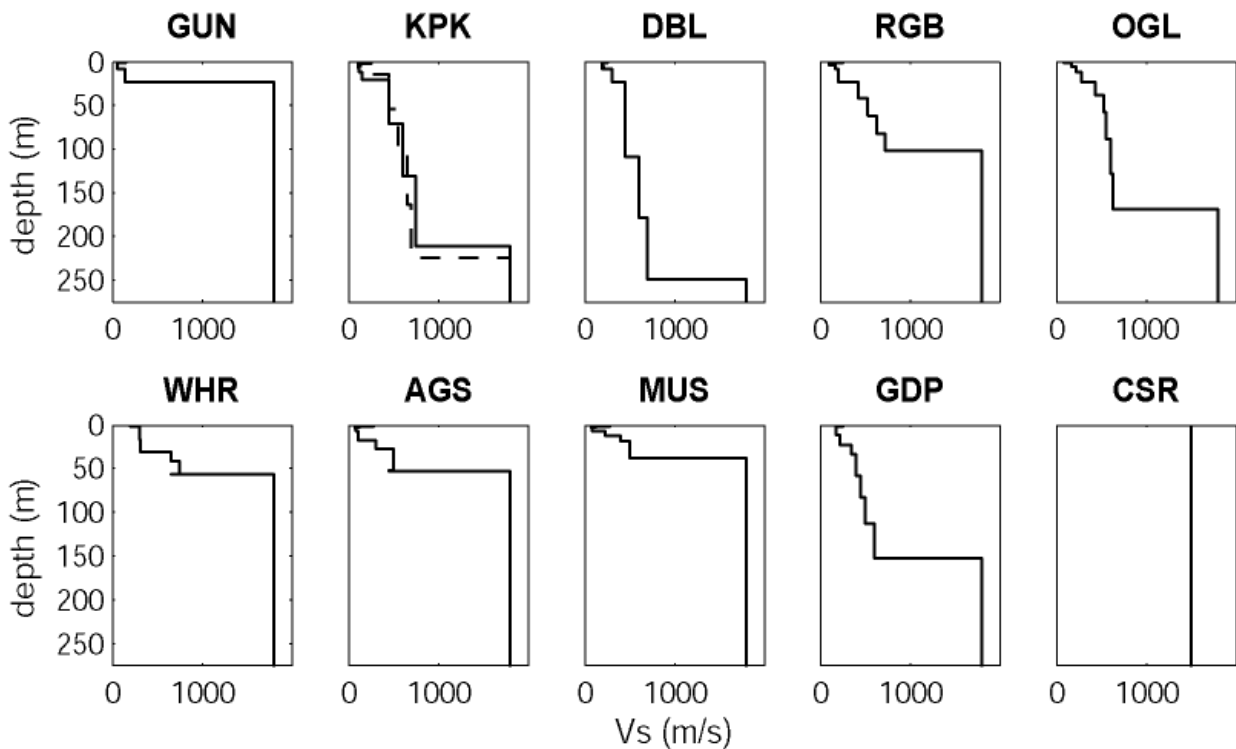


Figure 2.3.2-4. Preferred  $V_S$  profiles at all 10 sites in Launceston from interpretation of SPAC observations. Dashed  $V_S$  profile at site KPK is obtained from 100m radius centred triangular arrays (not presented).

$V_S$  profiles evaluated by the SPAC method (Figure 2.3.2-4) agree well with information derived from boreholes drilled at (or near) sites GUN, MUS, and DBL for the shallowest 20 m, and resolve the shallowest layers with accuracy. By choosing adequate inter-station separation in the array, the SPAC method could be used with confidence to assign seismic site class ( $V_{S30}$ ). When recording SPAC observations with larger inter-station separations, it also had enough resolution to evaluate  $V_S$  of deeper sediments; such as sites DBL, KPK which location and depth to bedrock agree well with the interpretation of gravity profiles.

## Acknowledgments

Financial support was provided by the Monash Graduate Scholarship, the International Postgraduate Research Scholarship, and a Québec's Funds for Nature and Technology Scholarship. Seismometers used the Launceston case study were loaned to Monash University by the Australian National Seismic Imaging Resource (ANSIR) Research Facility. The cooperation of Launceston City Council for their assistance during field surveys was much appreciated.

## References

- Aki, K., 1957. Space and time spectra of stationary stochastic waves, with special reference to microtremors; *Bulletin Earthquake Research Institute*, v. 35, p. 415–456.
- Asten, M., 2006. On bias and noise in passive seismic data from finite circular array data processed using SPAC methods; *Geophysics*, v. 71, V153–V162, doi: 10.1190/1.2345054.
- Asten, M., Dhu, T. and Lam, N., 2004. Optimised array design for microtremor array studies applied to site classification; comparison of results with SCPT logs; *in Proceedings, 13<sup>th</sup> World Conference on Earthquake Engineering*, Vancouver, Canada, Paper No.2903.
- Bettig, B., Bard, P.-Y., Scherbaum, F., Riepl, J., Cotton, F., Cornou, C. and Hatzfeld, D., 2001. Analysis of dense array noise measurements using the modified spatial auto-correlation method (SPAC). Application to the Grenoble area; *Bolletino di Geofisica Teorica ed Applicata*, v. 42, p. 281–304.
- Chavez-Garcia, F., Rodriguez, M. and Stephenson, W., 2005. An alternative approach to the SPAC analysis of microtremors: exploiting stationarity of noise; *Bulletin of the Seismological Society of America*, v. 95, p.277–293, doi: 10.1785/0120030179.
- Cho, I., Tada, T. and Shinozaki, Y., 2004. A new method to determine phase velocities of Rayleigh waves from microseisms; *Geophysics*, v. 69, p.1535–1551, doi: 10.1190/1.1836827.
- Claprod, M. and Asten, M.W., 2009a. Initial results from spatially averaged coherency, frequency-wavenumber, and horizontal to vertical spectrum ratio microtremor survey methods for site hazard study at Launceston, Tasmania; *Exploration Geophysics*, v. 40, no.1, Butsuri-Tansa, v. 62, Mulli-Tansa, v. 12, p. 132-142, doi: 10.1071/EG08106.
- Claprod, M. and Asten, M.W., 2009b. Variability of shear wave velocity structures in Launceston, Tasmania, Australia; *in Proceedings, 2009 AEES Conference, Australian Earthquake Engineering Society*, Newcastle, Australia.
- Claprod, M. and Asten, M., 2010. Statistical validity control on SPAC microtremor observations recorded with a restricted number of sensors; *Bulletin of the Seismological Society of America*, v. 100, p.776–791, doi 10.1785/0120090133.
- Claprod, M., Asten, M. and Kristek, J., 2011. Using the SPAC microtremor method to identify 2D effects and evaluate 1D shear-wave velocity profile in valleys; *Bulletin of the Seismological Society of America*, v.101, p.826-847, doi: 10.1785/0120090232.
- Cornou, C., Ohrnberger, M., Boore, D.M., Kudo, K. and Bard, P.-Y., 2006. Derivation of structural models from ambient vibration array recordings: Results from an International blind test; *in Proceedings, 3<sup>rd</sup> International Symposium on the Effects of Surface Geology on Seismic Motion*, Grenoble, France.
- Henstridge, J., 1979. A signal processing method for circular arrays; *Geophysics*, v. 44, p.179–184.

Jongmans, D., Ohrnberger, M. and Wathelet, M., 2005. Final report WP13: Recommendations for quality array measurements and processing; European Commission – Research General Directorate, Site Effects Assessment Using Ambient Excitations (SESAME), Deliverable 24.13. <<http://sesame-fp5.obs.ujf-grenoble.fr/Delivrables/Del-D24-Wp13.pdf>> [accessed March 2012]

Köhler, A., Ohrnberger, M., Scherbaum, F., Wathelet, M. and Cornou, C., 2007. Assessing the reliability of the modified three-component spatial autocorrelation technique; *Geophysical Journal International*, v. 168, p. 779–796, doi: 10.1111/j.1365-246X.2006.03253.x.

Leaman, D., 1994. Assessment of gravity survey City of Launceston; Technical Report, Leaman Geophysics, Hobart, Tasmania, Australia, for Launceston City Corporation Seismic Zonation Study.

Michael-Leiba, M., 1995. Microtremor survey and seismic microzonation Launceston, Tasmania, Technical Report, Australian Geological Survey, Canberra, ACT, Australia, for Launceston City Council.

Molnar, S., Dosso, S.E. and Cassidy, J.F., 2010. Bayesian inversion of microtremor array dispersion data in southwestern British Columbia; *Geophysical Journal International*, v. 183, p. 923–940.

Ohori, M., Nobata, A. and Wakamatsu, K., 2002. A comparison of ESAC and FK methods of estimating phase velocity using arbitrarily shaped microtremor arrays, *Bulletin of the Seismological Society of America*, v. 92, p. 2323–2332.

Okada, H., 2003. The microtremor survey method, no.12; *in* Geophysical Monograph Series, Society of Exploration Geophysicists, USA.

Okada, H., 2006. Theory of efficient array observations of microtremors with special reference to the SPAC method; *Exploration Geophysics*, v. 37, p.73–85.

Roberts, J. and Asten, M., 2008. A study of near source effects in array-based (SPAC) microtremor surveys; *Geophysical Journal International*, v. 174, p. 159–177, doi 10.1111/j.1365-246X.2008.03729.x.

Stephenson, W., Hartzell, S., Frankel, A., Asten, M., Carver, D. and Kim, W., 2009. Site characterization for urban seismic hazards in lower Manhattan, New York City, from microtremor array analysis; *Geophysical Research Letters*, v. 36, L03301, doi 10.1029/2008GL036444.

Wathelet, M., Jongmans, D., Ohrnberger, M. and Bonnefoy-Claudet, S., 2003. Array performances for ambient vibrations on a shallow structure and consequences over Vs inversion; *Journal of Seismology*, v.12, p.1–19, doi 10.1007/s10950-007-9067-x.

### **Additional Readings**

SESARRAY ([www.geopsy.org](http://www.geopsy.org)) is a free open-source software for ambient vibration analysis, with fairly high level of experience required (training courses provided). Several in-house toolboxes exist for SPAC interpretation. For example, IDL toolbox developed by Pr. Michael Asten ([Michael.Asten@sci.monash.edu](mailto:Michael.Asten@sci.monash.edu) for access, permission, and training) and MATLAB toolbox programmed by Dr. Maxime Claproud ([Maxime.Claproud@ete.inrs.ca](mailto:Maxime.Claproud@ete.inrs.ca) for permission and training).

## 2.3.3 Frequency-wavenumber (*f-k*) Ambient Noise Array Method

Sheri Molnar

Geological Survey of Canada, Sidney, BC

### Introduction

#### Principles of Method

Frequency-wavenumber (*f-k*) techniques extract surface wave dispersion curves from ambient vibration recordings. The phase velocity and propagation direction of the dominant wave propagating across the array is defined by the vector of the peak in the wavenumber spectrum for a particular frequency. A histogram of phase velocities is constructed from all time-windowed recordings for all sensors at all particular frequencies to provide the dispersion curve(s). By only using vertical-component recordings, Rayleigh waves are assumed to be the dominant wave type.  $V_S$  profiles are estimated by inverting the measured dispersion curve(s).

#### Current State of Engineering Practice

The use of *f-k* processing techniques to extract dispersion data from array-based ambient vibration recordings for the purpose of providing  $V_S$  profiles was first demonstrated by Asten and Henstridge (1984) and Horike (1985) based on the *f-k* methods of Capon (1969) and Lacoss et al. (1969), respectively. The European consortium, SESAME, investigated noise (single-station and array) techniques and produced recommended guidelines (Bard, 2004) and free open-source software for storage, processing, and inversion of array-based ambient vibration data. There is no global optimum array geometry, size, etc., as the source and direction of seismic noise and the urban built environment are unique to each geological setting.

#### Limitations

The same forward modeling assumptions as other surface-wave techniques of a flat-layered earth beneath the spatial extent of the array and propagation of plane waves applies for the *f-k* method. Rapidly varying topography of the ground surface is also a limiting factor. In contrast to the SPAC method, the *f-k* method works best for surface waves of high energy with a limited azimuth distribution. Array-based ambient vibration methods generally do not resolve fine/layered structure (< few metres) and poorly resolves bedrock (half-space) velocity (Cornou et al., 2006, Molnar et al., 2010).

### Data Collection

#### Required Equipment

An array of three or more vertical-component low-frequency ( $\leq 1$  Hz) seismic sensors is recommended. Equipment includes the use of three-component broad-band sensors connected to a digitizer, an external GPS antenna for timing, a small external battery, and associated cables (Figure 2.3.3-1). For sensor positioning in an array, a tape measure, hand-held GPS, and/or compass are beneficial. When using all three components of ambient noise records, a compass is also recommended to align all horizontal sensors to the same orientation (i.e. north).

#### **Recommended citation:**

Molnar, S., 2012. Frequency-wavenumber (*f-k*) Ambient Noise Array Method; *in* Shear Wave Velocity Measurement Guidelines for Canadian Seismic Site Characterization in Soil and Rock, (ed.) J.A. Hunter and H.L. Crow; Geological Survey of Canada, Open File 7078, p. 103-110.

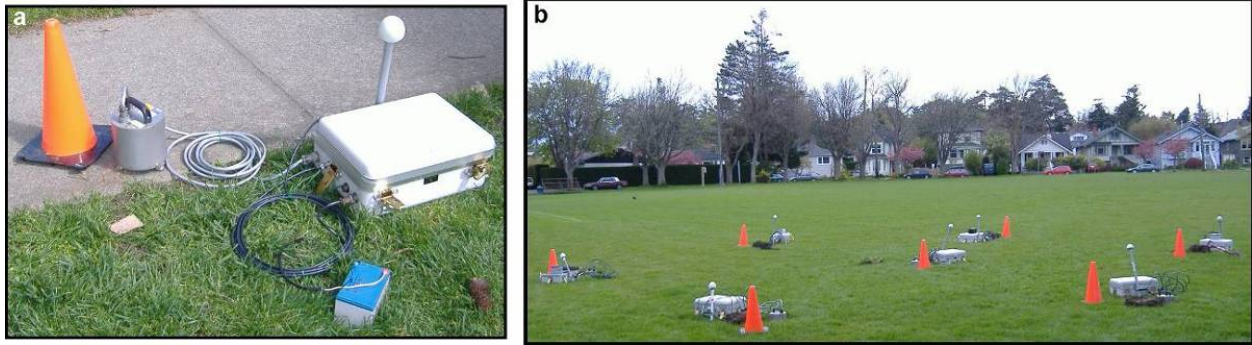


Figure 2.3.3-1. a) Single field unit of seismic sensor, digitizer, battery, and GPS antenna. b) Layout of a 5 m spaced hexagonal array of seven field units in Victoria, British Columbia.

### **Data Collection Procedures**

As with single-station data collection, good sensor/ground coupling is required. Symmetric array geometries are ideal to gain redundancy in data for noise reduction. To obtain dispersion characteristics over as wide a frequency band as possible, the array aperture is adjusted several times in the field to account for the trade-off between resolution and aliasing of the narrow target wavelength (depth) associated with each aperture (Jongmans et al., 2005). The spatial extent of each array is therefore related to the depth of investigation. For a particular array aperture, the theoretical minimum and maximum wavelengths are proposed to be greater than twice the minimum sensor spacing and less than three times the maximum sensor spacing, respectively (Tokimatsu, 1995). A minimum sensor spacing of 5 m is recommended and observed maximum wavelengths are approximately twice the maximum sensor spacing. Recording length is also primarily dependent on intended depth (lowest frequency) of investigation; if unknown, a minimum of ~30 minutes of continuous and simultaneous recording for each array aperture is recommended.

## **Processing Techniques**

### **Theory of Analysis**

The Fourier transform of the cross-correlation of array recordings provides an  $f$ - $k$  spectrum, the amplitude of which is associated with the dominance (i.e. power or coherence) of the signal. For each frequency, the wavenumber coordinates of the peak of the  $f$ - $k$  spectrum ( $k_x, k_y$ ) determines the phase velocity ( $c$ ) of the dominant wave as well as its propagation direction ( $\phi$ ) by

$$c = \frac{2\pi f}{\sqrt{k_x^2 + k_y^2}} \quad [2.3.3-1]$$

$$\phi = \tan^{-1}\left(\frac{k_x}{k_y}\right) \quad [2.3.3-2]$$

The  $f$ - $k$  method (Lacoss et al., 1969) sums spectra phase-shifted by the wavenumber difference between array sensors (or sums time-shifted seismograms) to provide a peak in the  $f$ - $k$  spectrum. In comparison, the high-resolution  $f$ - $k$  method (Capon, 1969) provides a peak in the  $f$ - $k$  spectrum by passing the most coherent signal unsuppressed while suppressing less coherent signals corresponding to other wavenumbers.

Figure 2.3.3-2 depicts an example of the processing flow to estimate phase velocities from microtremor array measurements for a 5 m spaced array.

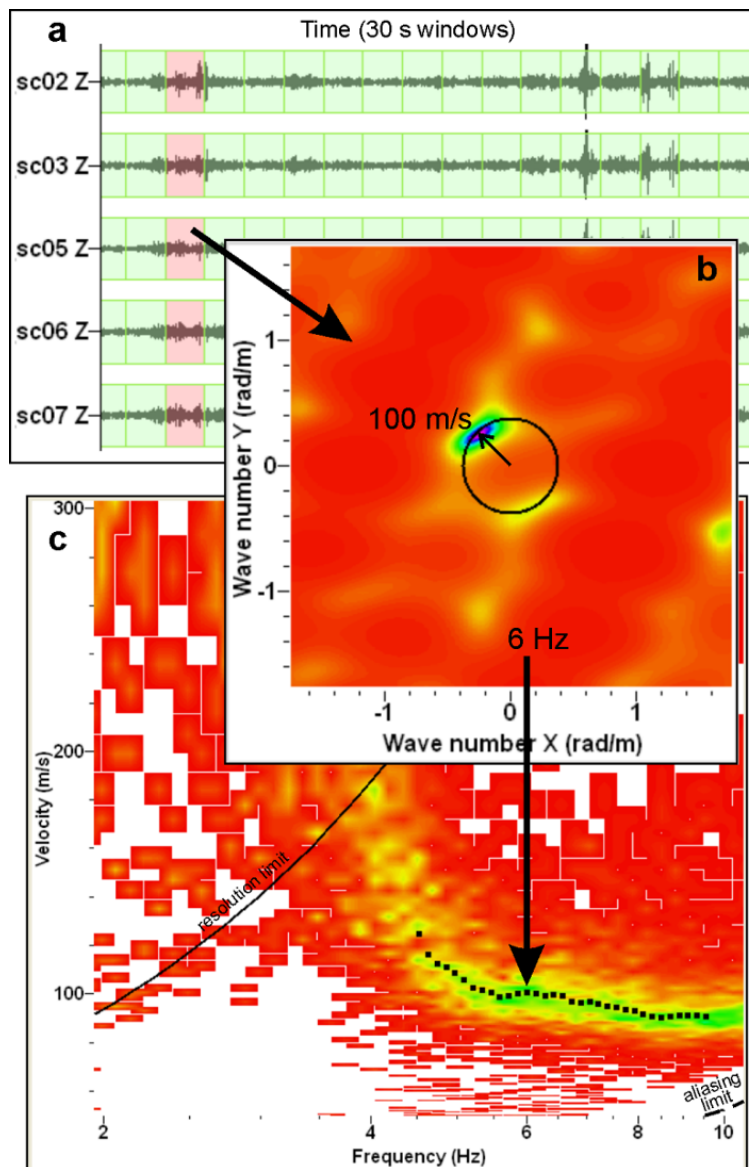


Figure 2.3.3-2. Example of processing flow to estimate phase velocities from ambient vibration recordings for a 5 m spaced array at the Victoria site (high-resolution  $f$ - $k$  results are shown). (from Molnar et al., 2011).

For a particular centre frequency, the ambient vibration recordings (Figure 2.3.3-2a) are first band-pass filtered in a 0.1 Hz band centred on that frequency. The filtered data are time windowed and Fourier transformed. The phase velocity for each window is determined using the above equation with a grid search applied to locate the maximum in the wavenumber plane (Figure 2.3.3-2b). This procedure is repeated for user-specified centre frequencies. A histogram of phase velocity values is computed for all time windows and all frequencies (Figure 2.3.3-2c). Following the methodology of Wathelet et al. (2008), resolution and aliasing frequency limits for each array aperture are based on the minimum ( $k_{\min}$ ) and maximum ( $k_{\max}$ ) wavenumbers of the theoretical array response to a vertically incident plane wave, respectively. The recommended grid spacing and search area for  $f$ - $k$  (high-resolution  $f$ - $k$ ) analysis are

$k_{min}/2$  ( $k_{min}/3$ ) and  $1.5*k_{max}$  ( $2*k_{max}$ ), respectively. The median phase velocity value is then calculated at each centre frequency and, if reliable (e.g. within theoretical limits, high bin count, etc.), are kept (squares in Figure 2.3.3-2c).

### **Uncertainty Assessment**

Molnar et al. (2010, 2011) provide unbiased uncertainty estimation of  $V_S$  structure from Bayesian inversion of array-based ambient vibration dispersion data using Markov-chain Monte Carlo methods, combining data error covariance estimation with objective model parameterization based on the Bayesian information criterion. Generally, best-fit  $V_S$  models from the optimization-based inversion of surface wave dispersion data have been used for calculating site amplification, with uncertainties approximated using all or a subset of the models sampled during the inversion process (Fäh et al., 2003; Scherbaum et al., 2003; Di Giulio et al., 2006; Parolai et al., 2007; Foti et al., 2009). However, it should be noted that none of these approaches properly estimate  $V_S$  profile uncertainties for use in characterizing site amplification uncertainties. Quantitative and unbiased uncertainty estimation requires not only a nonlinear sampling approach that draws models proportional to their probability, but also rigorous estimation of the data error statistics and an appropriate model parameterization.

### **Recommended Guidelines for Reporting**

The field procedure must be reported (array layout, number of sensors, spacing, etc.), and processing procedure(s) to extract dispersion characteristics, with presentation of empirical dispersion curve and associated fit obtained by  $V_S$  profiles (models) from the inversion. Avenues recommended to assess the quality of  $f$ - $k$  derived dispersion data includes: verification of consistency between different array apertures and/or active-source (SASW and/or MASW) techniques, if applicable (i.e. data overlap); comparison with modified SPAC analysis; and verification of feasibility from forward modeling of Rayleigh and/or Love wave dispersion based on an educated guess of the geology (*a priori*  $V_S$  profile), also beneficial for mode interpretation. Generally, non-linear optimization-based inversion procedures are applied with presentation of best-fit  $V_S$  profile with/out all or a sub-set of models sampled during the inversion. Amplitude spectra are usually predicted based on the  $V_S$  profiles and compared with empirical earthquake and/or ambient vibration spectral ratios for evaluation of site response characterization. The reader is referred to Di Giulio et al. (2006), Maresca et al. (2006), Parolai et al. (2007), Picozzi et al. (2009), Foti et al. (2009), and Molnar et al. (2011) as representative examples.

### **Hazard-Related Case Studies**

#### **Microtremor arrays in Victoria and Fraser River delta, BC.**

Bayesian inversion of microtremor array data was applied at two sites of high seismic risk in British Columbia (Figure 2.3.3-3a) to study the ability to recover an accurate  $V_S$  profile in relatively deep (> 200 m) and shallow (< 20 m) geological settings on the Fraser River delta in Greater Vancouver and in Victoria, respectively. For the site in Victoria,  $f$ - $k$  and modified SPAC derived dispersion data were obtained using semi-circular (7 sensors), hexagonal (7 sensors), non-symmetrical square (5 sensors), and T-shaped (4 sensors) arrays. Invasive  $V_S$  measurements were used to assess the reliability of the Bayesian microtremor inversion results; array sites were co-located with invasive  $V_S$  profiling sites (seismic cone penetration (SCPT) and surface-to-downhole). Ambient vibrations were collected using seismic arrays of five to six sensors with the largest array aperture set according to the depth of interest, i.e. maximum sensor spacing of 70 m at the shallow-sediment Victoria site (Figure 2.3.3-3b) and 180 m at the thick-sediment delta site (Figure 2.3.3-3d). Both  $f$ - $k$  (squares in Figure 2.3.3-3c,e) and high-resolution  $f$ - $k$  (circles in Figure 2.3.3-3c,e) processing techniques were applied to estimate the fundamental-mode Rayleigh wave phase velocity from the ambient vibration recordings. Reliable phase velocity estimates were obtained between 2.4-9.0 Hz (Figure 2.3.3-3c) and 1.2-6.7 Hz (Figure 2.3.3-3e) for the Victoria and delta sites, respectively.

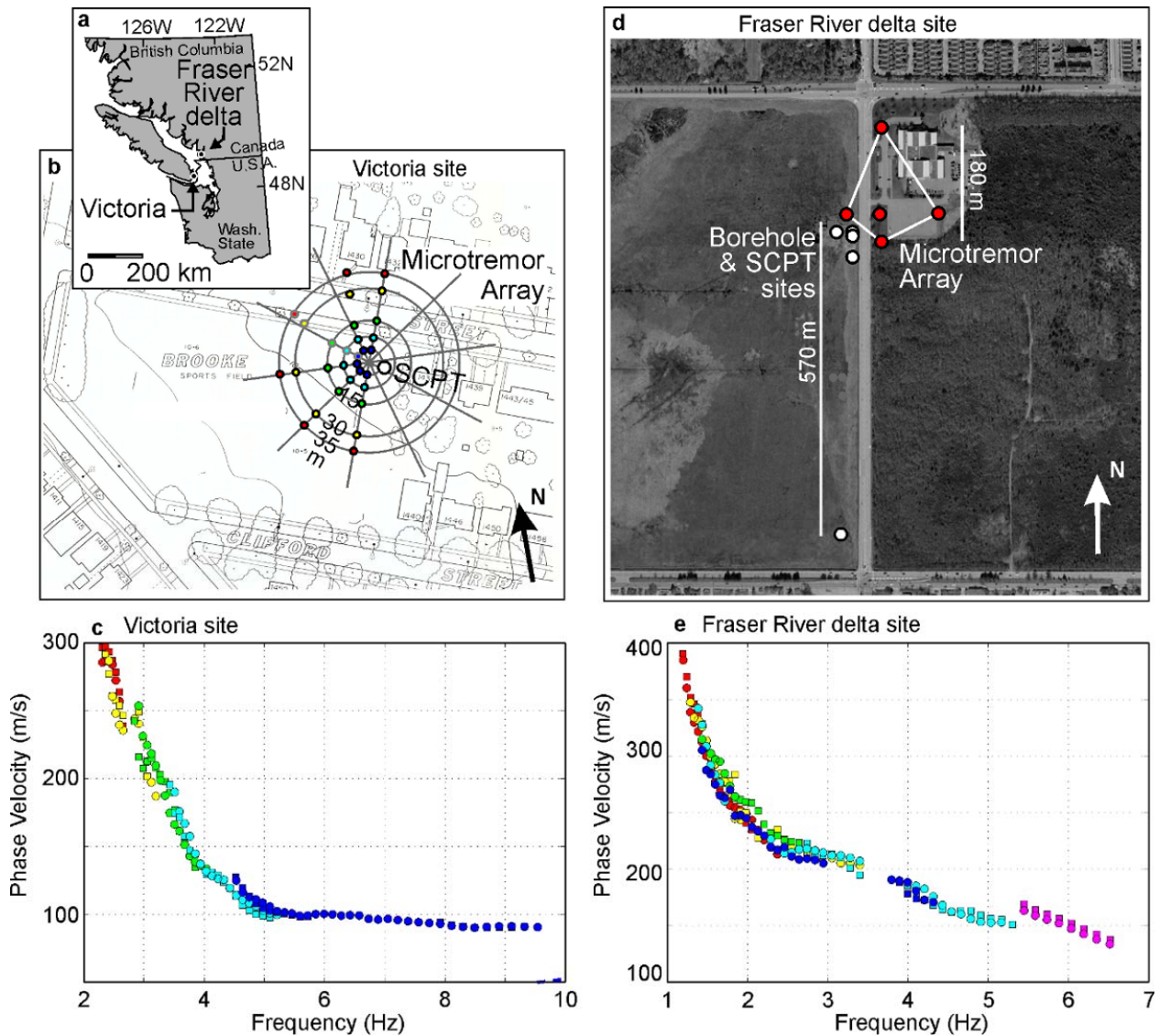


Figure 2.3.3-3. a) Location of the Victoria and Fraser River delta sites in southwestern British Columbia. b) Victoria microtremor array site showing the five semi-circular arrays (circles coloured according to array radius, greyed circles denote non-working sensor) and SCPT site (white circle). c) Phase velocity estimates for Victoria. d) Delta microtremor array site with the largest aperture array indicated by red circles, borehole and SCPT sites denoted by white circles. e) Phase velocity estimates for the delta site coloured according to array aperture (modified from Molnar et al. 2011).

Unbiased uncertainty estimates of  $V_S$  structure were obtained via Bayesian inversion of the dispersion curves shown in Figure 2.3.3-3c,e using Markov-chain Monte Carlo methods, combining data error covariance estimation with objective model parameterization based on the Bayesian information criterion (Molnar et al., 2010). For Victoria, Figure 2.3.3-4a shows a layer with low  $V_S$  and a weak linear gradient indicated between 15-18 m depth, above much higher velocity material. For the delta site, Figure 2.3.3-4b shows a well resolved  $V_S$  profile to at least 110 m depth for a power-law gradient parameterization. Excellent agreement is obtained between the inversion results and the invasive methods over the depth interval for which the inversion results are well resolved: the average relative difference is 5% from surface to 120 m depth for the delta site, and is 11% to 17 m depth for Victoria.

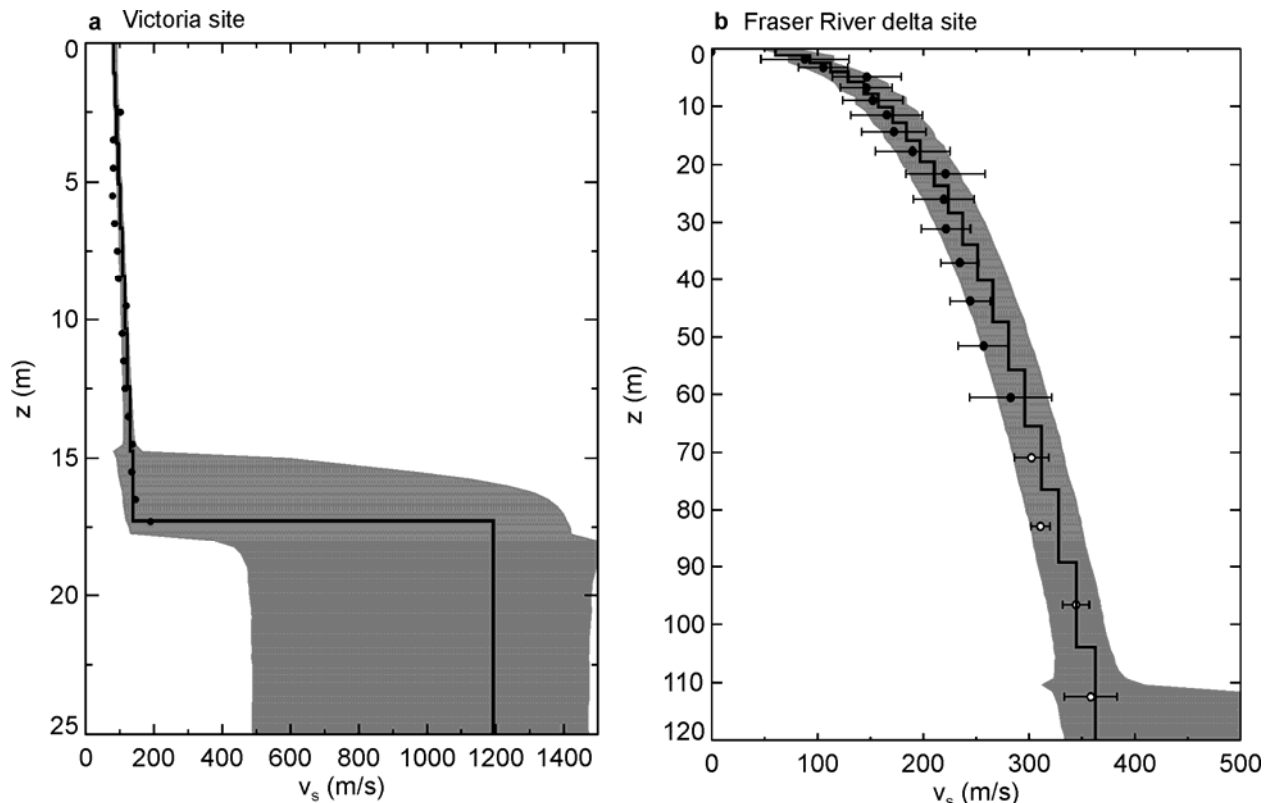


Figure 2.3.3-4. Comparison of  $V_s$  profiles at the (a) Victoria site and (b) Fraser River delta sites. Bayesian inversion results are shown as the maximum *a posteriori* (MAP) model (black line) and 95% highest-probability density credibility interval (shaded region). In (a), SCPT  $V_s$  measurements are shown as filled circles. In (b), averaged SCPT and downhole  $V_s$  measurements (according to the logarithmic depth partitioning of the MAP model) are shown as filled circles; open circles denote downhole-only averages (error bars indicate one standard deviation about the mean). (modified from Molnar et al. 2010).

## Acknowledgments

Financial support was provided by the National Sciences and Engineering Research Council of Canada, Geological Survey of Canada, and University of Victoria. Equipment provided by the Geological Survey of Canada.

## References

- Asten, M.W. and Henstridge, J.D., 1984. Array estimators and the use of microseisms for reconnaissance of sedimentary basins; *Geophysics*, v.49, p.1828-1837.
- Bard, P.-Y. (co-ordinator), 2004. Site EffectS assessment using Ambient Excitations (SESAME), Final report: European Commission - Research General Directorate, Project No. EVG1-CT-2000-00026, SESAME 33 p. <[http://sesame-fp5.obs.ujf-grenoble.fr/Delivrables/SESAME-Finalreport\\_april05.pdf](http://sesame-fp5.obs.ujf-grenoble.fr/Delivrables/SESAME-Finalreport_april05.pdf)> [accessed March 2012]
- Capon, J., 1969. High-resolution frequency-wavenumber spectrum analysis; *in Proceedings, IEEE*, v. 57, p.1408-1418.

Cornou, C., Ohrnberger, M., Boore, D.M., Kudo, K. and Bard, P.-Y., 2006. Derivation of structural models from ambient vibration array recordings: Results from an International blind test; *in* Proceedings, 3<sup>rd</sup> International Symposium on the Effects of Surface Geology on Seismic Motion, Grenoble, France.

Di Giulio, G., Cornou, C., Ohrnberger, M., Wathelet, M. and Rovelli, A., 2006. Deriving wavefield characteristics and shear-velocity profiles from two-dimensional small-aperture arrays analysis of ambient vibrations in a small-size alluvial basin, Colfiorito, Italy; *Bulletin of the Seismological Society of America*, v. 96, p. 1915-1933.

Fäh, D., Kind, F. and Giardini, D., 2003. Inversion of local S-wave velocity structures from average H/V ratios, and their use for the estimation of site-effects; *Journal of Seismology*, v. 7, p. 449-467.

Foti, S., Comina, C., Boiero, D. and Socco, L.V., 2009. Non-uniqueness in surface-wave inversion and consequences on seismic site analyses; *Soil Dynamics and Earthquake Engineering*, v. 29, p. 982-993.

Horike, M., 1985. Inversion of phase velocity of long-period microtremors to the S-wave velocity structure down to the basement in urbanized areas; *Journal of the Physics of the Earth*, v. 33, p. 59-96.

Jongmans, D., Ohrnberger, M. and Wathelet, M., 2005. Final report WP13: Recommendations for quality array measurements and processing; European Commission – Research General Directorate, Site Effects Assessment Using Ambient Excitations (SESAME), Deliverable 24.13. <<http://sesame-fp5.obs.ujf-grenoble.fr/Delivrables/Del-D24-Wp13.pdf>> [accessed March 2012]

Lacoss, R.T., Kelly, E.J. and Toksoz, M.N., 1969. Estimation of seismic noise structure using arrays; *Geophysics*, v. 34, p. 21-38.

Maresca, R., Galluzzo, D. and Del Pezzo, E., 2006. H/V Spectral ratios and array techniques applied to ambient noise recorded in the Colfiorito basin, central Italy; *Bulletin of the Seismological Society of America*, v. 96, p. 490-505.

Molnar, S., Dosso, S.E. and Cassidy, J.F., 2010. Bayesian inversion of microtremor array dispersion data in southwestern British Columbia; *Geophysical Journal International*, v. 183, p. 923-940.

Molnar, S., Dosso, S.E. and Cassidy, J.F., 2011. Site response probability analysis from Bayesian inversion of microtremor array data; *Soil Dynamics and Earthquake Engineering*, in review.

Parolai, S., Mucciarelli, M., Gallipoli, M.R., Richwalski, S.M. and Strollo, A., 2007. Comparison of empirical and numerical site responses at the Tito test site, southern Italy; *Bulletin of the Seismological Society of America*, v. 97, p. 1413-1431.

Picozzi, M., Strollo, A., Parolai, S., Durukal, E., Ozel, O., Karabulut, S., Zschau, J. and Erdik, M., 2009. Site characterization by seismic noise in Istanbul, Turkey; *Soil Dynamics and Earthquake Engineering*, v. 29, p. 469-482.

Scherbaum, F., Hinzen, K.-G. and Ohrnberger, M., 2003. Determination of shallow shear wave velocity profiles in the Cologne, Germany area using ambient vibrations; *Geophysical Journal International*, v. 152, p.597-612.

Tokimatsu, K., 1995. Geotechnical site characterization using surface waves; *in* Proceedings, 1<sup>st</sup> International Conference on Earthquake Geotechnical Engineering, Tokyo, Balkema Publishers, Netherlands, p.1333-1368.

Wathelet, M., Jongmans, D., Ohrnberger, M. and Bonnefoy-Claudet, S., 2008. Array performances for ambient vibrations on a shallow structure and consequences over  $V_S$  inversion; *Journal of Seismology*, v. 12, p. 1-19.

## **Additional Readings**

SESARRAY ([www.geopsy.org](http://www.geopsy.org)) is a free, open-source software for ambient vibration analysis. It provides a database structure for seismograms with multiple processing tools including: basic waveform processing, calculation of H/V spectral ratios, and  $f-k$ , high-resolution  $f-k$ , and modified SPAC processing. Inversion routine is based on a non-linear modified-neighbourhood algorithm. A fairly high level of experience is required (training courses provided).

Bayesian inversion algorithms developed by Dr. Stan Dosso and Sheri Molnar ([smolnar@nrcan.gc.ca](mailto:smolnar@nrcan.gc.ca), for access, permission, and training), with basic knowledge of FORTRAN and IDL programming language required.

## Chapter 3.0 Invasive Seismic Techniques

*Chapter Leaders:*

*Heather Crow*  
*Geological Survey of Canada, Ottawa, ON*

*Ilmar Weemees*  
*ConeTec Investigations Ltd., Vancouver, BC*

Invasive shear wave seismic methods involve travel time measurements using receivers which are pushed into soft soil (seismic cone penetration testing, SCPT) or lowered into one or more boreholes. The seismic source may be located on surface, within the test borehole, or in an adjacent borehole.

SCPT methods are generally considered the most reliable approach for shear wave travel time measurements (and thus velocity), as the seismic cone remains in contact with the soil. This is a particular advantage in sensitive soils, as it reduces disturbance caused by drilling and fluid invasion, and removes uncertainty caused by a poorly bonded casing. A source at surface (sledge or automatic hammer) is used to generate horizontally polarized shear (SH) waves, and traveltimes are measured at discrete depths by receivers in the cone as it advances. In cases where the material is too stiff for cone pushing, a boring must be drilled.

Four common borehole measurement techniques are also discussed:

- Vertical seismic profiling (single borehole),
- Full waveform sonic logging (single borehole),
- Crosshole (two or more boreholes), and
- Multichannel crosshole (two or more boreholes).

Vertical seismic profiling (VSP) is the most straightforward and commonly used of the downhole shear wave methods, and requires a source on surface (sledge or automatic hammer) to measure SH wave transit times downhole at discrete depths, typically 0.5 to 1m intervals. This method can be used in any combination of soil (cased) or rock (open or cased) borings, and holes do not need to be fluid-filled.

Full waveform acoustic (sonic) tools use a high frequency (1-50 kHz) source and two or more receivers all mounted on the sonde to measure traveltimes of compressional and shear headwaves and guided waves (pseudo-Rayleigh and tube (Stoneley) waves) along the borehole wall. Complexity with this method arises when the shear wave velocity in the formation is lower than the compressional velocity of the wave in the borehole fluid (called a "slow formation"). Therefore, this method is recommended only for open rock holes, which must be fluid-filled.

The standard crosshole test utilizes one borehole for the downhole source and either one or (preferably) two closely-spaced boreholes for the receivers. A horizontally propagating, vertically polarized shear wave (SV) is generated at the source and the traveltime between the receivers located at the same elevation are used to determine shear wave velocity. This method, when used in a three borehole configuration, is regarded as one of the more accurate approaches since two downhole receivers in different boreholes removes the uncertainty of time zero errors originating at the source. An extension of this method is the multichannel crosshole tomography survey, in which the single cross-hole receiver is replaced with a downhole array capable of measuring shear wave velocity simultaneously over multiple ray paths. This allows for an assessment of the shear wave velocity distribution in the region between two boreholes

When selecting one of these methods for  $V_s$  measurement, the variation of shear wave velocity between the horizontal and vertical directions (called 'formation anisotropy') should be considered. Although typically not highly varying (less than a few percent), shear wave anisotropy may be present in highly stratified materials, or materials under significant shear stresses in one orientation (open slopes, cuts, embankments, etc). The methods generating downward propagating SH waves are those with the

closest resemblance to earthquake energy as it travels to the surface. If significant anisotropy is present, a vertically travelling wave will yield a velocity with predominantly horizontal particle motion which may be lower than a horizontally travelling shear wave.

## **3.1 Seismic Cone Penetrometer (SCPT) Technique for Hazard Studies**

*Ilmar Weemees & David Woeller,  
ConeTec Investigations Ltd, Vancouver, BC*

### **Introduction**

#### **Principles of the Method**

The seismic piezocone test (SCPT) combines the standard piezocone test (CPTu) with one or more integrated geophones or accelerometers to record in situ body wave motion (Figure 3.1-1). The test measures the in situ interval travel time of body waves generated at or near the ground (or mudline) surface. Body waves generated are most commonly horizontally polarized shear waves (SH) but can also be compression (P) waves. Typically the quasi interval technique is used where the test is performed at fixed intervals when the penetration of the cone is halted. By recording the wave traces at successive depths a profile of interval travel times can be determined. The velocity of the shear wave (or P wave) is then calculated on the basis of net difference of the interval wave path distance between each test depth (Figure 3.1-2). The velocity can then be used to directly calculate small strain moduli.

#### **Current State of Engineering Practice**

The seismic cone test equipment and procedure developed at the University of British Columbia (UBC) (Campanella and Robertson, 1984) is the basis for the current accepted test procedure. Over time there have been improvements to deployment and in situ equipment and refinements to data reduction procedures (Campanella and Stewart, 1992; Howie and Amini, 2005). Whereas the test was first considered highly specialized it is now incorporated commonly in cone penetration site investigations. The CPT procedure and data analysis should conform to ASTM D5778-07, Standard Test Method for Performing Electronic Friction Cone and Piezocone Penetration Testing of Soils, while the seismic portion of the test should conform to ASTM D 7400-07, Standard Test Methods for Downhole Seismic Testing. Usually the seismic cone is equipped with a single horizontally oriented geophone or accelerometer though tri-axial receiver packages may be used as well. While the test is incremental in general practice, developments in continuous seismic testing have been made. By recording wave arrivals from an automatically operating source and recording wave traces while the cone is in motion, a near continuous profile and shear wave velocity can be developed (Figure 3.1-3).

#### **Limitations**

The test depth is limited to site conditions and the equipment used. This limitation is a function of the cone capacity, the hydraulic pushing capacity of the deployment system, and ground conditions. In some cases localized layers can be drilled out and the cone can be redeployed. Depth can become a limiting issue where accumulated friction force on the deployment rods plus the end bearing exceeds the pushing capacity of the deployment system.

Generally the detection of shear waves is not limited by depth; SCPT's of over 100m from the ground surface wave have been performed. Signal transmission can be a problem when there are soft low velocity soils at the surface, such as in the case of peat or very soft clay. In these soils the shear wave amplitude is often low, and when higher velocity layers are encountered a portion of the energy is reflected, thus decreasing transmission through to deeper soils. In these cases a source can be pushed or hammered into more competent soil.

#### **Recommended citation:**

Weemees, I. and Woeller, D., 2012. Seismic Cone Penetrometer (SCPT) Technique for Hazard Studies; *in* Shear Wave Velocity Measurement Guidelines for Canadian Seismic Site Characterization in Soil and Rock, (ed.) J.A. Hunter and H.L. Crow; Geological Survey of Canada, Open File 7078, p. 113-122.

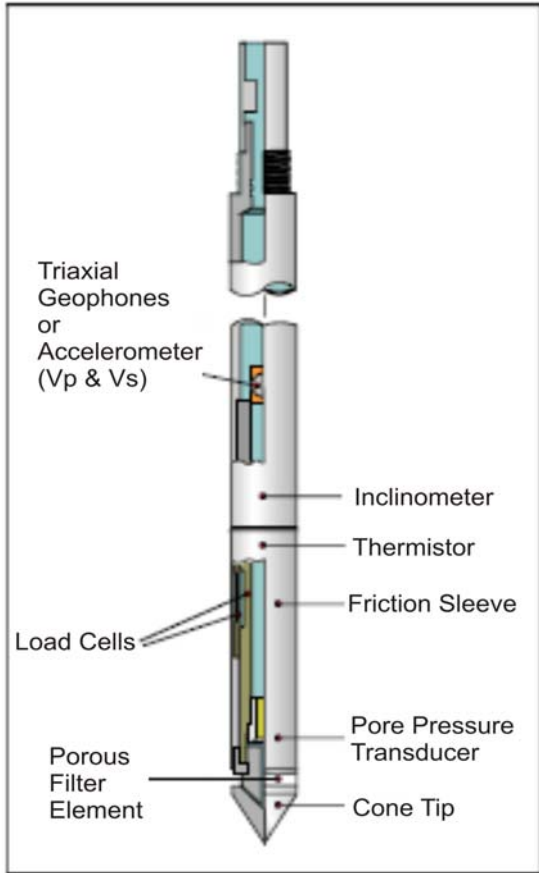


Figure 3.1-1. Elements of the seismic cone.

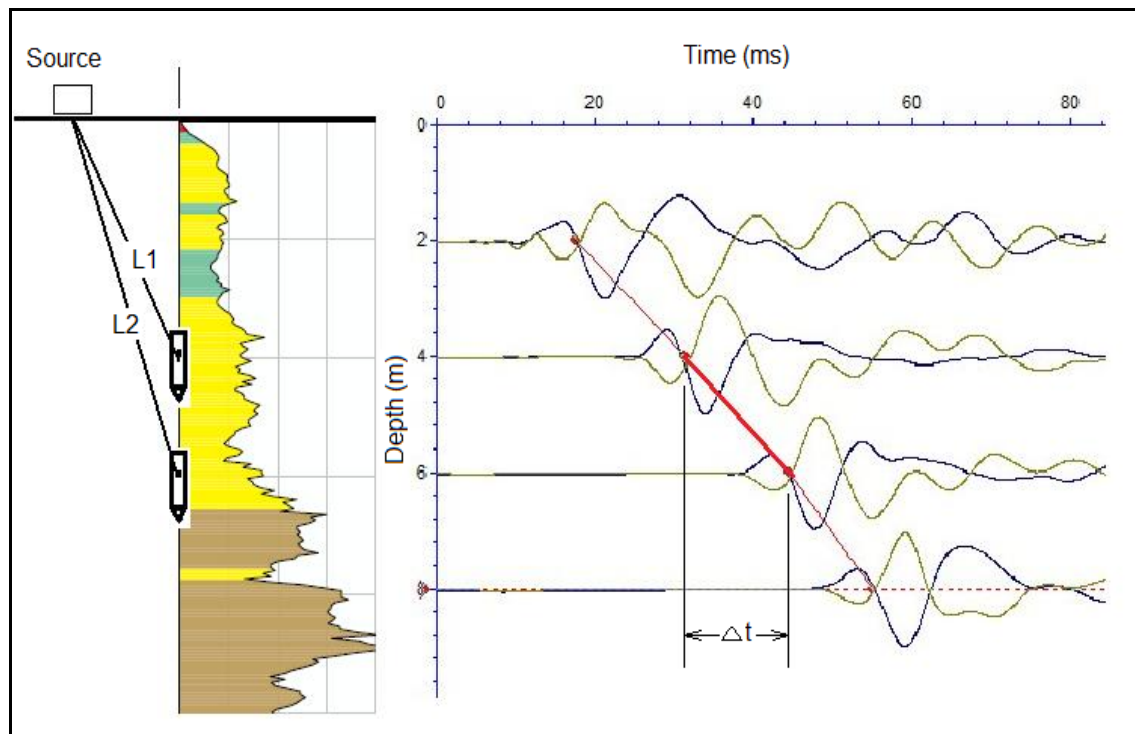


Figure 3.1-2. Determination of the interval travel time for the SCPT using the crossover method.

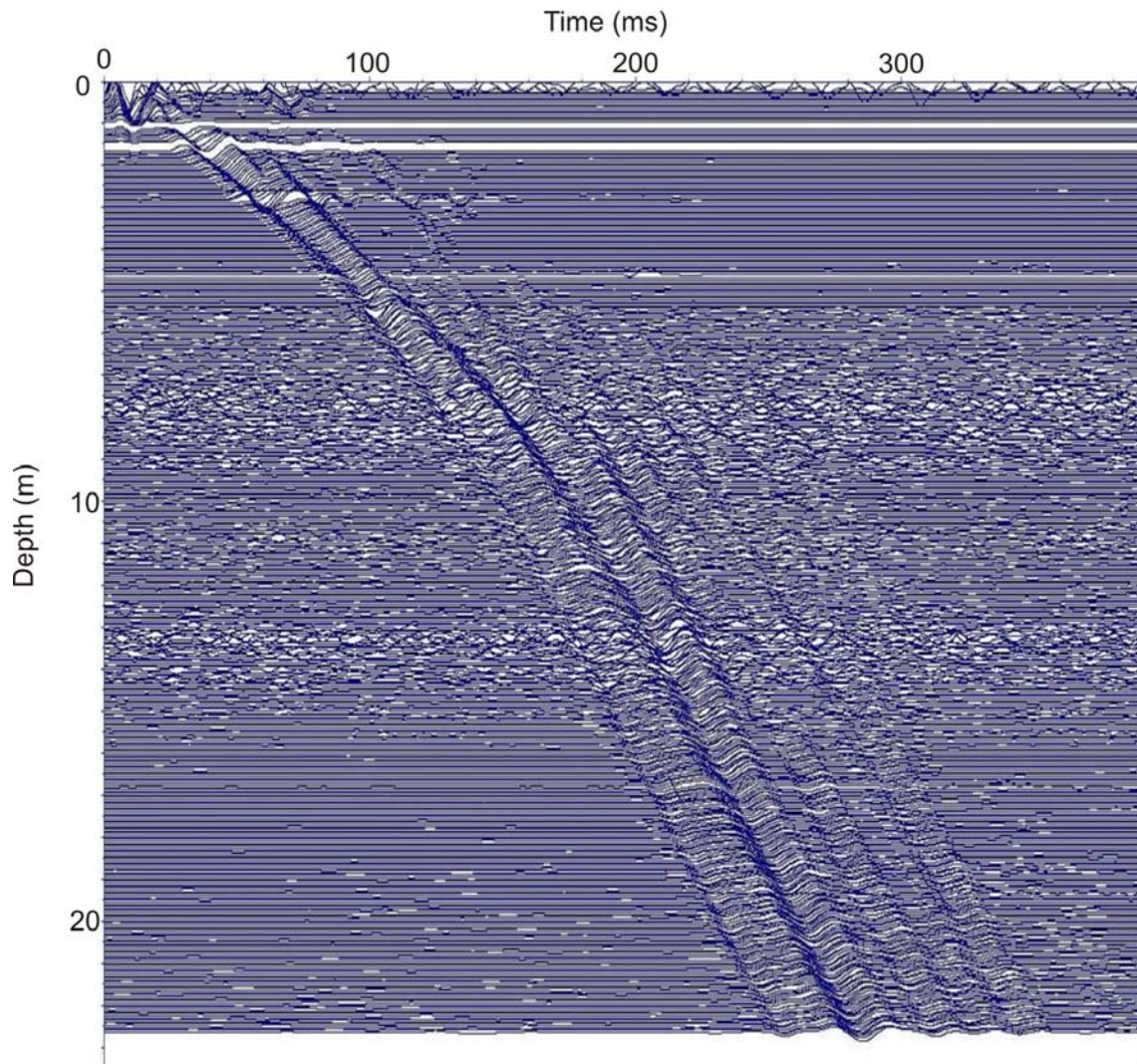


Figure 3.1-3. Continuous seismic testing results to 22m (test intervals=0.1m).

## Data Collection

### Required Equipment

The equipment required to push the cone in the ground can be a drill rig equipped with suitable hydraulics, or a purpose built cone pushing rig, which may be either truck or track mounted. Portable hydraulic rams can also be used in a number of scenarios in which the ram can be either bolted to a floor slab, mounted on a piece of heavy construction equipment, or the deck of a barge for over water testing. The choice of deployment equipment is a function of equipment availability, site access, anticipated ground conditions, and required depth.

The seismic cone penetrometer is usually equipped with a single horizontally oriented geophone or accelerometer. Cones can also be equipped with triaxial geophone packages or can be set up as true interval cones with two receivers separated by a distance of 0.5 m.



The most commonly used source is a sledge hammer impact against the end of steel I-beam equipped with end mounted striking plates (Figure 3.1-4). The normal load on the beam is supplied by the cone or drill rig outriggers, or purpose built cylinder integrated into the cone vehicle. Striking the beam at each end generates clean oppositely polarized SH waves which is ideal for measuring shear wave velocity. For P wave acquisition a vertical impact source is used, alternatively a buffalo gun (Pullan and MacAulay, 1987) may be used which generates both P and S wave energy. More recently, automatic hammers (AutoSeis) systems for SH wave generation has also been used in practice. These sources improve impact repeatability and can speed up the overall test procedure (Casey and Mayne, 2002). When testing over water, sources that use blasting caps or submersible automatic hammers are used. For over water work the horizontal offset from the source to the cone rod string should be minimized.

Triggering can be either an electric contact trigger or an accelerometer trigger when using an automatic hammer. The recording system should have adjustable gain for each channel and be equipped with anti-aliasing filters.

Figure 3.1-4. CPT truck with integrated beam for generating SH waves.

### **Data Collection Procedures**

As with any cone test the deployment rig must be properly leveled and cone push rods are vertical at the start of the test. Attention should be paid to the near surface such that obstructions or fill will not deflect the cone off the vertical axis. In most circumstances a shear beam or autoseis will be set within 0.3 to 1.0m of the cone rods in an orientation such that the primary axis of the source is parallel to the active axis of the receiver in the cone. Having a small offset minimizes the opportunity to receive wave travel paths that are refracted at velocity boundaries. In order to get good quality data the shear source must rest on a flat level surface, any inconsistencies in the surface should be removed such that there are no gaps between the base of the source and the testing surface.

Data is usual collected at 1 metre (but sometimes 0.5,2, or 3m) intervals when the cone penetration is stopped. Usually a minimum of 2 repeatable impacts from each side of the shear beam are collected. When an autoseis is used only one impact direction is normally collected. While it is possible to conduct the test with just one impact per depth, multiple impacts are preferred to provide better confidence in the data, and allow for the time domain stacking of signals if random ambient noise is present. The short time to acquire extra data usually benefits in reduced post processing time.

### **Processing Techniques**

#### **Theory of Analysis**

The first step in the analysis of seismic CPT data is the determination of the interval shear and compression wave travel times. This is still commonly done using the cross over method as shown in Figure 2. When non-polarized shear wave data or P wave data is being analyzed then a consistent marker such as the first peak is used. Other methods such as cross correlation or the phase of the cross-spectrum (Howie and Amini, 2005) can be used to automate the determination of interval time. The body waves measured by the test are effectively non dispersive so they should have the same velocity over the source frequency range used in the SCPT. For the shear wave sources used in the SCPT this is typically

in the range of 20 to 200 Hz. if required, digital filtering is often useful in isolating the source signal in the case where background noise is present.

Once the interval times have been determined the velocity (V) can be simply calculated (Equation 3.1-1) using a straight ray path assumption as shown in Figure 3.1-2.

$$V = \frac{L_2 - L_1}{\Delta t} \quad [3.1-1]$$

This method assumes no wave refraction. This assumption is valid in cases where the source is close to the cone rods, and the cone has not significantly deviated from vertical. With a large offset and when layers of large velocity contrast are encountered refraction of the ray paths according to Snell's Law must be considered (ASTM D7400-07 and Baziw, 2002).

Once the velocity profile has been generated shear wave velocity can be used for site classification and as an indicator of resistance to liquefaction. The small strain shear modulus ( $G_{\max}$ ) can be determined from the shear wave velocity, and if P wave velocity is being measured, Poison's ratio ( $\nu$ ) and Elastic modulus ( $E_{\max}$ ) can be calculated (Equations 3.1-2,-3, and -4).

$$G_{\max} = \rho V_s^2 \quad [3.1-2]$$

$$\nu = \frac{\left(\frac{V_p}{V_s}\right)^2 - 2}{2\left(\frac{V_p}{V_s}\right)^2 - 1} \quad [3.1-3]$$

$$E_{\max} = 2(1 + \nu)G_{\max} \quad [3.1-4]$$

### **Uncertainty Assessment**

The primary source of error in the test is the determination of the interval travel time. With data of typical quality the uncertainty is usually less than  $\pm 0.1\text{ms}$  when making first cross over picks from oppositely polarized shear waves. At a velocity of 200 m/s this would be an uncertainty of  $\pm 4$  m/s. In cases where the oppositely polarized waveforms are somewhat asymmetric, or there is significant background noise, the uncertainty will be greater. Uncertainty can be better quantified with multiple hits at each depth.

### **Recommended Guidelines for Reporting**

The test location must be identified with a unique name and coordinates (UTM, Lat Long, or site specific datum). Data required for reporting must include the source type, offset distance and depth if the source is embedded.

The tabular data should include the tip depth, receiver depth, travel time interval, and velocity for each depth interval. The basic SCPT plot should include tip resistance, sleeve friction, dynamic pore pressure and velocity.

If the interval shear wave velocity data is being used to calculate  $V_{s30}$ , then most shallow velocity data layer is assumed to project to the surface. If the data does not reach 30m the deepest velocity value is assumed to extend to 30m. Since  $V_{s30}$  is defined as the travel time weighted averaged shear wave

velocity (Equation 3.1-5a) the reported velocities need to be converted to equivalent travel times for each velocity interval layer (Equation 3.1-5b).

$$V_{s30} = \frac{30}{\Sigma t_{30}} \quad [3.1-5a]$$

$$V_{s30} = \frac{30}{\Sigma \left( \frac{z_n}{V_{s_n}} \right)} \quad [3.1-5b]$$

## Hazard-Related Case Studies

### **Comox, BC**

This case history describes the test results of an SCPT conducted at Goose Spit, near Comox BC. This site is of particular interest in that there was documented liquefaction of the sands at this location caused by the 1946 magnitude 7.3 earthquake. The epicenter of the earthquake was 32km to the NW, and the site is described in detail by Mosher et al. (2001). Estimates of peak ground acceleration at the site are between 0.2 and 0.4g.

SCPT was chosen at this site because the method would induce the least amount of soil disturbance (desirable for a liquefaction site) while providing continuously recorded cone tip resistance which would contribute to liquefaction risk assessment calculations. Test holes at the location indicated medium to coarse sand with some shells and gravel. This is consistent with the characteristics of the CPT tip and sleeve data (Figure 3.1-5). The hydrostatic dynamic pore pressure also indicates a clean soil that is drained during penetration.

The  $V_{s30}$  value of 221 m/s of the site would result in it classified as zone D (stiff soil) under the NBCC 2005 criteria, however due to significant ground acceleration combined with relatively loose sands in the upper 5m, the site would be classified as zone F. To assess the liquefaction risk at the site the Cyclic Resistance Ratio (CRR) has been presented for the upper 10m using both the cone tip resistance and the shear wave velocity. These values of CRR are compared to the calculated Cyclic Stress Ratio (CSR) for the design earthquake to identify zones where cyclic liquefaction is possible.

An estimation of cyclic resistance ratio (CRR) for clean sands and silty sands can be made using corrected cone penetration resistance (Robertson and Wride, 1998a). The estimation of CRR from the CPT is based on an equivalent clean sand normalized cone penetration resistance  $(q_{c1n})_{cs}$ . The shear wave velocity method for evaluating cyclic resistance ratio is outlined in the summary documents of the NCEER Workshop on Evaluation of Liquefaction Resistance of Soils (Youd et al., 1998; Robertson and Wride, 1998b). The results of the analysis are plotted in Figure 3.1-6. Both the cone and shear wave velocity analyses identify the zone below the water table at 2.2m to a depth of 6m as liquefiable at the peak ground accelerations induced during the earthquake.

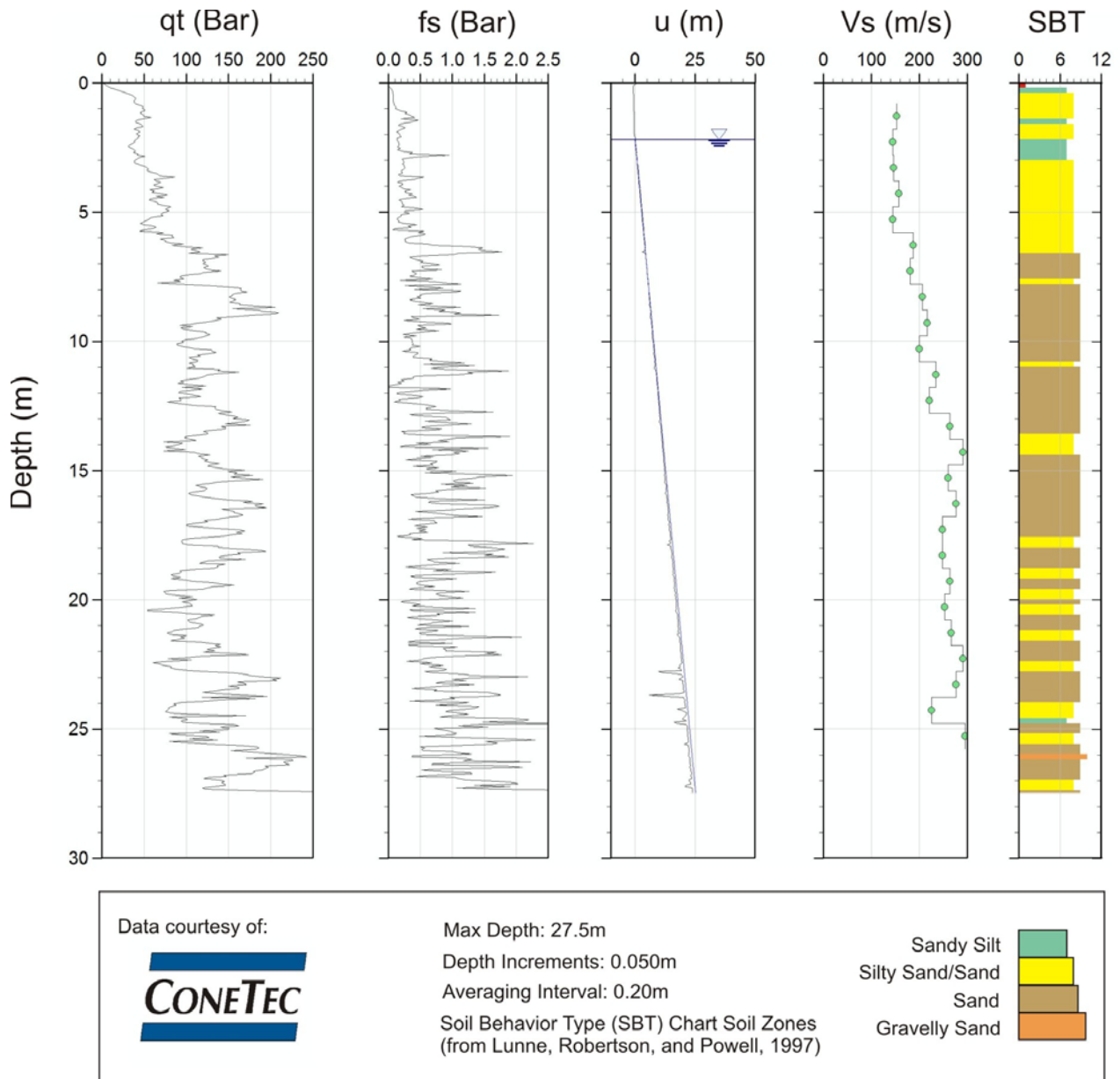


Figure 3.1-5. SCPT Profile, Goose Spit, Comox B.C.

**Winnipeg Manitoba**

The deposits at this site consist of firm clayey silt with a traveltime-weighted shear wave velocity of 122 m/s to a depth of 19.2 m below ground surface. Surficial deposits noted in this area are Lake Agassiz glaciolacustrine sediments (Matile and Keller, 2004). From a depth of 19.2 m to penetration refusal at 21.25 m, the deposits are sand and very stiff silt, with a much higher shear wave velocity, approaching 400 m/s. Since the final shear wave velocity measurement was at less than 30 m the deepest shear value was assumed to carry on to a depth of 30m for the purposes of computing  $V_{s30}$ . The traveltime-weighted shear wave velocity was then calculated to be 163 m/s, which classifies the material as a site class E under the NBCC 2010 criteria (Figure 3.1-7). It should be noted, however, that the projection of traveltimes down to 30 m is not the method outlined in the NBCC, and can result in an incorrect site class assignment.

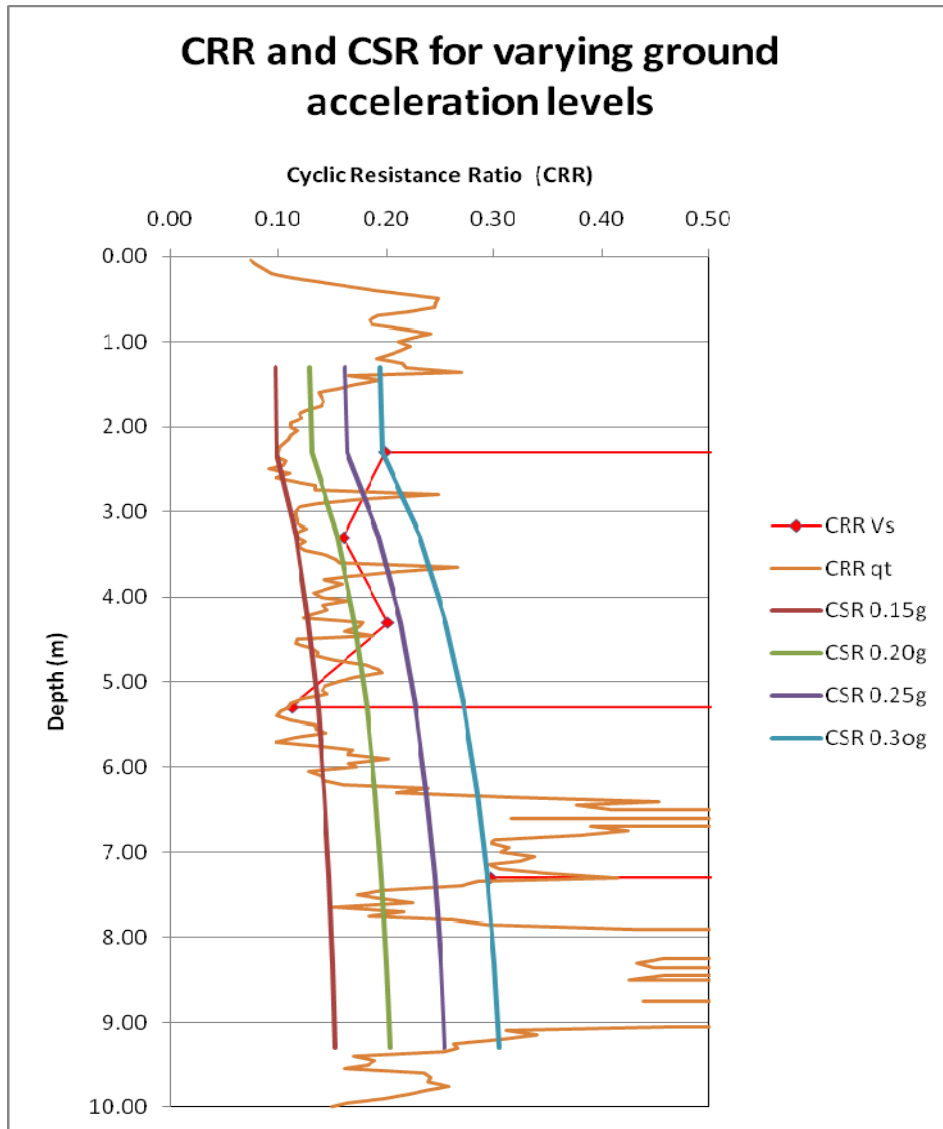


Figure 3.1-6. CSR and CRR determined from SCPT data, Goose Spit, Comox BC

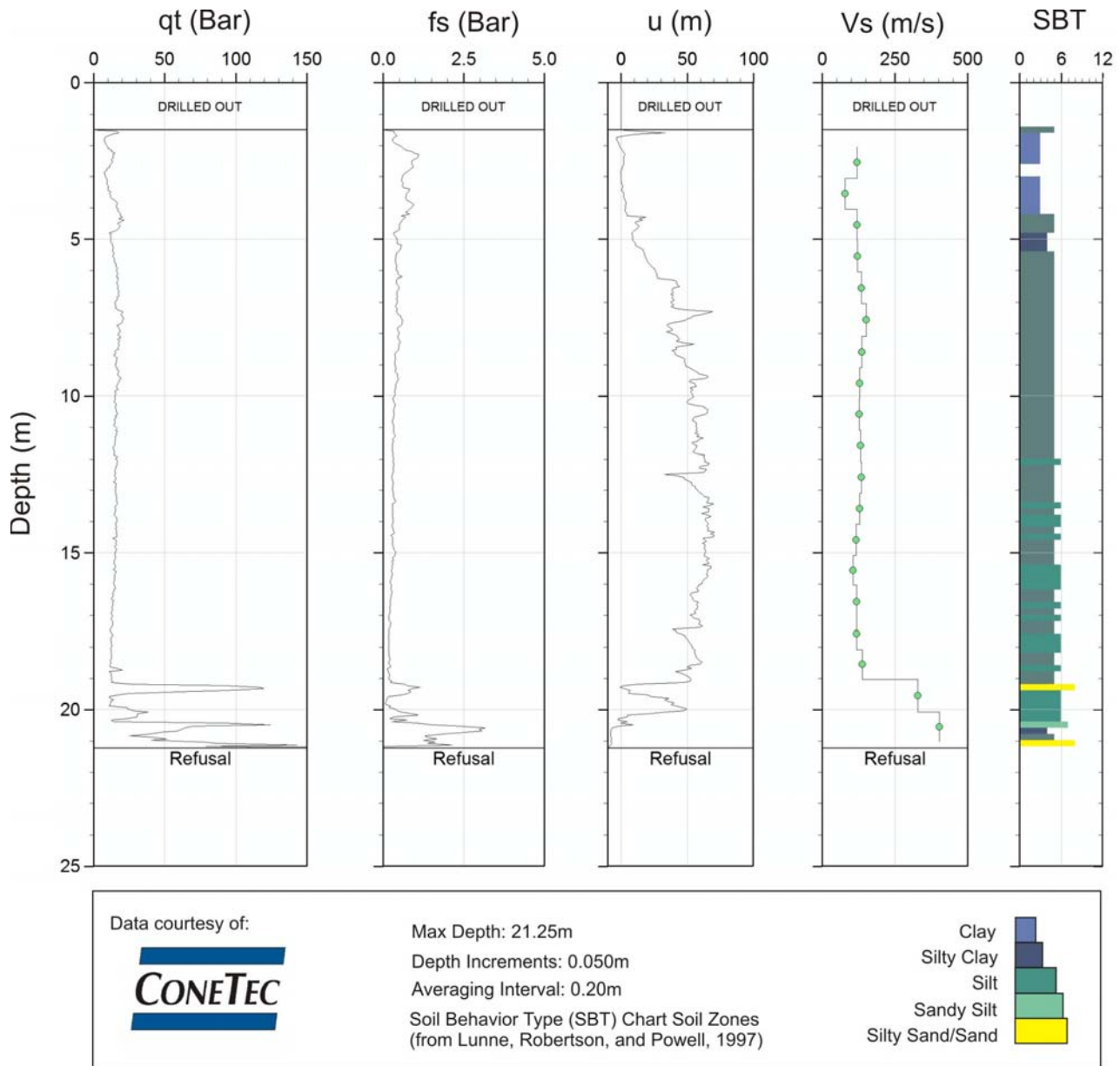


Figure 3.1-7. SCPT Profile, Winnipeg MB.

## References

ASTM D5778-07 (2012). Standard Test Method for Performing Electronic Friction Cone and Piezocone Penetration Testing of Soils, ASTM International, West Conshohoken, PA, 2012, DOI: 10.1520/D5778-12, [www.astm.org](http://www.astm.org).

ASTM D7400-07 (2008). Standard Test Methods for Downhole Seismic Testing, ASTM International, West Conshohoken, PA, 2008, DOI: 10.1520/D7400-08, [www.astm.org](http://www.astm.org).

Baziw, E.J., 2002. Derivation of seismic cone interval velocities utilizing forward modeling and the downhill simplex method; Canadian Geotechnical Journal, v. 39, p. 1181-1192.

Campanella, R.G. and Stewart, W.P., 1991. Downhole Seismic Cone Analysis Using Digital Signal Processing; *in* Proceedings, 2<sup>nd</sup> International Conference on Recent Advances in Geotechnical Earthquake Engineering and Soil Dynamics, v. 1, p. 77-83 (SM #144).

Campanella, R.G. and Stewart, W.P., 1992. Seismic Cone Analysis using digital signal processing for dynamic site characterization; *Canadian Geotechnical Journal*, v. 29, p. 477-486.

Campanella, R.G. and Robertson, P.K., 1984. A Seismic Cone Penetrometer to Measure Engineering Properties of Soil; *in* Proceedings, 54<sup>th</sup> Annual International Meeting and Exposition of the Society of Exploration Geophysicists (SEG), Atlanta, Georgia, U.B.C. Soil Mech Series No. 84.

Casey, T.J. and Mayne, P.W., 2002. Development of an electrically-driven automatic downhole seismic source; *Soil Dynamics and Earthquake Engineering*, v. 22, p. 951-957.

Howie, J.A. and Amini, A., 2005. Numerical simulation of seismic cone signals; *Canadian Geotechnical Journal*, v. 42, p. 574-586.

Matile, G.L.D. and Keller, G.R., 2004. Surficial geology of the Winnipeg map sheet (NTS 62H), Manitoba; Manitoba Industry, Economic Development and Mines, Manitoba Geological Survey, Surficial Geology Compilation Map Series, SG-62H, scale 1:2500000.

Mosher, D.C., Monahan, P.A. and Barrie, J.V., 2001. Submarine failures in the Strait of Georgia, British Columbia: landslides of the 1946 Vancouver Island Earthquake; *in* Proceedings, 54<sup>th</sup> Canadian Geotechnical Conference, Calgary, AB, (eds.) M. Mahmoud, R. Van Everdingen, and J. Carss; Bitech Publishers Ltd., Richmond, B.C. Vol. 2, p. 744-751.

Pullan, S.E. and MacAulay, H.A., 1987. An in-hole shotgun source for engineering seismic surveys; *Geophysics*, v. 52, p. 985-996.

Robertson, P.K. and Wride, C.E., 1998a. Evaluating cyclic liquefaction potential using the cone penetration test; *Canadian Geotechnical Journal*, v. 35, p. 442-459.

Robertson, P. K. and Wride, C. E., 1998b. Cyclic Liquefaction and its Evaluation based on the SPT and CPT; *in* Proceedings, 1996 NCEER workshop on soil liquefaction, Report No. NCEER-97-02.

Youd, T.L., Idriss, I.M., Andrus, R.D., Arango, I., Castro, G., Christian, J.T., Dobry, R., Finn, W.D.L., Harder, L.F., Hynes, M.E., Ishihara, K., Koester, J., Liao, S., Marcuson III, W.F., Martin, G.R., Mitchell, J.K., Moriwaki, Y., Power, M.S., Robertson, P.K., Seed, R. and Stokoe, K.H., 1998. Liquefaction Resistance of Soils: Summary Report from the 1996 NCEER and 1998 NCEER/NSF Workshop on Evaluation of Liquefaction Resistance of Soils, ASCE, *Journal of Geotechnical & Geoenvironmental Engineering*, v. 127, p. 817-833.

#### **Further Reading:**

Lunne, T., Robertson, P.K. and Powell, J.J.M., 1997. Cone Penetration testing in Geotechnical Practice; Blackie Academic & Professional, London, 312 p.

## 3.2 Borehole Methods

### 3.2.1 Shear Wave Velocity Logs from Vertical Seismic Profiles (VSP)

Jean-Luc Arsenault  
Geophysics GPR International Inc., Longueuil, QC

Jim Hunter & Heather Crow  
Geological Survey of Canada, Ottawa, ON

#### Introduction

##### Principles of the Method

A shear wave velocity log is calculated from a vertical seismic profile (VSP) by measuring the traveltimes of waves propagating from a source to a receiver. The method can be conducted as a “downhole” VSP analysis, where a seismic signal generated at the surface is detected by a receiver in a PVC-cased borehole; or an “uphole” VSP analysis where seismic signals originating from a borehole source are measured by receivers placed on the surface. The most commonly used method, and the one described in the case studies in this article, is the downhole approach. In VSP velocity logging, the entire wave train is recorded allowing for the interpretation of later arriving events (e.g. reflections below the bottom of the borehole, converted waves, signal-generated tube waves, etc).

An average shear wave velocity ( $V_{s_{av}}$ ) can be calculated by dividing the source-geophone distance by the traveltime of a wave to that depth.  $V_{s_{av}}$  differs from the definition of interval velocity ( $V_{s_{int}}$ ), which represents the vertical velocity of a particular layer or short interval. A  $V_{s_{30}}$  measurement value is an average traveltime-weighted vertical velocity to a depth of 30 metres, calculated by dividing 30 (m) by the summed vertical travel-times (milliseconds) within all of the layers. This approach is equivalent to dividing 30 m by a single vertical traveltime measurement at 30m depth. The summation method of layer velocities and travel-times as given by the NBCC is preferred, since the interpreter can be guided by the development of a time-depth “wobble-trace” record suite and correlation of shear wave events can be more reliably made.

##### Current State of Engineering Practice

The VSP velocity analysis method has been primarily used for petroleum exploration for over 50 years, but near-surface engineering applications have become popular only in recent decades. The interpretation of compressional (P) and shear (S) wave velocity structure of soils and rock allows for the evaluation of variations in dynamic Poisson's ratio, and supports the estimation of different dynamic mechanical moduli (shear, Young, elastic, and bulk). Horizontally polarized shear waves (SH) created at the surface or in the borehole allow for easier interpretation of the shear wave velocities. Downhole test procedures are described in ASTM standard D7400-07, and further practical aspects of shear wave surveying are described in Hunter et al. (1998, 2002, and 2007).

It should be noted that borehole shear wave velocity measurements are made vertically down through the soil in contrast to shear wave refraction and MASW techniques. Therefore, the downhole approach may be a preferred measurement for one-dimensional earthquake modeling, should vertical-to-horizontal anisotropy exist in the near-surface materials.

##### **Recommended citation:**

Arsenault, J.-L., Hunter, J.A. and Crow, H.L., 2012. Shear Wave Velocity Logs From Vertical Seismic Profiles; *in* Shear Wave Velocity Measurement Guidelines for Canadian Seismic Site Characterization in Soil and Rock, (ed.) J.A. Hunter and H.L. Crow; Geological Survey of Canada, Open File 7078, p.123-138.

## **Limitations**

One of the principal limitations of this method is the clear recognition of the shear wave arrival at short source-receiver offsets near ground surface, as a result of signal-generated P-wave and surface wave noise. Some exceptional site conditions also do not favor the use of this method; dry swamps or significant accumulations of other organic material on surface could jeopardize survey success due to signal damping. When casing (PVC or metal) is inadequately grouted to the formation, poor coupling of shear waves can result; large amplitude “tube” waves and apparent oscillations of the downhole tool can be correlated with areas where poor bonding of the cement grout exists behind the casing.

In stratified soils and fractured rock, there is a potential for shear wave anisotropy to exist wherein the velocity in the horizontal plane (SH) differs from the velocity in the vertical plane (SV). SH velocities may also vary azimuthally; such azimuthal anisotropy commonly is caused by changes in soil fabric, or in the local stress fields. In these cases, the calculated horizontal velocities will be different depending on the polarization of the source and geophone orientation. Where present, azimuthal anisotropy in near surface deposits is often in the range of 5% - 10%, and has been measured on a Fraser River Delta shelf edge at 7% in the upper 40m (Harris et al., 1996; Hunter et al., 2002). In exceptional circumstances, it has been measured up to 25% (Lynn, 1991).

## **Data Collection**

### **Required Equipment**

Three basic components are required to conduct a VSP survey: a seismograph (and recording computer), a downhole tool (3-component is standard), and a source/triggering system (Figure 3.2.1-1). For shear wave velocity measurements in unconsolidated materials, the seismograph should have a sampling rate as low as 50  $\mu$ s (frequency sampling of 20 kHz) and a minimum of 3 recording channels; these basic elements are standard for almost all modern engineering seismographs.

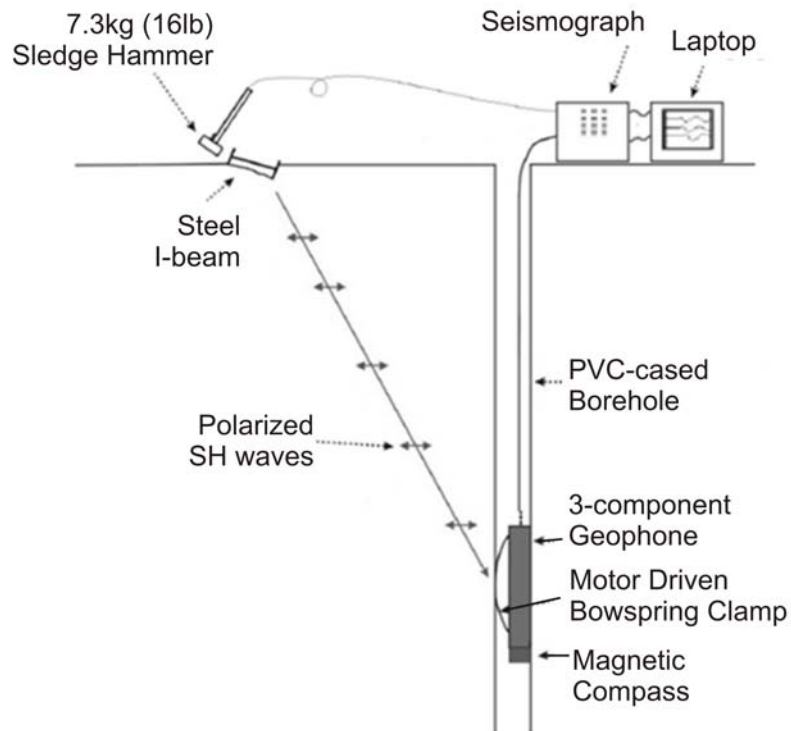


Figure 3.2.1-1. Downhole VSP survey configuration for polarized shear wave data acquisition.

Typically, a three-component downhole tool is used with geophones or accelerometers mounted rigidly in a block, oriented in orthogonal horizontal positions (H1, H2) and one vertical (V) component. It is recommended to use geophones with 8 – 15 Hz resonant frequencies with 60-70% damping in order to adequately capture low frequency horizontally polarized shear waves (SH), and yet have an adequate frequency range (up to 100 Hz). The receivers are contained within an impermeable probe, with an outer mechanical clamping device to ensure that the tool is well coupled with the casing. Such a coupling device could be a bowspring arm (triggered by an impact at the base of the borehole), or an inflatable packer or mechanical/electrical bowspring arm controlled from the surface. To ensure the geophones are aligned in the same orientation for each shot, thin fiberglass rods can be attached to the cable immediately above the tool. Some modern tools contain a fluxgate compass to aid rotation of the sonde prior to clamping; others contain a compass and rotating motor to orient the geophone block to magnetic north once the tool is clamped to the borehole wall (may not work well in the presence of concentrations of ferromagnetic minerals).

The most commonly used seismic source is a 5.5 – 8.0 kg (12-18 lb) sledge hammer, impacted against a loaded I-beam or wooden plank. Firm coupling of the source with the ground surface is of great importance to the success of the survey. If surface conditions consist of rigid or semi-rigid materials (compacted gravel, pavement or concrete), it is common to use a 2 - 3-metre long, 15cm x 15cm, wooden beam loaded by the wheels of a heavy vehicle. When on soft ground, it is preferable to use small (0.3 - 0.5 metre) length of steel I-beam with one flange sunk partially into the ground. For uphole surveys, the in-hole source can be a clamped downhole shear-wave hammer for shallow surveys (<100 m). Other compressive sources such as an air-gun or water-gun, as well as small explosives, can provide adequate shear wave energy at other hole depths. Triggering (time zero) for hammer surveys utilizes either a piezoelectric contact closure device attached to the top side of the hammer handle, or a contact closure circuit from the steel hammer head to the metal I-beam.

### **Data Collection Procedures**

For near-surface logging (< 100m below ground surface), a 1 – 5 metre source offset from the borehole is usually far enough away to reduce significant tube wave coupling to the casing (signal generated noise), but close enough to minimize non-vertical travel paths (refractive effects). The I-beam source is commonly oriented with respect to magnetic north to focus most of the energy in-line with one of the horizontal components; however, some operators prefer equal shear wave energy to be observed on both horizontal components and hence orient the source at 45° to the horizontal axes.

The geophone sonde is commonly moved up or down the borehole at intervals required to adequately delineate velocities associated with geological layers (e.g. small increments to obtain interval velocity estimates of sand layering for liquefaction studies). For most general purpose  $V_{s30}$  surveys, 0.5 or 1 metre intervals are deemed adequate. It is recommended to record shots with opposite source polarities ('toward' and 'away' records) to assist in identifying the onset of shear wave energy. In cases where noise levels are high (e.g. urban environments), stacking (signal record summation) is recommended to improve the signal-to-noise ratio. Special care should be used when stacking to reject poor records. When a 3-component probe is used, vertical impacts on a flat steel plate can also be useful to enhance the visibility of the P wave in the signal.

As a further check on trigger timing a fourth channel can be recorded from a high frequency vertical geophone placed on surface at a standard location (5 to 10 m) away from the borehole. A compilation of these geophone traces can usually help correction of anomalous timing at any sonde location.

## **Processing Techniques**

### **Theory of Analysis**

Superimposing or comparing the "wiggle trace" display of the 'toward' and 'away' shots at any one depth location can assist in the identification of the onset of shear wave motion (Figure 3.2.1-2). Seismic processing packages have a variety of trace gain controls which enhance amplitudes at different times in the signal, or boost overall signal strength to investigate low amplitude events. Filtering can also be used

to remove unwanted noise, but should only be applied when absolutely necessary, as this may alter the signal shape and deteriorate the first arrival onset by the addition of filtering artifacts. If data are noisy, cross-correlation techniques using adjacent depth interval traces will assist in the interpretation of shear wave traveltimes. In datasets with very poor signal-to-noise ratios, it may be possible to detect the onset of shear wave arrivals through the use of hodogram software to closely examine particle motion plots in all three components of motion.

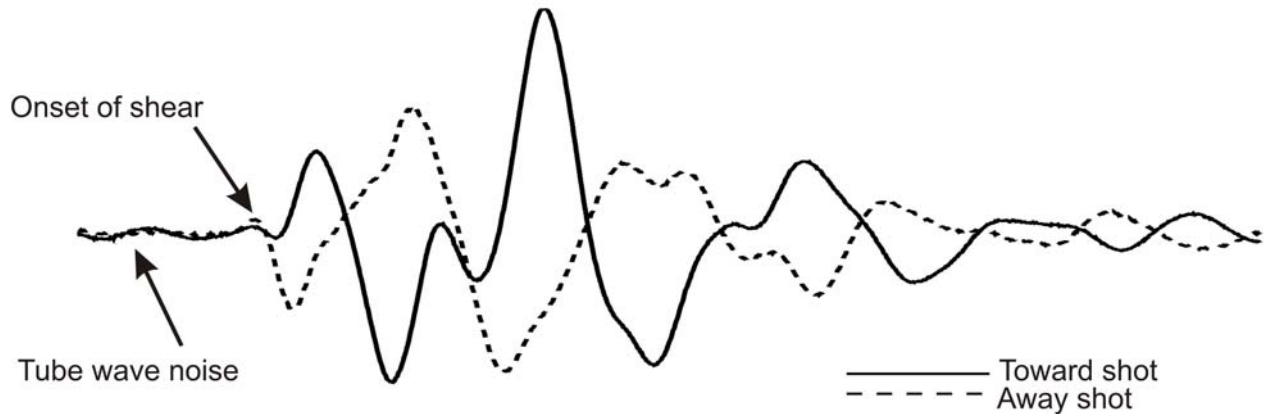


Figure 3.2.1-2. Superimposing toward and away shots at each depth helps to identify the onset time of the shear wave, particularly in cases where traces are noisy.

For a given horizontal component, a compilation of seismic traces can be plotted together as a function of depth. This aids in the identification of arrival times for traces with possible time zero errors or high noise levels which will interfere with arrival time picking. Figure 3.2.1-3 shows a shot gather from a 30 metre borehole in an urban area of Ottawa drilled into clayey silts. With the longer time window, the bedrock reflection and its surface-reflected multiple can be identified. Although the borehole was not drilled to the bedrock interface, the backward projection of the upgoing bedrock reflection can be used to estimate the depth.

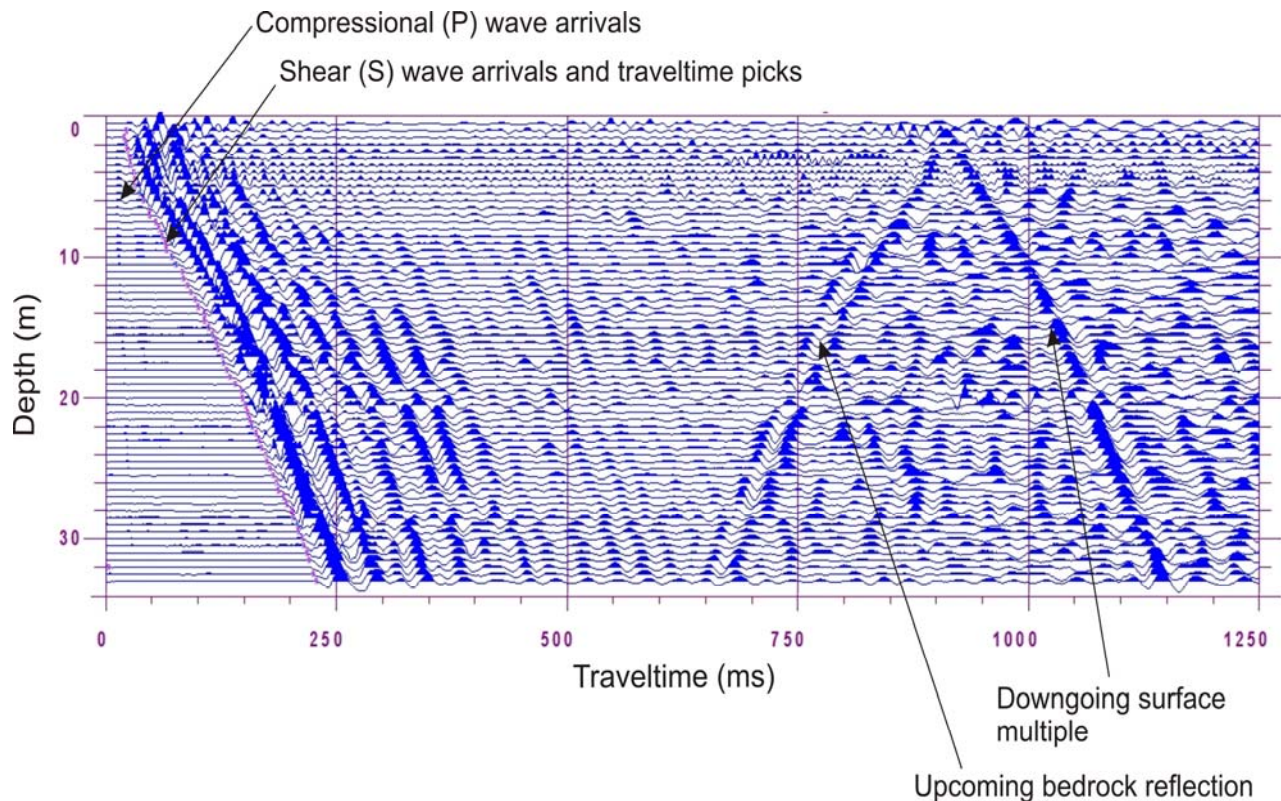


Figure 3.2.1-3. Raw Vertical Seismic Profile (VSP) assembled from merged seismic traces from an Ottawa borehole showing the direct shear wave arrivals and picked traveltimes in the soft, silty, soils. The extended recording window shows the bedrock reflection (from 80m depth), as well as its downgoing multiple, reflected from the surface. The data is presented using an automatic gain control (AGC) display gain to enhance the amplitude of the later arriving events.

The depths and first arrival picks can be exported to a spreadsheet, as shown in Table 3.2.1-1. The recommended processing method is that developed by Hunter et al. (1998, 2002). The distance between the source and receiver is the hypotenuse of the source-borehole offset and the depth of the geophone, which must be calculated to take into account the actual travel path of the wave to the receiver (Figure 3.2.1-4a). The interpreted traveltimes plotted against source-receiver distance and the interval (or layer) velocities between measurement points are calculated by taking the inverse of the slope of a three, five, or more point least-squares fit (Figure 3.2.1-4b). Once the layer  $V_s$  is known ( $V_{s_{int}}$ ), the traveltime within the layer ( $dT$ ) can be calculated. The value of 30 m divided by the sum of all the layer  $dT$ 's, provides the traveltime-weighted  $V_{s_{30}}$  value (as recommended by the NBCC). Alternatively an estimate of  $V_{s_{30}}$  can be obtained by assuming a single "layer" over 30 metres and dividing the source-receiver distance at 30 m depth by the travel time of the shear wave at that depth. As shown in Table 3.2.1-1, the two values should give similar results. However, the "single layer" assumption should only be used as a check on the procedure recommended by NBCC. It is possible that a single travel-time measurement at 30 m depth can be subject to considerable picking error because of poor signal-to-noise and, if this is the only seismic trace taken in the borehole, it cannot be correlated with adjacent traces; a single sonde location and a single trace procedure is not recommended. It is preferable that all downhole surveys for  $V_{s_{30}}$  estimations be conducted using short increments (0.5 m), so that correlations of downhole shear wave arrival times and interval velocities can be used to guide the estimate of traveltime at the depth of 30 m.

Downhole Depth (m)	Source-Receiver Distance (m)	Interpreted Travel time (s)	Vs <sub>int</sub> (m/s) 3pt fit	Error (2σ from LSF)	Layer thickness (m)	Layer dT (s)
0.0	3.0	no reading				
1.0	3.2	0.0122				
2.0	3.6	0.0113	355.7	8.0	2	0.0056
3.0	4.2	0.0130	242.9	2.0	1	0.0041
4.0	5.0	0.0168	167.6	0.0	1	0.0060
5.0	5.8	0.0224	109.6	3.0	1	0.0091
6.0	6.7	0.0321	89.6	0.0	1	0.0112
7.0	7.6	0.0423	101.6	2.0	1	0.0098
8.0	8.5	0.0500	105.2	3.0	1	0.0095
9.0	9.5	0.0600	103.6	3.0	1	0.0097
10.0	10.4	0.0683	112.6	2.0	1	0.0089
11.0	11.4	0.0770	118.5	2.0	1	0.0084
12.0	12.4	0.0845	133.7	1.0	1	0.0075
13.0	13.3	0.0915	150.9	7.0	1	0.0066
14.0	14.3	0.0974	148.4	2.0	1	0.0067
15.0	15.3	0.1046	134.1	0.0	1	0.0075
16.0	16.3	0.1120	134.4	0.0	1	0.0074
17.0	17.3	0.1193	140.6	2.0	1	0.0071
18.0	18.2	0.1260	133.4	5.0	1	0.0075
19.0	19.2	0.1340	133.6	4.0	1	0.0075
20.0	20.2	0.1408	154.9	7.0	1	0.0065
21.0	21.2	0.1468	161.6	4.0	1	0.0062
22.0	22.2	0.1530	157.0	3.0	1	0.0064
23.0	23.2	0.1594	160.2	2.0	1	0.0062
24.0	24.2	0.1654	157.1	5.0	1	0.0064
25.0	25.2	0.1720	147.1	0.0	1	0.0068
26.0	26.2	0.1789	155.5	5.0	1	0.0064
27.0	27.2	0.1848	163.9	6.0	1	0.0061
28.0	28.2	0.1910	151.4	2.0	1	0.0066
29.0	29.2	0.1979	154.3	2.0	1	0.0065
30.0	30.1	<b>0.2039</b>	165.8	3.0	1	0.0060

$$\Sigma dT = 0.2102$$

$$\text{NBCC recommended } Vs_{30} = 30 / \Sigma dt = 142.7$$

$$\text{Error Check: } Vs_{30} \text{ single layer} = 30.1 \text{ m} / \mathbf{0.2039 \text{ s}} = 147.6$$

Table 3.2.1-1: Sample Vs<sub>30</sub> calculation for a 30 m borehole drilled into clayey silt. Note that the NBCC recommended summed travelttime method provides a slightly different result than a single layer approximation at 30 m depth. As a check, these two methods should produce results within a few m/s.

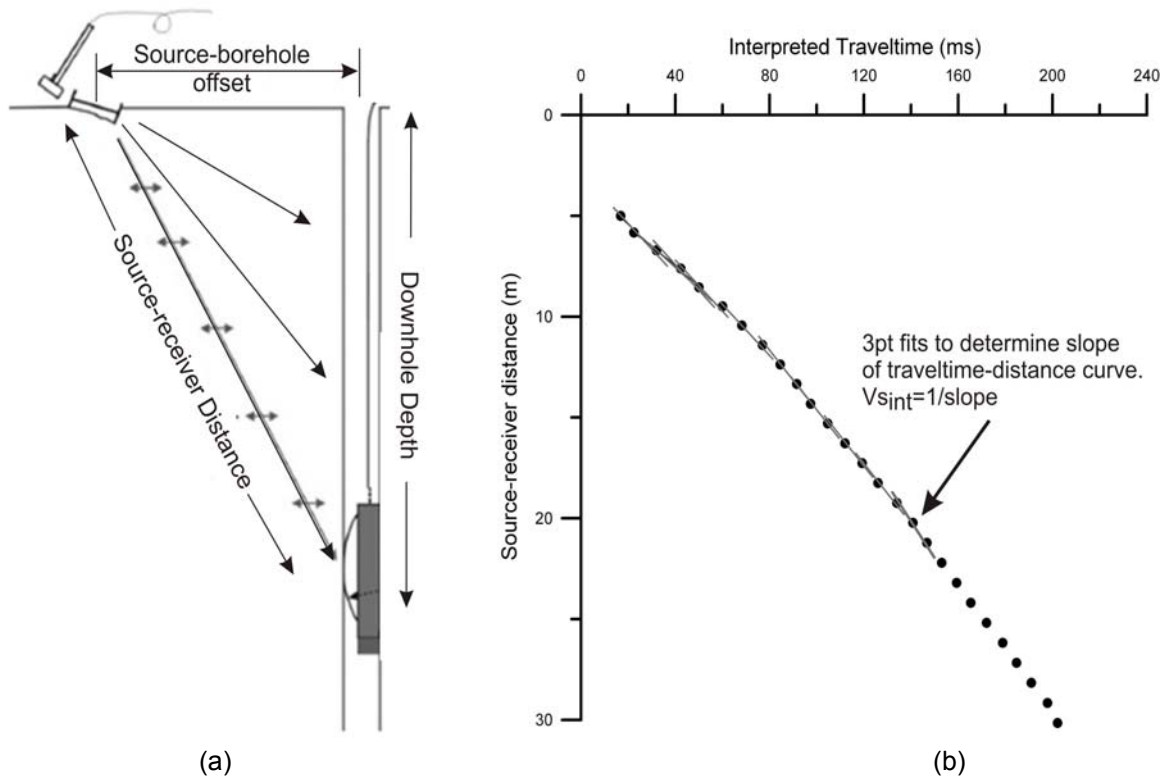


Figure 3.2.1-4. (a) The travel distance of the wave to the geophones is the hypotenuse of the source-borehole offset and the downhole depth of the tool. (b) The interpreted travelttime distances from the seismic records are plotted against the source-receiver distances (not depth of sonde). The inverse slope of a three or five point linear least-squares regression between points provides the layer shear wave velocities between downhole measurement intervals. The travel-time in each interval can be calculated from the downhole interval thicknesses and layer velocities. 30 metres divided by these summed traveltimes yields the  $V_{s_{30}}$  value for the site (refer to Table 3.2.1-1).

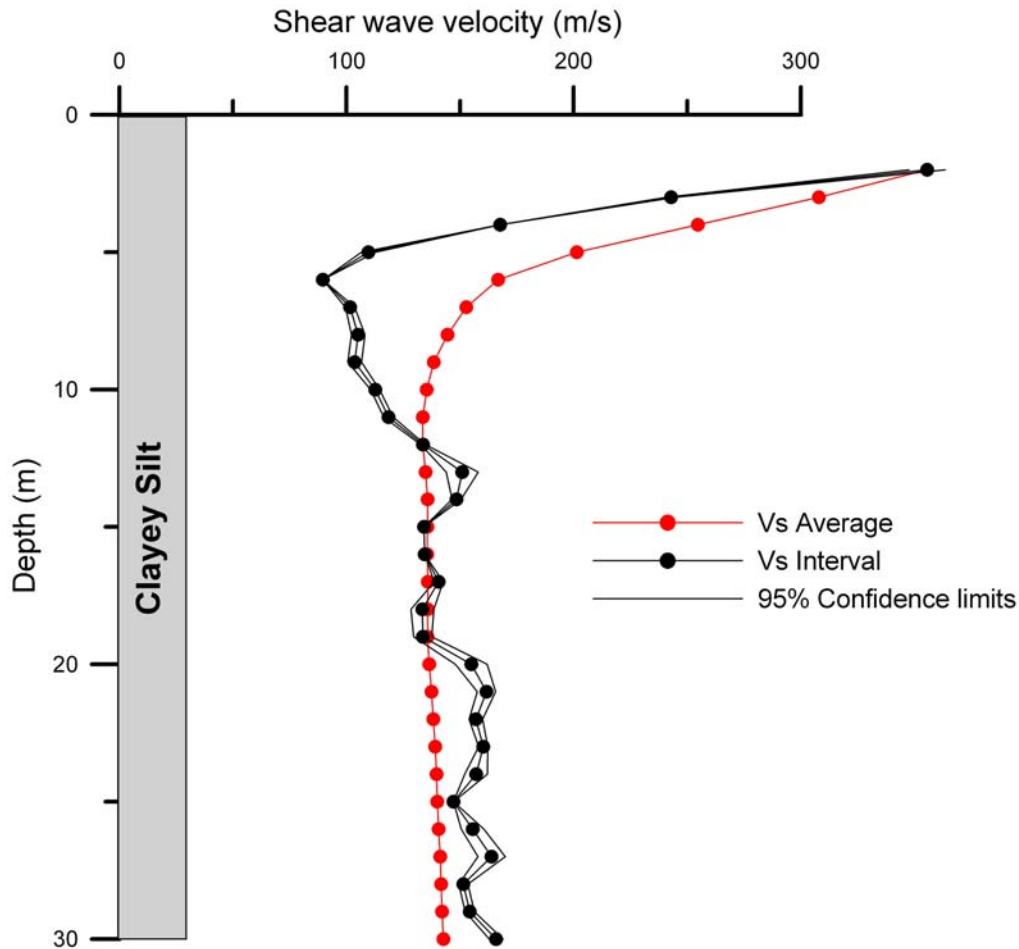


Figure 3.2.1-5. Interval and average shear wave velocity logs, resulting in a  $V_{s30}$  calculation of 142.7 m/s using a 3-point least squares fit. Shear wave velocity measurement alone in this fine-grained cohesive soil cannot be used to define a site class; therefore, this site would be classified as E from the computed  $V_{s30}$  but could also be F based on other geotechnical measurements.

### **Uncertainty Assessment**

A 3-, 5- (or more) point least squares fit on the slope of the traveltime dataset provides an estimate of standard deviation for each of the interval velocities. However, since the error associated with the estimation of 95% confidence limits (2 standard deviations  $\sigma$ ) for a small number of measurements is itself very large, the  $2\sigma$  error limits can only be used as a qualitative estimate of the scatter in the traveltime data. As a check of the  $V_{s30}$  value, it is suggested that the summed interval traveltime method recommended by the NBCC and the direct measurement of traveltime (single layer assumption) at 30m should yield values that are within a few m/s of one another. If the values differ substantially, it is possible that first arrival shear wave onset has been incorrectly interpreted, either because of poor signal-to-noise at the single 30 m sonde depth, or possibly a mis-pick of all arrival times down the compiled trace sections for one or both horizontals. One such possibility is a pick of a first peak or first trough on the shear wave event for all depths; in this case all interval velocities down the hole will most likely be correct but adjustments will have to be made at the near surface to compensate for the incorrect shear wave onset in the upper layer. Alternatively, if evidence exists, after close observation, to correctly identify the first break on some traces, it may be possible to “phantom forward” the pick on the first peak or first trough of each trace using a standard correction time. Such techniques can also be applied at shallow depths where the first arrival may be obscured by source-generated noise. In very noisy environments or very poorly bonded boreholes, it can be helpful to use a secondary surface method (e.g. MASW, or

reflection) which can be collected quickly once on site, and useful for comparison with the downhole results.

The potential for error also exists in first arrival picking when the casing is not well bonded to the formation. Ringing in the casing (tube waves) can distort the true shear wave arrival, which cannot be filtered away (Figure 3.2.1-6)

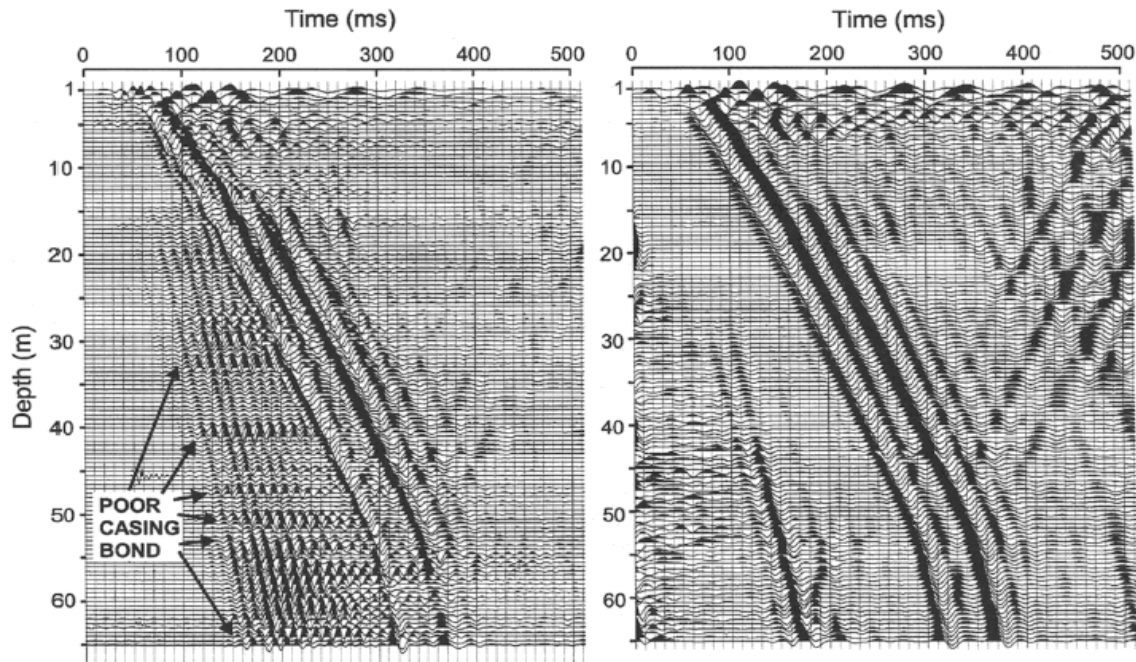


Figure 3.2.1-6. Raw (left panel) and filtered (right panel) downhole records showing interfering ringing effects of 'tube waves' caused by poor casing bond (Geological Survey of Canada, Fraser Delta, BC).

## Recommended Guidelines for Reporting

The field equipment, the acquisition parameters and the description of the field set-up should be specified in the report (including source-borehole offset, logging interval, number of stacks, record length, seismograph sampling rate, etc.) as well as the details of the drilling and any particulars (casing depth, grouting details, etc). The seismogram plot versus depth should be presented to provide a sense of data quality (see Figure 3.2.1-3). The picking results should be presented in tabular form as shown in Table 3.2.1-1, along with the  $V_{s30}$  calculation, as per the NBCC requirements. Average and interval velocities should be presented graphically, preferably with borehole stratigraphy (see Figure 3.2.1-5). As a measure of uncertainty, it is recommended to include the direct "single layer" measurement of travel-time at 30m depth and the resulting  $V_{s30}$  single layer. This result should be within a few percent of the reported travelttime-weighted  $V_{s30}$ .

## Hazard-Related Case Studies

### Bedrock Case:

Limestone and dolostone bedrock with shale interbeds are commonly found throughout south and eastern regions of Ontario and along the Ottawa-Quebec City corridor. A 30 m-deep borehole was drilled within a suburban neighbourhood in Ottawa to investigate the local geotechnical properties of the bedrock and provide a boring for  $V_s$  data collection. The source, a metal I-beam struck with a 16 lb sledge hammer, was positioned 1m from the borehole. Merged seismic traces are shown in Figure 3.2.1-7. Using a 5pt least squares fit of the traveltimes, the travelttime-weighted analysis resulted in a  $V_{s30}$  calculation of 1486 m/s. The 'direct' measurement of travelttime at 30 m depth resulted in a  $V_{s30}$  value of

1362 m/s. Sources of error for this discrepancy include a noisy suburban environment (site near roadway), and a weak tube wave interfering event preceding the shear wave first arrival in the lower part of the hole. Here, the first arrival picks are influenced by the presence of the tube wave. Larger error would probably result from a single arrival time estimate at 30 m depth (the single layer approximation) compared to the recommended travel-time summation approach.

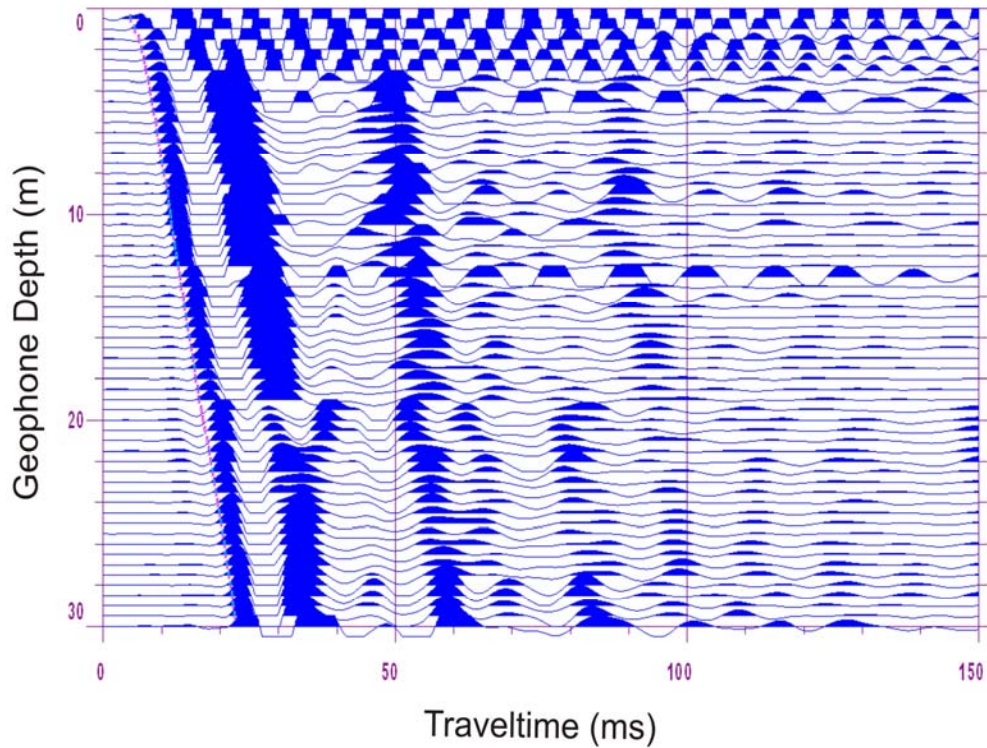


Figure 3.2.1-7. Interpreted arrival picks from the H2 component VSP for a 30 m borehole drilled into limestone/dolostone/shale bedrock in Ontario. Source-borehole offset was 1m. Records were collected at 0.5 m geophone intervals. Note that a weak tube wave interfering event precedes the shear wave first arrival in the lower part of the hole; hence first arrival event picking is guided by the first peak excursion.

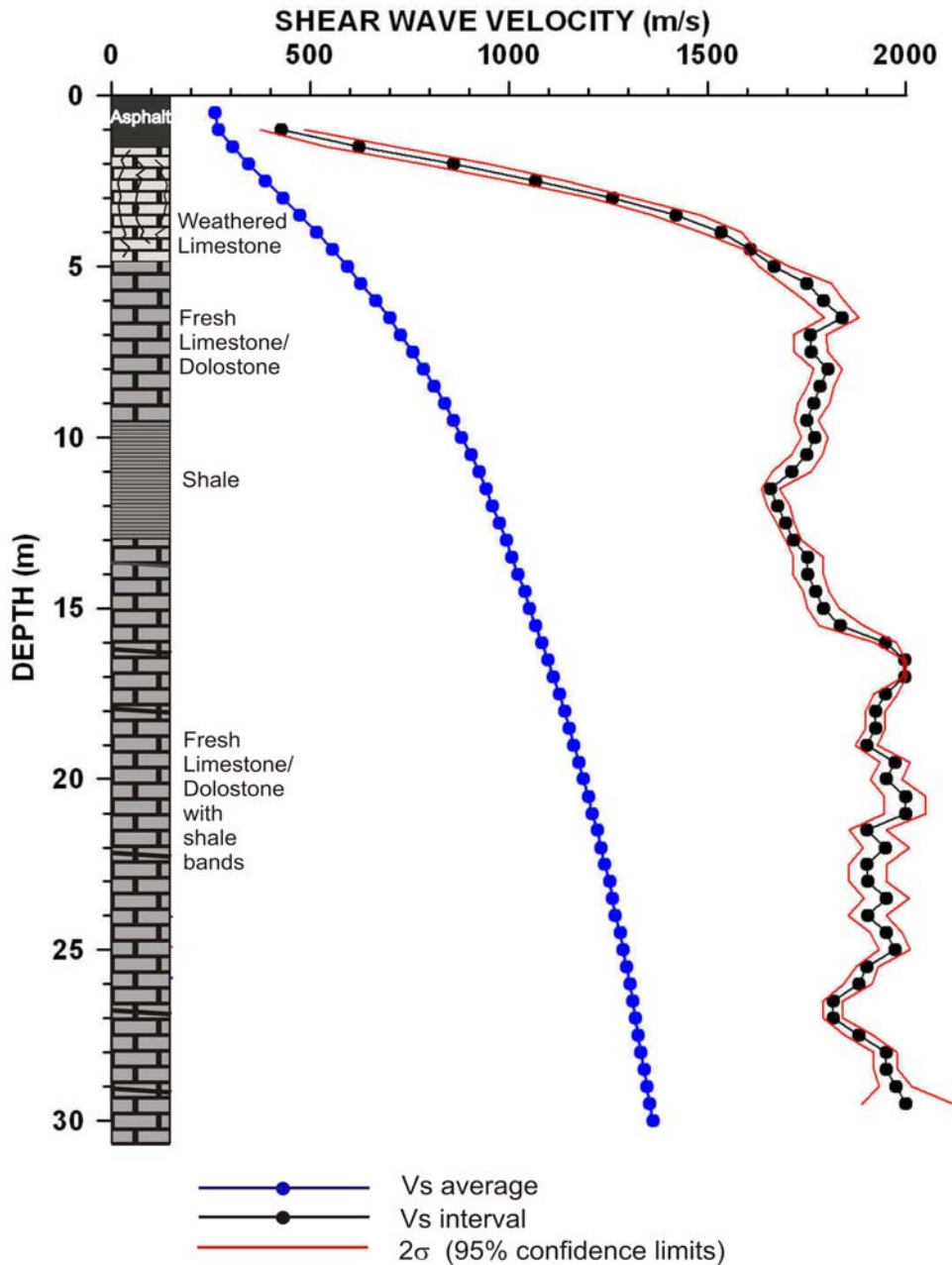


Figure 3.2.1-8. Resulting shear wave velocity logs for a typical eastern-Canadian bedrock site. Traveltime-weighted analysis leads to a  $V_{s30}$  value of 1486 m/s, while the direct single-layer approximation measured traveltime produced a  $V_{s30}$  of 1362 m/s (note; the travel time value at 30 m depth has a probable large error due to noise interference).

**Glacially-derived Soils Case:**

Prior to development, a 30 m borehole was drilled at a site where glacially-derived sands, silts, and gravels were deposited in a 29 m-thick sequence over limestone bedrock. VSP from merged seismic traces, collected at 0.5 m intervals, showed that the casing was well grouted within the formation, providing a high quality downhole record. A recording window of 250 ms allowed for the detection of the bedrock reflection (Figure 3.2.1-9). Traveltime-weighted shear wave analysis yielded a  $V_{s30}$  value of 245 m/s. As a check, the 'direct' traveltime measurement at 30m depth yielded a  $V_{s30}$  of 250 m/s, providing a good measure of confidence in the  $V_{s30}$  calculations (Figure 3.2.1-10).

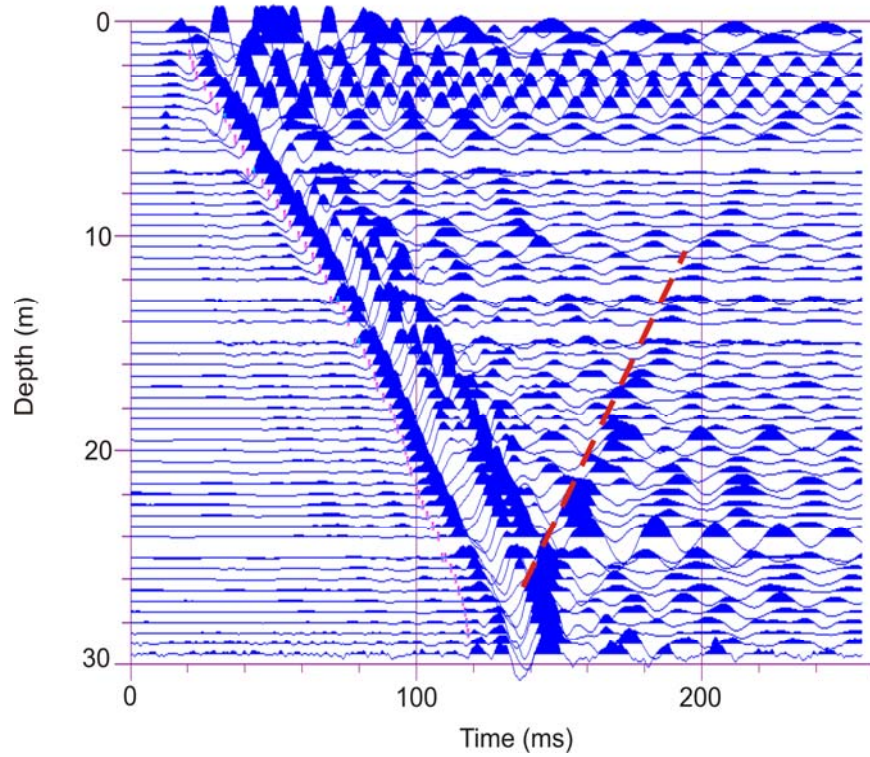


Figure 3.2.1-9. Interpreted arrival picks from the H2 component VSP for a 29.5-m borehole drilled into glacial soils (sands, silty clays, gravels). Source-borehole offset was 3 m. Red dashed line indicates bedrock reflection.



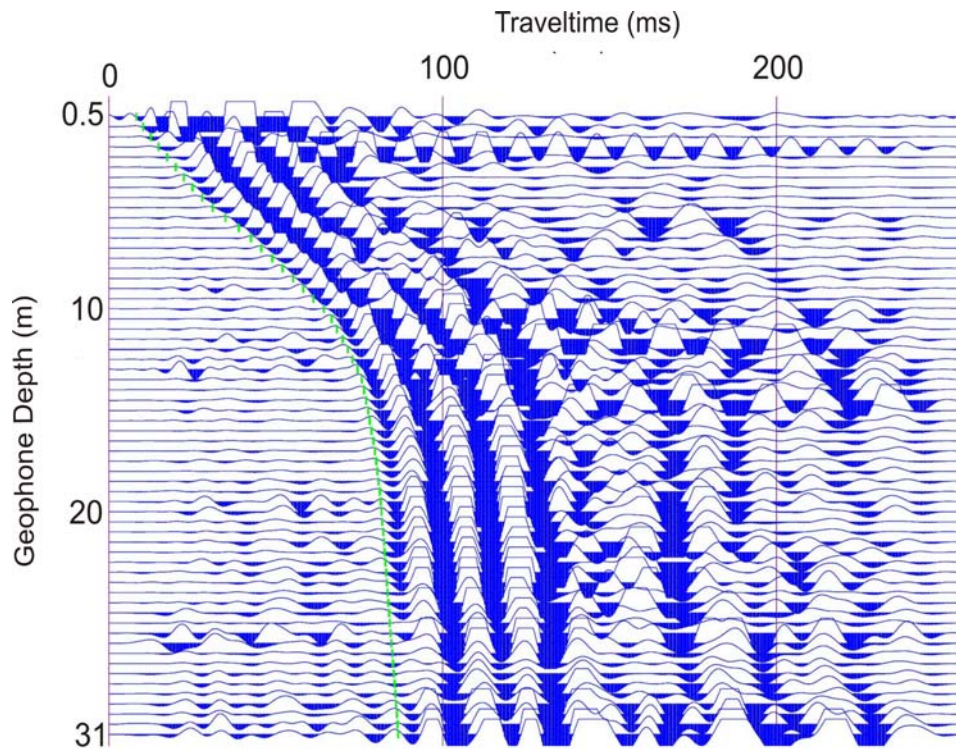


Figure 3.2.1-11. Interpreted arrival picks from the H2 component VSP for a 31-m borehole drilled into shallow soils over bedrock. Source-borehole offset was 3m. Note first arrival interference from tube wave events in the 27 – 29 metre range. The second cross-over was used as a guide to “phantom” in the first arrivals in that zone.

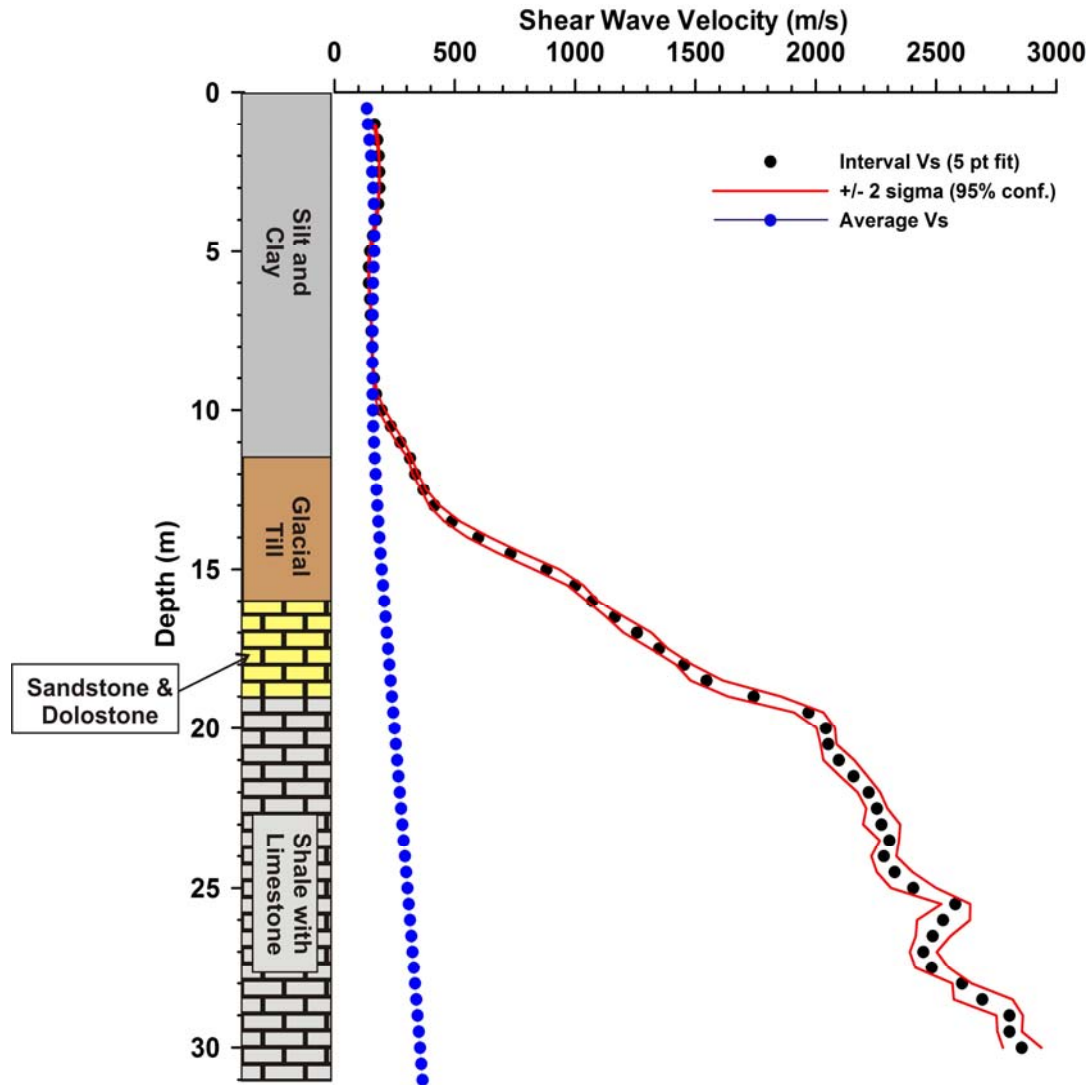


Figure 3.2.1-12. Resulting shear wave velocity logs for a shallow (<16 m) overburden and bedrock site. Traveltime-weighted analysis led to a  $V_{s30}$  value of 370 m/s, while the traveltime for the single-layer approximation at 30 m depth yielded a  $V_{s30}$  of 356 m/s.

## References

ASTM D7400-07 (2008). Standard Test Methods for Downhole Seismic Testing, ASTM International, West Conshohoken, PA, 2008, DOI: 10.1520/D7400-08, [www.astm.org](http://www.astm.org).

Harris J.B., Hunter J.A., Burns, R.A., Good, R.L. and Luternauer, J.L., 1996. Observation of shear-wave splitting in Holocene sediments of the Fraser River delta, British Columbia, Canada; *in* Proceedings, 7<sup>th</sup> International Workshop on Seismic Anisotropy, Miami, FL, (abstract).

Hunter, J.A., Pullan, S.E., Burns, R.A., Good, R.L., Harris, J.B., Pugin, A., Skvortsov, A. and Goriainov, N.N., 1998. Downhole seismic logging for high-resolution reflection surveying in unconsolidated overburden; *Geophysics*, v.63, p.1371-1384.

Hunter, J.A., Benjumea, B., Harris, J.B., Miller, R.D., Pullan, S.E., Burns, R.A. and Good, R.L., 2002. Surface and downhole shear wave seismic methods for thick soil site investigations; *Soil Dynamics and Earthquake Engineering*, v.22, p.931-941.

Hunter, J.A., Burns, R.A., Good, R.L., Aylsworth, J.M., Pullan, S.E., Perret, D. and Douma, M., 2007. Borehole shear wave velocity measurements of the Champlain Sea sediments in the Ottawa-Montréal region, Geological Survey of Canada, Open File 5345, 30 (+ app.) p., 1 CD-ROM. <[ftp://ftp2.cits.mcan.gc.ca/pub/geott/ess\\_pubs/223/223226/of\\_5345.zip](ftp://ftp2.cits.mcan.gc.ca/pub/geott/ess_pubs/223/223226/of_5345.zip)> [accessed: Jan 2012]

Lynn, H. B., 1991. Field measurements of azimuthal anisotropy: First 60m, San Francisco Bay area, CA, and estimation of horizontal stresses' ratio from  $V_{s1}/V_{s2}$ ; *Geophysics*, v. 56, p. 822-832.

### Further Reading

Hunter, J.A., Woeller, D.J. and Luternauer, J.L., 1991. Comparison of surface, borehole, and seismic cone penetrometer methods of determining the shallow shear wave velocity structure in the Fraser River delta, British Columbia; *in Current Research, Part A, Geological Survey of Canada, Paper 91-1A*, p. 23-26.

Hunter, J.A., Crow, H., Brooks, G.R., Pyne, M., Lamontagne, M., Pugin, A., Pullan, S.E., Cartwright, T., Douma, M., Burns, R.A., Good, R. L., Motazedian, D., Kaheshi-Banab, K., Caron, R., Kolaj, M., Folahan, I., Dixon, L., Dion, K. and Duxbury, A.. 2010. Seismic site classification and site period mapping in the Ottawa area using geophysical methods. Geological Survey of Canada, Open File Report 6273, 80 pages 1 DVD. <[ftp://ftp2.cits.mcan.gc.ca/pub/geott/ess\\_pubs/286/286323/of\\_6273.zip](ftp://ftp2.cits.mcan.gc.ca/pub/geott/ess_pubs/286/286323/of_6273.zip)> [accessed: Jan 2012]

Sol, S., Phillips, S., Walters, D.L. and Bidhendi, H., 2011. A comparison of different methods for the estimation of NBCC 2005 seismic hazard site classification: A case study from the Toronto-York Spadina Subway extension project; *in Proceedings, 14<sup>th</sup> Pan-American Conference on Soil Mechanics and Geotechnical Engineering / 64<sup>th</sup> Canadian Geotechnical Conference*, Toronto, ON, BiTech Publishers Ltd., Richmond, BC.

## 3.2.2 Full Waveform Sonic Logging for Shear Wave Velocity

Heather Crow

Geological Survey of Canada, Ottawa, ON

### Introduction

#### Principles of the Method

In full waveform sonic logging, one or two transmitters at the base of a centralized sonic probe emit pulses of high frequency mechanical energy (ranging between 1 and 50 kHz) into a fluid filled borehole. The compressional energy is refracted at the borehole wall as compressional (P) and shear (S) head waves and reflected as numerous modes, which are recorded by two or more receivers on the probe (Figure 3.2.2-1). An advantage of full waveform sonic logging over earlier sonic methods is the ability to record the full wavetrain, and thereby calculate shear wave velocity through later arrivals in the signal.

Downhole sonic tools have a long history in the petroleum industry for porosity estimation using P-wave transit times measured in open rock boreholes. In the mid 1970's, it was recognized that acoustic logs were not just recording body waves ( $V_p$  &  $V_s$ ), but compressional and shear head waves, and a potentially large number of trapped P-, S-, and Stoneley wave modes travelling along the borehole wall (Paillet & Cheng, 1991). The use of synthetic microseismograms significantly improved the understanding of borehole wave propagation (and attenuation) through comparison with waves collected during carefully controlled experiments. Although these multiple modes complicated the analysis of the recorded signals, they also established a connection between formation properties, borehole conditions, and the shape of the recorded wave. It was also found that certain transmitter frequencies could excite the desired wave modes and suppress unwanted modes, depending on borehole diameter, condition, and lithology. Modern full waveform tools now allow the user to select the most optimal single transmitter frequency for logging, thereby reducing the complexity of the waveform and enabling clearer shear wave analysis.

#### Current State of Engineering Practice

While a specific ASTM standard does not exist for full waveform sonic logging, recommended reference texts are written by White (1983) on the theory of acoustic waves in boreholes, and Paillet & Cheng (1991) and Hearst et al. (2000) on the theory and experimental evidence necessary to model, collect, and interpret sonic logs.

Modern downhole sonic tools must have a minimum of two receivers, and three or more are required for high quality semblance processing, recommended for S-wave interpretation. Most modern tools allow the user to select the optimal transmitter frequencies, and have a monopole source configuration (some can be altered to operate as dipole sources), meaning that indirect methods must be used to interpret shear wave velocities in slow formations. For geotechnical applications, P- and S-wave velocity logs are being combined with density logs to calculate elastic parameters (Young, bulk, and shear moduli).

Other sonic log applications include 'bond logging', where compressional wave amplitudes from a cased borehole are interpreted to determine the presence of cement or grout behind the casing wall. This is used to assess the degree of bonding between the casing and the formation, and is typically used for groundwater applications.

#### **Recommended citation:**

Crow, H.L., 2012. Full waveform Sonic Logging for Shear Wave Velocity; *in* Shear Wave Velocity Measurement Guidelines for Canadian Seismic Site Characterization in Soil and Rock, (ed.) J.A. Hunter and H.L. Crow; Geological Survey of Canada, Open File 7078, p. 139-149.

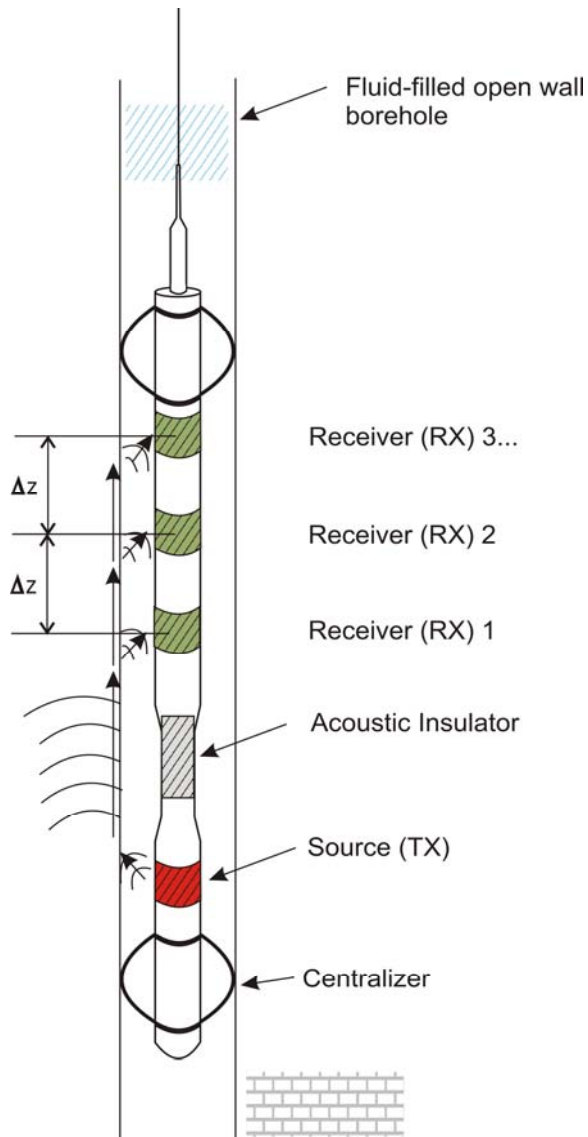


Figure 3.2.2-1. Generalized schematic of a three receiver-one transmitter full waveform sonic tool in a fluid-filled borehole with simplified ray path transmission.

### **Limitations**

This method can be used to determine formation velocities in cased boreholes where a well bonded casing velocity exceeds the formation velocity (approximate PVC P-wave velocity:  $\sim 1900$  m/s, approximate steel P-wave velocity:  $\sim 5900$  m/s), but a correction must be made to take into account the reduced traveltime of the raypaths in the higher velocity casing/cement (Paillet and Cheng, 1991, p.152). Therefore, this method is best suited for shear wave logging in open-rock boreholes, and must be carried out in fluid-filled borings. The tool must also be well centralized; otherwise, signals reflected from opposite sides of the borehole wall can interfere destructively with the waveform and reduce signal quality. A caliper log can determine zones in which the borehole may be washed out or fractured, thereby affecting tool centralization.

Shear wave measurement using a monopole full waveform sonic tool is interpreted differently in a “fast” versus “slow” formation. “Slow” formations are those which have a lower shear wave velocity than the compressional velocity of the borehole fluid (water  $V_p \sim 1450$  m/s) or mud ( $V_p \sim 1800$  m/s) (Paillet & Cheng, 1991). In “soft” formations, most of the transmitted energy is partitioned into P-wave modes, making the interpretation of shear wave velocities in slower materials much more difficult. In these cases, it is necessary to measure  $V_s$  through indirect methods, such as tube (Stoneley) wave interpretation (Cheng

and Toksöz, 1983; Stevens and Day, 1986; Oden and LoCoco, 2000). Although recent US research has been carried out on S-wave interpretation using Stoneley wave measurements, this approach is not known to be used in practice and a different downhole seismic method is strongly recommended in these conditions (e.g. VSP, cross-hole). In a “fast” formation, shear wave arrivals can be picked either visually, or more accurately, through semblance processing or other advanced picking techniques.

An alternative to measuring shear wave velocities with a monopole source is to use a dipole transmitter configuration, which some modern tools can be adapted for. A dipole system can excite a flexural wave in the borehole, where the first arrival will travel at the formation’s shear wave velocity (Paillet & Cheng, 1991). Therefore, flexural waves can be used to measure both fast and slow shear velocities with a straightforward two receiver moveout algorithm.

## Data Collection

### Required Equipment

Modern logging systems consist of a winch with several hundred metres of wireline, a logging console or digital interface, a series of interchangeable downhole probes, and a digital or optical encoder which records depth to the nearest 0.01 m. Systems are controlled with manufacturer’s logging software on a portable field computer, and data are recorded digitally. Waterfall displays on the computer screen allow for the data to be quality controlled in real time. A portable power source, such as a generator or battery, is required and should be used with a sine wave inverter for optimal system performance. Modern tools can often be configured to run with transmitters in monopole or multi-pole modes.

While borehole diameter and mode content have a large effect on resulting waveforms, Paillet and Cheng (1986) demonstrated that the most important element for head wave excitation is choosing the correct frequency of the source signal centered on one of the cut-off frequencies of the lowest compressional or shear mode. The cut-off frequency is the frequency below which a given mode cannot exist. Because the modes are highly dispersive (velocity varies with frequency), the mode velocity approaches the desired head wave velocity as the frequency approaches the mode cut-off frequency. For P-wave surveys, the desired frequency is above the compressional cut-off frequency, but not so high as to excite normal modes that complicate the received waveform. To allow maximum flexibility, modern full waveform sonic tools typically have a range of user-selectable transmitter frequencies ranging between 1-50kHz.

### Data Collection Procedures

Several uphole passes of the tool may need to be carried out at various frequencies to collect optimal waveforms for P- and S-wave analyses. As a rule of thumb, P- and S-wave signal excitation cut-off frequencies can be estimated using the following equation (Oden et al., 2000):

$$f_{co} \propto \frac{v_{mode}}{BoreholeDiameter} \quad [3.2.2-1]$$

where  $v_{mode}$  is the anticipated P- or S-wave mode velocity in the formation.

Before lowering a sonic tool down an open borehole, a dummy probe should always be run. The weight of the tool and scraping of the centralizers in potential fracture zones can lead to dislodging of rock fragments which could lodge the tool. Depth ‘zeroing’ of the tool at surface must be performed to ensure the readings reflect the position of the receivers. Typically, an average receiver offset from some reference point on the tool is used for the ‘sensor’ depth. Recommended logging speed is in the range of 3m/minute.

Logs should be run uphole to keep constant tension on the wireline. Repeat logs are recommended at a variety of frequency settings with the range of the target cut-off frequency(ies). A depth check should be performed at the end of the up run and compared to the start depth at the outset to look for discrepancies.

## Processing Techniques

### Theory of Analysis - Monopole Sources

#### **“Fast” Formations**

The picking of S-wave arrivals from full waveforms is much more complicated than the picking of P-wave first arrivals due to the presence of constructive interference from the normal modes. In “fast” formations, shear wave arrivals can sometimes be picked visually or, more reliably, through semblance cross-correlation. Visual picking is aided by a high amplitude pseudo-Rayleigh wave which travels with the shear wave packet (Paillet & Cheng, 1991). Semblance cross-correlation processing helps improve the picking when the shear arrival is difficult to identify. An early algorithm was developed by Willis and Toksöz (1983) which takes into account the amplitudes and coherency of the waveform and compares this with the signals recorded by the other receivers to establish a more robust shear wave arrival. Semblance routines are usually provided in sonic processing packages. Prior to beginning semblance processing, it is advised to first use signal stacking or filtering to remove front-end noise from the individual receiver traces.

#### **“Slow” Formations**

In “slow” formations, indirect methods to determine shear wave velocity must be employed when using a monopole source. As mentioned earlier, these methods are interpretive and not known to be used in practice. They are based on idealized borehole models (i.e. cylindrical borehole in an elastic, homogenous formation; no borehole irregularities) which can lead to results which deviate from reality, particularly in horizontally heterogeneous units, like shales. The first and more common method is Stoneley (or tube) wave interpretation, as the Stoneley wave phase velocity is quite sensitive to formation shear velocity in slow formations (Cheng and Toksöz, 1982; White, 1983; Stevens and Day, 1986; Oden and Lococo, 2000; Oden et al., 2000). The other factor influencing the Stoneley wave velocity is the borehole fluid. Therefore, if Stoneley velocity and the fluid compressional velocity can be measured, shear wave velocity can be solved through inversion (Stevens and Day, 1986).

A second processing approach is through leaky-P mode interpretation. A leaky-P mode is one which follows closely behind the P head wave arrival but has lost some of its energy by conversion to shear wave energy during refraction. This approach is useful when a tube wave was not excited due to the use of a higher frequency source (i.e. 13-15 kHz). In principle, the amount of energy being radiated into the formation from a leaky-P wave is dependant on Poisson’s ratio, and thus on shear wave velocity. Details of the inversion process are described by Cheng (1989). This method is reported to be unstable in formations with shear wave velocities below 800 m/s (Paillet & Cheng, 1991).

### Theory of Analysis - Multi-pole Sources

As mentioned, the most direct method of measuring shear wave transit times is through the use of a dipole or quadrupole source. However, the theory behind analysis of nonaxisymmetric waveforms is more complicated than with monopole sources, and good resources on topic are found in Schmitt (1988), and Chen (1988, 1989).

#### **Uncertainty Assessment**

To correctly interpret P- and S-wave arrivals, it is critical to have a good understanding of wave propagation theory in fluid-filled boreholes. Choice of the optimal signal frequency and processing method must depend on knowledge of the physical conditions and lithological units in the borehole. The presence of cavities, fractures, and zones of weakness in the borehole wall will affect tool response and may lead to misinterpretation of the arrival times. In addition, interpretation of waveforms and inversion processing should not be undertaken without suitable understanding of the principles of analysis.

## Recommended Guidelines for Reporting

Minimum reporting requirements must include basic survey information such as tool configuration, details of tool runs and transmitter frequencies used, and survey date(s). Drilling details, such as date, borehole and casing diameters, drilling method, total drill depth, and any particulars of the drilling fluids must also be included. The shear (and compression) wave logs must be accompanied by a geological or drilling log, and caliper log. In addition to the interpreted velocity logs, the VDL (variable density log) display or wiggle trace display of the raw downhole data must be provided along with interpreted arrival time picks. A sample time pick should be shown on two or three sample traces in separate figures. The geophysical and geological logs should be presented side-by-side in a suite with the caliper log and any others collected for interpretation. Details of any inversion process used must be described along with the assumptions and inherent velocity and depth errors.

## Hazard-Related Case Studies

### Case 1: FWS logs at a fractured bedrock site

A large-scale geotechnical study was undertaken to investigate faulted bedrock beneath a historic building complex. Vertical and inclined boreholes were drilled across the site and a suite of geophysical logs were collected to assess the *in situ* characteristics of the rock mass. The suite was composed of full waveform sonic (FWS), optical (OTV) and acoustic (ATV) televiewers, natural gamma, apparent conductivity, caliper, fluid temperature & conductivity, and flowmeter logs.

Figure 3.2.2-2 presents a sample 1.20m interval from the OTV and ATV logs, showing an ‘unwrapped’ 360° image of the inside of an inclined borehole wall. OTV images provide a high resolution picture of the rock wall, while ATV panels show the amplitude of high-frequency sound waves reflected off the borehole wall. Where the wall widens due to fracturing or cavities, the amplitude is reduced and the image darkens. The OTV and ATV images greatly assist in the interpretation of the FWS data, as they provide information on the condition of the rock wall *in situ* such as fracture aperture and depth of penetration into the borehole wall.

Figure 3.2.2-3 shows a sample of the raw waveform data from one of the inclined holes (35° from horizontal), and the resulting velocity interpretation. The variable density log (VDL) in the first column presents raw waveform data from the first of the tool’s three receivers (RX-1) and the interpreted arrival times of the P-wave downhole. The second column presents the results of the semblance processing which uses waveform data from all three of the tool’s receivers. This technique produces high correlation bands of the interpreted P- and S-wave slowness, which can then be inverted to produce velocity logs (column 4). The caliper log identifies areas in the borehole where large fractures were encountered (column 3), correlating with P- and S-wave velocity decreases.

Once depths are corrected for the inclination of the borehole, an analysis of  $V_{s30}$  using the travelttime-weighted method can be completed. At this site, however, the degree of fracturing in the near-surface bedrock was found to be a controlling factor for the design criteria at the site.

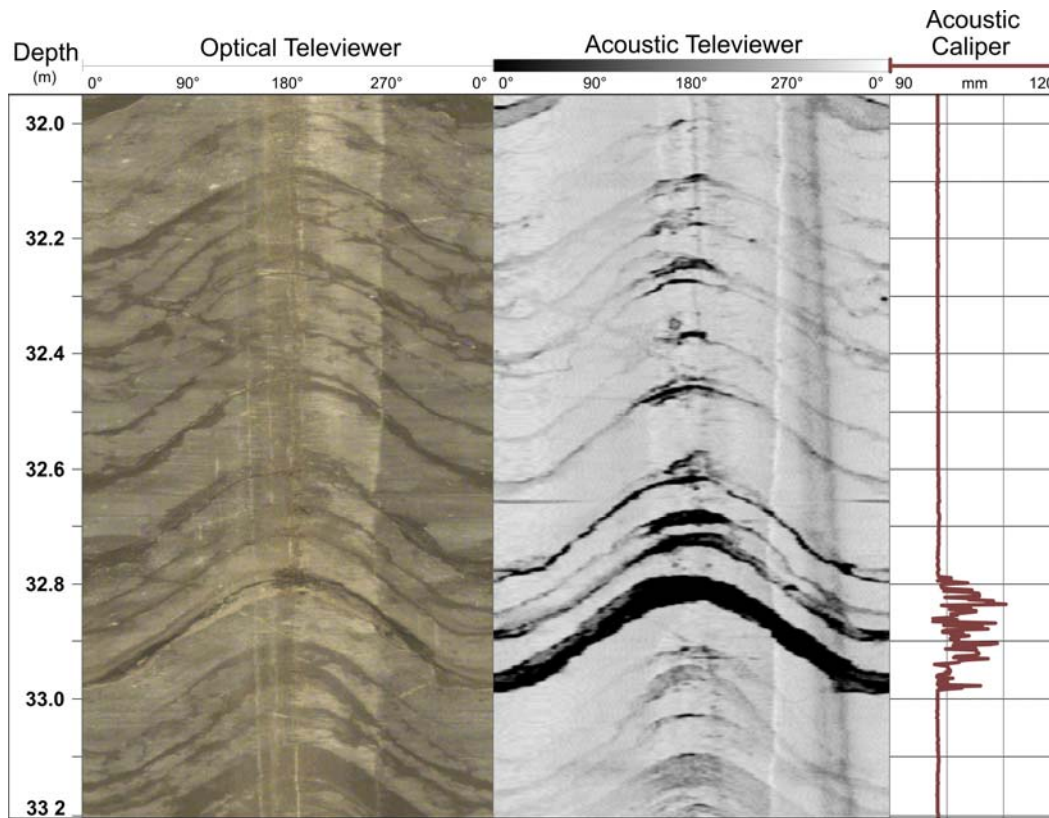


Figure 3.2.2-2. Sample optical (OTV) and acoustic (ATV) televiewer data segment showing an 'unwrapped' 360° image of the inside of an inclined borehole wall. The OTV-ATV images are complimentary, permitting an improved inspection of the condition of the rock wall *in situ*, and are helpful in the interpretation of full waveform sonic data by highlighting zones of fracture.

At a vertical borehole on the same property but some distance away, a VSP (vertical seismic profile, see Section 3.2.1 for VSP methodology) was also collected. The source, a metal beam struck on its edges with a sledge hammer to produce horizontally polarized shear waves, was positioned 1.5m from the borehole. The results of the survey are plotted next to the FWS results, which are shown adjusted to vertical (Figure 3.2.2-4). Where both boreholes intersect zones of relatively competent bedrock, the results indicate velocities average approximately 2800-3000 m/s, but on different scales: the VSP averages over larger volumes, while the FWS is looking at smaller intervals within a few centimetres around the borehole wall, hence the variability in log (b). The FWS sampling interval is 8 cm, whereas the VSP was collected with 1 m intervals, therefore, inherent smoothing is seen in the VSP data when comparing the two datasets. In addition to the differences in the data collection methods, this figure also illustrates how variable conditions can appear to be between two boreholes on the same site.

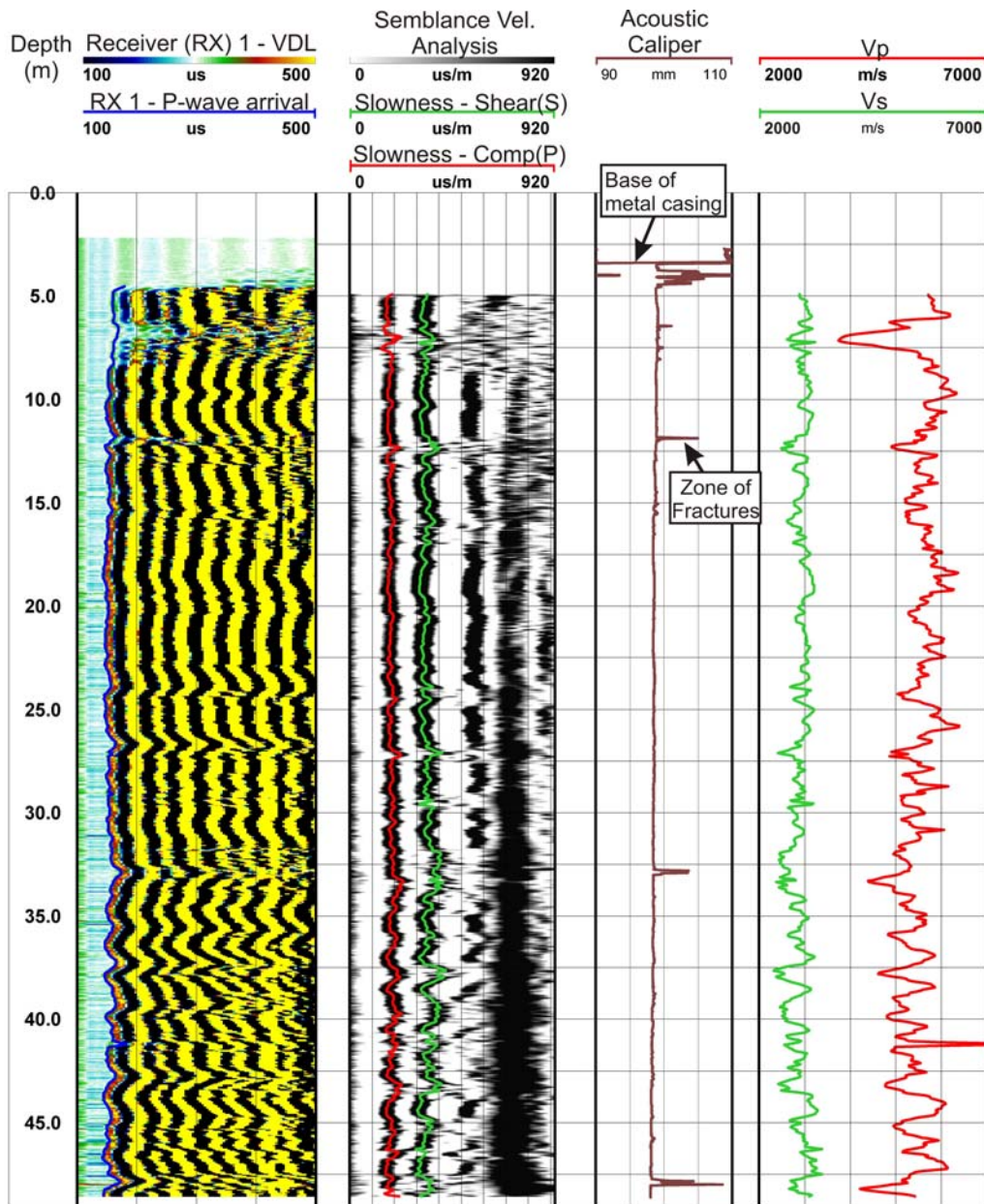


Figure 3.2.2-3. Sample full waveform sonic velocity logs and interpreted velocities. The variable density log (VDL) represents raw waveform data from the first of three receivers (RX-1). Semblance processing using waveforms from all three receivers produces high correlation bands of the interpreted P and S wave slowness. The interpreted slowness can then be inverted to produce velocity logs. The caliper log is shown to identify areas in the borehole where fracture zones were encountered.

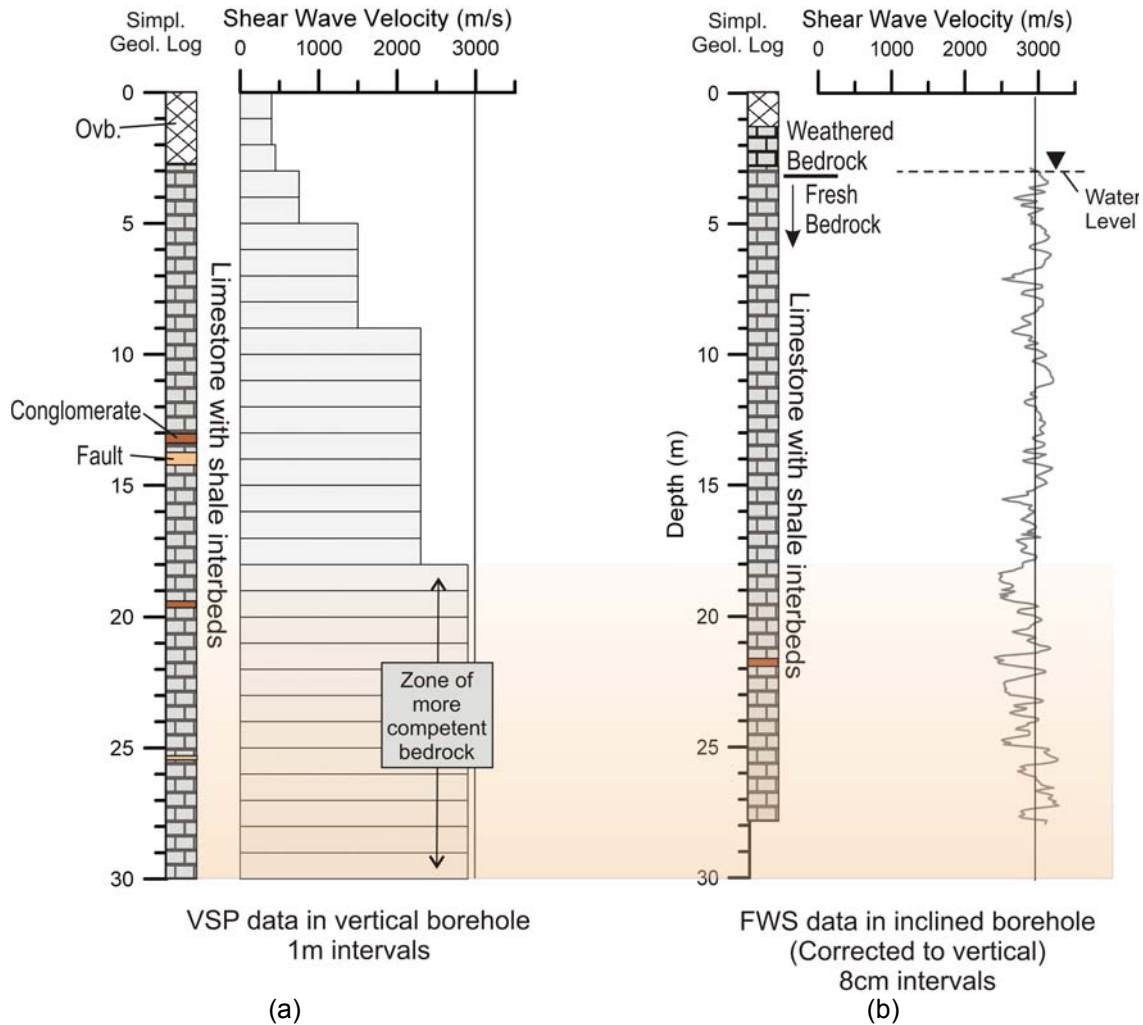


Figure 3.2.2-4. Comparison of FWS and VSP log data. These data are from the same site but different boreholes. Borehole A intersects zones of faulted bedrock in the upper 20m, while borehole B, inclined at 35° to the horizontal, does not. Where both boreholes intersect zones of relatively competent bedrock, the results of the two methods are comparable, but on different scales: the VSP averages over larger volumes, while the FWS is looking at smaller intervals within a few centimetres around the borehole wall, hence the variability in log B. This figure illustrates the differences between the two methods.

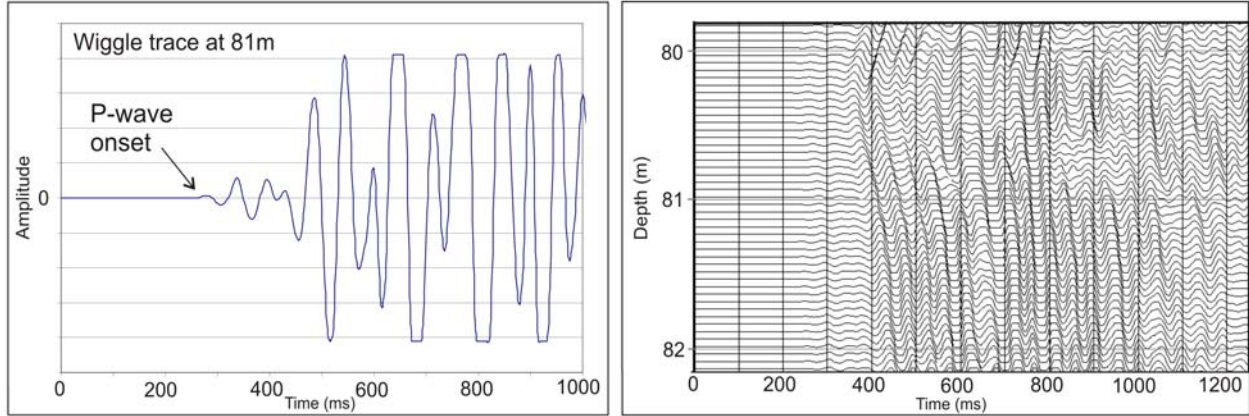
### **Case 2: Acoustic logs for geotechnical hazard assessment**

A Canada/US geotechnical and environmental study was undertaken in 2005 to investigate potential Detroit River crossing locations for a new highway bridge joining Windsor, Ontario and Detroit, Michigan. Salt solution mining carried out in the late 19<sup>th</sup> century in the vicinity of the proposed crossings led to concern for rock mass stability, as a large sinkhole had developed on the Canadian shoreline in the 1950's. A comprehensive investigation program was developed to assess boundaries around the mine sites beyond which the ground would be deemed strong enough to support bridge piers.

A phase of this investigation involved an intensive drilling program of twelve 500 m boreholes, advanced to the base of the salt formation. As only one of the boreholes was cored, the program relied heavily on the downhole geophysical survey results to assess rock mass properties in the vicinity of the holes. Logs included the full waveform sonic, caliper, natural gamma, EM induction, and acoustic televiewer. Crosshole seismic imaging was also carried out to investigate the condition of the rock mass between holes, and infer the location of cavities caused by the solution mining.

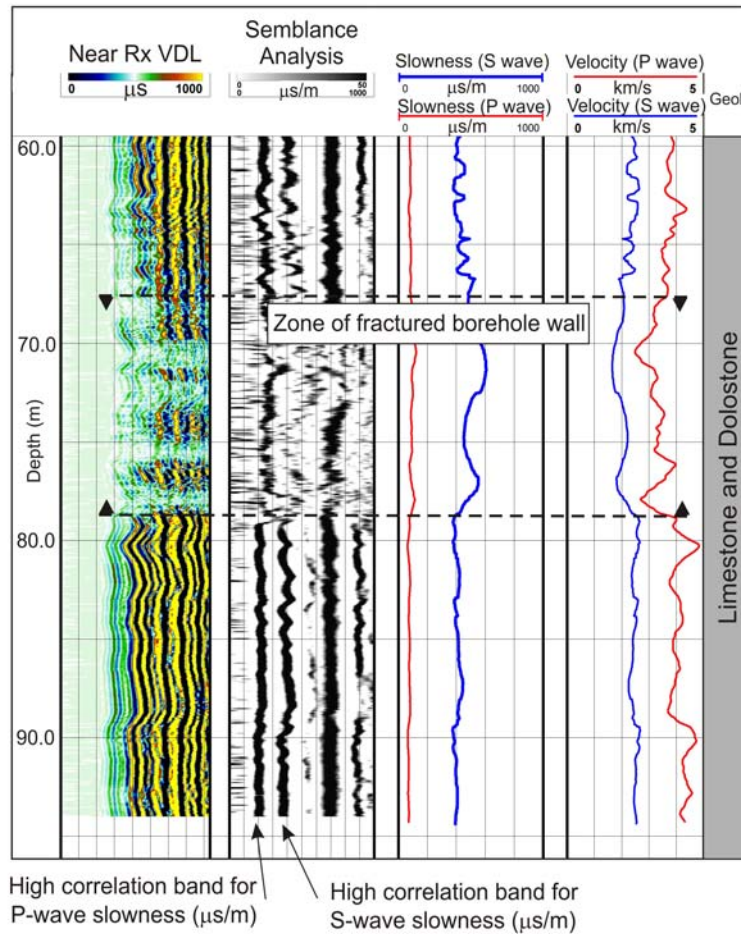
The sonic logs were interpreted to provide measurements of compression and shear wave velocity, engineering properties, acoustic porosity and, in combination with the acoustic televiewer data, apparent rock hardness and apparent density. Figure 3.2.2-5 shows sample full waveform sonic data collected in one of the boreholes. Single traces from each receiver (a) are plotted together versus depth, either as wiggle traces (b), or variable density logs (VDL) (c) which present amplitude with the aid of a color scale. In zones of competent limestone bedrock, travel times of the first arrivals can be interpreted manually. However, due to the potential mixing of the shear wave and pseudo Rayleigh wave packet, the shear wave velocity logs were processed using a semblance routine. Here, cross-correlation takes into account the relative amplitude and the coherency of subsequent waveforms. The result is a plot showing bands of higher correlation (c, column 2) from which slowness (column 3), and then velocity (column 4), can be interpreted.

These sonic data, in combination with the other borehole geophysical data and the cross-well surveys (and subsequent numerical modeling) provided considerable insight to the subsurface structure at this site. The results provided a basis for establishing limits on the zone of influence of the solution mining with respect to locating and designing the bridge foundations. Modelling support and the borehole geophysical data were vital aids in the interpretation of the data (Boone et al., 2008).



a)

b)



c)

Figure 3.2.2-5. (a) Trace recorded by a single receiver. (b) Merged traces from a single receiver are shown plotted versus depth. (c) Wiggle traces are shown plotted as a variable density log (VDL) in column 1, where amplitude is represented by a color scale. Semblance processing, which uses a cross-correlation routine, takes into account the relative amplitude and the coherency of subsequent waveforms. The result is a plot showing bands of higher correlation (c, column 2) from which slowness (column 3), and then velocity (column 4), can be interpreted.

## Acknowledgements

With thanks to Mark Monier-Williams (Golder Associates Ltd.) and Kim Davis (Golder Associates Inc.) for supplying case studies and article input.

## References

Boone, S.J., Beddoes, R., Carter, T.G., Monier-Williams, M. and Turpening, R., 2008. Bridges, Salt and Sinkholes: Applications of Geophysics for the Detroit River International Crossing, Keynote address, *in* Proceedings, Federal Highway Administration (FHWA) Accelerated Bridge Construction Conference, Baltimore, MD.

Chen, S.T., 1988. Shear wave logging with dipole sources; *Geophysics*, v.53, pp. 659-667.

Chen, S.T., 1989. Shear wave logging with quadrupole sources; *Geophysics*, v.54, pp. 590-597.

Cheng, C.H., 1989. Full waveform inversion of P waves for Vs and Qp; *Journal of Geophysical Research*, v.94, p.15,619-15,625.

Cheng, C.H. and Toksöz, M.N., 1982. Generation, propagation, and analysis of tube waves in a borehole; *in* Proceedings, 23<sup>rd</sup> Society of Professional Well Log Analysts Annual Logging Symposium, Corpus Christi, TX, Transactions, Paper P.

Cheng, C.H. and Toksöz, M.N., 1983. Determination of shear wave velocities in "slow" formations; *in* Proceedings, 24<sup>th</sup> Society of Professional Well Log Analysts Annual Logging Symposium, Calgary, AB, Transactions, Paper V.

Hearst, J.R., Nelson, P.H. and Paillet, F.L., 2000. Well Logging for Physical Properties; John Wiley and Sons Ltd., England, 483 p.

Oden, C.O. and LoCoco, J.J., 2000. Variable Frequency Monopole-Dipole Sonic Logging for Mechanical and Hydrogeologic Parameters; *in* Proceedings, Annual Meeting of the Environmental and Engineering Geophysical Society (EEGS), Denver, CO, p. 493-502.

Oden, C.O., Lococo, J.J., and Staples, P.L., 2000. Sonic Logging Case Histories Using Advanced Equipment and Data Processing Techniques, Mount Sopris Instruments Ltd., <<http://www.mountsopris.com/PDF%20Documents/Sonic%20Case%20Histories-1.pdf>> [Accessed February 2012]

Paillet, F.L., and Cheng, C.H., 1986. A numerical investigation of head waves and leaky modes in fluid-filled boreholes; *Geophysics*, v.51, p.1438-1449.

Paillet, F.L. and Cheng, C.H., 1991. Acoustic Waves in Boreholes; CRC Press Inc, FL, 264 p.

Schmitt, D.P., Zhu, Y. and Cheng, C.H., 1988. Shear wave logging in semi-infinite saturated porous formations; *Journal of the Acoustic Society of America*, v.84.

Stevens, J.L. and Day, S.M., 1986. Shear velocity logging in slow formations using the Stoneley wave; *Geophysics*, v.51, p.137-147.

White, J.E., 1983. Underground Sound: Application of Seismic Waves. v.18; *in* Methods in Geochemistry and Geophysics, Elsevier Science Publishers, Amsterdam.

Willis, M.E. and Toksöz, M.N., 1983. Automatic P and S velocity determination from full waveform acoustic logs; *Geophysics*, v.48, p.1631-1644.

### 3.2.3 Crosshole Logging for Shear Wave Velocity

*Jean-Jacques Sincennes  
Géophysique SIGMA, St. Bruno, QC.*

#### Introduction

##### **Principles of Method**

Crosshole techniques measure traveltimes between boreholes using a downhole source and receivers placed in two or more adjacent boreholes drilled in-line, 3 to 4.5 metres apart. A downhole impact source generates a horizontally propagating, vertically polarized shear wave (SV), and the interval traveltime between two receivers positioned at the same elevation is used to calculate shear wave velocity at that depth. Once the shots are recorded at a particular depth, the source and receivers are moved up the hole together at 0.5 or 1.0 m intervals until the entire hole is logged. The logging configuration is shown in Figure 3.2.3-1.

The crosshole technique, although more expensive due to the cost of drilling, casing, and grouting multiple boreholes, is considered one of the most accurate downhole methods of measuring velocities because the uncertainty of time zero errors are removed. In addition, traveltime measurement is relatively independent of depth as the source-receiver distance remains nearly constant throughout the survey. As discussed in the next article, the crosshole approach also offers the ability to record multiple inclined raypaths for tomographic analyses. Due to cost, this technique is typically used for critical projects where highest quality velocity data are required, or complex geology and velocity reversals limit the effectiveness of other methods.

##### **Current State of Engineering Practice**

ASTM standard D-4428 / D-4428-07 describes conventional crosshole measurement techniques, and compliance with the preferred ASTM method requires that three equidistant, PVC-cased, boreholes be drilled in a row. The ASTM also describes an optional method where two boreholes are used if the time and expense of the preferred method is not warranted. Typically, a 3m separation is sufficient unless the shear wave velocities in the near-surface materials exceed 450 m/s. In this case, a borehole separation up to 4.5m is recommended by the ASTM. This close spacing increases the likelihood of measuring a direct wave as opposed to a refracted wave, and ensures the same phase of the wave is propagated to the receivers (Stokoe and Hoar, 1977).

When both P and S wave velocities are calculated, Poisson's ratio ( $\nu$ ) and the various dynamic moduli can be calculated (Young's and bulk). Maximum shear modulus,  $G_{\max}$ , can be calculated directly from interval shear wave velocity and bulk density. Relationships for these moduli can be found in most standard geotechnical textbooks and require knowledge of the soil's density. Crosshole techniques have also been used to investigate low strain damping ratio and dispersion in soft soils (Hall and Bodare, 2000), and in urban seismic zonation studies where complex geology exists (Cardarelli et al., 2008).

Downhole SH-type sources have also been developed for crosshole applications as described by Roblee et al. (1994), but the most commonly used sources are those which generate SV waves.

##### **Recommended citation:**

Sincennes, J.-J., 2012. Crosshole Logging for Shear Wave Velocity; *in* Shear Wave Velocity Measurement Guidelines for Canadian Seismic Site Characterization in Soil and Rock, (ed.) J.A. Hunter and H.L. Crow; Geological Survey of Canada, Open File 7078, p. 150-159.

### Limitations

The methods generating downward propagating SH waves are those with the closest resemblance to earthquake energy as it travels to the surface (i.e. vertical seismic profiling, VSP). If significant horizontal anisotropy is present in the near-surface materials, the crosshole approach will calculate velocity based on SV waves traveling predominantly along a horizontal raypath, which could lead to an overestimation of shear wave velocity in the vertical direction.

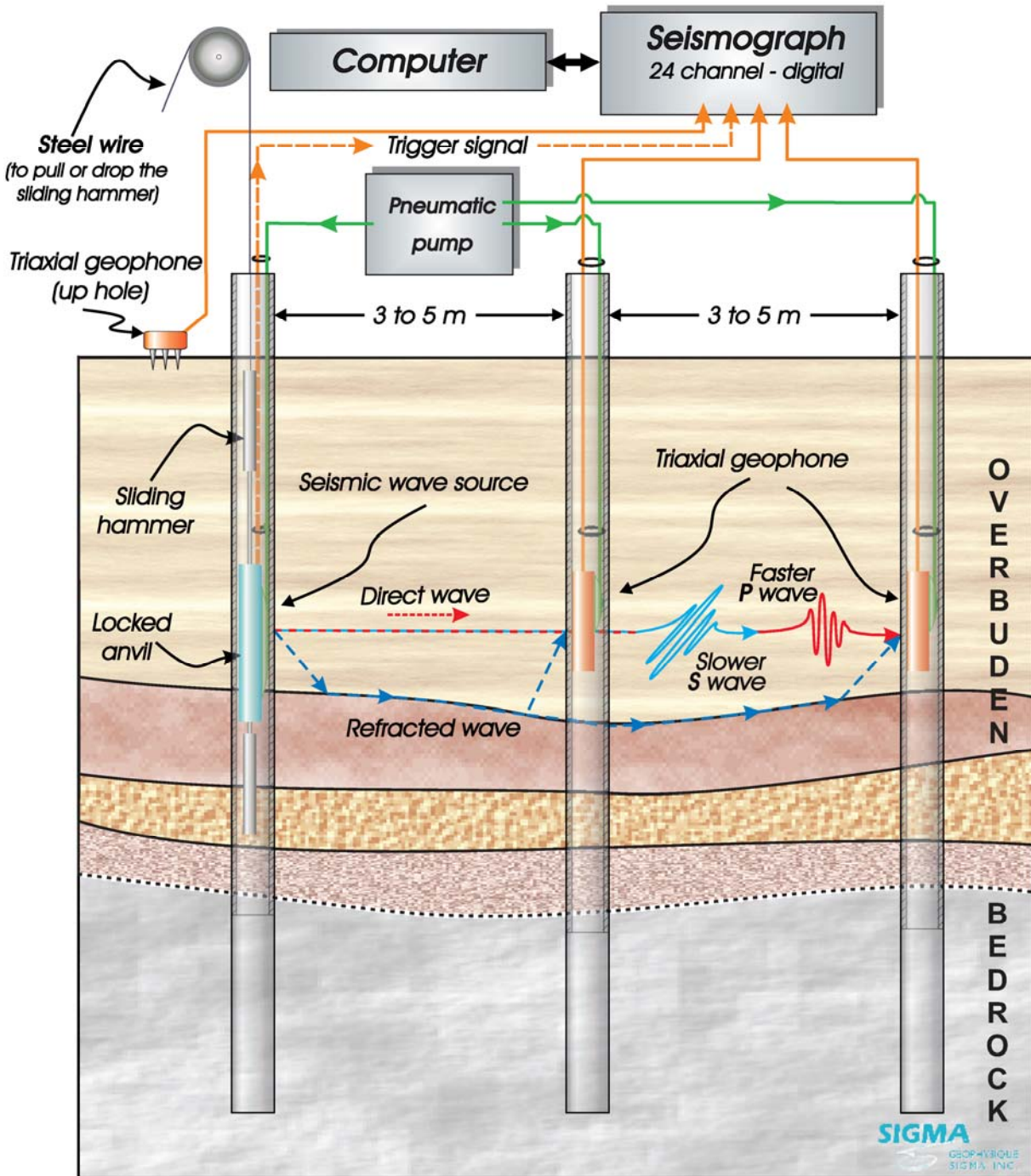


Figure 3.2.3-1. Seismic crosshole survey set-up.

Vertical boreholes are required for this survey and must be logged with a deviation tool if borings exceed 15 m depth to determine the correct in-line distance between the holes (ASTM D-4428). Even a very small change in borehole verticality could cause an increase or decrease in cross-hole traveltime, leading to a misinterpretation of material velocities.

As with all borehole methods, the casing must be carefully grouted in the formation, but this requirement is especially important for multiple boreholes used in the crosshole method. The procedure requires the use of a pump and a grout pipe advanced to the base of the borehole, grouting from the bottom up. Grouting must be completed several days before logging can take place to allow the grout to set.

## Data Collection

### Required Equipment

The survey equipment must include a multi-channel seismograph connected to a recording computer, a downhole shear wave source, and two wall-locking triaxial geophones for the three-borehole configuration (Figure 3.2.3-2). Geophone frequency should be selected based on the range of operating frequencies produced by the source, but it is generally recommended that the geophones have a natural roll off frequency of approximately 15 Hz (or less) to capture lower shear wave frequencies. Wall-locking can be accomplished through a mechanical bowspring arm, or a bladder inflated by a pneumatic pump. Modern downhole geophones often have a magnetometer which can be used to orient one of the horizontal components to magnetic north. Otherwise, a method should be used (such as thin fiberglass rods running to surface) to ensure the horizontal components of the tools in both boreholes are oriented in the same direction. This will improve the identification of the shear wave arrival on the two sets of recorded signals.

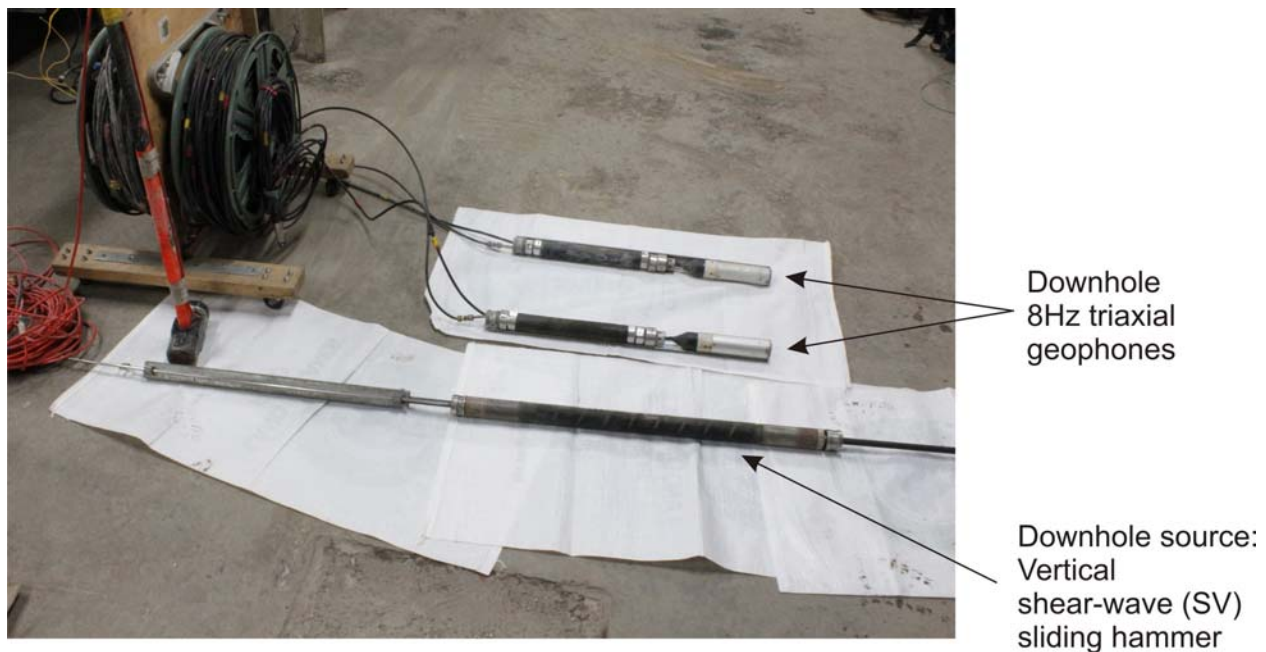


Figure 3.2.3-2. Photograph of source and receiver equipment. With this system, tools are lowered downhole to desired depths and locked in place using inflatable bladders.

### Data Collection Procedures

During data collection, the shear wave hammer is locked in place at the base of one of the outer boreholes and the two downhole triaxial geophones are placed at the same elevation in the other two holes and also locked in place, as shown in Figure 3.2.3-1. Cables should then be slacked to reduce transmission of vibrations from surface to the geophones. An impact (upward or downward) is produced

by the source and the received waveforms are recorded by the seismograph. Although the main signal produced is a vertically polarized shear wave, some compressional (P) wave energy is also produced through energy mode conversion. Both upward and downward shots should be recorded separately at each depth, and if necessary, records can be stacked to improve the signal-to-noise ratio.

## Processing Techniques

### Theory of Analysis

Borehole records from both downhole receivers are displayed at each depth to pick shear wave arrival times (see Figure 3.2.3-4 for sample). It is helpful to overlay oppositely polarized signals in the picking of the shear wave onset. The center-to-center distance between the two outer boreholes, divided by the difference in traveltimes between the shear wave arrivals provides the interval shear wave velocity ( $V_{s_{int}}$ ) at that depth. In some cases, filtering may be necessary if the survey was carried out in a noisy urban environment, but with the proximity of the source to the receiver, good signal-to-noise levels should be achieved.

To calculate a  $V_{s_{30}}$  value, the traveltimes within each of the depth intervals must be calculated by dividing the distance between the receivers (as determined by the deviation surveys) by the calculated  $V_{s_{int}}$ . The traveltimes to 30m must be summed and divided into 30m, providing the travelttime-weighted  $V_{s_{30}}$  value (see VSP article for sample calculations). It needs to be remembered that although the waveforms generated from the downhole shear wave source are vertically polarized (SV), the wave is travelling horizontally. If horizontal-to-vertical anisotropy is present, this  $V_{s_{30}}$  value will represent an upper bound value.

### Uncertainty Assessment

Provided that the sources of potential error are minimized (boreholes carefully grouted, deviation survey carried out, oppositely polarized waveforms are used in the interpretation, etc.), onset of shear motion can be picked to less than  $\frac{1}{4}$  cycle; these generally result in errors of  $V_{s_{int}}$  values less than  $\pm 5\%$  error.

## Recommended Guidelines for Reporting

Reports should include the details of the borehole drilling and completion, such as borehole separation, diameter, drilling method, grouting materials and methods, and results of deviation surveys. Details of the seismic survey should be presented in the form of a table with sensor details (including geophone frequency), record length, and sampling interval. Record depths should be presented, along with sample seismic survey results in the form of wiggle traces (see Figure 3.2.3-4) with picked arrival times. A table of interpreted traveltimes should be presented, showing the calculated interval velocities, calculated interval traveltimes within each of the depth intervals, and the calculated  $V_{s_{30}}$ .

## Hazard-Related Case Studies

### Case 1: Dam foundation study

Crosshole logging and vertical seismic profiling (VSP) were carried out at a dam site to investigate the velocity characteristics and geotechnical properties of the dam and its underlying foundation (Figure 3.2.3-3). A crosshole survey was completed in the downstream coffer dam in three 32 m boreholes each spaced 4.5 m apart and cased with PVC. A 24-channel seismograph was used, along with 8Hz-triaxial geophones and a sliding hammer downhole source, capable of generating SV waves with upward and downward blows. Traces were recorded at 1 m downhole intervals.

Figure 3.2.3-4 presents sample traces from the three-component receivers in boreholes 1 and 2. The difference in P- and S-wave arrival times divided into the distance between the boreholes gives the P- and S-wave interval velocities. The downhole seismic profile and associated stratigraphy are shown in Figure 3.2.3-5. Having both seismic velocities, and a measured or assumed density, allows for the calculation of additional engineering properties, including Poisson's ratio, and Young and shear moduli.

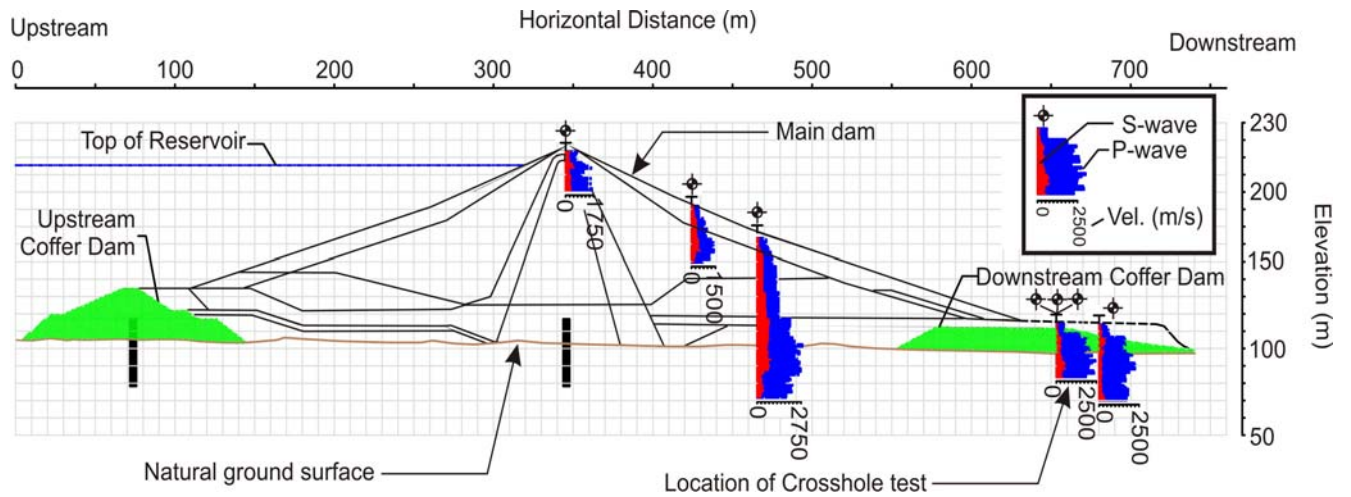


Figure 3.2.3-3. Location of crosshole test at downstream coffer dam. Locations of other single borehole VSP logs are also shown.

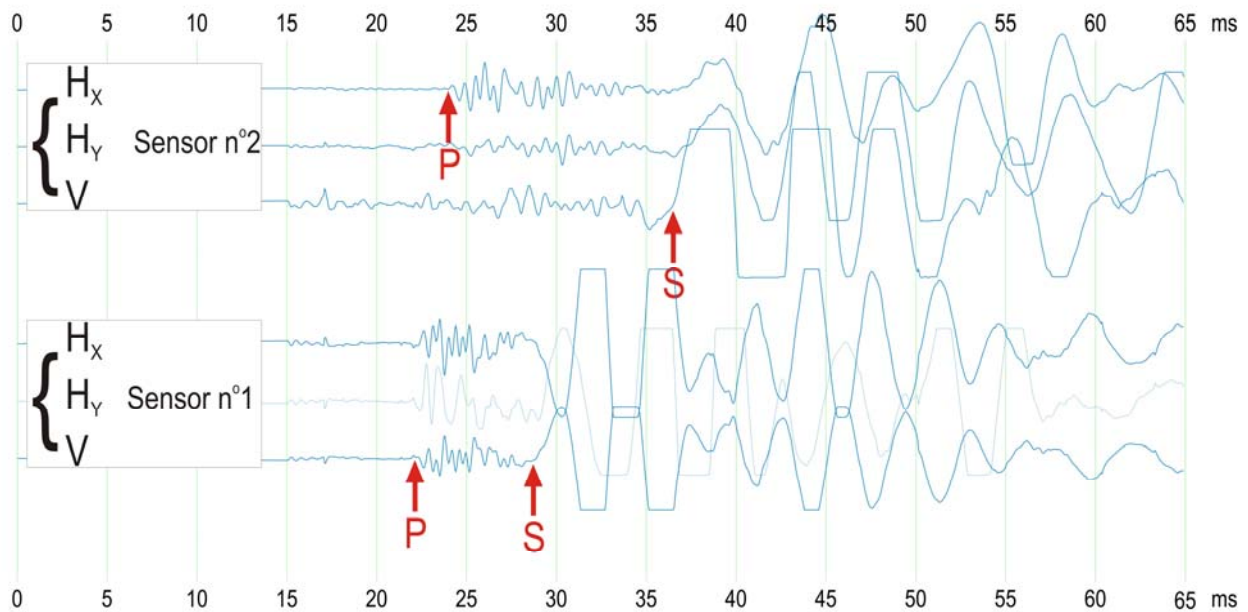


Figure 3.2.3-4. Sample traces from 24m depth recorded by receivers in boreholes 2 and 3. Travelttime analysis ( $dx/dT$ ) produces interval velocities of  $V_p=2250$  m/s and  $V_s=610$  m/s.

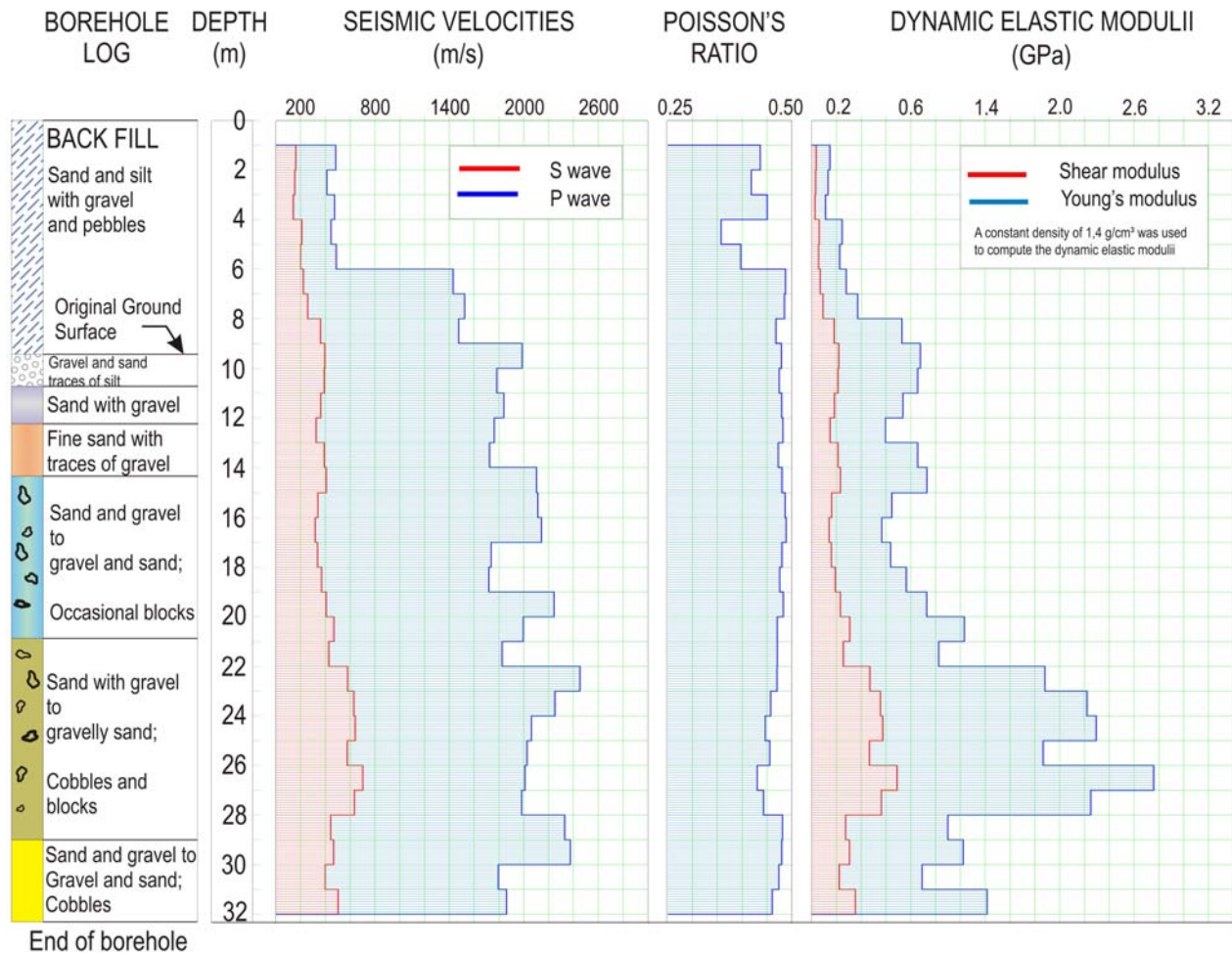


Figure 3.2.3-5. Resulting interval shear and compressional velocities from crosshole traveltime interpretations. Using an estimated density of 1.4g/cm<sup>3</sup>, elastic moduli were computed from the velocity data.

**Case 2: NBCC Seismic Site Class assessment for subway expansion project**

Seismic site class assessments were carried out by Golder Associates Ltd. at two locations in Toronto in support of the Toronto-York Spadina Subway Extension (TYSSE) project (Sol et al., 2011). Results presented here focus on Site 1, the deeper of the two sites. Figure 3.2.3-6 shows the types of materials encountered during the investigation, ranging from gravels and sands to clays and silts. Crosshole surveys were carried out at both sites within three PVC-cased boreholes, each spaced 3m apart. As a comparison with other Vs methods, vertical seismic profiling (VSP, see Chapter 3, Article 3.2.1) and multichannel analysis of surface waves (MASW, see Chapter 2, Article 2.2.3) methods were also carried out and compared with N<sub>60</sub> counts from standard penetration testing (SPT) for Vs<sub>30</sub> determination.

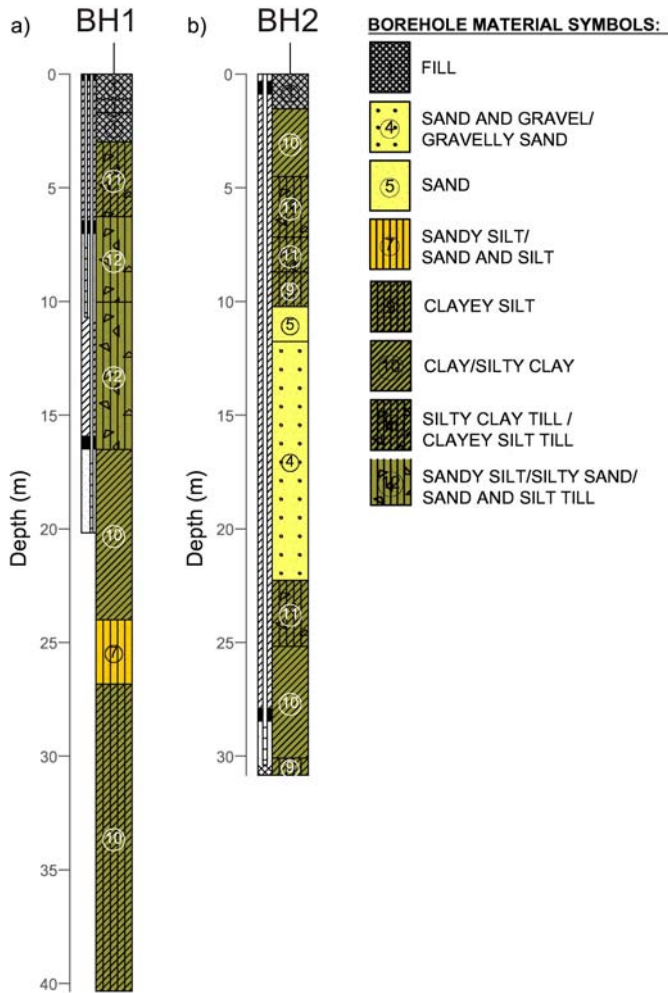


Figure 3.2.3-6. Overburden stratigraphy at crosshole Site 1 (a) and Site 2 (b).

Prior to testing, grout was allowed to set for 48 hours, followed by borehole deviation surveying in all six holes. The crosshole surveys were carried out using downhole P- and S-wave hammers and two downhole 3-component geophones, all wall-locking using spring-loaded clamps. Readings were collected a 1m intervals, and upward and downward hammer blows were recorded at each depth with the S-wave source.

Figure 3.2.3-7 presents the recorded shear wave traces from Site 1 with picked arrival times from one of the horizontal components in each of the downhole tools. Upward and downward hammer blows were superimposed at each depth to assist in the picking of shear wave arrival times. Interval velocities were calculated based on the borehole separations calculated from the deviation surveys. In one of the boreholes at each site, a VSP was collected using a loaded wooden beam struck horizontally to generate shear waves (Figure 3.2.3-8).

Figure 3.2.3-9 presents a comparison of shear and compressional wave velocities at Site 1 calculated using the crosshole, VSP, and MASW datasets. The 2010 NBCC seismic site class calculated in all three cases is a "C", but the  $V_{s30}$  values differ slightly: crosshole ( $V_{s30}=484$  m/s), VSP ( $V_{s30}=402$  m/s), and MASW ( $V_{s30}=482$  m/s). It should be noted that in the MASW case, the  $V_s$  inversion was not able to produce a profile down to 30 m depth, and was therefore only extrapolated for  $V_{s30}$  comparison with the other methods.

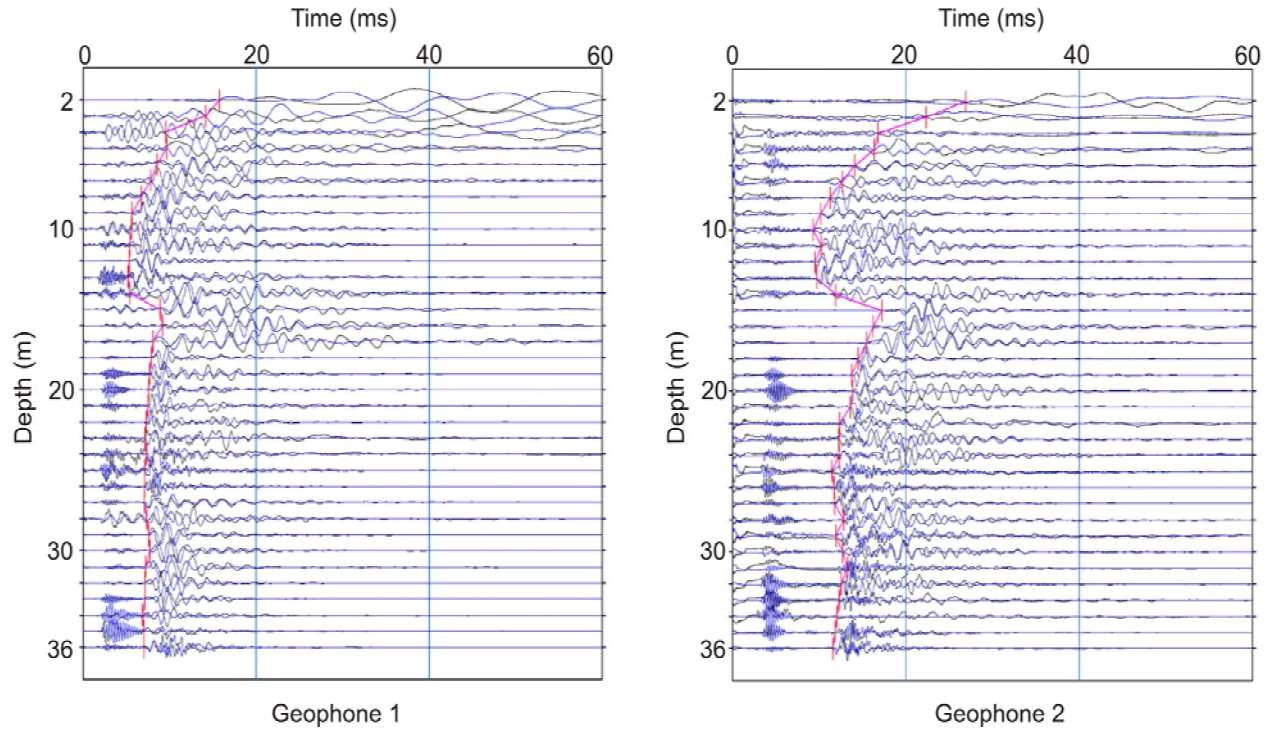


Figure 3.2.3-7. First break picks of shear wave arrivals at geophones 1 (3m from source) and 2 (6m from source) at Site 1. Upward and downhole hammer blows are superimposed to aid in shear wave picking.

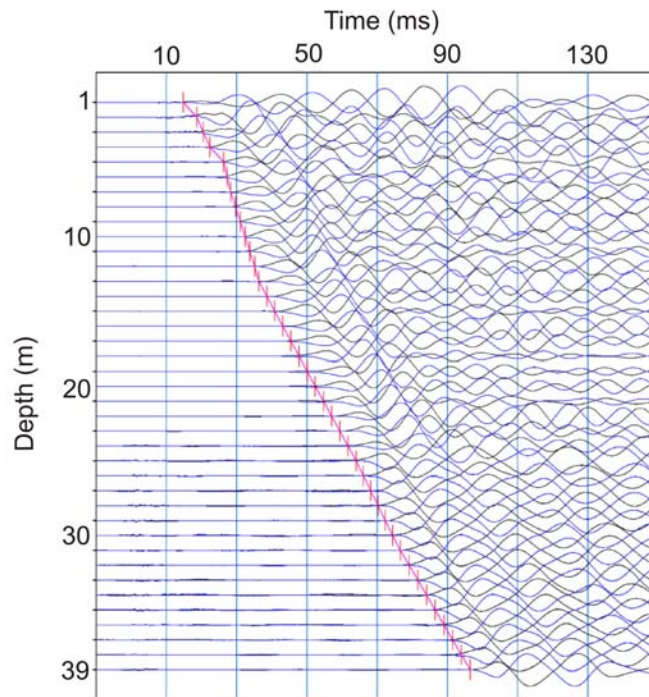


Figure 3.2.3-8. First break picks of shear wave arrivals from vertical seismic profiling (VSP) survey for comparison. Away and toward shots are superimposed to aid in picking the onset of shear waves.

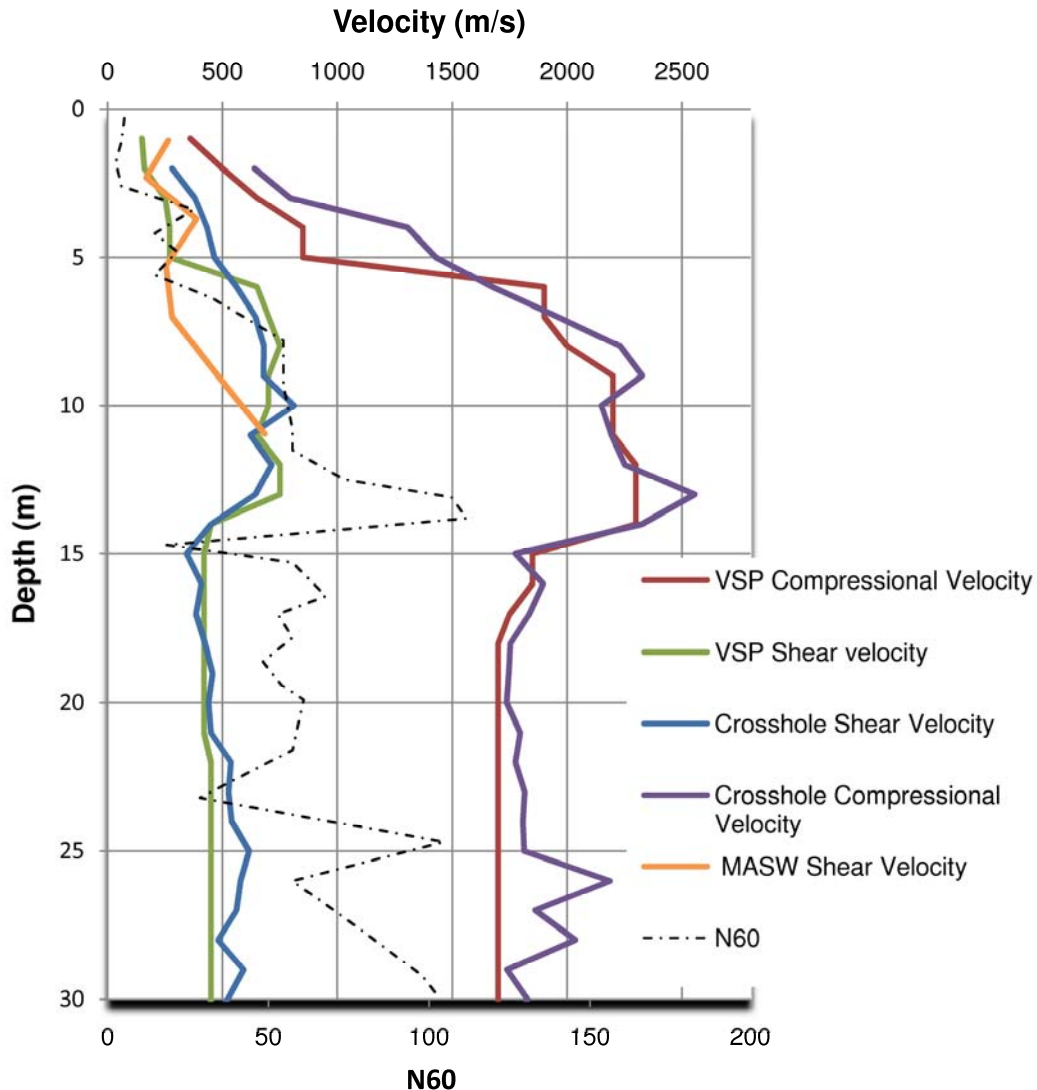


Figure 3.2.3-9. Comparison of shear and compressional wave velocities at Site 1 for crosshole, VSP, and MASW methods. Results of the SPT tests are also shown.

### Acknowledgements

The author thanks the Toronto Transit Commission (TTC) and Golder Associates Ltd. (S. Sol and C. Phillips) for contributing the TYSSE case study.

### References

ASTM D4428 / D4428M - 07. Standard Test Methods for Crosshole Seismic Testing, ASTM International, West Conshohocken, PA, 2007, DOI: 10.1520/D4428\_D4428M-07, [www.astm.org](http://www.astm.org).

Cardarelli E, Cercato, M., deNardis, R., DiFilippo, G. and Milana, G., 2008. Geophysical investigation for seismic zonation in municipal areas with complex geology: The case study of Celano, Italy; Soil Dynamics and Earthquake Engineering, v. 28, p. 950-963.

Hall, L. and Bodare, A., 2000. Analyses of the cross-hole method for determining shear wave velocities and damping ratios; *Soil Dynamics and Earthquake Engineering*, v.20, p. 167-175.

Roblee, C.J., Stokoe, K.H., Fuhrman, M.D. and Nelson, P.P., 1994. Crosshole SH-wave measurement in rock and soil; *in* *Dynamic Geotechnical Testing II*, ASTM special technical publication 1213, (eds.) R. J. Ebelhar, V. P. Drnevich, and B. L. Kutter; American Society for Testing and Materials, Philadelphia, PA., p. 58-72.

Sol, S., Phillips, S., Walters, D.L. and Bidhendi, H., 2011. A comparison of different methods for the estimation of NBCC 2005 seismic hazard site classification: A case study from the Toronto-York Spadina Subway extension project; *in* *Proceedings, 14<sup>th</sup> Pan-American Conference on Soil Mechanics and Geotechnical Engineering / 64<sup>th</sup> Canadian Geotechnical Conference*, Toronto, ON, BiTech Publishers Ltd., Richmond, BC.

Stokoe, K.H. and Hoar, R.J., 1977. Field measurement of shear wave velocity by crosshole and downhole seismic methods; *in* *Proceedings, Dynamical Methods in Soil and Rock Mechanics 1977*, Karlsruhe, Germany, v.3, p. 115-137.

## 3.2.4 Multichannel Crosshole Shear Wave Surveys

*Cliff Candy & Russell Hillman  
Frontier Geosciences Inc, North Vancouver, B.C*

### Introduction

The multichannel crosshole shear wave method provides a means of efficiently gathering a large number of ray-paths to investigate the shear wave velocity distribution in the region between two boreholes. This dataset may also be further interpreted using a 3D tomographic approach. The multichannel information includes, as a sub-set, the basic velocity information that would be produced by a simple cross-borehole survey, as discussed in the previous article. However, the multichannel method adds considerable spatial information on such details as layer dip, thickening or thinning of layers, and the ability to detect velocity anomalies that are present between the boreholes, but not intersected.

### Principles of the Method

At each survey depth point, a downhole seismic shear wave source is fixed against the drillhole wall by means of a suitable wall lock mechanism. An upward or downward blow at the source creates a vertically polarised shear wave which travels radially away from the source point. For crosshole tomography, the shear wave generated at each source elevation is measured at multiple points in the receiver hole using a string of multiple vertical geophones.

The primary arrival at the receiver geophone package is the vertically polarised shear wave, although other waves (such as compressional waves) cannot be entirely eliminated as energy mode conversions take place whenever a wave passes through a contrast in seismic velocity. Both upward and downward polarised shear waves are recorded at each test depth, primarily to enable recognition of the onset of oppositely polarised shear wave arrivals. The wave traces from both upward and downward blows are plotted at each depth point, and used together to interpret the shear wave arrival time.

### Current State of Engineering Practice

The operational methodologies are guided by the approach defined in the ASTM D4428/D4428M-07. Crosshole tomography is typically carried out in a two-borehole configuration with the source in one borehole and the receiver array in the second. Therefore, the high quality zero time initiation of the seismograph is of key importance. In our practice, the zero time is determined by the hammer contact for each impact of the down-hole source, and ensures accurate sub-millisecond timing initiation.

Experimentation with various down-hole wall locking approaches led to the use of a passive geophone coupling approach. The device does not involve an active wall lock mechanism, but rather uses stainless steel band springs that hold the geophones against the wall with sufficient force to be well coupled, but allows the string to be drawn down the hole by a moderate weight.

### Limitations

As noted in the previous article, the methods generating downward propagating SH waves are those with the closest resemblance to earthquake energy as it travels to the surface. If significant horizontal anisotropy is present in the near-surface materials, the crosshole approach will calculate velocity based on SV waves traveling predominantly along a horizontal raypath. This could lead to an overestimation of the velocity for vertically travelling shear waves with SH orientation. Issues of anisotropy are discussed in the vertical seismic profiling (VSP) article.

### **Recommended citation:**

Candy, C. and Hillman, R., 2012. Multichannel Crosshole Shear Wave Surveys; *in* Shear Wave Velocity Measurement Guidelines for Canadian Seismic Site Characterization in Soil and Rock, (ed.) J.A. Hunter and H.L. Crow; Geological Survey of Canada, Open File 7078, p. 160-169.

Prior to surveying, care must be taken to ensure that the annulus between the borehole wall and the plastic pipe is filled with a grout of similar density to the formation, injected using the Tremi tube displacement method. The boreholes must be accurately surveyed using a high-quality borehole deviation tool, as the interpretation software takes the 3D position of the boreholes into account. This ensures that variations in borehole separation are not mistakenly represented as variations in earth material velocity.

If the source to receiver borehole separation is large with respect to the thickness of a higher velocity layer, refraction along this layer can produce errors in the thickness of the layer. This is mitigated to some extent by the curved ray inversion embodied in the tomography software.

In a typical Canadian project, particularly in complex glacio-lacustrine environments, weaker clay or silt layers may be present. Identification of these lower velocity zones require that source to receiver borehole separations be reduced. As well, the data must be of sufficient spatial density and high quality that subtle offsets in first breaks can be observed. Closely spaced boreholes provide the best conditions for testing in-situ material properties. However, the borehole locations are often chosen for other testing purposes, and seismic testing is conducted over relatively large separations. Good results can be achieved with borehole separations of about 10 to 20 metres, depending on soil properties, hole grouting conditions, source signal strength, receiver sensitivity, and background seismic noise conditions. Large borehole separations are also more acceptable when monitoring for changes in seismic velocity over time.

## **Data Collection**

### **Required Equipment**

The seismic survey is carried out utilising a seismograph that meets the ASTM D4428 specifications for recording systems. Frontier Geosciences have designed a source and receiver system specifically for crosshole shear wave seismic testing, although some equipment is also available commercially. This seismic source is a specially constructed packer, lined with metal sheathing and with metal anvils at each end. A multi-strand high strength steel cable is attached securely to the upper anvil as a means of lowering and raising the source. A small diameter air-line tube, attached directly to the seismic source, accompanies the source down the hole to supply compressed air from a surface bottle via a pressure control valve as a means of inflating the rubber bladder within the metal sheathing to secure the source against the borehole wall. A small diameter metal rod passes through the packer with cylindrical hammers at each end. The source is reversible, allowing upward and downward-blow shear waves to be generated. Seismograph initiation is provided by the contact of the hammer to the fixed anvil. This timing mechanism produces circuit closure/seismic recording initiation of very high accuracy.

The receiver arrays were constructed using 14 Hz geophones fitted within compact pressure cylinders. The 24 geophones are spaced every 0.5 metres and vertically oriented for optimal recording of the vertically polarised shear wave arrival. Each geophone is held against the casing wall by a spring steel carrier, with the entire array acoustically decoupled from the suspending cable and the weight that draws the carrier down the hole.

A common approach to borehole deviation measurement is to employ a digital borehole survey tool at 1 metre intervals. This tool is a borehole inclinometer that uses data from a miniature three-axis fluxgate magnetometer and a three-axis accelerometer and tilt meters to very accurately determine the instrument position and orientation in three dimensions.

### **Data Collection Procedures**

The shear wave source is lowered to the initial survey depth in the source hole. The array of 24 geophones is lowered into the receiver borehole, in this case, spanning 11.5 metres. The source is locked, and the double-ended hammer pulled upward, providing an upward blow seismogram. Similarly, a downward-blow is obtained, and after inspection for quality, the data is recorded. In general, the upward and downward blows are found to be independently repeatable at each depth. Once satisfactory signals

for the upward and downward blows are collected, the shear wave source and geophone array are lowered to the next source depth and the procedure repeated.

Depending on the geological environment, and depth and separation of boreholes, a number of possible source and receiver array deployments can be used. The objective of the source/receiver pattern is to provide the greatest possible uniform distribution of source to receiver ray-paths to fully sample the 'panel' between the source and receiver boreholes. A simple method that is easy to manage in the field, and provides a controlled density of coverage at the top and bottom of a panel is used. This approach sets the source at the same elevation at the upper geophone in the array and both source and array proceed downward at 1 m intervals in this fashion. For the return pass to surface, the source is located at the elevation of the lowest geophone in the array and both are moved upward together at 1m intervals. This provides approximately 47 ray-paths from the source at mid-depth, and a progressive reduction at the top and bottom of the panel (Figure 3.2.4-1). The data are generally sampled fairly densely, such as at 0.125 millisecond intervals.

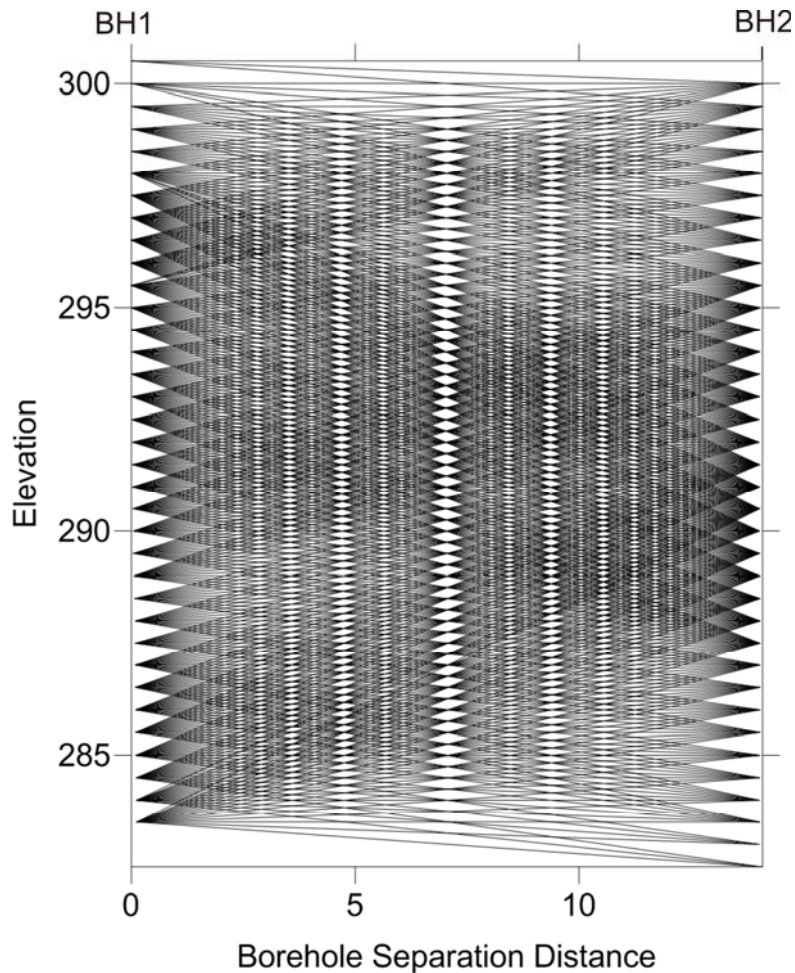


Figure 3.2.4-1. Crosshole tomography raypath diagram for two 18m boreholes.

If more than two boreholes are available in a test location, a set of panels between combinations of boreholes is possible. For instance, if three boreholes are available, the three panels of ray-path information can be simultaneously inverted in 3D to provide a volumetric representation of the zone of interest.

## Processing Techniques

### Theory of Analysis

At each source location, two seismic shots are taken to create both upward and downward polarised shear waves. All 24 traces that were created from each source location are displayed together in turn, with the upward and downward polarised traces plotted on a common baseline. This allows the interpreter to follow the phase of the arrival event from one depth station to the next. For each source location, the shear wave arrival times are picked at multiple receiver depths. The true source and receiver locations are calculated from surveyed measurements of the borehole collars and measurements of the borehole deviation. Finally, all of the picked arrival times are combined with the source and receiver locations and written into a file for modelling purposes.

The ASTM D4428 wave train identification process is followed in picking the first arrivals. This involves the identification of the shear wave break on the basis of its polarity, amplitude increase and abrupt change in frequency. This process is greatly aided by plotting the data in a 'gather' format such as the collective common elevation plot, as shown in Figure 3.2.4-2. In this format, the phase of the arrivals from elevation to elevation can be readily tracked. This improves the consistency of the picking by strongly reducing the likelihood of mis-tracking the arrival of the true wavelet by one wavelength early or late.

The picking procedure consists of the following steps, in order of increasing precision:

- 1) Observation of the general location of the shear wave energy 'packet' within the overall wave train. This signal will be approximately a two period wavelet of generally lower frequency and higher amplitude than the other components of the wave train. The wavelet will most often have similar phase and character to the traces gathered above and below this elevation. The fixed gain plots are useful at this step in defining the relative amplitudes of the shear wave energy packet within the context of the arrivals at similar depths.
- 2) The first period of this wavelet is identified on the basis of its character and polarity. The first movement of this period will be consistent with the known blow direction. As well, the peak of the second half of the first period will be of higher amplitude as compared to the first break peak. When an ambiguity exists between possible pick phases due to the presence of noise, no pick can be made.
- 3) Identification of the moment of first break, which is greatly aided by comparison with the opposing blow data. High frequency content in the wavetrain which departs from the envelope of the first period of the wavelet may be disregarded in this step.

The multichannel downhole method produces very large datasets. The process of arriving at high quality first arrival picks is critical to the successful outcome of the survey. The process of picking a very large volume of data is strongly facilitated by the use of a first arrival picking tool that is linked to dataset management, and incorporates some auto-picking and previous/next overlay capabilities.

The seismic tomography dataset is then modelled using a tomographic imaging program that develops a best-fit distribution of shear wave velocities in the model, based on the input file containing raypaths and travel times. Plots for quality control include travel time versus distance, residual versus raypath angle, velocity versus raypath angle and others. Depending on geometry the data can be modelled as either a two-dimensional (2D) section, or a three-dimensional (3D) volume. The program uses an inversion process such as the Simultaneous Iterative Reconstruction Technique (SIRT), which repeatedly modifies an initial model to obtain the best possible fit to the data. This modification of the initial velocity values consists of repeated cycles of three steps: forward computation of model times, calculation of residuals and application of velocity corrections.

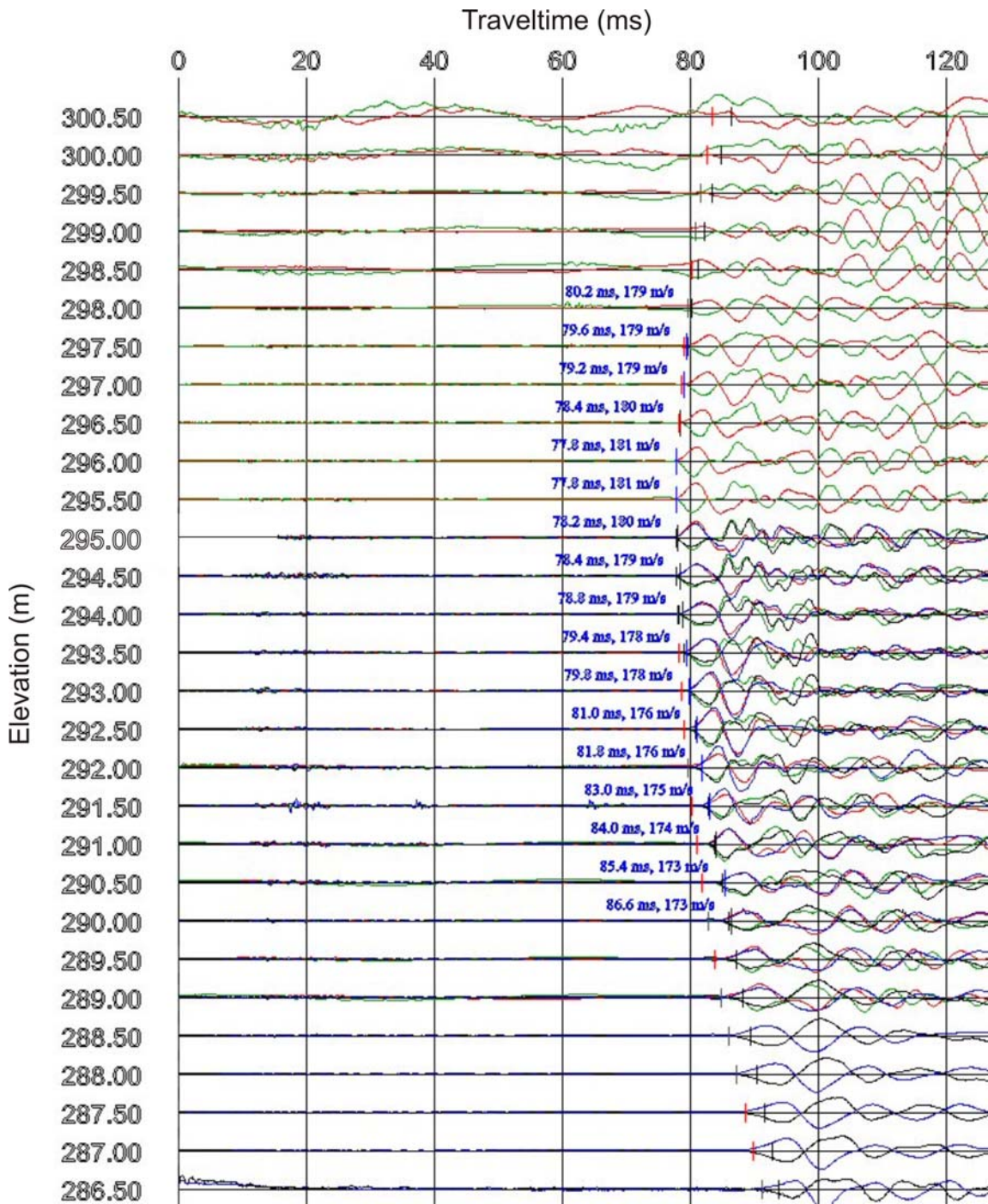


Figure 3.2.4-2. Common gather plot of shear wave arrival times showing superimposed up and down shots.

In the software, the seismic tomography raypath coordinates and arrival times are loaded into a 2D or 3D model, with a choice of vertical and horizontal model mesh intervals. The mesh grid density is chosen to reflect the source and receiver station spacing and to divide the hole separation distances by a reasonable factor. A two-dimensional, vertical plane of the shear wave velocities can then be extracted from the three-dimensional model by using the surface coordinates of the source and receiver drillholes to

define the plane. The extracted panels can then be contoured, or if a 3D data volume is produced from multiple drillhole pairs, then the model can be imported into a volume visualiser.

## Uncertainty Assessment

The accuracy of the crosshole shear wave velocities is dependent on timing errors, geometric position errors, and the inversion modelling process. Timing errors include any error in the source triggering system, and uncertainty associated with picking the arrival time of the relatively low frequency shear wave. Geometric positioning error can largely be attributed to the accuracy of the borehole deviation survey of the source and receiver boreholes. An estimate of the accuracy of the shear wave velocity computations can be made with the following formula:

$$V_{s_{\text{error}}} = V_s * (dL / L + dT / T) \quad [3.2.4-1]$$

where  $V_s$  = shear wave velocity,  $L$  = raypath length,  $dL$  = geometric error,  $T$  = arrival time, and  $dT$  = error in arrival time. For example, if the borehole separation is 10 metres  $\pm$  0.2 metres, and the arrival time is 50 milliseconds  $\pm$  1 ms, then the velocity is 200 m/s  $\pm$  8 m/s.

Further uncertainty is due to the crosshole modelling process, which produces best fit model to the data set. The difference between the measured shear wave arrival time and the modelled arrival time is referred to as the residual time. The residual times of all raypaths can be plotted to identify spurious data which can be removed to prevent distortion of the resulting model.

Another method of checking for uncertainty is to plot the average velocity of each raypath against the raypath angle, to identify anisotropy in the shear wave velocity.

When assessing the velocity panel results of the modelling process, it is instructive to compare the results against the sampling density of the crosshole seismic testing. This can be achieved by either plotting the number of raypaths that intersect each element in the modelling grid, or by producing a raypath diagram as shown in Figure 3.2.4-1.

## Recommended Guidelines for Reporting

The final form of the report is generally a contour plot of the velocity distribution for each panel of data gathered. In the case of a multiple borehole survey where a 3D volume is surveyed, a set of 3D renderings using the simplest possible isosurface choice to convey a sense of the data may be supplied. Due to the difficulties in displaying a 3D volume as 2D views, it is recommended that the data volume be supplied to the user with a volume visualisation program.

These final products should be backed up with at least a sub-set of the quality control products such as travel-time vs. distance plots, inversion residuals, example shot gathers, and the results of the borehole deviation surveys. Reporting should also include a table of velocities that represent the cross-borehole velocities determined solely from the sub-set of data where the source and receiver occupy the same elevation. Textual information will include a description of the methodology and issues encountered during the survey.

## Hazard-Related Case Study

### **Multichannel Shear Wave Investigation of a Tailings Storage Facility Dam**

Frontier Geosciences Inc. carried out a crosshole seismic survey at a tar sands tailings dam in Fort McMurray, Alberta. The purpose of the survey was to assess the degree of soil densification caused by overburden loading. The crosshole method would allow for the detection of changes in shear wave velocities during the construction of the dam, by measuring traveltimes between a network of drillholes installed on the dam site.

The primary survey method was crosshole shear wave tomography. Eight pairs of drillholes were tested in each phase of the field work, on materials immediately at the base of the superimposed structure. These tested materials ranged in elevation from approximately 280 metres to 298 metres. The first phase of testing was conducted when the dam elevation at the survey site was about 299 metres. The second phase of testing repeated the shear wave velocity measurements after construction had raised the dam elevation to about 308 m, a further addition of about nine metres of overlying materials. In addition to the shear wave velocity measurements, downhole compressional (P) wave velocities were measured during both phases of field testing.

In general, a large increase in shear wave velocity was measured in the second phase of the survey, after about nine metres of materials were placed over the test area. In the first phase of the survey, the shear wave velocities ranged from about 100 to 165 m/s. The compressional wave velocity was approximately 1500 m/s. In the second phase of the survey, the shear wave velocities ranged from about 160 to 208 m/s. The compressional wave velocity increased slightly, to about 1700 m/s. The largest increase occurred between drillholes DH-1, DH-2, and DH-3, at the higher elevations of the tested zone. These three planes show an increase of about 30 to 100 m/s in shear wave velocity. In general, the degree of change in shear wave velocity decreased downward, reducing from a maximum increase of about 100 m/s at the top of the tested zone, down to a minimum increase of about 30 m/s at the bottom.

Examples of the shear wave tomograms are shown in Figures 3.2.4-3 and 3.2.4-4. The shear wave distributions in the plane prior to loading are illustrated in Figure 3.2.4-3. The velocities increase with depth, from approximately 100 m/s at the ground surface, to about 130 to 160 m/s at the bottom of the tested zone. The tested zone extended up to 18 metres below the original ground surface. The range in shear wave velocities suggests loose, unconsolidated materials. Compressional wave velocities were determined to be about 1500 m/s, also suggesting loose, unconsolidated, saturated soil.

Figure 3.2.4-4 illustrates the shear wave velocity distributions after an additional layer of about nine metres of materials were placed over the tested zone. The crosshole velocities increased by as much as 100 m/s at the higher elevations of the tested zone, and by about 30 m/s at the bottom. These increases in shear wave velocity were not uniform for all of the planes, which suggest that stress levels in the soils, the degree of densification, and changes in void ratio were varied at the site. The compressional wave velocity also increased slightly to 1700 m/s in the second phase of the survey, which suggests that soils had densified enough to allow the P wave to travel through the matrix of solid soil particles, rather than travelling through the fluids in the pore spaces.

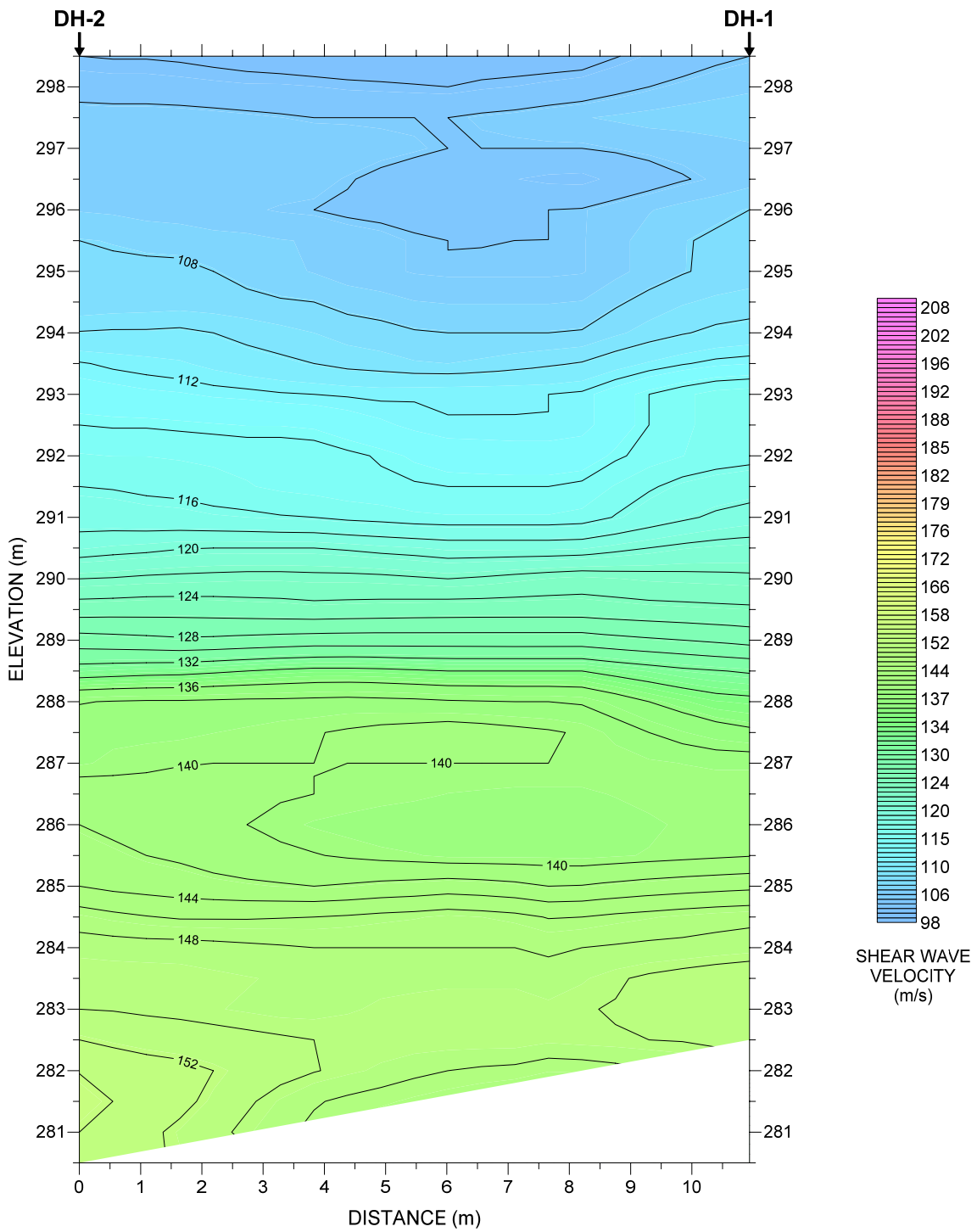


**Figure 3.2.4-3: Plane prior to loading.**

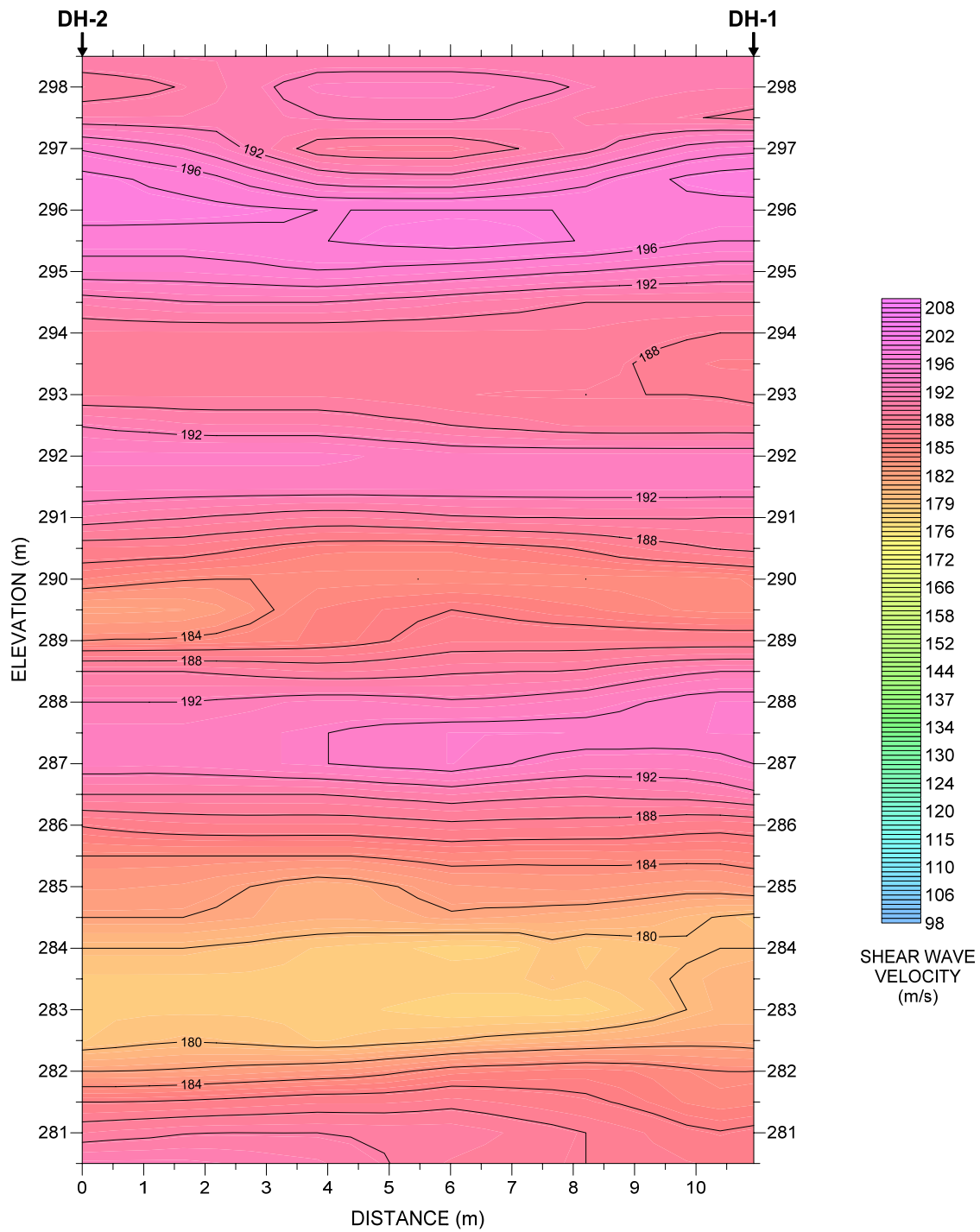


Figure 3.2.4-4: Plane after loading.

## References

ASTM D4428 / D4428M - 07. Standard Test Methods for Crosshole Seismic Testing, ASTM International, West Conshohocken, PA, 2007, DOI: 10.1520/D4428\_D4428M-07, [www.astm.org](http://www.astm.org).

## Further Reading

Bregman, N.D., Bailey, R.C. and Chapman, C.H., 1989. Crosshole seismic tomography; *Geophysics*, v. 54, p.200-215

Tweeton, D.R., 1988. A Tomographic computer program with constraints to improve reconstructions for monitoring in situ mining leachate; Report of Investigations No. 9159, United States Bureau of Mines (USBM), 70 p.

Vazinkhoo, S. and Gaffran, P., 2002. Crosshole Seismic Measurements to Characterise and Monitor the Internal Condition of Embankment Dams; *in* Proceedings, Canadian Dam Association Annual Conference, Victoria, B.C.

Xia, J., Miller, R.D. and Park, C. B., 1999. Estimation of near-surface shear-wave velocity by inversion of Rayleigh waves; *Geophysics*, v. 64, p. 691-700.

Jackson, P.D. and McCann, D.M., 1997. Cross-hole seismic tomography for engineering site investigation; *in* Modern Geophysics in Engineering Geology, (ed.) D.M. McCann, M. Eddleston, P.J. Fenning, and G.M. Reeves; The Geological Society, London, 441 p.

## Chapter 4.0 Complementary Geophysical Techniques for Site Geometry Assessment

*Chapter Leader:*

*Réjean Paul  
Géophysique GPR International, Longueuil, QC*

Depending on the footprint of a proposed structure, uncertainty in the number of boreholes or surface seismic surveys required to properly classify a site is common. The use of complementary geophysical techniques to assess subsurface stratigraphy over the site may be the only way to answer these questions, and much of this reconnaissance can be done quickly and cost effectively if planned in advance. Locations can then be targeted to carry out one or more shear wave surveys so that the seismic site classification(s) is representative of the site conditions.

The primary reasons for requiring additional site coverage may include having:

- A large site or structural footprint,
- Unknown geology and/or stratigraphy,
- Shallow or varying bedrock topography,
- Background noise too high for seismic techniques,
- Limited site access, or
- Known/suspected karstic conditions.

The techniques presented in this chapter include electromagnetic (EM), resistivity, ground penetrating radar (GPR), borehole logging, and small scale gravity methods. The choice of an appropriate survey method should be based on the types of materials present in the near surface. Therefore, this chapter aims to address the advantages and limitations of each technique, and provides a series of case studies in Canadian settings. It must be noted however that while these techniques will supply complementary information on a site's near surface geology, the results cannot be used in place of a seismic survey as per the 2005 / 2010 NBCC requirements for seismic site classification.

## 4.1 Electromagnetic (EM) Methods

Melvyn E. Best  
Bemex Consulting International

### Introduction

#### Principles of the method

Electromagnetic (EM) methods are based on Faraday's Law of induction (Jackson, 1975; Nabighian, 1988). A time-dependent current is applied to a transmitter loop consisting of one or more turns of wire. The current in the loop generates a time varying electromagnetic field which induces eddy currents in subsurface geological formations. These eddy currents generate secondary electromagnetic fields as shown in Figure 4.1-1. Receiver coils are used to measure the voltage associated with the secondary field. Frequency-domain systems produce an alternating current in the transmitter loop and measure the components of the secondary voltage in the receiver which are in-phase and 90° phase-shifted with the transmitter current. Time-domain systems produce a current pulse or pulses in the transmitter loop and measure the decaying voltage after the pulse is turned off.

This article focuses primarily on ground time-domain EM systems which are increasingly being used for shallow sub-surface geotechnical investigations, although a hazard-related frequency-domain example is also provided in the case studies.

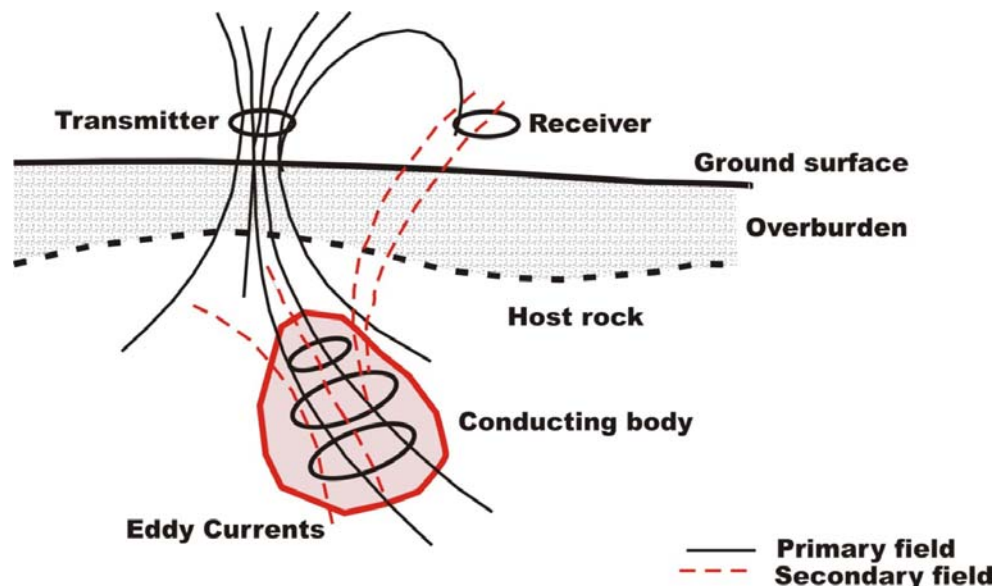


Figure 4.1-1. Schematic diagram of electromagnetic induction

#### Current state of engineering practice

Electromagnetic techniques provide estimates of resistivity versus depth for shallow sub-surface layers which can be used to verify layer thicknesses and composition. In addition, porosity can be estimated from the resistivity using Archie's Law (Archie, 1942), thus providing another estimated geotechnical parameter.

#### **Recommended citation:**

Best, M.E., 2012. Electromagnetic (EM) Methods; *in* Shear Wave Velocity Measurement Guidelines for Canadian Seismic Site Characterization in Soil and Rock, (ed.) J.A. Hunter and H.L. Crow; Geological Survey of Canada, Open File 7078, p. 171-181.

EM methods have been in use for more than 50 years (Frischknecht, 1959). The first EM systems were frequency-domain systems designed for mineral exploration and were used to locate finite conductive bodies (anomaly hunting). More modern frequency EM systems have been designed using low induction numbers to directly measure the surface conductivity of the top 10 or so metres of the earth (ASTM D6639-01, 2008; McNeil, 1980). Although they are ideal for detection of buried conductive bodies, they are not as well suited for delineation of subsurface structure.

Time-domain systems began to appear in the 1970's and are now the most commonly used EM technique. With more sophisticated hardware and software, modern EM systems have been increasingly used for mapping the resistivity of the shallow sub-surface. Time-domain systems provide information to significantly greater depths than frequency based systems, but require the use of more sophisticated inversion methods to estimate sub-surface resistivity from the data. ASTM standard D6820-02 (2007) describes the procedures for data collections using time domain EM systems.

**Limitations**

Grounded metal and electric fences, high voltage power lines, and spherics (electromagnetic energy generated from local and distant lighting storms) distort the signals produced from geological formations. These must be avoided if possible or, if not, corrections must be made for them. Resistive geological formations, greater than approximately 1000 ohm-m, are difficult to detect using EM methods since eddy currents tend to flow in more conductive geological formations (Figure 4.1-2). For example the contact between a resistive sand or gravel located above resistive bedrock can be difficult to detect.

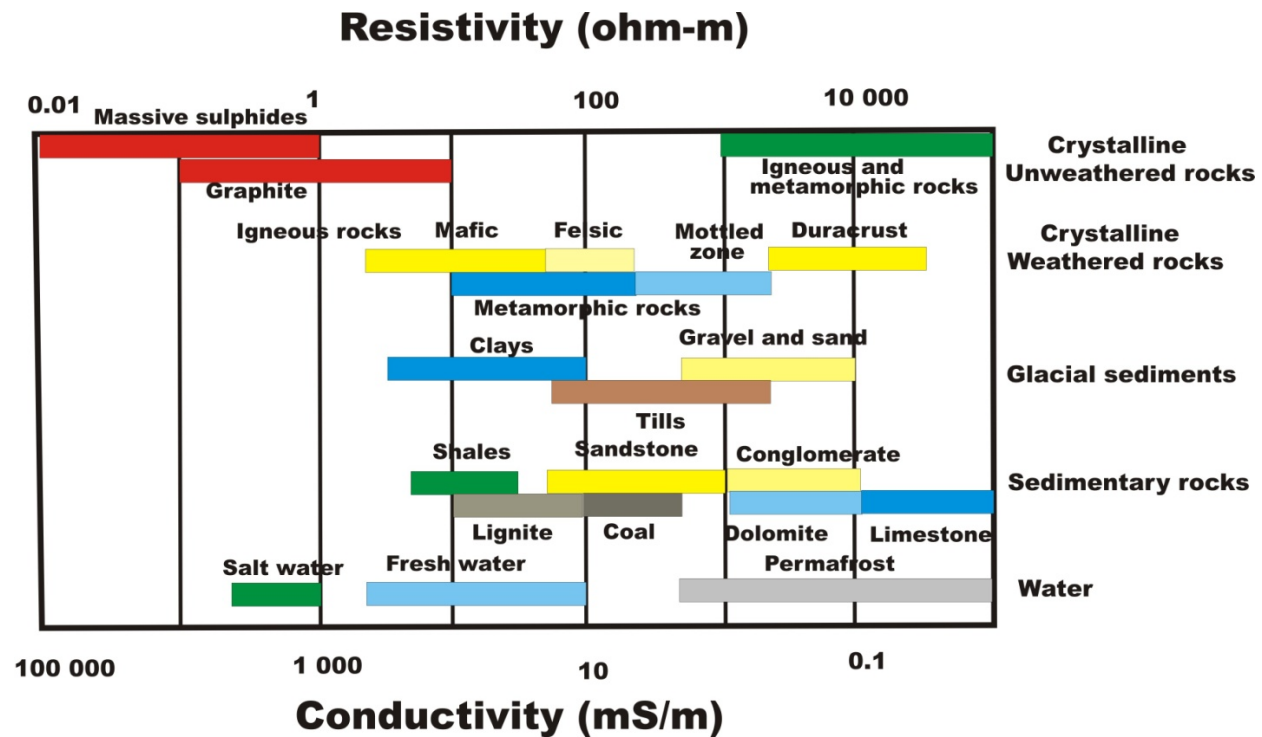


Figure 4.1-2. Typical resistivity (conductivity) ranges for rocks and unconsolidated materials.

**Data Collection**

**Required Equipment**

Ground time-domain EM systems require a transmitter loop, a transmitter console, receiver coil(s), receiver console, and a reference cable or crystal clock synchronization between the transmitter and receiver console. The transmitter loop is usually a single turn of wire laid out in a square. The length of the sides of the square depends on the resistivity of the near surface layers and the anticipated depth of investigation. Typical lengths are between 20 and 40 m for depths up to 100 m. The standard

configuration for depth sounding is the central sounding mode with a horizontal receiver coil measuring the vertical magnetic field placed at the centre of the transmitter loop (Figure 4.1-3).

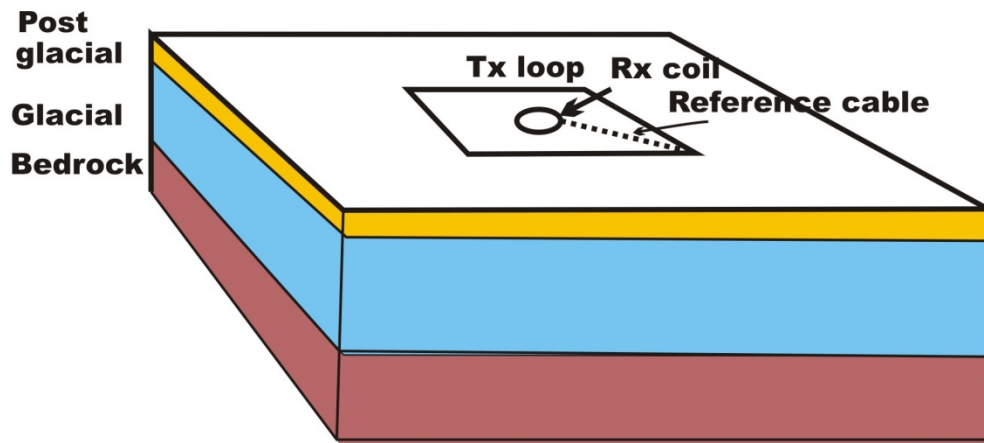


Figure 4.1-3. Field configuration of the central sounding mode of operation for time-domain soundings.

#### Data collection procedures

A current is injected into the transmitter and quickly turned off (square wave pulse). During the off time, the decaying voltage in the receiver is measured as a function of the time after the transmitter is turned off. The current is reversed and the measurements repeated with the sign of the receiver reversed. The cycle of on-off times determines the frequency of the transmitted current (Figure 4.1-4a). Different frequencies provide voltage information covering different time ranges. Usually the windows used to measure voltage versus time (Figure 4.1-4b) for different frequencies are overlapped to provide redundancy in the data. In noisy areas the measurements are repeated several times at each frequency to improve signal to noise. Later these measurements can be edited and stacked (averaged) using appropriate software to reduce the noise and improve the overall signal-to-noise (Figures 4.1-5a-d).

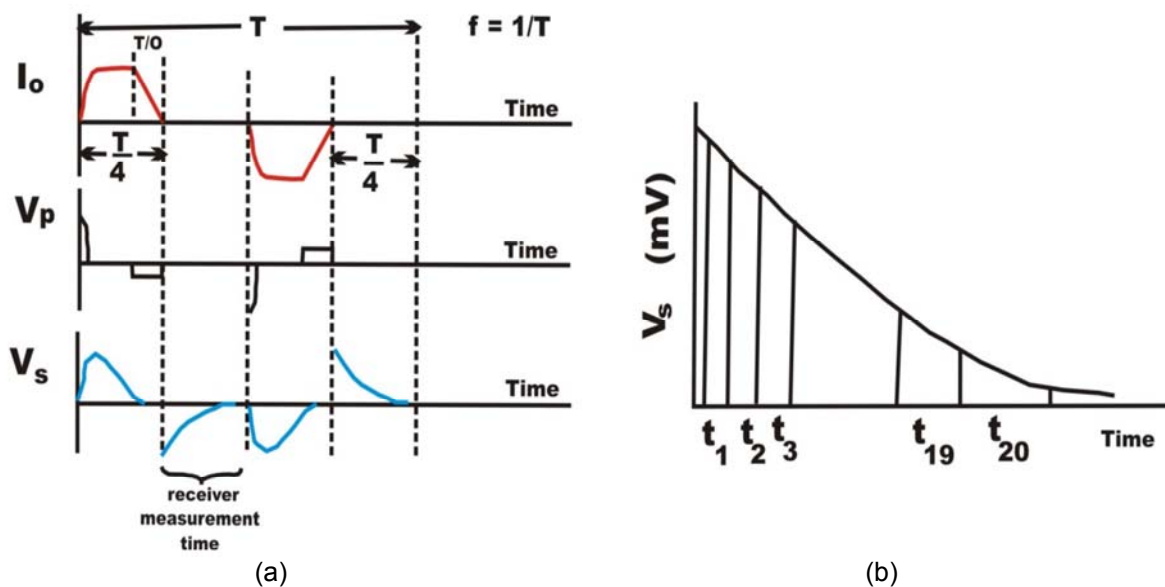


Figure 4.1-4 a) Transmitter current ( $I_o$ ), primary voltage ( $V_p$ ), and secondary voltage ( $V_s$ ). The frequency ( $f$ ) is equal to  $1/T$  where  $T$  is the period of the transmitted pulse in seconds.  $T/O$  is the turn off time of the transmitter. b) Time channels measured by the receiver.

## Processing Techniques

### Theory of analysis

The data from the EM system consist of the secondary voltage versus time measured at one or more frequencies. The voltage versus time data are first edited to remove spikes and obvious noise (Figure 4.1-5a) and then averaged to produce the final stacked data. This data set is normally converted into apparent resistivity versus time using an asymptotic approximation of the voltages at long times (Spies and Eggers, 1986). Apparent resistivity versus time plots are similar to DC resistivity sounding plots (Kearey and Brooks, 1984). Although this approximation distorts the short time portion of the apparent resistivity versus time plot inversion programs compensate for this (Spies and Eggers, 1986; Fitterman and Stewart, 1986; Stoyer, 1990). A one dimensional inversion program (Stoyer, 1990; Maxwell, 1998) is then used to generate a 1D resistivity depth image at each sounding location (Figures 4.1-5a-d).

A number of software programs are available to edit and average the voltage data, generate the apparent resistivity plots, and carry out the inversion to produce a one dimensional resistivity versus depth image. Software exists to splice the individual soundings together to make a two dimensional resistivity cross section. Two-dimensional and three-dimensional modelling software programs are also available but are not normally required for shallow hazard applications.

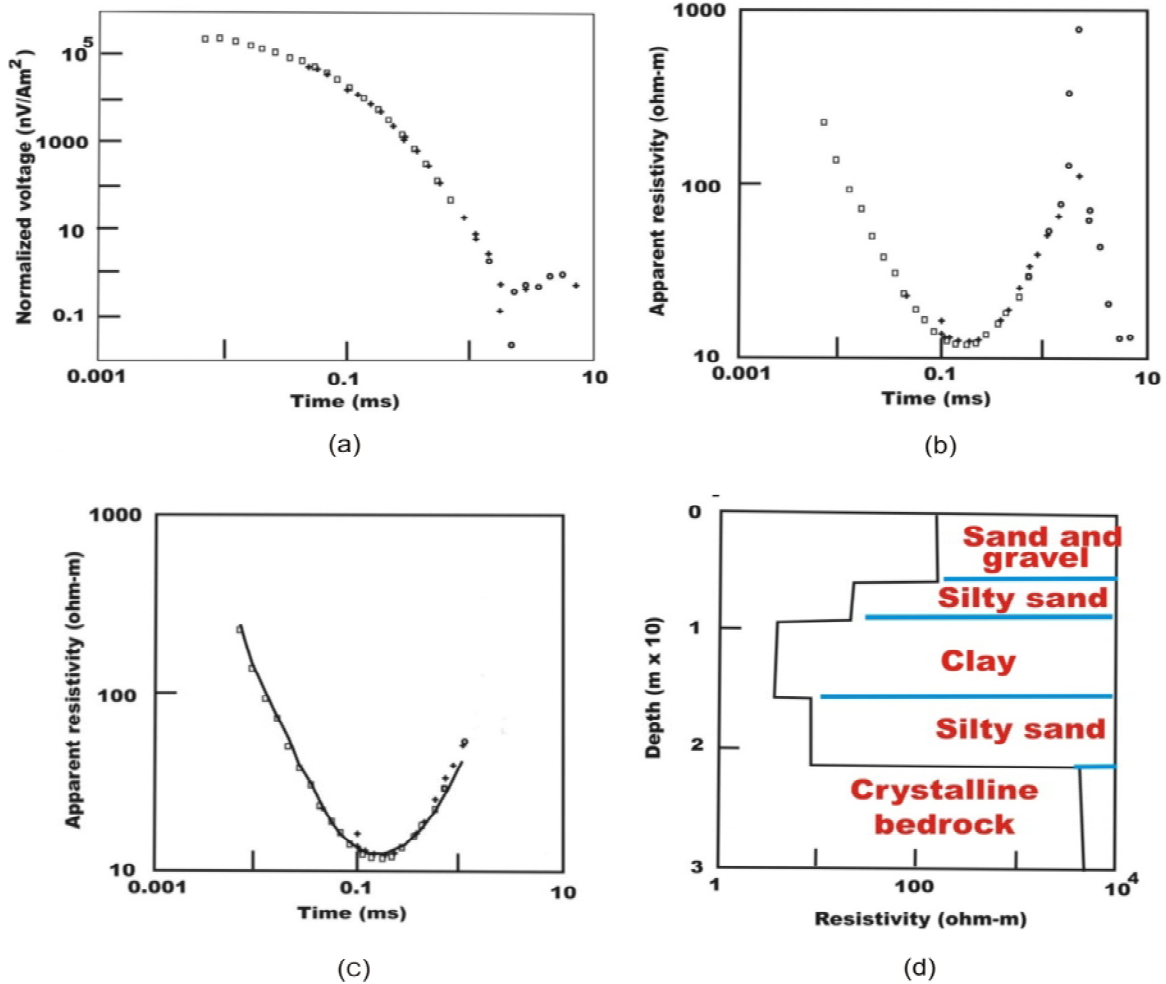


Figure 4.1-5 Unedited voltage (a) and apparent resistivity (b) measured directly by the EM system. Edited apparent resistivity (dots) with the solid line representing the best fit from the 1D inversion (c). The right hand side is the best fit resistivity versus depth model which, in this case, is a 5 layer model (d).

### **Uncertainty assessment**

One-dimensional time-domain inversion methods provide ranges of the model parameters by computing those models that fit the data to the same level of fit as the best fit models (shown in Figures 4.1-5 and 4.1-7). This procedure is called equivalence analysis. Figure 4.1-6 is an example of an equivalence analysis for a sounding carried out on the Brookwood aquifer in the Fraser Valley near Langley, British Columbia. The black line is the best fit model while the coloured lines show the range of models that fit data to the same accuracy as the best fit model. Note that conductive layers tend to have smaller errors of fit compared with resistive layers as expected and the depth errors increase with depth. This 3 layer model consists of sand and gravel overlying silty sand overlying clay. In this example the range of depths for the upper and lower boundaries is approximately +/- 7m.

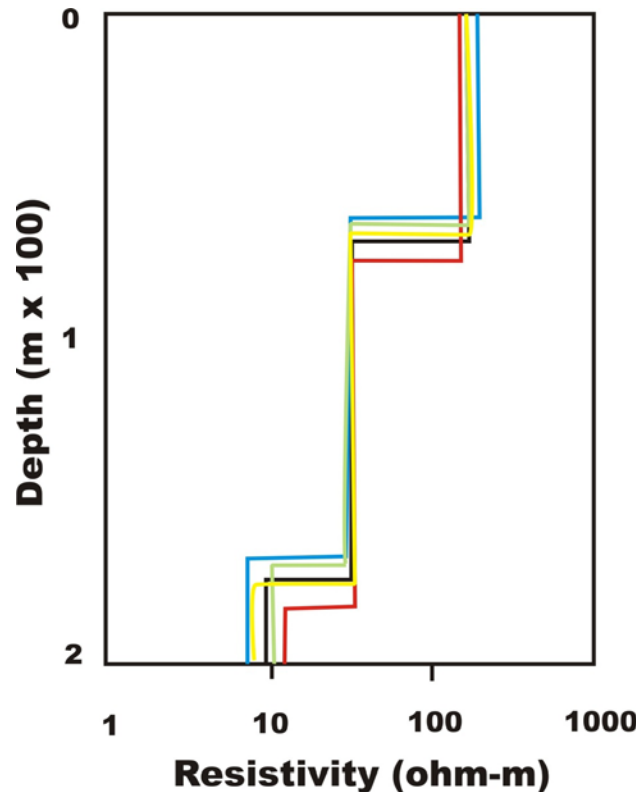


Figure 4.1-6. Equivalence analysis of a typical time-domain sounding (example from the Fraser Valley, British Columbia). The black line is the best fit model and the coloured lines represent the range of models that fit the data to the same level of error.

### **Recommended Guidelines for Reporting**

Minimum reporting requirements must describe survey system and components, survey configuration used, as well as any impediments, such as space limitations to lay out transmitter loops, noise levels at the time of the survey, and topography in the survey area. Other geological limitations must also be described (e.g. possibility of non one-dimensional structures, highly resistive layers expected to overlie each other, based on analysis of available borehole data, etc). Electromagnetic site classification reports must present sample voltage and apparent resistivity versus time data (Figure 4.1-5a, b). Interpreted resistivity depth sections (Figure 4.1-5c, d) must also be presented.

## Hazard Related Case Studies

### Case 1: Time-Domain EM in the Fraser River delta, BC.

In the Fraser River Delta, the boundary between Holocene and Pleistocene sediments is important for seismic hazard studies, as the Holocene sediments have a lower velocity than the Pleistocene sediments leading to possible focusing (amplification) effects of seismic waves. Figure 4.1-7 presents an EM sounding in unconsolidated Holocene Fraser River soft sediments which overlie consolidated glacial Pleistocene sediments. Also presented is the 1D interpretation and resistivity log. The Holocene and Pleistocene sediments are similar in lithology but have significantly different resistivity values due to salt water intrusion into the Holocene sediments. An impermeable shell bed separates the upper saline water from the underlying fresh water at the boundary between. This provided an easy mapping horizon for the top of the Pleistocene sediments using time-domain EM.

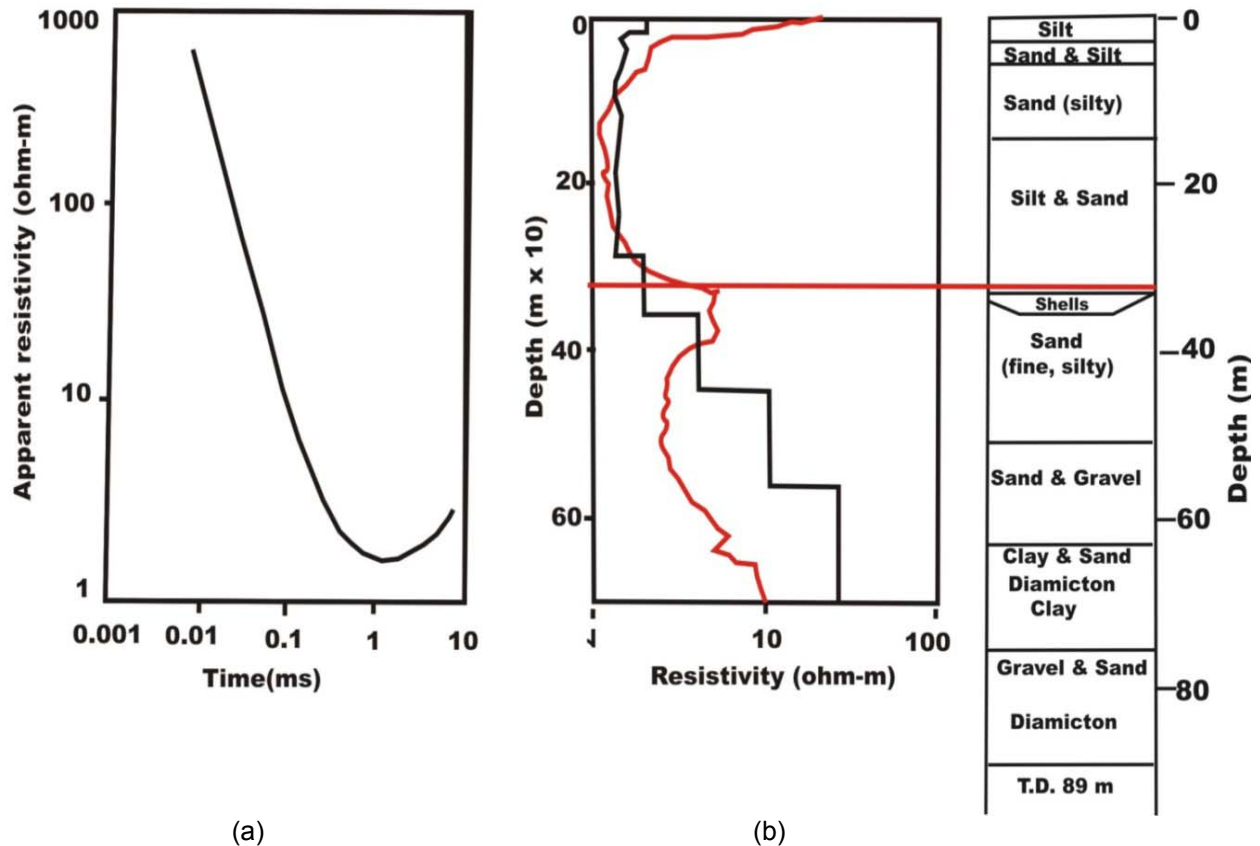
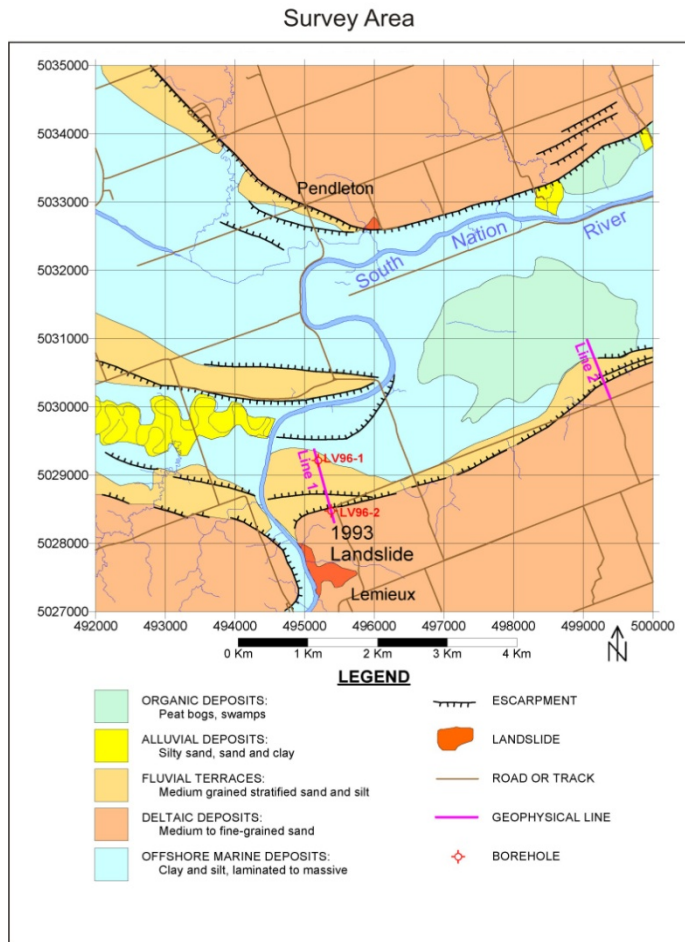


Figure 4.1-7 a) Edited apparent resistivity versus time. The solid black line is the best fit 1D inversion model for the multi-layer resistivity model shown in the left hand side of (b). The data and inversion results are coincident so the dots for the field data are not shown. The red curve in (b) is a down-hole resistivity log measured using the Geonics EM39 system. The right hand side of (b) is a geological log for the same well. The horizontal red line shows the contact between the Holocene and Pleistocene sediments and its relationship to the shell bed.

### **Case 2: Frequency-Domain EM for landslide investigation applications, Ottawa Valley, ON.**

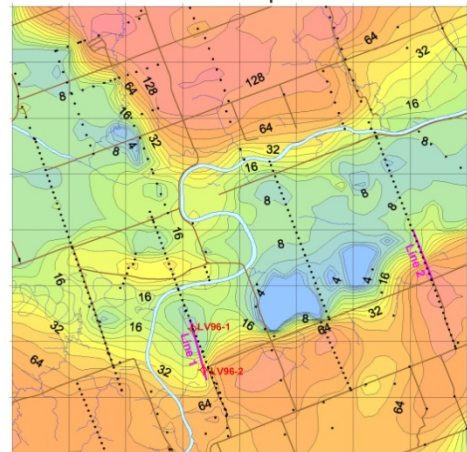
In the Ottawa Valley, large landslides have occurred on slopes that are underlain by sensitive marine sediments, known locally as Leda Clays. Slope failures in the area are known to be associated with several factors. First, an overlying sand layer is often present which creates a hydrostatic load when saturated. Second, if sufficient leaching of salts has occurred in the Leda Clay porewater, sensitivity of the soil is high. Finally, the landslide must be triggered at the toe of the slope by erosion or some other force. Once initiated, the Leda Clay can flow quite rapidly, even in areas with relatively low topographic relief (Aylsworth and Hunter, 2004). Previous work by Hyde and Hunter (1998) had shown that electrical conductivity of glaciomarine sediments of the Ottawa Valley is primarily controlled by pore-water salinity. Therefore, an EM34 inductive conductivity survey near the 1993 Lemieux landslide was effective in identifying the distribution of these sediments and overlying deltaic sands (Calvert and Hyde, 2002). Figure 4.1-8 presents sample results of the EM34 apparent resistivity maps. Coil separations of 10, 20 and 40m were used with horizontal and vertical dipoles to investigate variation of resistivity with depth. Figure 4.1-9 presents one of several complimentary electrical resistivity profiles collected to investigate the subsurface conditions near an existing landslide. Apparent conductivity downhole logs along the alignment were used to constrain the resistivities during the inversion process.

Examples estimating porosity from time-domain and frequency-domain conductivity metres in eastern and western Canada can be found in Best and Todd (1998), Hunter et al. (1998), and Hyde and Hunter (1998).

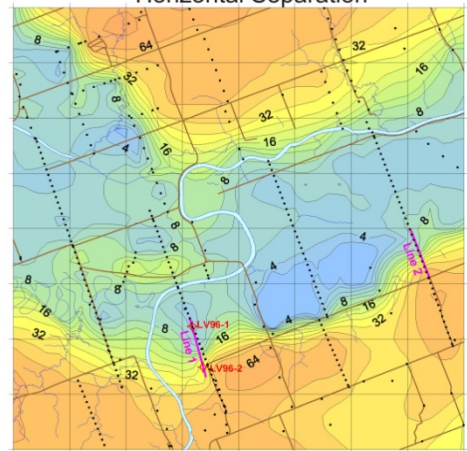


a)

b) EM34 - 10m Dipoles  
Horizontal Separation



c) EM34 - 20m Dipoles  
Horizontal Separation



d) EM34 - 40m Dipoles  
Horizontal Separation

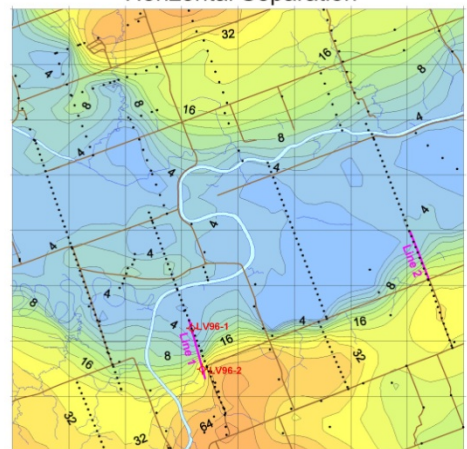


Figure 4.1-8. EM34 survey results collected near a large Leda Clay landslide. a) Surficial geology of the survey area. b) Apparent resistivity results using 10m horizontal dipoles. c) 20 m horizontal dipoles. d) 40 m horizontal dipoles.

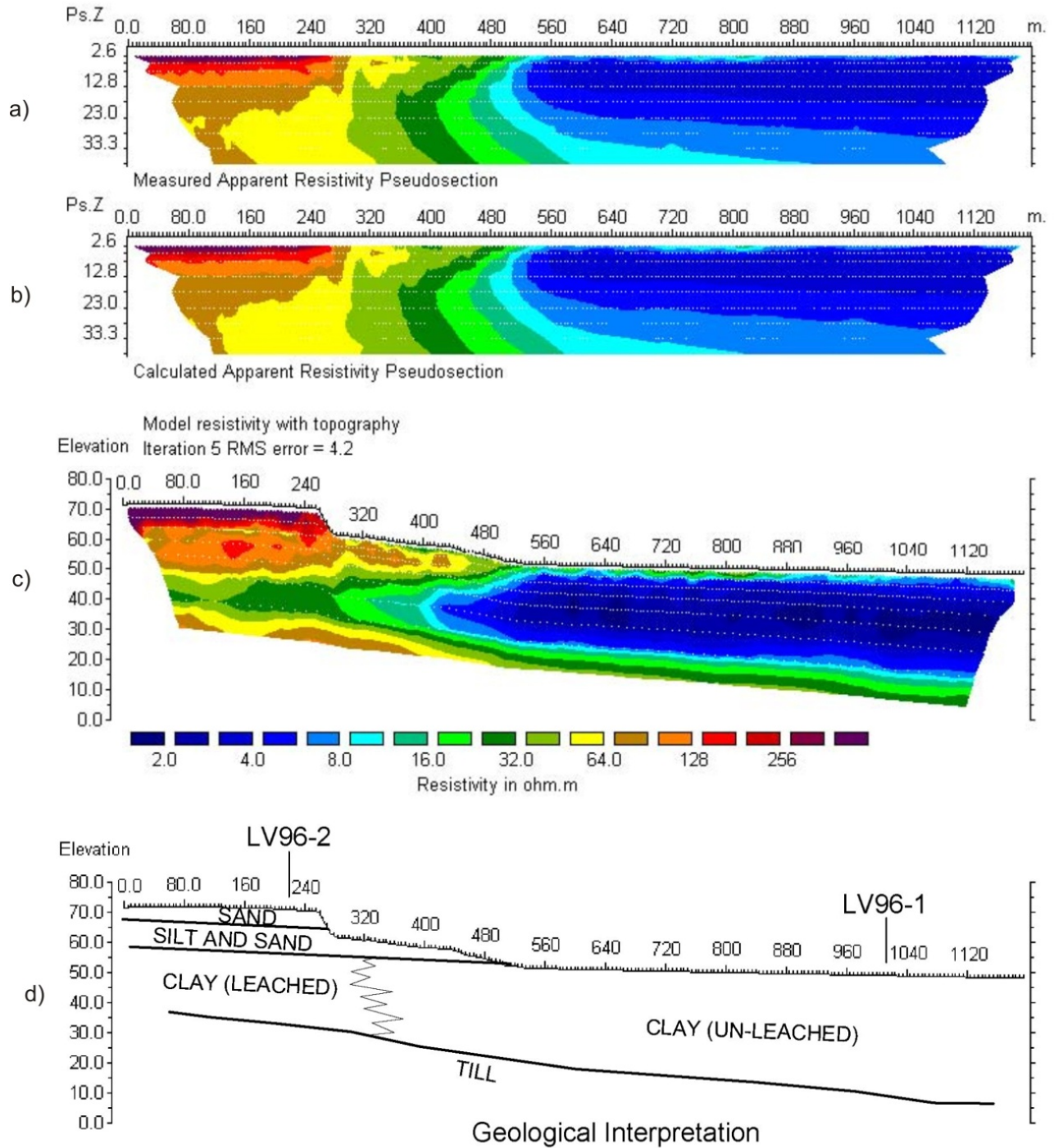


Figure 4.1-9. Resistivity section collected over the landslide slope. Images represent a) the measured apparent resistivity pseudosection, b) calculated apparent resistivity pseudosection, c) modelled resistivity section with topography, and d) the interpreted soil conditions. The location of boreholes where apparent conductivity downhole logs were collected are shown on the section

## References

- Archie G.E., 1942. The electrical resistivity log as an aid in determining some reservoir characteristics; American Institute of Mining, Metallurgical, and Petroleum Engineers (AIME) Transactions, v. 146, p.54-62.
- ASTM D6639-01 (2008). Standard Guide for Use of the Frequency Domain Electromagnetic Method for Subsurface Investigations, ASTM International, West Conshohocken, PA, 2008, DOI: 10.1520/D6639-01R08, [www.astm.org](http://www.astm.org).
- ASTM D6820-02 (2007). Standard Guide for Use of the Time Domain Electromagnetic Method for Subsurface Investigations, ASTM International, West Conshohocken, PA, 2007, DOI: 10.1520/D6820-02R07, [www.astm.org](http://www.astm.org).
- Aylsworth, J.M. and Hunter, J.A., 2004. A geophysical investigation of the geological controls on landsliding and soft deformation in sensitive marine clay near Ottawa; *in* Proceedings, 57<sup>th</sup> Canadian Geotechnical Congress, Quebec city, Quebec, p. 30-37.
- Best, M.E. and Todd, B.J., 1996. Electromagnetic soundings, pseudo-resistivity logs and implications for porosity and groundwater salinity; *in* Proceedings, Symposium on the Application of Geophysics to Environmental and Engineering Problems (SAGEEP), Keystone, CO, p. 1061-1074.
- Calvert, H.T. and Hyde, C.S.B., 2002. Assessing landslide hazards in the Ottawa Valley using electrical and electromagnetic methods; *in* Proceedings, Symposium on the Application of Geophysics to Environmental and Engineering Problems (SAGEEP), Las Vegas, NV, 11 p.
- Fitterman, D.V. and Stewart, M.T., 1986. Transient electromagnetic soundings for ground water; *Geophysics*, v. 51, p. 995-1005.
- Frischknecht, F.C., 1959. Scandinavian electromagnetic prospecting; American Institute of Mining, Metallurgical, and Petroleum Engineers (AIME) Transactions, v. 214, p. 932-937.
- Hunter, J.A., Burns, R.A., Good, R.L., Douma, M., Pullan, S.E., Harris, J.B., Luternauer, J.K. and Best, M.E., 1998. Application of geophysical techniques in the Fraser River delta, for earthquake hazard studies, (eds.) J.J. Clague, J.K. Luternauer and D. Mosher; Geological Survey of Canada, Bulletin 525, p. 123-145.
- Hyde, C.S.B. and Hunter, J.A., 1998. Formation electrical conductivity-porewater salinity relationships in Quaternary sediments from two Canadian sites; *in* Proceedings, Symposium on the Application of Geophysics to Environmental and Engineering Problems (SAGEEP), Chicago, IL, p. 499-510.
- Jackson, J.D., 1999. Classical electrodynamics; John Wiley and Sons, Inc., Hoboken, NJ, 832p. (third edition).
- Kearey, P. and Brooks, M., 1984. An introduction to geophysical exploration; Blackwell Scientific Publishing, Boston, MA, 296p.
- Maxwell, A. M., 1998. A simple method of transient electromagnetic data analysis; *Geophysics*, v. 63, p. 505-419.
- McNeil, J.D., 1980. Electromagnetic terrain conductivity measurement at low induction numbers; Technical Note TN-6, Geonics Limited, Mississauga, ON, 15p.
- Nabighian, M.N., 1988, Electromagnetic methods in applied geophysics: Theory (Vol 1, 972p.), and Applications (Vol 2, 452p.); Society of Exploration Geophysicists, Tulsa, Oklahoma, USA.

Spies, B.R. and Eggers, D.E., 1986. The use and misuse of apparent resistivity in electromagnetic methods; *Geophysics*, v. 51, p. 1462-1471.

Stoyer, C.H., 1990. Efficient computation of transient sounding curves for wire segments of finite length using an equivalent dipole approximation; *Geophysical Prospecting*, v. 38, p. 87-89.

## 4.2 Resistivity Methods

Michael Maxwell  
Golder Associates Ltd., Burnaby, B.C.

### Introduction

#### Principles of the Method

The physical principles for electrical resistivity methods are a simple extension of Ohm's Law applied to the half-space or whole space of earth media, rather than an electrical circuit. The current density,  $J$ , at a point in a media is proportional to the electric field,  $E$ , and related to the resistivity of the media,  $\rho$ , or its reciprocal, conductivity,  $\sigma = 1/\rho$ , in an alternative expression of Ohm's Law, ( $J = \sigma E$ ). This form of the equation is usually used for inverse modeling of resistivity data. Resistivity variations of natural ground media vary by more than 10 orders of magnitude ( $10^{-6}$  to  $10^{+6}$ , metals to dry rocks) and presence of water can provide significant variation in soils and rocks. Ward (1990) provides an excellent summary of the theory and practice of electrical resistivity.

In the simplest form of the DC resistivity method, the apparent resistivity of the subsurface can be calculated by injecting a current into the ground using two electrodes and measuring the potential difference (voltage) between two different electrodes. The current flow into the ground will be affected by the resistive properties of the media, therefore by measuring the resultant electric field, information about these properties can be determined. The 'depth' of investigation is a function of electrode separation, with larger electrode separations providing information from greater depth or distance as a result of the electrical current flow extending further into the ground. Complex resistivity in contrast to DC resistivity incorporates the effects of induction and chargeability due to varying the injected current flow.

#### Current State of Engineering Practice

Traditional DC sounding techniques measure the potential differences for various positioning and separations of the four electrodes or quadrapoles. Traditional interpretation techniques used analytically-modeled type curves, 1D forward modeling, or pseudo-sections of data with an assigned geometric factor to develop a ground resistivity stratigraphy that approximated the measured data. In the modern implementation termed electrical resistivity imaging or tomography (ERI/ERT), ground response is measured from sequentially-sampled quadrapole sets of 2D or 3D arrays of electrodes. Multi-channel data collection systems allow rapid collection of large data sets. Inverse modeling is used to process the large resistivity/conductivity data sets to develop ground resistivity models that are used to infer rock/soil types, stratigraphy, and soil conditions. Electrode arrays and measurement sequences extend from standard 2D types that were established in traditional DC surveys (e.g. Wenner, Schlumberger) to random 2D and 3D dipole-dipole and pole-pole arrays. The combination of high speed data collection and inverse modeling of large data sets has made ERI/ERT a powerful tool for subsurface imaging.

Ward (1990) provides a good summary and includes an extensive reference list. For more current practices and especially for interpretation methodology, the various manufacturers of software and hardware provide good summaries/tutorial information (see Loke, 2012).

#### **Recommended citation:**

Maxwell, M., 2012. Resistivity Methods; *in* Shear Wave Velocity Measurement Guidelines for Canadian Seismic Site Characterization in Soil and Rock, (ed.) J.A. Hunter and H.L. Crow; Geological Survey of Canada, Open File 7078, p. 182-190.

### **Limitations**

Resistivity relies upon establishing sufficient potential field for measurement and sufficient receiver geometry to successfully sample the ground for inversion modeling to be valid. Conductive overburden situations can limit depth penetration and highly conductive channels can mask more subtle resistivity variations which may be of interest. In highly resistive environments, low currents can result in noisy data sets. Abrupt resistivity variations can be difficult to inverse model and small but resistive or conductive structures can be difficult to resolve. Data collection is usually a compromise between resolution and depth penetration in regard to electrode spacing. Finally, it is important to note that electrical resistivity delineates soil and rock electrical property variations which are only indirect indicators of mechanical engineering properties of soils.

## **Data Collection**

### **Required Equipment**

Commercial electrical resistivity and IP data collection systems consist of power, control, and data collection units (often in a common box or separately computer-controlled) connected to individual electrodes through multi-core cables. Injection and measurement electrodes are typically stainless steel but sometimes potential measurement electrodes are porous pots for low field measurements. Borehole electrodes include cables with exposed takeouts that are below water level or grouted in place or spring-style electrodes that keep contact with the media. Marine cables are available for water-based surveys. Typical power units use 12V batteries (often car batteries in parallel) to inject up to 3 amperes at 1000 volts, and higher power systems are available that use generators (i.e. 10 kW) that inject higher currents at higher voltages for very resistive environments or maximum depth penetration. Some units use smart electrodes that are addressed from a central computer control and which allow smaller conductor count cables and reduce any potential crosstalk on long cable lengths. There are also wireless systems available which use GPS timing to reduce wire layouts. Electrode spacing varies from 1 to 10 metres typically for non-mineral exploration applications.

### **Data Collection Procedures**

Prior to surveying using automated multi-channel systems (manual data collection is rarely used in modern work), quadrapole sequence files are prepared to control current injection and potential voltage measurements based on selected array types and electrode layouts. ERI survey planning, especially for 2D surveys, is similar to seismic refraction in that electrode spacing is selected to balance resolution and depth penetration. General rules-of-thumb are that resolution provides an inversion model cell-size of similar order to electrode spacing, and depth penetration is between  $\frac{1}{4}$  and  $\frac{1}{10}$  of the total line length or separation between injection/measurement electrodes and dependent upon ground resistivity conditions. Higher resistivity generally permits deeper penetration but potentially noisier data. With automatic data collection systems, injected current and potential measurement levels can be adjusted on-the-fly based on input parameters for minimum potential voltage levels and/or injection currents. Statistical evaluation of data measurements during current reversals are used to control data quality and repeat measurements can be completed or poor data is flagged by the poor repeat statistics. Modern microprocessor-controlled systems usually remove drift due to SP (self-potential) variations.

Selection of a survey array type is dependent upon the goals of a survey, but each type has general characteristics that help in the selection and often multiple arrays are collected for each layout. Generally, Dipole-Dipole provides shallower penetration with good delineation of lateral variations. Wenner surveys provide deeper penetration and good delineation of horizontal layering but not lateral variations. Wenner-Schlumberger is a compromise between Dipole-Dipole and Wenner. Pole-pole surveys use remote electrodes for both injection and potential measurements and can provide deeper penetration with less noisy data and combinations of pole-dipole and the older style gradient array setup are often used in specific situations. Dipole-dipole and pole-pole surveys have the advantage of faster data collection because of simultaneous multi-channel capability and typical surveys of 100 or more electrodes with good resolution and depth penetration can be collected in one hour compared to a Wenner-Schlumberger survey requiring 3-4 hours.

3D electrode arrays are of increasing interest and there is focus on optimizing survey designs based on forward modeling of expected targets to reduce the number of data measurements. Typical 3D surveys will collect data from more than 15,000 quadrupoles and often require multi-day data collection.

Survey layouts usually require planting of each electrode either by hammer placement and watering of stainless steel electrodes or in high resistivity situations (dry ground, rock, frozen ground), use of porous pots or other creative preparation including bentonite or cloth (e.g. diaper) saturation to reduce contact resistances. The first step in all surveys is to test the contact resistances of all electrodes and ensure that they are all within approximately 1-2 orders of each other. Some geophysicists prefer to get contact resistances below 10,000 ohm-m, but generally, if during a survey they all remain within 1-2 orders as noted, the data are of good quality. This is especially true in very dry highly resistive situations.

## **Processing Techniques**

### **Theory of Analysis**

There are extensive treatments of theoretical and practical aspects of the theory of analysis of electrical resistivity, however, the most appropriate are the manuals provided by various commercial software producers. Inverse modeling is the main tool for interpreting electrical resistivity data that is used in modern surveys. The programs are all based on solving the potential field for the injected current and electrode locations.

Generally, a block or mesh model is set up with elements that match the data distribution reasonably well based on pseudosections, geometric factors, or calculated potentials from a full solution of the potential field for each injection dipole. Software packages use a variety of finite difference and finite element models for a sequence of forward and inverse steps with optimization using different tradeoffs. The result is an inverse model that provides an optimal fit to the measured data. The results of inverse modeling have been truthed in many different field situations and they have been successful at delineating subsurface conditions and identifying drill targets.

### **Uncertainty Assessment**

Any inversion modeling results in a smoothing of the resistivity conditions unless there is a truly homogeneous earth. Newer adaptive meshes are reducing the smoothing effect but models are still restricted by the size of the blocks or meshes. Inversion modeling, and especially 3D inversions, can reveal resistivity contrasts but may not accurately reproduce true apparent resistivities (10% to 50% differences) especially in low resistivity situations (more conductive). A number of measures can be evaluated to consider how well a model fits reality. Measured and modeled pseudosections can be examined as a first level of how well the modeled data fits the measured data. Numerically, the misfit of the model with the measured data can be calculated and is used during the modeling process to reject potentially bad data. The total misfit is used as a measure of how well the model fits and if it is in the same order as the number of data points, the inversion is considered to be good. The sensitivity of each block or mesh cell can be evaluated as well to determine its weighting in the inversion modeling which can assist in determining whether a resistivity feature is valid.

For interpretation of ground geology or stratigraphy, the general rule-of-thumb is that the resolution of an inversion model is in the order of the separation of electrodes given that the inversion used an appropriate block or cell size and is of good quality. However, generally depth uncertainty is taken as 10% to 20% of depth (as for seismic refraction). Lateral uncertainty of the location of a resistivity feature is taken as one electrode separation.

## **Recommended Guidelines For Reporting**

Minimum reporting requirements should be inverse models of apparent resistivity/conductivity with model uncertainties and calibration with other data (borehole, seismic) when available. Original data with current levels and potential voltage levels along with statistical information and SP data should be supplied as well. For 2D data sets, original data pseudosections and inverse modeled data pseudosections are available from commercial software and should be provided at least as an appendix.

3D and 2D inverse models could also be supplied with a sensitivity analysis to indicate where there is good information for model solutions.

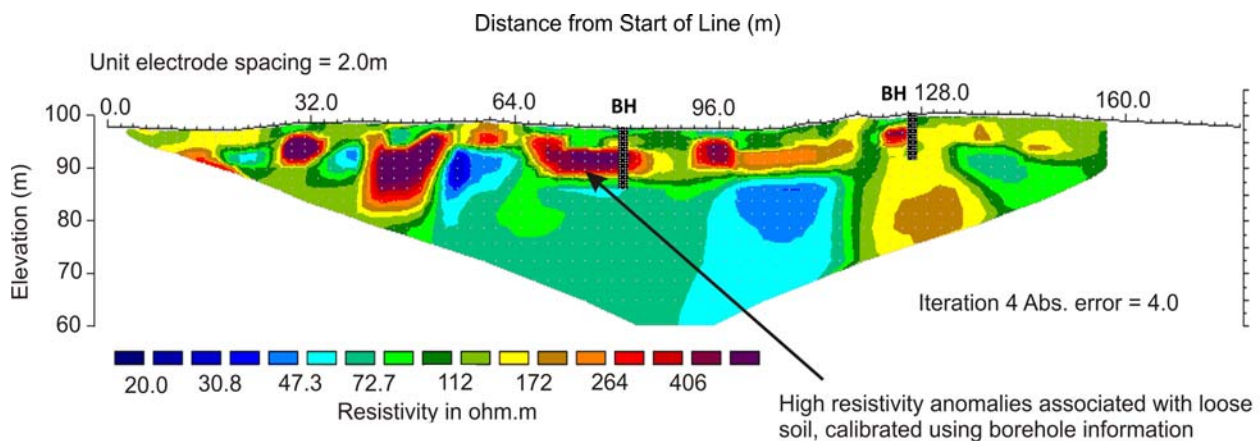
## Hazard-Related Case Studies

Electrical resistivity is often used as a geophysical screening tool to look for soil and rock variations at sites where seismic surveys may be difficult to carry out or non-conclusive. 3D deployments and interpretation of electrical resistivity data are often more efficient than using seismic methodology, particularly where there are opportunities to obtain complementary information. In addition, seismic or borehole investigations may be used for follow-up work. Many soil and rock development regimes result in resistivity contrasts due to interstitial water and air variations in soils/rocks incorporating particle size differences. Example situations include voids, loose soil, and water exploration.

For illustration purposes, various case histories are presented in which electrical resistivity was used to look for resistivity variations in common engineering investigations of soil, dams, and rock. In some cases, seismic investigations were also completed before or after the electrical resistivity investigation.

### Case 1: Soil Variations

Loose soil development is common in the interior of British Columbia, but this also occurs at soil sites around the world. At a project site in BC, site construction plans were changed once these conditions were identified, to allow for the shallow loose soils. Examples of the 2D ERI profiles from the site are shown in Figure 4.2-1. Wenner-Schlumberger data were collected with an electrode spacing of 2m. RES2DINV inversion models indicate resistive zones in the subsurface (purple, red, orange, and brown colour contours). Calibration with borehole data confirmed that the resistive zones are associated with loose silt soils. Visual evidence is present at the site with a series of regularly spaced slumps extending across the terrain near the surveyed site (and the reason for geophysical surveying).



#### Model Notes:

- Horizontal scale is 10.63 pixels per unit spacing
- First electrode is located at 0.0 m
- Last electrode is located at 178.0 m

Figure 4.2-1. ERI delineation of soil variations. Modeled inverse resistivity profile shows anomalies of relatively high resistivity where drilling indicated loose soils had developed.

ERI is frequently used to characterize soil variations due to changes in subsurface resistivity properties. Figures 4.2-2a and b are from the same site, and Figure 4.2-2c is from a nearby site. Figure 4.2-2a illustrates a typical 2D inversion model of an ERI survey at a sand and gravel deposit to delineate silt zones which can have lower resistivity due to water in the interstitial void space. Typically 2D arrays are deployed with 50 to 100 electrodes and standard Wenner or Wenner-Schlumberger arrays are sampled. A cutoff resistivity was used to delineate volumes of aggregate resource for development of the pit as shown in Figure 4.2-2b.

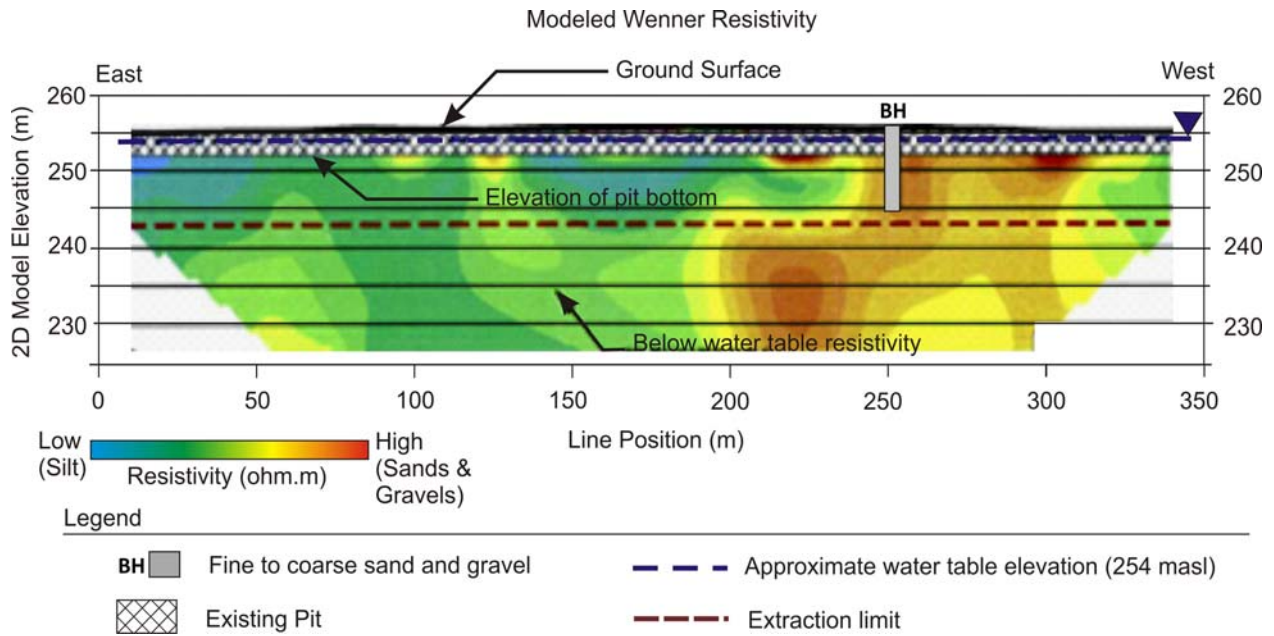


Figure 4.2-2a. ERI is used as a complementary method to, or in place of, seismic surveying to characterize aggregate deposits between boreholes. Here, the ERI model was correlated to grain size distribution and moisture content obtained from soil samples.

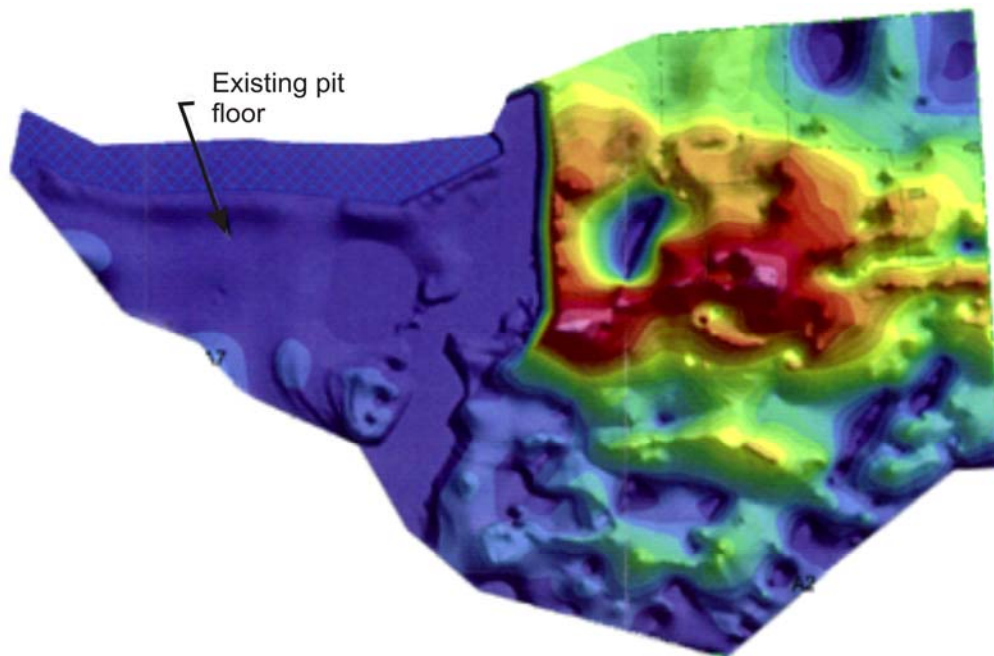


Figure 4.2-2b. Modeled thickness contours of aggregate based on ERI profiles.

In Figure 4.2-2c, a series of ERI lines were collected near an open pit gravel deposit and used to guide a program of PQ overburden coring. The data gathered from both datasets (resistivity and coring) were used to develop a 3D model of the estimated reserves at the site which proved very effective for continued pit development.

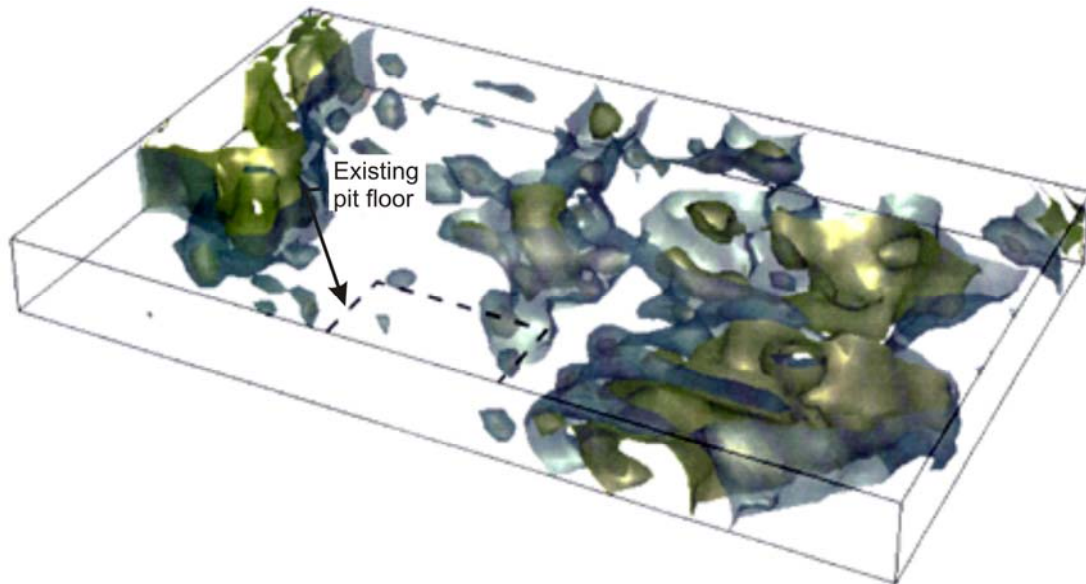


Figure 4.2-2c. Resulting modeled gravel resource volumes based on cut-off resistivities and overburden coring results.

**Case 2: Dam Investigations**

ERI was used in combination with seismic methodology to investigate dam soil conditions for stability as well as soil-water properties and potentially to delineate seepage. Figure 4.2-3 shows the results of a standard 2D Wenner-Schlumberger survey over a dam to delineate the different dam component materials. Figure 4.2-4 shows the results of 2D surveys over a proposed dam site to characterize the soil overburden and potential bedrock issues. The complementary nature of ERI is evident in this result as seismic refraction methodology could measure the engineering properties of the overburden but would have had difficulty delineating the bedrock variations.

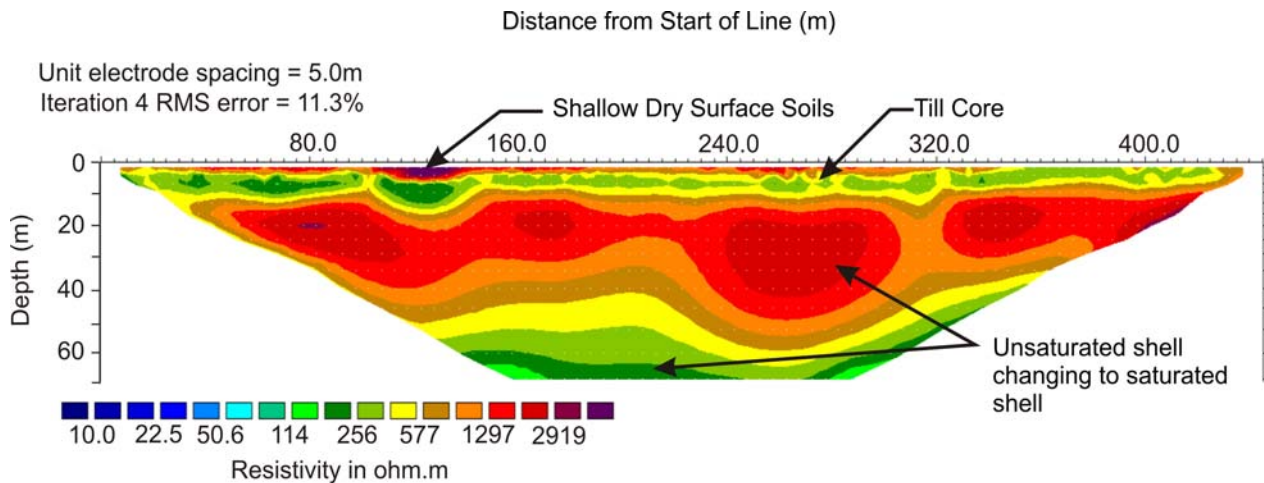


Figure 4.2-3. ERI delineation of dam soils. Modeled inverse resistivity profile is shown with interpretations, based on a synthesis of ERI, surface seismic, and borehole data.

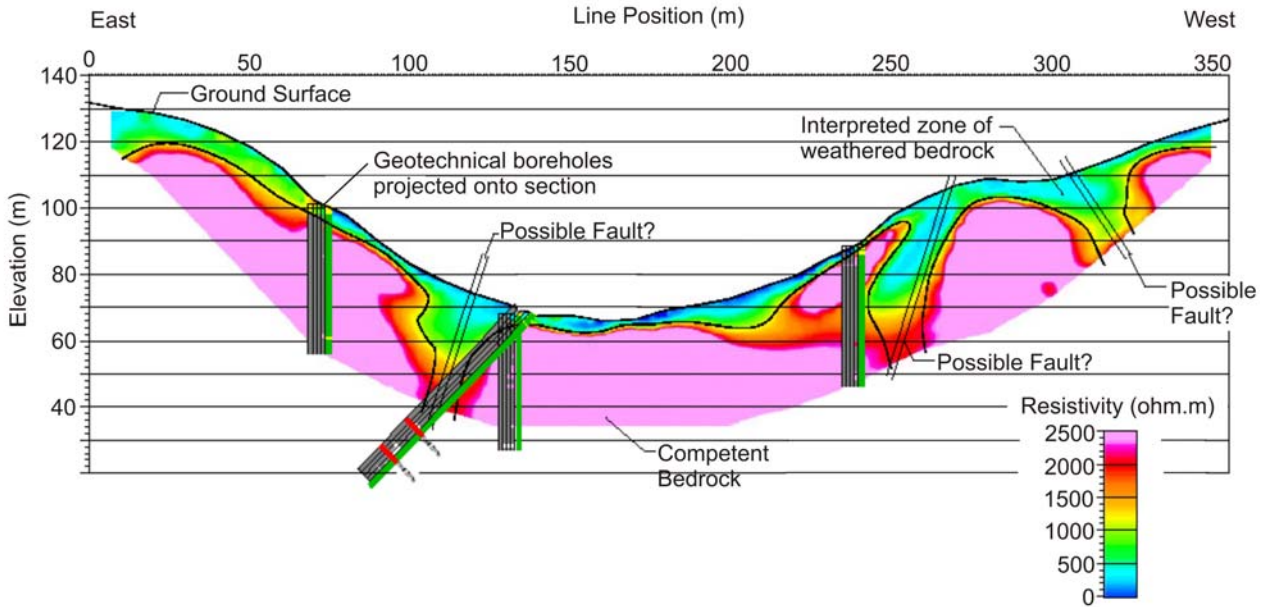


Figure 4.2-4. Example of ERI used in conjunction with surface seismic and borehole techniques to characterize soils and rock for a dam foundation. Shown is the modeled inverse resistivity profile with geotechnical borehole information projected onto the section.

### Case 3: Rock Variations

Electrical resistivity surveys are often used to investigate sites for overburden thickness and underlying rock conditions. In particular, abandoned underground mine sites are often surveyed to delineate old mine workings. 2D and 3D ERI surveys are carried out for this purpose and often borehole electrodes are used to provide better geometry. Figure 4.2-5 shows an application of 2D ERI for imaging a void in limestone under soil overburden.

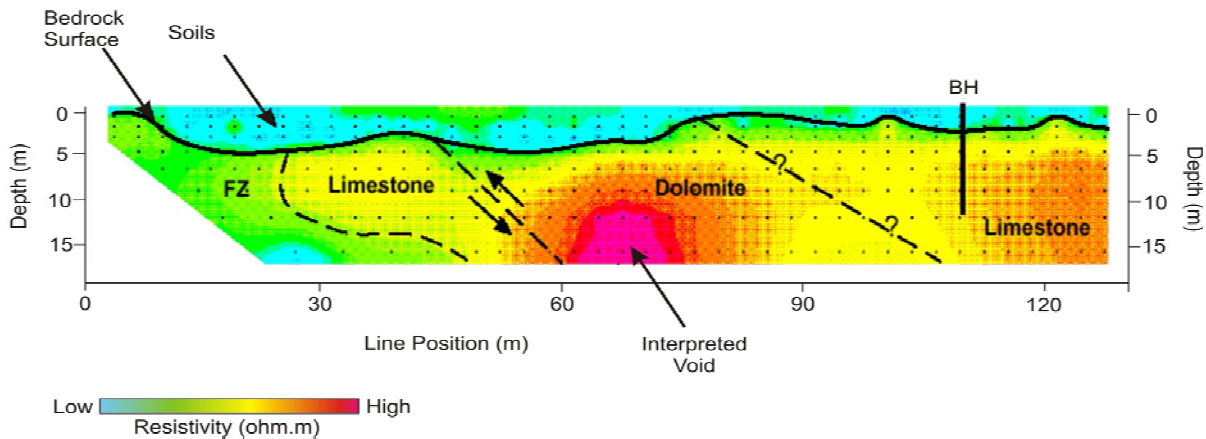
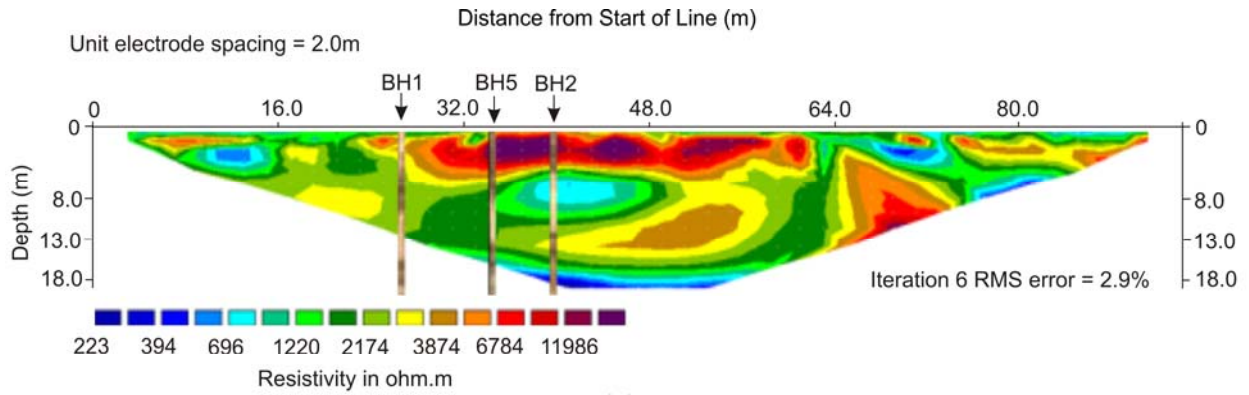
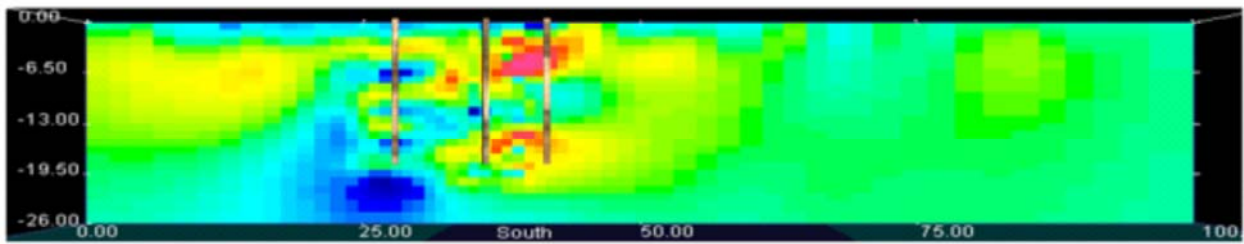


Figure 4.2-5. Example of ERI survey being used to delineate voids in bedrock underlying a soil layer.

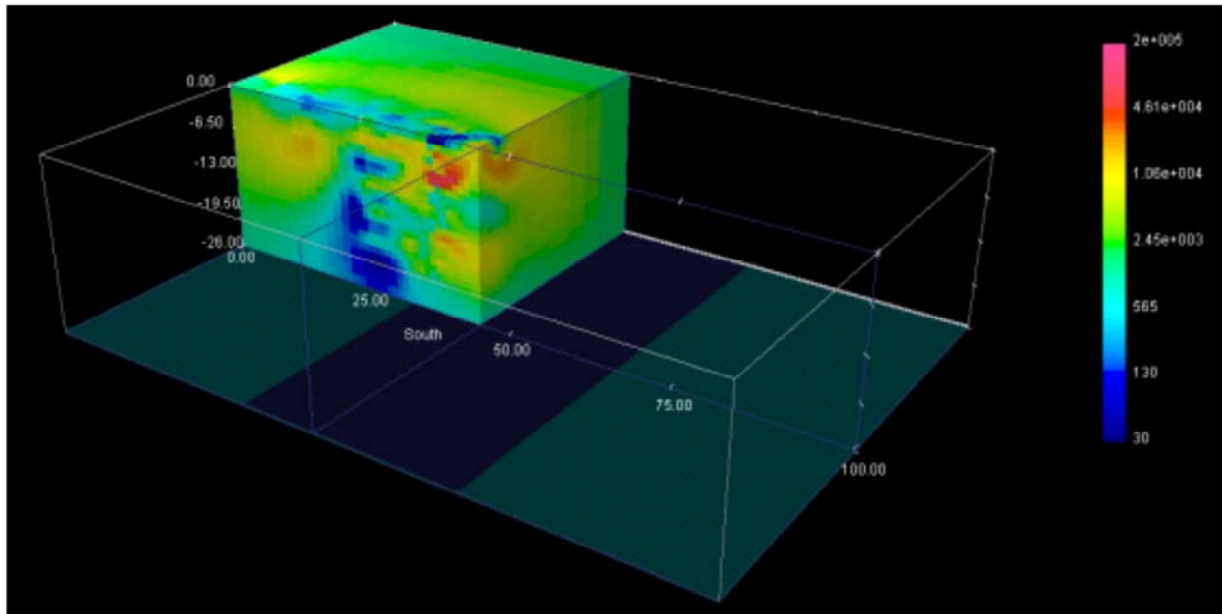
Maxwell et al. (2005) provides a summary of applications of 2D and 3D ERI for delineation of voids and wet salt in an underground potash mine. 3D ERI surveys have the capability of delineating even finer scales of media variations as illustrated in Figure 4.2-6. A 3D ERI investigation used 120 electrodes in a drift into a limestone aquifer at the underground Laboratoire Souterrain à Bas Bruit research facility in southern France. The electrical resistivity imaged subtle variations in the limestone porosity due to alteration of resistivity by interstitial water. This result has been confirmed from borehole data as well as borehole seismic and GPR surveys.



(a)



(b)



(c)

Figure 4.2-6. Underground 2D and 3D ERI Investigation. (a) Comparison of 2D inversion of Wenner-Schlumberger data and 3D inversion slice of complete data set (b) on similar plane with borehole televiewer data overlaid. The light coloured zone in televiewer data is higher porosity zone in limestone and correlates with lower resistivity zone in 2D and 3D ERI data sets. (c) Full 3D resistivity interpretation is presented.

## Acknowledgements

The author thanks Dr. Doug Oldenburg and Rob Eso of University of British Columbia Geophysical Inversion Facility (UBC-GIF) for 3D interpretations and designs of 3D ERI surveys; Golder Associates Limited geophysicists including Christopher Phillips, Mark Monier-Williams, Jeffrey Schmok, and Fern Webb for the variety of case histories; and Dr. Stéphane Gaffet of the Laboratoire Souterrain à Bas Bruit in Rustrel, France and Dr. Matt Yedlin of the University of British Columbia for the opportunity to conduct ERI experiments in the underground laboratory.

## References

Maxwell, M.G., Unrau, J., Eso, R., Oldenburg, D. and Song, L.P., 2005. Advancement of 2D and 3D electrical resistivity techniques for underground applications in a potash mine; *in* Proceedings, Rock Mechanics and Geotechnical Applications – International Symposium on Mine Planning and Equipment Selection, Banff , AB.

Loke, M. H., 2012. [Tutorial: 2-D and 3-D electrical imaging surveys](http://www.geoelectrical.com/coursenotes.zip). (Revised Mar 2012) <<http://www.geoelectrical.com/coursenotes.zip>> [accessed: Mar 2012]

Ward, S.H., 1990. Resistivity and Induced Polarization Methods; *in* Geotechnical and Environmental Geophysics, Volume I, Society of Exploration Geophysics, Tulsa, OK, 389 p.

### Further Reading:

Note: The above notes by Dr. Loke contain numerous references to further readings, and free downloadable software is available from <<http://www.geoelectrical.com/downloads.php>>.

## 4.3 Ground Penetrating Radar (GPR) Methods

*Daniel Campos*

*Géophysique GPR International Inc., Longueuil, QC*

### Introduction

#### **Principles of the Method**

Ground penetrating radar (GPR) is a non-intrusive method that uses electromagnetic radiation to image the earth's materials. High-frequency radio waves (MHz to GHz range) are transmitted into the ground using a GPR system coupled to a transmitter-receiver antenna. When the transmitted wave hits a boundary between two materials having different dielectric constants, a portion of the energy is reflected back to the surface and detected by the antenna. Antennas of different peak frequencies can be used to investigate the ground at different depths. GPR results are presented in the form of radargrams. These are similar to seismograms except that reflections appear at boundaries with differing dielectric constants instead of acoustic impedance boundaries.

#### **Current State of Engineering Practice**

GPR is used for various applications ranging from mineral exploration to high resolution concrete investigations. In the engineering field, GPR is mostly used for non-invasive subsurface characterization. ASTM standard D6432 - 11 describes the equipment and methodology of the GPR technique, which allows for layer mapping, material characterization, and detecting objects, voids, and cracks. It can be used over bedrock, soil, ice, fresh water, pavement, and within structures.

Constant advances in electronics and computer technology have allowed newer generation GPR systems to have better performance in terms of resolution, penetration and automation. The latest GPR technology includes handheld systems, multiple-antenna array 3D systems, multi-frequency antennas, wireless communications and automated data interpretation.

#### **Limitations**

The most important limitation of this method is the poor signal penetration in conductive materials. In soils with high electrical conductivity, such as clays or mine tailings, penetration can be very limited. This is caused by signal dissipation as it quickly travels through the conductive material away from the receiver. Another condition that affects penetration is signal scattering in very heterogeneous soils. In these conditions, GPR signal is lost because a high portion of the transmitted energy does not return to the surface. The use of lower frequency antennas can sometimes overcome poor signal penetration, but lower frequency antennas will reduce resolution.

The presence of underground utilities, reinforced concrete slabs, buried waste, metallic fences, etc. can cause interference to the GPR signal when carrying out work in urban sites. The use of shielded antennas is recommended on such sites.

Data quality is optimal when the antenna is in direct coupling with the ground. Work in uneven terrain such as forest and bush can be difficult with common antennas. Data interpretation may also be limited. Understanding how different materials react to GPR signal and radargram interpretation can be difficult for someone not familiar with the technique. Recommended further reading includes texts by Ulriksen (1982), Bristow and Jol (2003), Yelf (2007), and Reynolds (2011).

#### **Recommended citation:**

Campos, D., 2012. Ground Penetrating Radar (GPR) Methods; *in* Shear Wave Velocity Measurement Guidelines for Canadian Seismic Site Characterization in Soil and Rock, (ed.) J.A. Hunter and H.L. Crow; Geological Survey of Canada, Open File 7078, p. 191-197.

## Data Collection

### Required Equipment

GPR equipment consists of a control unit and transmitter-receiver antennas. The control unit is a computer that operates the antennas and records the acquired data. It is normally powered by an internal battery or 12V external source. A graphic interface allows the user to set the desired acquisition parameters (antenna frequency, data range, sampling interval, gain functions, frequency filters, etc.) and view the data in real time. GPS loggers and electronic odometers are normally used for accurate data positioning. Figure 4.3-1 shows a basic GPR system.

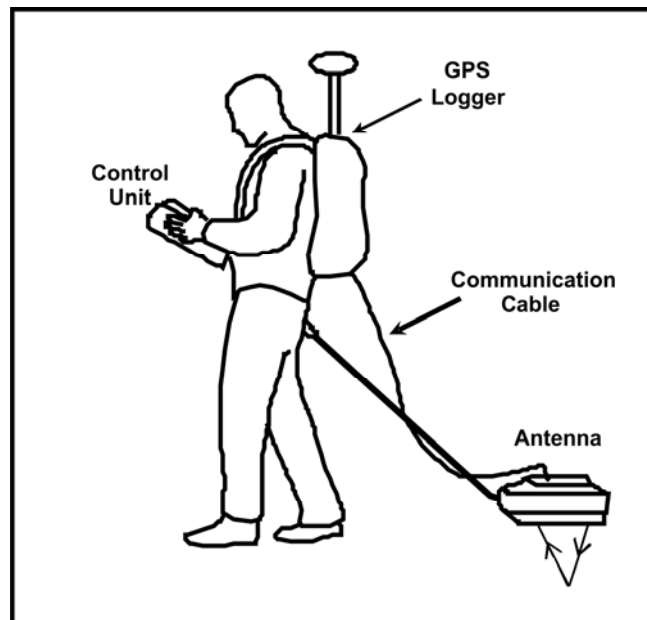


Figure 4.3-1. Basic GPR system.

The antennas are connected to the control unit through a communications cable. Depending on the type of survey being undertaken, one or several antennas of different frequencies can be used. GPR antennas are either monostatic (using the same antenna housing for the transmitter and receiver), or bistatic (antennas have separate transmitter and receiver housings). GPR antennas can be shielded to ensure that the transmitted radar energy is only emitted from the bottom of the antenna and to protect the receiver from external interference. Shielded antennas are mainly used for medium to high resolution surveys in urban applications. Commercially available GPR antennas have frequencies ranging from 12.5 MHz to 2.6 GHz.

### Data Collection Procedures

Survey planning is very important for GPR data acquisition. Prior to starting the field work, site conditions and expected geology should be known. The studied area should be surveyed along a grid of parallel and evenly spaced survey lines. Line spacing will be determined by the desired resolution and the size of the targets. The type, depth and orientation of the targets have to be specified in order to choose the right antenna and acquisition parameters. It is recommended that a series of trial reflection and CMP (common midpoint) surveys be undertaken upon arrival at a new site to optimize acquisition.

Data range should be set so the record length is sufficient to record only coherent data. The sampling interval (the distance between readings) will be determined by the size of the targets. For small targets to be detected, sampling intervals at close spacings are needed. For geological mapping, sampling at larger intervals is generally sufficient. Frequency filters should be set to isolate the antenna's main frequency. Finally, gain functions can be applied during data acquisition. It is important that the applied gain does not saturate the signal. Figure 4.3-2 shows two radargrams comparing good and poor acquisition parameters.

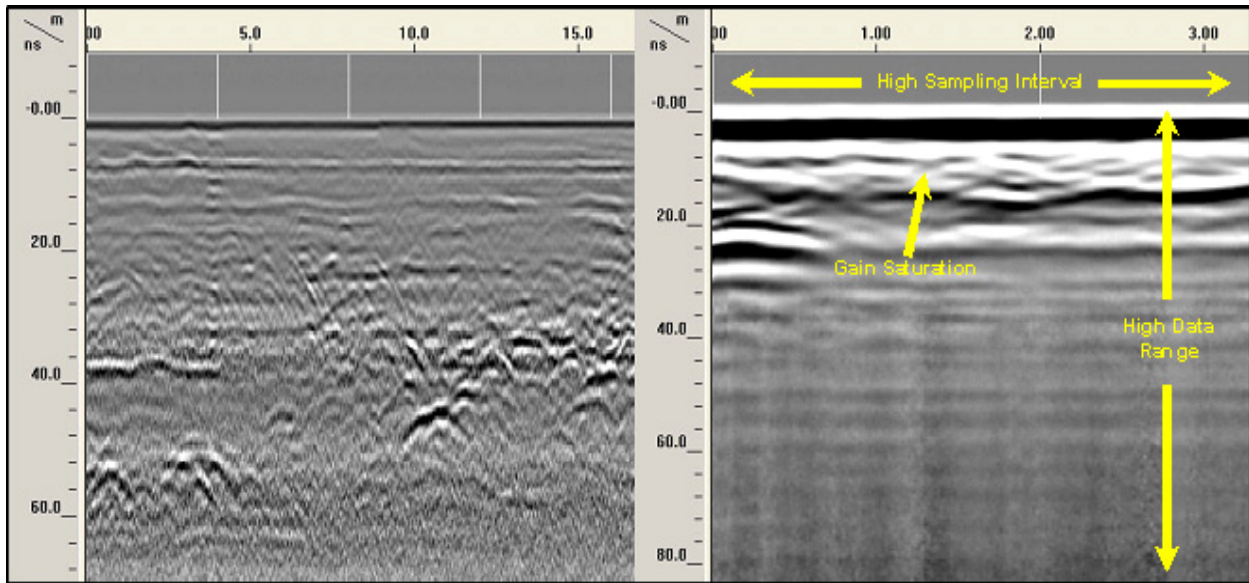


Figure 4.3-2. Radargrams showing correct (left) and poor (right) acquisition parameters.

When mapping depth to stratigraphic layers, the soil's electromagnetic (EM) velocity (m/ns) should be measured by performing a CMP survey. CMP acquisition requires bistatic antennas, as the distance between the antennas is increased stepwise around a fixed midpoint. Reflected waves in the CMP gather are used to determine EM velocity by manually fitting hyperbola to the reflected waves, a routine which is available in most GPR software packages.

## Processing Techniques

### Theory of Analysis

GPR data processing was mainly adapted from reflection seismology interpretation techniques. Specialized software allows the use of many post-processing functions in a user friendly format. The goal of GPR data processing is to obtain a clear radargram for graphic interpretation. Common processing functions include spatial corrections, trace stacking, background removal, bandpass filtering, deconvolution and migration. Figure 4.3-3 shows a typical GPR processing workflow.

Graphic interpretation allows for the identification of geological layers, buried objects, voids and other targets. Radargrams can easily be digitized in order to produce 2D profiles, contour maps and 3D surface slices. Quantitative analysis can also be performed on GPR data. EM velocity analysis of CMP data will allow for accurate velocity interpretation for each layer, thereby improving depth estimates. Yilmaz (2001) presents an in-depth view of velocity analysis for seismic reflection surveys. The techniques shown in this reference are very similar to the ones used in GPR software packages. GPR data can also be correlated with other data (such as hydrogeological, geochemistry, geophysical, etc.) in order to estimate soil properties (i.e. Gloaguen et al., 2001).

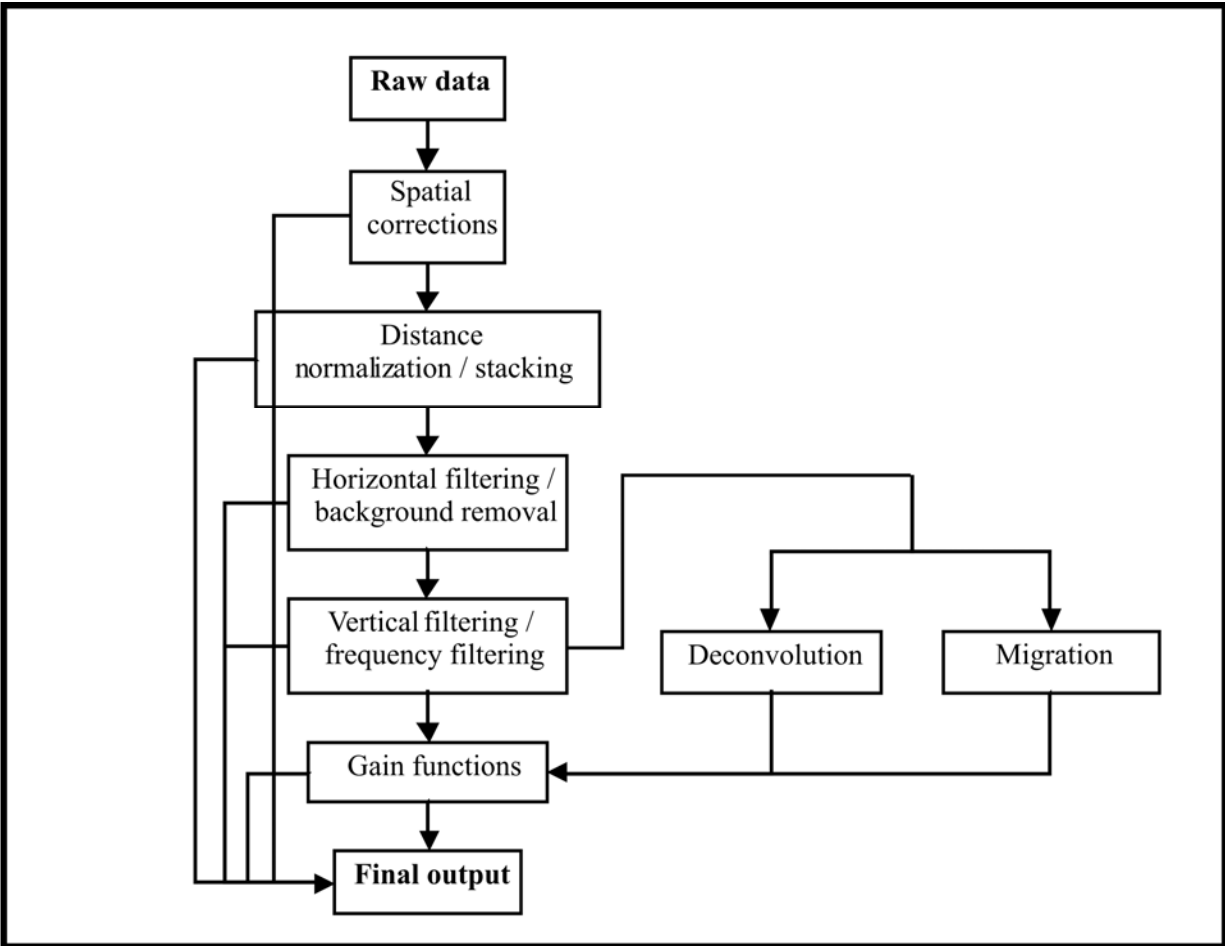


Figure 4.3-3. Basic GPR data processing workflow.

### **Uncertainty Assessment**

There are two main uncertainties resulting from GPR investigations: the depth and the nature of the target. Frequently, target depth is estimated by assuming a uniform dielectric constant for the investigated material. This can lead to significant errors, since the dielectric constant differs in space and between different layers. Velocity analysis of CMP data can increase the precision of depth estimations. One such example is presented in Figure 4.3-4. A CMP survey was carried out to estimate the EM velocity of three soil layers. Figure 4.3-4 shows the analysis window taken from GPR interpretation software. This allowed for the calculation of the velocity of each layer which was later used to calibrate the data for a full scale survey in the area.

### **Recommended Guidelines for Reporting**

Field equipment as well as acquisition parameters and description of the on site set-up should be specified in the report. Data quality and limitations of the interpretation should be discussed in the results. CMP survey gathers and EM velocity results should also be presented with calculations providing a measure of error for the depth estimates. Radargram examples are recommended and should be annotated since they can be difficult to understand for the untrained eye. Interpreted results should also be presented in a familiar layout such as anomaly maps, 2D profiles or 3D models.

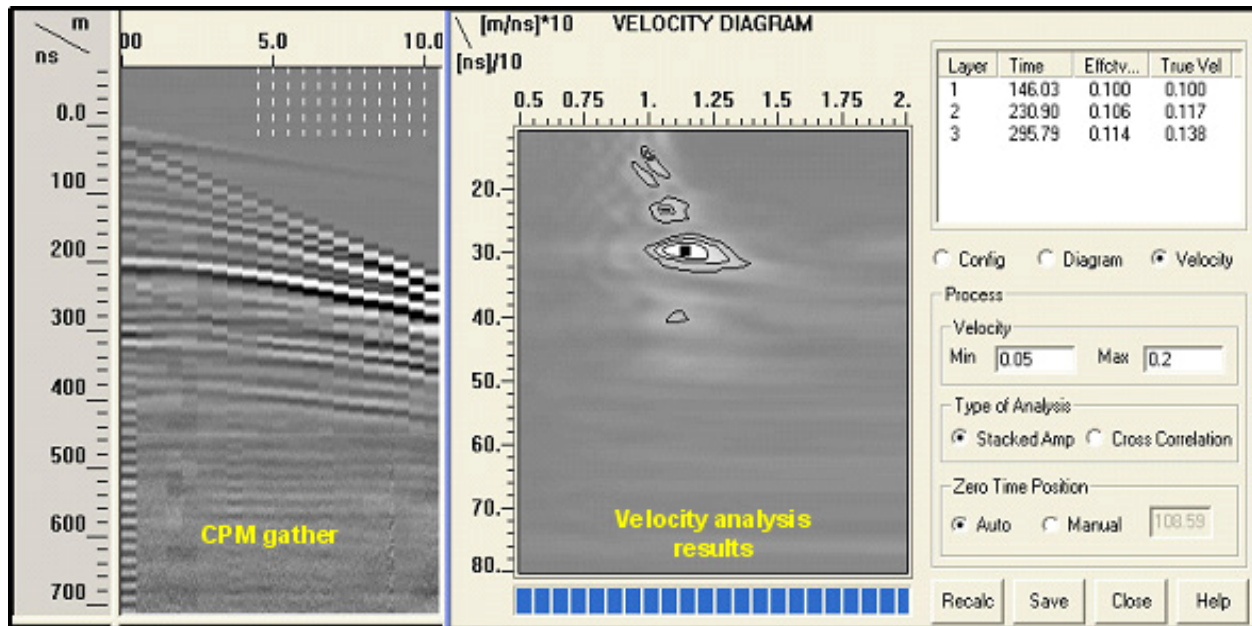


Figure 4.3-4. CMP gather and velocity analysis results

Due to the non-invasive nature of GPR, determining the composition of a target can also lead to interpretation errors. For example, voids and large boulders can easily be mistaken. GPR data interpretation should be performed by experienced geoscientists.

## Hazard-Related Case Studies

### Case 1: Bedrock mapping

GPR was used in Southern Quebec to locate bedrock surface for the design of a municipal sewer. Five kilometres of data along three roads were acquired in less than one day of fieldwork. Overburden material was silty sand, and underlying bedrock was believed to be located at a depth of 2 to 3 metres. A 270 MHz antenna was chosen to maximize resolution of the shallow overburden/bedrock interface.

An odometer wheel was used along the roadways, assuring a constant sampling interval of 20 scans/metre was achieved. Basic data processing (offset correction and background removal) was performed. Figure 4.3-5a shows a GPR profile along a 160 m section from this survey. A strong reflector corresponding to the bedrock was identified between depths of 2 to 4 metres, and different overburden layers, possibly dense till, were also identified within the section.

Complementary geophysical methods were also very important in this study. A seismic refraction survey was carried out between chainages 480 and 540 m (results not shown) and a calibration borehole was drilled to confirm the stratigraphic interpretations from the GPR profiles. In one section, a strong reflector at about 2 metres below the surface could have been interpreted as the bedrock, since borehole refusal was observed. However, seismic refraction data showed that this was due to a dense till layer and that the bedrock was located at greater depths.

These surveys revealed that the dense till layer was the interface formerly believed to be the bedrock surface. The actual bedrock interface was located generally above 4 metres beneath the surface.

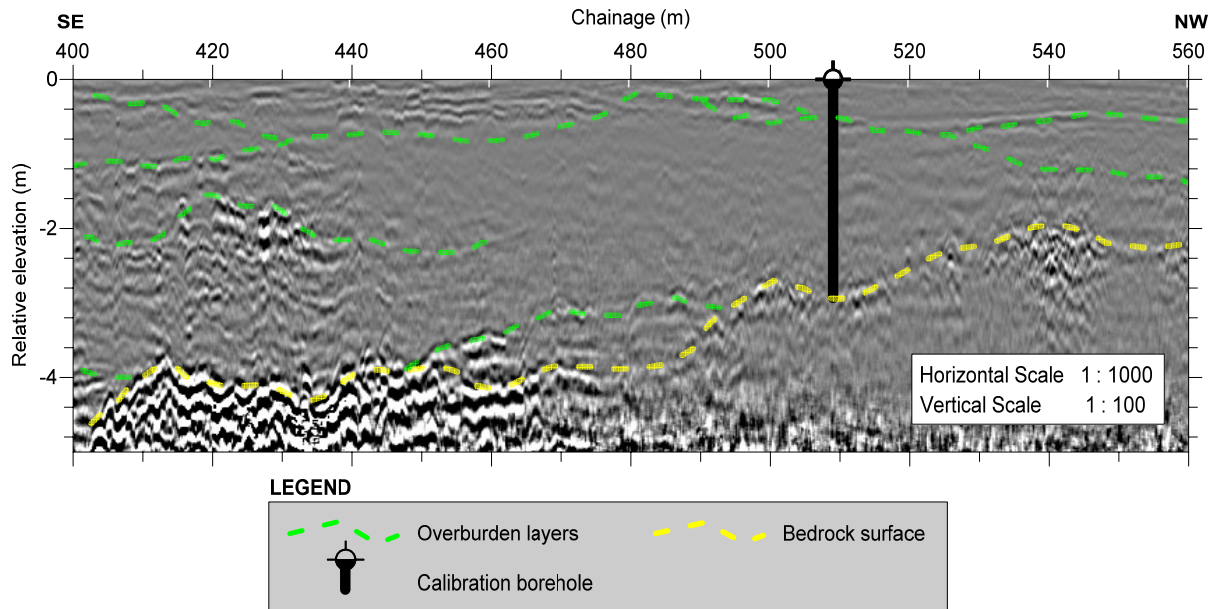


Figure 4.3-5. Radargram showing interpreted bedrock interface and intra-overburden layers.

Figure 4.3-6 shows a GPR profile used for bedrock mapping in another municipal sewer design project in the Laurentians region of Quebec. Here, a 400 MHz antenna was used with a sampling interval of 30 scans/metre. Basic data processing (offset correction and background removal) was performed. The technique allowed for the detection of intra-overburden layers and the bedrock surface along approximately 60% of the 3 line-km of survey profiles.

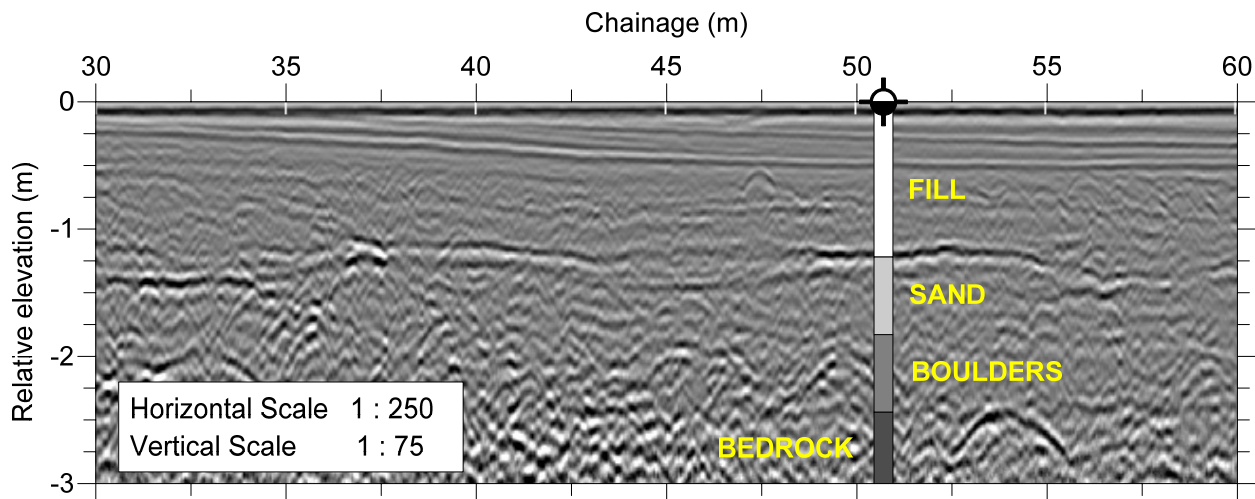


Figure 4.3-6. Radargram showing intra-overburden layers and borehole data.

### **Case 2: Stratigraphic modeling**

A high resolution 3D GPR survey was carried out at a site in central Quebec to study the site's stratigraphy for an environmental assessment project. An area of about 375 m<sup>2</sup> was surveyed along a grid with 1 metre line spacing at a sampling interval of 50 scans/metre. Regional geology suggested that various sand layers would be intercepted, so a 270 MHz antenna was selected to acquire the GPR data. Figure 4.3-7 shows the 3D model obtained with the GPR data. Basic data processing (offset correction and background removal) was performed. Signal penetration at this site was excellent and allowed for

detection of sand layers located at about 6 metres below the surface. Multiple reflectors were identified, showing a sub-horizontal stratigraphy with a slight dip to the north-east. Three layers showed stronger reflection interfaces, suggesting greater dielectric contrasts. This indicates changes in composition between the different layers. No borehole data was available to correlate with these results.

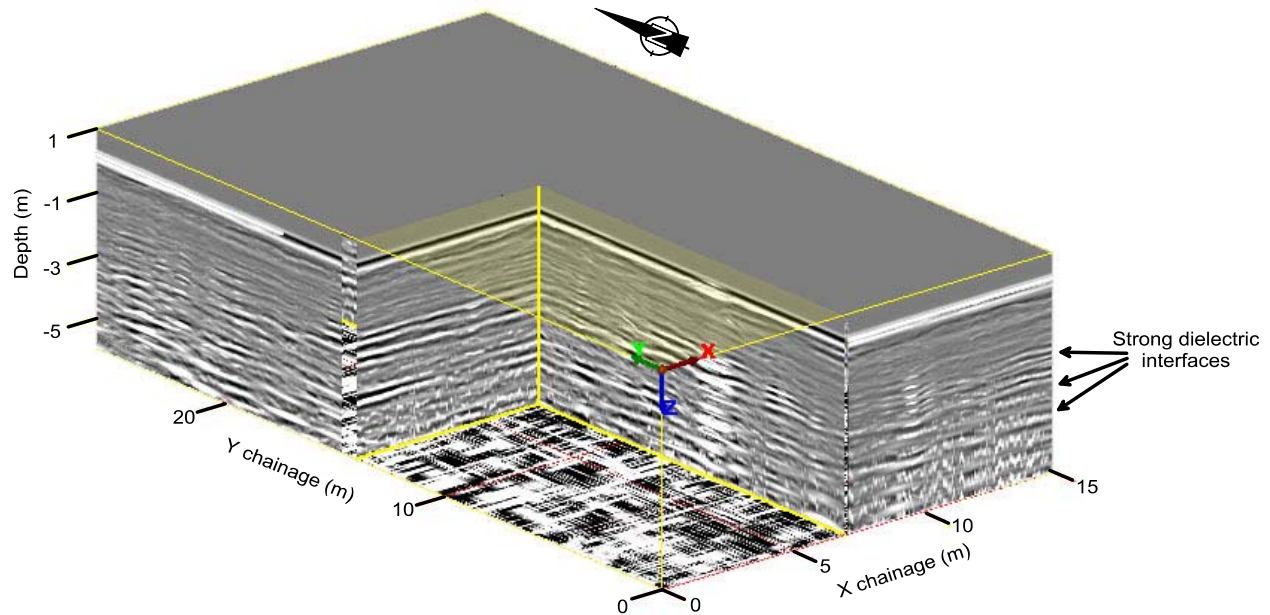


Figure 4.3-7. 3D model obtained with the GPR data for stratigraphic modeling

## References

ASTM D6432–11. Standard Guide for Using the Surface Ground Penetrating Radar Method for Subsurface Investigation, ASTM International, West Conshohocken, PA, 2011, DOI: 10.1520/D6432-11, [www.astm.org](http://www.astm.org).

Bristow, C.S. and Jol, H.M. (ed.), 2003. Ground Penetrating Radar in Sediments; Geological Society Special Publication 211, Geological Society Publishing House, Bath, UK, 330 p.

Gloaguen, E., Chouteau, M., Marcotte, D. and Chapuis, R., 2001. Estimation of hydraulic conductivity of an unconfined aquifer using cokriging of GPR and hydrogeological data; *Journal of Applied Geophysics*, v 47, p.135-152.

Reynolds, J.M., 2011. An Introduction to Applied and Environmental Geophysics; John Wiley and Sons, Inc., New York, 712 p. (second edition).

Ulriksen, C.P.F., 1982. Application of Impulse Radar to Civil Engineering; Geophysical Survey Systems Inc., North Salem, NH, 175 p.

Yelf, R.J., 2007. Application of Ground Penetrating Radar to Civil and Geotechnical Engineering; *Electromagnetic Phenomena*, v 7, p.103-116.

Yilmaz, O., 2001. Seismic Data Analysis – Processing, Inversion and Interpretation of Seismic Data; Volume 1, Investigations in Geophysics No.10; Society of Exploration Geophysics, Tulsa, OK, 1000 p.

## 4.4 Borehole Logging Techniques in Unconsolidated Sediments for Hazard Studies

Heather Crow & James Hunter  
Geological Survey of Canada, Ottawa, ON

### Introduction

#### Principles of the Method

In addition to downhole shear wave logging (see Chapter 3.2), complementary geophysical logs can provide additional information on soil properties which influence ground motion response. During logging, a borehole probe, or sonde, is lowered down a cased or open borehole using a motorized winch. Sensors in the tools sample a volume of soil up to several feet into the borehole wall. Within the context of this article, natural gamma, gamma-gamma density, and induction (conductivity and magnetic susceptibility) logs are discussed within PVC-cased overburden boreholes. When interpreted as a suite, these logs provide information on changes in lithology, relative grain size, density, and formation conductivity.

#### Current State of Engineering Practice

Logging tools have been developed for various hard rock, and later, overburden applications over the past 80 years. Many of the techniques used in logging practice today were developed for mining or environmental applications (Hearst et al., 1985; Killeen, 1986; Keys, 1990; Keys, 1997). However, it is also recognized that downhole geophysical techniques can provide important information for geotechnical soil investigations (Paillet and Saunders, 1990) provided that a careful drilling approach is used and a well grouted casing is installed. Several ASTM standards exist for the planning and collection of downhole logging data (D5753-05 (2010) for planning, D6274-98 for Gamma, and D6726-01(2007) for Electromagnetic Induction).

#### Limitations

Minimizing the width of the annulus (grouted region between borehole wall and PVC casing) is a consideration for natural gamma tools, as they have a smaller radius of investigation (~30 - 60 cm) than induction tools. This is particularly important for the gamma-gamma probe, as much of the backscattered signal comes from a distance of 10 - 15 cm into the borehole wall. In addition, the presence of cavities behind the casing reduces tool response, which can lead to misinterpretation of lithological conditions. The gamma tools can be run through a metal casing, but the count levels will be significantly attenuated, requiring a compensation correction. Also, certain bentonite grouts are high in potassium, giving false elevated natural gamma count levels at the depth of a bentonite seal. Ideally, grout type and seal locations should be known in advance if gamma logging is planned.

A PVC casing is necessary for induction logging, as the tools go off-scale in the presence of metal. Induction instruments induce magnetic fields over a large volume of soil, which limits their ability to detect thin variations in lithology. It is important to be aware that log response in unconsolidated materials typically tends to be relatively low, so tools, particularly the magnetic susceptibility tool, must be highly sensitive in the low end of the operating range.

Although downhole logs are used to measure/infer soil properties, they cannot entirely replace a geotechnical sampling program. Whenever possible, lab testing results and core logs should be displayed with the geophysical logs.

#### **Recommended citation:**

Crow, H.L. and Hunter, J.A., 2012. Borehole Logging Techniques in Unconsolidated Sediments for Hazard Studies; *in* Shear Wave Velocity Measurement Guidelines for Canadian Seismic Site Characterization in Soil and Rock, (ed.) J.A. Hunter and H.L. Crow; Geological Survey of Canada, Open File 7078, p. 198-205.

## Data Collection

### Required Equipment

Modern logging systems consist of a winch with several hundred metres of wireline, a logging console or digital interface, a series of interchangeable downhole probes, and a digital or optical encoder which records depth to the nearest 0.01 m. Systems are controlled with manufacturer's logging software on a portable field computer, and data is recorded digitally. Real-time log display on the computer screen allows for quality control during data collection. A portable power source, such as a generator or battery, is required and should be coupled with a sine wave inverter for optimal system performance.

Modern gamma-gamma tools are composed of dual sensors located at near and far points above a radioactive source positioned at the base of the tool. Operating a nuclear logging source of any activity level is heavily regulated by the Canadian Nuclear Safety Commission and requires a nuclear licence. Only a few downhole operators in Canada are licensed for active gamma logging for environmental/geotechnical applications.

### Data Collection Procedures

Prior to lowering any tool into a borehole, it is recommended to run a dummy probe in open and cased boreholes, unless a temperature tool must first be run in the undisturbed borehole fluid. Depth 'zeroing' of the tools at surface must be performed to ensure the readings reflect the position of the sensors. Induction tools require coil calibrations (or nulling) after the tool has been powered on in borehole fluid for 10 - 15 minutes to warm up the electronics. For these tools, logging speed should be in the range of 3 - 4 m/min – even with the new higher bandwidth logging systems. It is recommended that gamma tools be run at 1 - 2 m/min for highest resolution, as logging too quickly will have the effect of 'smearing' the results, and reducing the count levels.

Repeat logs (up and down hole) are recommended to look for drift in the recording, often caused by temperature sensitivity of the electronics, which is particularly important in soils where tool response is low. A depth check should always be performed at the end of the up run and compared to the start depth on the down run to look for discrepancies, and allow for corrections during processing. Refer to Douma (1999) for detailed logging guidelines.

## Processing Techniques

### Theory of Analysis

Once imported into a software processing package, logs should immediately be corrected for any depth shift errors noted at the time of collection. The logs can then be interpreted as a suite to compare tool response at different depths.

The natural gamma tool measures naturally occurring gamma radiation from radioactive isotopes of potassium, uranium, and thorium which occur in unconsolidated sediments. Variation in radiation levels are used to track changes in lithology. In overburden materials usually low in counts, the gamma log provides a qualitative estimate of changes in grain size: increasing in zones of finer grain size, and decreasing in zones of coarser grain size (see Figure 4.4-1). True 'chemical' clays with elevated potassium levels are relatively rare in Canada. The active gamma-gamma tool bombards the formation with gamma radiation from a radioactive source in the tool, and records the levels of backscattered energy in terms of counts. Counts are converted to density using calibrations performed with blocks of known density in the lab, and can also be corrected with tool-specific compensation curves determined at well log calibration facilities in Canada or the US. Density values are important for geotechnical investigations as they can be used to calculate the maximum shear modulus ( $G_{max}$ ) from shear wave velocities, and estimate relative variations in porosity.

Inductive conductivity logs provide lithologic information as unconsolidated materials (gravels, sands, silts, and clays) generally have different electrical properties. A transmitting coil in the tool produces an AC current of several tens of kHz and a receiving coil detects variation in voltage from eddy currents

induced in the formation by the transmitter current. The magnitude of the received current is proportional to the electrical conductivity of the formation. Fine grained materials tend to be more conductive than coarser grained materials. However, when conductive porewaters are present (saline, or contaminated), the tool responds primarily to the fluids. In the presence of highly conductive materials (>800 mS/m), a correction factor will need to be applied to the conductivity log to account for a deviation from linearity (Kaufman and Keller, 1983). In silt and clay soils of the St Lawrence Lowlands and Fraser Delta, lack of saline porewater in the formation can also be an indicator of geotechnically sensitive soils.

Magnetic susceptibility represents the degree to which materials can be magnetized in the presence of the earth's magnetic field. Typically, in unconsolidated sediments of very low susceptibilities, the response of the tool is governed by very small amounts of magnetite contained in the coarser grained materials (sands and gravels). Therefore, small differences are generally observed between fine grained sediments of very low susceptibilities, and coarser grained sediments where slightly higher susceptibility levels are recorded (McNeill et al., 1996). For very near surface hazard studies, this can be useful for detecting the presence of sand in finer grained materials, which may be prone to liquefaction behaviour.

### **Uncertainty Assessment**

For gamma tools (passive and active), the decay rate of radioactive elements follows a Poisson's distribution, where the standard deviation is equal to the square root of the counts recorded. If the tools are run too quickly, a reduced number of counts will be recorded, resulting in a relatively higher error range.

Performing tool calibrations prior to, and post, logging reduces uncertainty. Density calibration should be performed using specially designed blocks of known density, typically in the lab at project start up. Induction tool calibration should be performed at each site once the tool has been allowed to warm up for a short period of time (10-20 minutes depending on the tool), and preferably in the conditions of logging (e.g. in the borehole fluid). The induction tools are calibrated by nulling them (in air), and some tools can also be calibrated at the high end of the range using a coil capable of inducing a known conductivity response. Uncertainty can also be reduced by overlaying up and down runs to look for repeatability. The detection of temperature drift in the tools becomes more important when tools are operating in the low-end of their range.

### **Recommended Guidelines for Reporting**

Minimum reporting requirements must include survey date, details (and dates) of all tool calibrations such as those described above, repeat runs up/down hole, and any site particulars (casing stick up, piezometric water level in the borehole, condition of the well, ID tag, etc.). Drilling details, such as date, borehole and casing diameters, drilling method, and total drill depth should be included if known. The geophysical logs should be accompanied by a geological or drilling log and well completion details (grout type, seal depths, native backfill or filter sand, etc.). Any processing details and correction factors should also be described. Final corrected logs should be presented side-by-side in a suite with interpretation.

### **Hazard-Related Case Studies**

#### **Case 1: Leda Clay studies, Ottawa, ON.**

As part of the seismic hazard studies carried out by the Geological Survey of Canada (GSC) and Carleton University to create a seismic site class map of Ottawa, borehole studies were undertaken to better understand the varying properties of Holocene-aged clayey silts (locally known as "Leda Clays") deposited in the region by the Champlain Sea (Hunter et al., 2010).

Prior to drilling, a 3km-long high-resolution seismic landstreamer profile collected by the GSC (see Chapter 2.1.2) was key in selecting the location for a 96 m borehole near Kinburn, ON. The profile identified the bedrock surface, an overlying sand and gravel unit, and two primary sedimentary horizons within the Leda Clays: a highly stratified low-velocity layer (5 - 20 m below surface), overlying a stiffer ~70 m homogenous unit. The borehole was drilled through the Leda Clays, terminating in sandy soils just

above a gravel aquifer. Borehole logging identified the upper unit as having a shear wave velocity range of 90 - 150m/s, and a density ranging between 1.40 - 1.75 g/cm<sup>3</sup> (Figure 4.4-1). Core sample testing at 2-to-3 m intervals confirmed the presence of elevated porosity (n=0.5 - 0.8) which is reflected in the most elevated conductivities in the borehole (caused by saline porewater) and the lowest densities. This is also reflected in the reduced natural gamma count levels. In the lower 70 m of the borehole, the silty marine deposits are fairly homogenous, but sand begins to appear at 62 m depth as shown by increased response in the magnetic susceptibility tool. This trend continues downward and is coupled with decreasing gamma counts, reflecting increasing sand content, shown in the grain size logs. A detailed report on the geophysical logging and coring results can be found in Medioli et al. (2011).

Of note in the conductivity log is the decreasing levels of apparent conductivity coupled with an increase in sensitivity (ratio of undisturbed to remoulded shear strength), which is a feature of Champlain Sea soils which have been leached of their saline porewater, or deposited in sea water which has been intermixed with fresher glacial melt-water. In Champlain Sea boreholes of low conductivity, sensitivity is generally high and could be of concern for terrain stability in the event of strong ground shaking (Quigley, 1983; Aylsworth, 2000).

Magnetic susceptibility readings may prove useful in hazard studies for reasons beyond lithologic indicators. Presence of sand in fine grained soils in the near surface could be a concern for liquefaction potential, and can be used alongside earthquake liquefaction resistance estimates derived from the downhole shear wave velocity measurements (Hunter et al., 1998a, Goda et al., 2011). Density is also an important modeling parameter in the response of soil to ground motion. It is often assumed that these sediments have one density value of 1.65g/cm<sup>3</sup>, but in fact, this value can vary from ~1.4 g/cm<sup>3</sup> up to nearly ~1.8 g/cm<sup>3</sup> at depth. The difference between using an assumed density of 1.65 g/cm<sup>3</sup> vs. 1.4 g/cm<sup>3</sup> in the calculation of shear modulus leads to a 15% overestimation of  $G_{max}$ .

### **Case 2: Holocene soil studies, Fraser River delta, BC.**

During the 1980's and 90's, more than 40 boreholes were drilled in the Fraser Delta by the GSC to measure the geophysical and geotechnical properties of the delta materials, and study the Quaternary stratigraphy in the region (Holocene-aged silts and clays, Pleistocene-aged diamictos). Natural gamma, inductive conductivity, and magnetic susceptibility logs were collected alongside compressional and shear wave logs, and interpreted to provide information on porewater salinity, ferromagnetic mineral content, and presence of gas charged sediments (Hunter et al., 1998a, Hunter et al., 1998b). Surface reflection and refraction surveys were also a large component of the study (Pullan et al. 1998).

The gamma and electrical logs provided complimentary information to the shear wave logs for earthquake hazard estimation parameters. As shown in Figure 4.4-2, the magnetic susceptibility and natural gamma logs were key in delineating the Holocene-Pleistocene boundary, which is the first major acoustic impedance layer in the seismic logs. A simple fundamental site period calculation (see Chapter 2.3) using this depth and the average shear wave velocity down to this boundary would predict the frequency (or period) at which resonance amplification would be greatest.

As in the Ottawa case, information on the variation of porewater salinity was obtained from apparent conductivity logs. If negative conductivity gradients are the result of post-depositional leaching of saline porewater by fresher groundwater, the soils may become geotechnically sensitive, resulting in potential instability under cyclic or increased static stresses.

# Geotechnical Logs (based on lab samples)

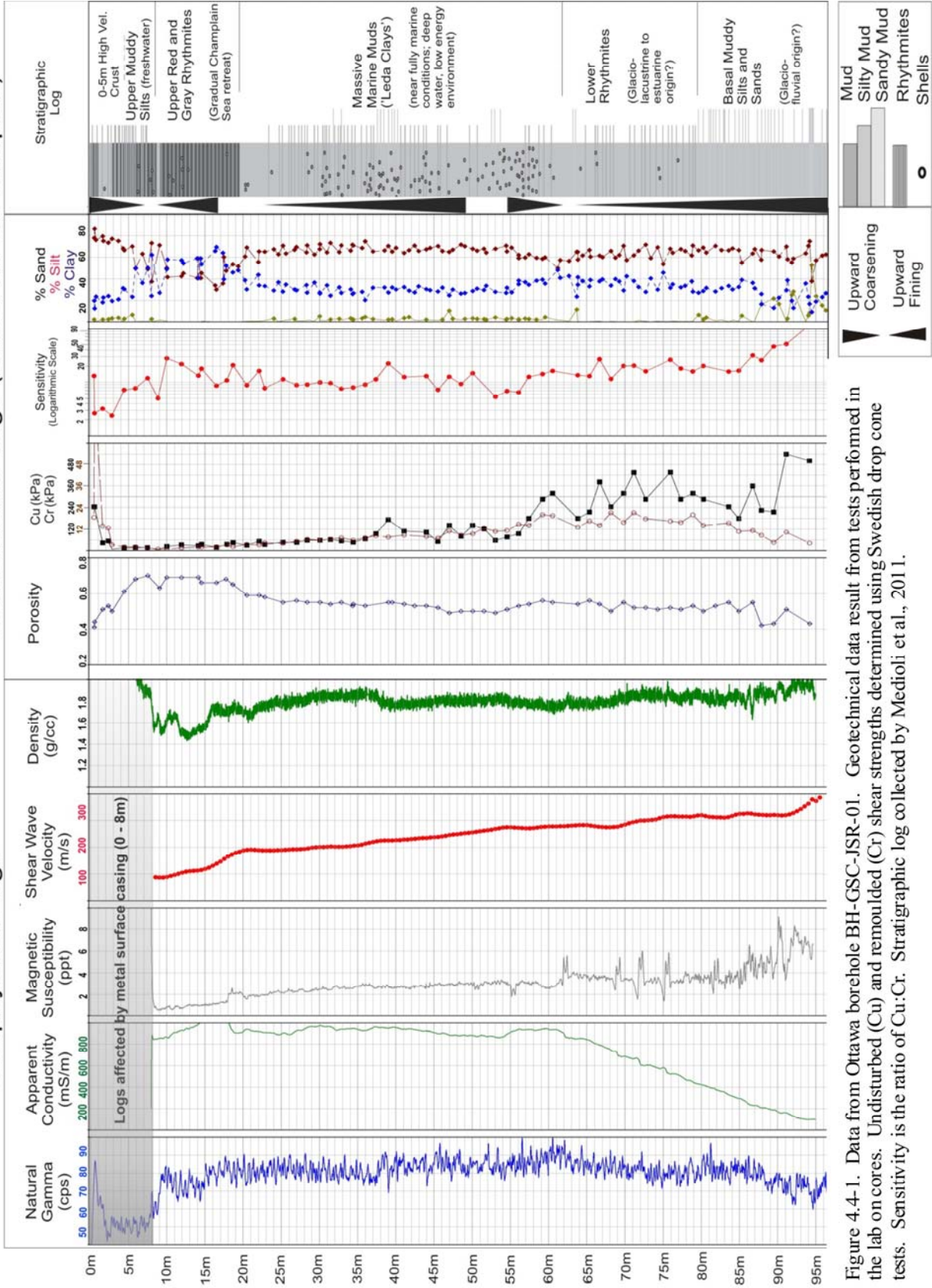


Figure 4.4-1. Data from Ottawa borehole BH-GSC-JSR-01. Geotechnical data result from tests performed in the lab on cores. Undisturbed (Cu) and remoulded (Cr) shear strengths determined using Swedish drop cone tests. Sensitivity is the ratio of Cu:Cr. Stratigraphic log collected by Medtoli et al., 2011.

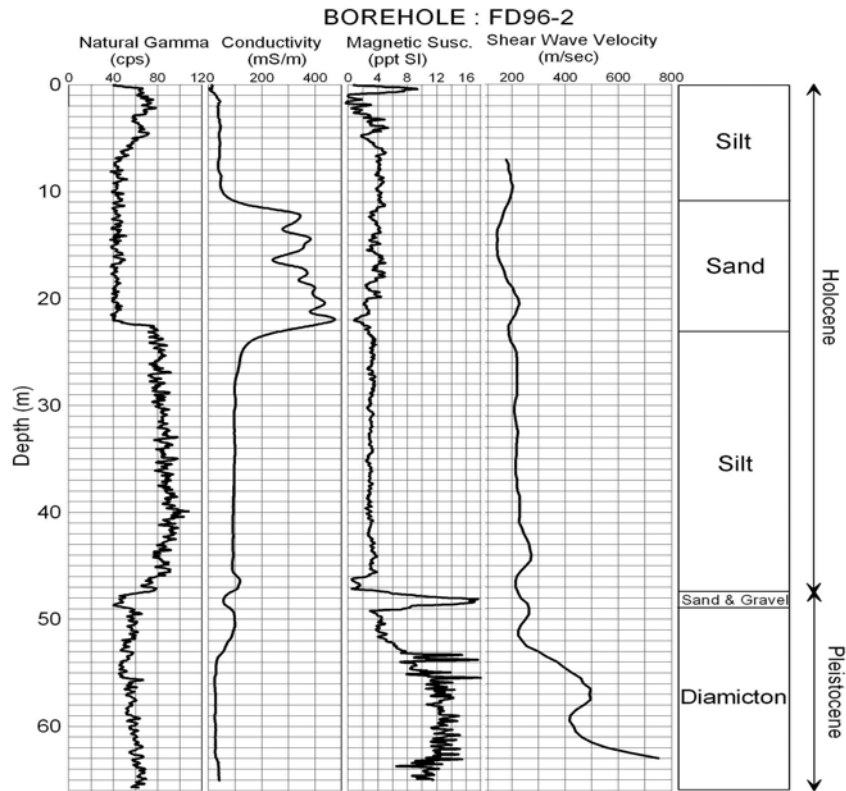


Figure 4.4-2. Two sample logs from the Fraser delta showing the complementary lithological data collected using the natural gamma, apparent conductivity, and magnetic susceptibility probes. Shear wave data is also shown, along with basic geological data.

## Acknowledgements

The authors would like to acknowledge funding support for the Ottawa work from Natural Resources Canada's Eastern Canada Geohazards Assessment Project and NSERC funding through Carleton University, part of the Canadian Seismic Research Network (CSRN).

The Fraser delta work was supported by numerous government, university, and industry partners including the Pacific and Northern GSC divisions, the BC Geological Survey, the Municipality of Delta, the Corporation of Richmond, the University of British Columbia, Simon Fraser University, the University of Wisconsin, Conetec Investigations Ltd., Golder Associates Ltd., and Sonic Drilling Ltd..

## References

ASTM D5753-05 (2010). Standard Guide for Planning and Conducting Borehole Geophysical Logging, ASTM International, West Conshohocken, PA, DOI: 10.1520/D5753-05R10, [www.astm.org](http://www.astm.org).

ASTM D6274-10. Standard Guide for Conducting Borehole Geophysical Logging - Gamma, ASTM International, West Conshohocken, PA, DOI: 10.1520/D6274-10, [www.astm.org](http://www.astm.org).

ASTM D6726-01 (2007). Standard Guide for Conducting Borehole Geophysical Logging-Electromagnetic Induction, ASTM International, West Conshohocken, PA, DOI: 10.1520/D6726-01R07, [www.astm.org](http://www.astm.org).

Aylsworth, J.M., Lawrence, D.E. and Guertin, J., 2000. Did two massive earthquakes in the Holocene induce widespread landsliding and near-surface deformation in part of the Ottawa Valley, Canada? *Geology*, v.28, p. 903-906.

Douma, M., Hunter, J.A., and Good, R.L., 1999. Borehole geophysical logging; *in* A handbook of geophysical techniques for geomorphic and environmental research, (ed.) R. Gilbert; Geological Survey of Canada, Open File 3731, p. 57-68.

Goda, K., Atkinson, G.M., Hunter, J.A., Crow H.L., and Motazedian, D., 2011. Probabilistic Liquefaction Hazard Analysis for Four Canadian Cities; *Bulletin of the Seismological Society of Canada*, v. 101, p.190-201.

Hearst, J.R., Nelson, P.H. and Paillett, F.L., 2000. *Well Logging for Physical Properties*; John Wiley & Sons, New York, 483p. (second edition).

Hunter, J.A., Douma, M., Burns, R.A., Good, R.L., Pullan, S.E., Harris, J.B., Luternauer, J.L., and Best, M.E., 1998a. Testing and application of near-surface geophysical techniques for earthquake hazards studies, Fraser River delta, British Columbia; *in* *Geology and the natural hazards of the Fraser River Delta, British Columbia*, (eds.) J.J. Clague, J.L. Luternauer, and D.C. Mosher; Geological Survey of Canada, Bulletin 525, p. 123-145.

Hunter, J.A., Burns, R.A., Good, R.L. and Pelletier, C.F., 1998b. A compilation of shear wave velocities and borehole geophysics logs in unconsolidated sediments of the Fraser River Delta, British Columbia; Geological Survey of Canada, Open File 3622, 1 CD-ROM.

[ftp://ftp2.cits.mcan.gc.ca/pub/geott/ess\\_pubs/209/209974/of\\_3622.zip](ftp://ftp2.cits.mcan.gc.ca/pub/geott/ess_pubs/209/209974/of_3622.zip) [accessed: Jan 2012]

Hunter, J.A., Crow, H.L., Brooks, G.R., Pyne, M., Motazedian, D., Lamontagne, M., Pugin, A. J.-M., Pullan, S.E., Cartwright, T., Douma, M., Burns, R.A., Good, R.L., Kaheshi-Banab, K., Caron, R., Kolaj, M., Folahan, I., Dixon, L., Dion, K., Duxbury, A., Landriault, A., Ter-Emmanuil, V., Jones, A., Plastow, G., and Muir, D., 2010. Seismic Site Classification and Site Period Mapping in the Ottawa Area Using Geophysical Methods; Geological Survey of Canada, Open File 6273, 1 DVD. [ftp://ftp2.cits.mcan.gc.ca/pub/geott/ess\\_pubs/286/286323/of\\_6273.zip](ftp://ftp2.cits.mcan.gc.ca/pub/geott/ess_pubs/286/286323/of_6273.zip) [accessed: Jan 2012]

Kaufman, A.A. and Keller, G.V., 1983. Frequency and Transient Soundings; Elsevier Publishing Co., Amsterdam, 685 p.

Keys, W.S., 1990. Chapter E2, Borehole Geophysics Applied to Ground-Water Investigations, in Techniques of Water-Resource Investigation, USGS <http://pubs.usgs.gov/twri/twri2-e2/> [accessed February 2012]

Keys, W.S., 1997. A practical guide to borehole geophysics in environmental investigations; CRC Press Inc., Boca Raton, FL., 176 p.

Killeen, P G. (ed.), 1986. Borehole geophysics for mining and geotechnical applications; Geological Survey of Canada, Paper 85-27, 400p.

McNeill, J.D., Hunter, J.A. and Bosnar, M., 1996. Application of a Borehole Induction Magnetic Susceptibility Logger to Shallow Lithological Mapping; Journal of Environmental and Engineering Geophysics, v.0, p. 77-90.

Medioli, B.E., Alpay, S. Crow, H.L., Cummings, D.I., Hinton, M.J., Knight, R.D., Logan, C., Pugin, A.J.-M., Russell, H.A.J. and Sharpe, D.R., 2011. Integrated data sets from a buried valley borehole, Champlain Sea basin, Kinburn, Ontario; Geological Survey of Canada, Current Research (Online) no. 2012-3, 20p. <[ftp://ftp2.cits.mcan.gc.ca/pub/geott/ess\\_pubs/289/289597/cr\\_2012\\_03\\_gsc.pdf](ftp://ftp2.cits.mcan.gc.ca/pub/geott/ess_pubs/289/289597/cr_2012_03_gsc.pdf)> [accessed Jul 2012]

Paillet, F.L. and Saunders, W.R. (ed.), 1990. Geophysical Applications for Geotechnical Investigations; ASTM Committee D-18 on Soil and Rock, ASTM International, 112 p.

Pullan, S.E., Hunter, J.A., Jol, H.M., Roberts, M.C., Burns, R.A. and Harris, J B., 1998. Seismostratigraphic investigations of the southern Fraser River delta; *in* Geology and the natural hazards of the Fraser River Delta, British Columbia; (ed.) J.J. Clague, J.L. Luternauer, and D.C. Mosher; Geological Survey of Canada, Bulletin 525, p. 91-122.

Quigley, R.M., Gwyn, Q.H.J., White, Q.L., Rowe, R.K., Haynes, J.E. and Bohdanowicz, A., 1983. Leda Clay from deep boreholes at Hawesbury, Ontario. Part I: Geology and Geotechnique; Canadian Geotechnical Journal, v. 20, p. 288-298.

## 4.5 Microgravity Technique for Hazard Studies

Stephane Sol & Jeff Fleming  
Golder Associates Ltd., Mississauga, Ontario

### Introduction

#### **Principles of the Method**

Microgravity is a geophysical method commonly used to infer subsurface density variations by measuring changes in the Earth's gravitational field. The method is based on the principles of Newton's law of gravitation that states that the gravitational force between two objects is proportional to the product of their masses and inversely proportional to the square of the distance between them (Telford et al., 1995). Similar to regional-scale gravity surveys, microgravity surveys, as indicated by its prefix micro, measure extremely small variations of the Earth's gravitational field. The standard unit for the acceleration of gravity is the Gal. The technique uses highly sensitive instruments called gravimeters capable of measuring variations of the Earth's gravitational field at the  $\mu\text{Gal}$  level. The very precise measurements of microgravity combined with a number of applied corrections allow for the detection of small voids, variations in depth to bedrock, buried valleys, and lateral changes in soil or rock density across a survey site.

#### **Current State of Engineering Practice**

The microgravity method is increasingly being applied for detection of near surface anomalies common in geotechnical, engineering, and archaeological investigations (Panisova and Pasteka, 2009). ASTM Standard D6430-99 (2010) describes the methodology for performing detailed microgravity surveys. This ASTM Standard includes a description of applicable corrections that are required to be applied to data.

#### **Limitations**

Microgravity relies on the assumption that target features have a sufficient density contrast with the overlying or surrounding materials to be detected. Data acquisition of microgravity is slow compared to other conventional geophysical techniques, such as electrical resistivity and seismic methods, and requires a considerable number of processing steps to reduce the collected data. The method is relatively sensitive to local sources of noise such as vibrations (e.g. traffic), wind, and even distant earthquakes. Very accurate elevation data is required at each reading location, as errors in measured topography can introduce errors in the range of  $\pm 3 \mu\text{Gal}$  per centimetre of elevation error. Similar error can be introduced due to variations in topography across a survey site between survey stations. Therefore, accurate elevation data is required for the local area within, and adjacent to, the survey site. Solutions to microgravity modelling and inversion are non-unique and often intrusive investigations are required to obtain a priori information and to confirm microgravity modelled results.

### Data Collection

#### **Required Equipment**

Microgravity surveys are carried out using high precision gravimeters that should detect  $\mu\text{Gal}$  changes in the gravitational field. New modern gravimeters should be repeatable to a few  $\mu\text{Gals}$ . Kaufmann and Doll (1998) describe suitable gravimeters for microgravity surveys.

#### **Recommended citation:**

Sol, S. and Fleming, J., 2012. Microgravity Technique for Hazard Studies; *in* Shear Wave Velocity Measurement Guidelines for Canadian Seismic Site Characterization in Soil and Rock, (ed.) J.A. Hunter and H.L. Crow; Geological Survey of Canada, Open File 7078, p. 206-210.

### **Data Collection Procedures**

A gravimeter should be warmed up for a few days to allow the internal system to stabilize before starting field measurements and should always be handled with care.

Gravity measurements are acquired at discrete points (stations) along profiles or grids with station spacing chosen as a function of the target size. Gravimeters must be properly deployed and levelled with care prior to taking measurements. Figure 4.5-1 shows an example of readings being performed during a typical microgravity survey. An accurate height between the ground surface and the gravimeter must be also recorded. Base stations must be established and reoccupied periodically throughout the day to account for instrument and tidal drift. At each station, the elevation and the positioning should be accurately surveyed to sub-centimetre accuracy to correct for elevation effects on the microgravity readings.



Figure 4.5-1. Typical microgravity station. The gravity meter, in the foreground, is levelled on a base before readings are taken. Each station location was marked, in this case, using a metal nail so that stations could be reoccupied to measure instrument drift and repeatability.

## **Processing Techniques**

### **Theory of Analysis**

Upon completion of data collection, several corrections must be applied to the raw microgravity data to take into account instrument drift, and external gravitational effects such as tides, elevation changes, variations in latitude, and topography. Instrumental drift is caused by changes in the internal spring and is accounted for by frequent reoccupation of the base station, and in some cases is automatically corrected by the gravity meter to minimize this drift. The effects of tides are corrected using existing tide tables by entering the date and time of the measurement. This is done automatically by the gravity meter at the time of the measurement in some cases. Elevation corrections are applied to the data and all the measurements are reduced to a common datum and the effects of mass between the datum and the gravity station are removed. Latitude corrections are applied to account for the centrifugal acceleration due to the spinning of the Earth and the equatorial bulge. The last step, known as terrain corrections, is to correct for topography variations around the gravity station. After all these corrections have been applied, the resulting values are known as Bouguer gravity and can be directly related to lateral variations in the subsurface density. The main interest in microgravity is to isolate local shallow features and therefore a fraction of the gravity anomalies that are caused by deep regional features should be removed from the

data by filtering a linear trend from the data. Proper interpretation of observed gravity anomalies often requires the use of 2D or 3D modelling to get a better control on the density contrast as well as the size and depth of the anomalies. The interpretation of the data should be based on the knowledge of the local geology and on existing relevant data, such as boreholes.

### **Uncertainty Assessment**

There are various sources of uncertainty and error that can be introduced during both the data collection and the processing stages of a microgravity survey. In the field the largest uncertainty is generated by the repeatability of the gravity measurements. Outside of the corrections to the data that are carried out during testing or in the processing stages (such as instrument drift and tidal drift, which are discussed below), errors in the measurements of the Earth's gravitational acceleration could be the result of various factors such as inaccurate leveling of the instrument, instrument vibration due to traffic, microseismic activity such as earthquakes, or other forms of external vibration. The best way to assess and reduce these errors is to make multiple readings at a single station to determine if the standard deviation is acceptable for the accuracy needed for the particular survey. Most microgravity meters do this as part of their testing, and provide these statistics so they can be assessed while surveying.

During the processing stage, the application of corrections (instrument drift, latitude, tidal, elevation, and terrain) to the dataset presents the largest potential source of error. Highly accurate control of elevation and position of the gravity meter at each test location is also required. To minimize errors associated with drift and tidal corrections, base station reoccupation time intervals should be optimized. Sources of uncertainty are also associated with the formulaic determination of the terrain corrections. Local and regional topographic information is also required to generate the terrain correction factor for each measurement location. The required accuracy of the regional and local terrain elevations can be minimized by choosing survey locations in relatively flat areas, although this is often not possible.

### **Recommended Guidelines for Reporting**

The report should describe the data acquisition, processing techniques, discussion of the results and recommendations. The quality control processes should clearly be documented and methods of data reduction clearly discussed. It should include a table presenting the raw data and the processed data at each station, base map indicating the site features, colour contour maps of the data overlaid on a basemap or profile lines (depending on the station setup), interpretation showing the site plan, and depth estimates for anomaly sources.

### **Hazard-Related Case Studies**

#### **Case 1: Paleochannel identification, Eastern Canada**

A microgravity survey was carried out by Golder Associates at a site in eastern Canada to support the installation of a new sewer trunk line in an urban setting. The area of installation was adjacent to a large river, and the presence of a paleochannel had been identified based on borehole drilling at an adjacent site. The paleochannel posed a risk to the tunnel boring machine if encountered along the proposed sewer trunk line. A microgravity survey was undertaken using a Scintrex CG-5 to aid in identifying the location and delineating depth of the paleochannel. The microgravity results indicated the location and extents of the paleochannel (Figure 4.5-2) which were confirmed through correlation with available borehole information from an adjacent property.

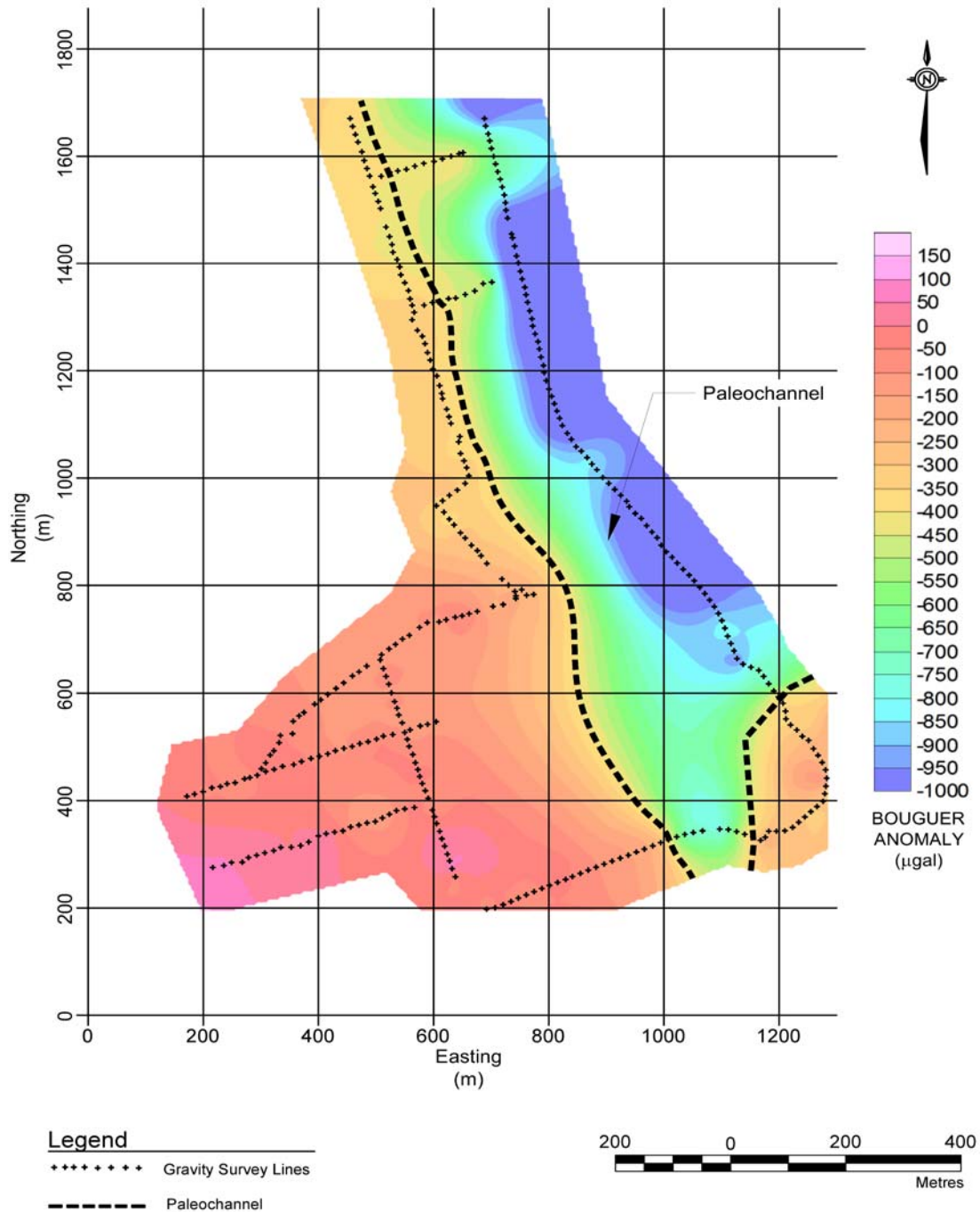


Figure 4.5-2. Interpreted paleochannel location based on microgravity survey.

**Case 2: Karstic terrain, Ireland**

A microgravity survey was carried out by Golder Associates at a site in Ireland well known for karst physiography. The objective of the survey was to delineate anomalies indicative of sinkholes as part of a landfill siting investigation. Drilling in the area had confirmed the presence of several sinkholes in the underlying dolomitic limestone. As there was typically no surface expression of these sinkholes (i.e. depressions in the ground surface), the location and extent of these karst features was unknown.

The microgravity results are shown as a contoured residual Bouguer anomaly map in units of microgals. The survey identified a large gravity low (shown in dark blue) indicative of a local deficiency in mass with respect to the surrounding geology (Figure 4.5-3). Drilling indicated that the bedrock in the area was typically found to be less than 30 metres below ground surface. The drill hole advanced in the centre of the microgravity low was abandoned at 90 metres, having never encountered bedrock, and confirming the presence of a sinkhole at that location.

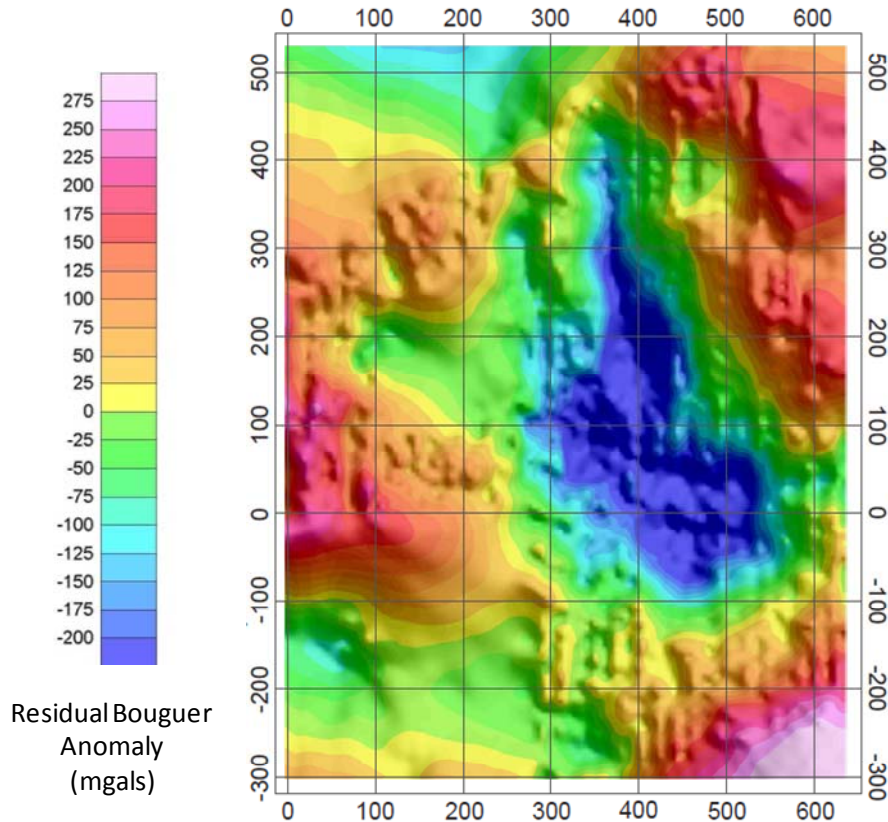


Figure 4.5-3. Microgravity residual Bouguer anomaly map identifying the location and extents of a sinkhole feature (dark blue area) in karstic limestone.

## References

ASTM D6430-99 (2010). Standard Guide for Using the Gravity Method for Subsurface Investigation, ASTM International, West Conshohocken, PA., DOI: 10.1520/D6430-99R10, [www.astm.org](http://www.astm.org).

Kaufmann, R.D. and Doll, W.E., 1998. Gravity Meter Comparison and Circular Error; Journal of Environmental and Engineering Geophysics, v. 2, p. 165-171.

Panisova, J. and Pasteka, R., 2009. The use of microgravity technique in archaeology: A case study from the St. Nicolas Church in Pukanec, Slovakia; Contributions to Geophysics and Geodesy, v. 39, p. 237-254.

Telford, W.M., Geldart, L.P. and Sheriff, R.E., 1995. Applied Geophysics, 2<sup>nd</sup> Ed; Cambridge University Press, New York, 770p.

# Chapter 5.0 Shear Wave Guidelines for Non-technical Users

Heather Crow & Jim Hunter,  
Geological Survey of Canada, Ottawa, ON

This chapter is directed towards non-technical professionals who may be required to review seismic site classification reports for municipal applications or engineering studies. It provides a brief review of seismic waves, the use of average shear wave velocity to 30 m depth ( $V_{s30}$ ) to account for site effects during earthquake shaking, and a summary of methods that can be used to measure  $V_{s30}$ . It also offers some guidance on the various types of information that may be contained, or asked for, in a contractor's technical report.

## 5.1 Seismic Waves

When an earthquake occurs deep within the earth, seismic (or sound) energy travels as waves in all directions, eventually reaching, and travelling along, the earth's surface. These waves fall into two broad categories: body waves, and surface waves. Body waves are like the motions of a slinky spring toy, while surface waves are like ripples on a pond. All waves attenuate with distance, and also change form and speed as they pass from one geological material to another.

Body wave motion in rocks and soils can be described by two main types: compressional (or primary, P), and shear (or secondary, S). They are called body waves because they travel within the body of the material, and their velocity varies with changes in soil and rock stiffness. Because geological materials are stiffest during compression, P-waves travel most quickly, with particle motion in the direction of the wave propagation. S-waves, which arrive later in time, have a particle motion which is perpendicular to the direction of wave propagation, exerting a shearing force on the ground. It is for this reason that large earthquake-generated S-waves are of concern to structural engineers, as they impart a lateral load to structures at, or below, the ground surface.

Another type of wave discussed within these Guidelines is the "surface" wave, where propagation is restricted to the near surface of a medium. Surface waves consist of Rayleigh waves, in which ground motion is both perpendicular and parallel to their wave front and direction of travel, and Love waves, for which ground motion is predominantly polarized in the horizontal plane. Rayleigh waves (also often referred to as ground roll) are important in this discussion as they can be used to indirectly estimate shear wave velocity.

## 5.2 Shear Waves and Ground Amplification

Shear waves travel faster in firmer materials (e.g. rock and glacial till soil) than in softer sediments (e.g. clay, silt and loose sands). As an earthquake-generated S-wave approaches the surface, it slows down as it passes from the harder, deeply buried, bedrock into softer bedrock and eventually into the surface soils. As the wave slows, its wavelength shortens, leading to an increase in the amplitude of the wave.

### Recommended citation:

Crow, H.L. and Hunter, J.A., 2012. Chapter 5.0: Shear Wave Guidelines for Non-technical Users; *in* Shear Wave Velocity Measurement Guidelines for Canadian Seismic Site Characterization in Soil and Rock, (ed.) J.A. Hunter and H.L. Crow; Geological Survey of Canada, Open File 7078, p. 211-223.

It has long been known by researchers in the field of earthquake engineering and seismology that the types of materials in the near surface affect how we experience earthquake shaking at ground level, often called 'site effects'. In very general terms, soft soils tend to amplify ground shaking, compared to the same earthquake shaking experienced on a bedrock site. There are some exceptions to this rule of thumb, such as when soft soils are shaken so intensely that they begin to act as dampers, reducing the level of shaking in some frequency ranges. Other phenomena that we can't see at the surface can also influence ground motion. For example, a bedrock valley infilled with softer materials can focus energy unevenly at the ground surface or cause basin edge effects. More detail on these effects can be found in Chapter 1, Section 1.3. The true nature of soil amplification can be quite complicated and is currently the subject of ongoing research worldwide.

One way the 2010 National Building Code of Canada (NBCC) accounts for site effects is through the average traveltime-weighted shear wave velocity in the top 30m of the ground ( $V_{s30}$ ). Based on a site's  $V_{s30}$  value, it assigns relative shaking levels at different seismic frequencies. These site provisions follow the system developed by NEHRP (National Earthquake Hazard Reduction Program) in the 1990s for building codes in the United States.

### 5.3 What is $V_{s30}$ ?

$V_{s30}$  is the measurement of the *average* shear wave velocity of the near surface materials down to a depth of 30m. This could be entirely bedrock, entirely soil, or any combination of these materials. The term  $V_{s30}$  must be further clarified as being a 'traveltime-weighted' average shear wave velocity, which is different from the "thickness-weighted" average shear wave velocity. A  $V_{s30}$  average velocity can be calculated by dividing 30 m by the total travel time of a shear wave from surface down to 30 m depth. .

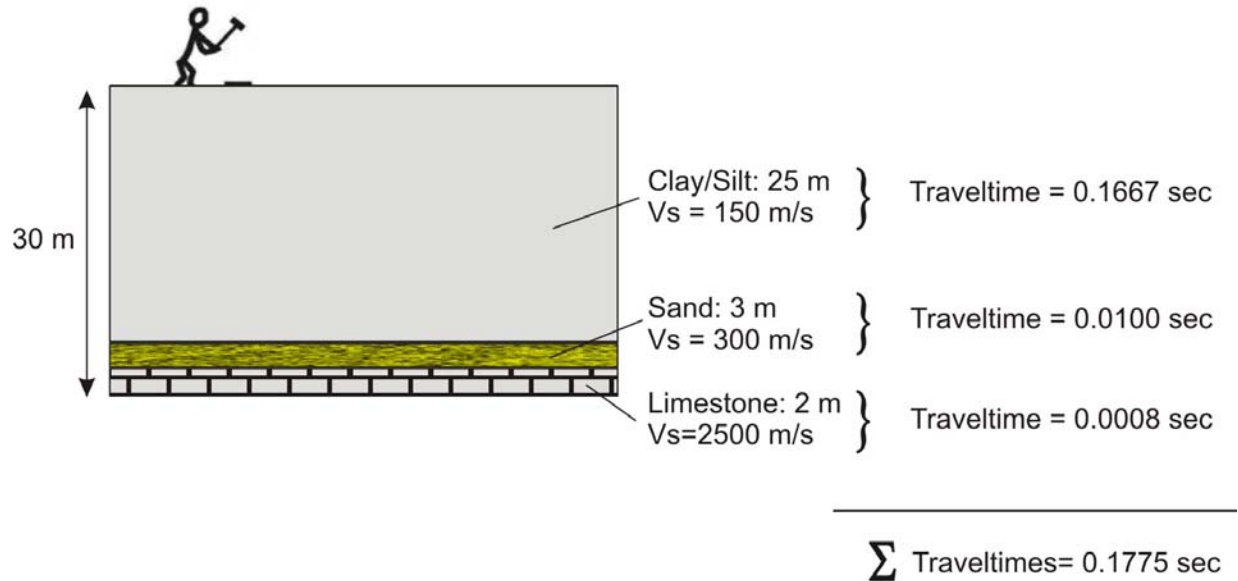
Commentary J in the Structural Commentaries of the NBCC (NRC, 2006) provides the formula:

$$V_{s30} = \frac{\text{total thickness of all layers (30 m)}}{\sum \left( \frac{\text{layer thickness}}{\text{layer shear wave velocity}} \right)}$$

which is equivalent to

$$V_{s30} = \frac{\text{total thickness of all layers (30 m)}}{\sum (\text{layer traveltimes})}$$

Hence, this measurement is referred to as a 'traveltime-weighted' average shear wave velocity since it is calculated based on the sum of the traveltimes through the all layers in the top 30m of the ground. Figure 5-1 illustrates this concept.



$$V_{s30} = \frac{\text{total thickness of all layers (30 m)}}{\Sigma (\text{layer traveltimes})} = \frac{30 \text{ m}}{0.1775 \text{ sec}} = 169 \text{ m/s} = \text{Site Class E}$$

Figure 5-1. Sample  $V_{s30}$  calculation illustration, based on the formula provided in Commentary J of the 2005 NBCC (NRC, 2006).

#### 5.4 Seismic Site Classes and Shear Waves in Near Surface Materials

$V_{s30}$  values fall within one of five ranges of shear wave velocities which define the seismic site categories, lettered A, B, C, D, & E. Other geotechnical parameters (undrained shear strength and standard penetration tests) also define the site categories but cannot be used in rock; only  $V_{s30}$  can define all categories A through E.

Generally speaking, **site class A** represents ‘**hard rock**’ with a  $V_{s30}$  value of greater than 1500 m/s. This velocity range encompasses unweathered bedrock, including igneous (e.g. granites) and competent sedimentary rocks (e.g. limestone, sandstone). The uppermost limit of S-wave velocity in very hard bedrock in Canada is approximately 4000 m/s in near surface Precambrian granites and gneisses. In Eastern Canada, sedimentary bedrock (limestones, dolostones, and sandstones) and Precambrian granites have shear wave velocities ranging between  $2700 \pm 700$  m/s (Hunter et al., 2010). In Western Canada, for geologically younger bedrock at depth beneath thick soils, the shear wave velocities can also be in the range of 1500 – 2500 m/s (Hunter et al., 1998).

Softer bedrock types (e.g. shales) or those weakened by chemical weathering or fracturing, generally fall into **site class B** ( $V_{s30} = 760 - 1500$  m/s), referred to as ‘**rock**’. In some cases, very hard soils consolidated by loading from glaciers (called tills) fall into this category.

**Site class C** describes ‘**firm ground**’ ( $V_{s30} = 360 - 760$  m/s) and encompasses soft rock (may be highly weathered) or very dense soils. In Canada, these dense soils will commonly include glacial materials, such as gravels, sands, and glacial tills.

**Site class D** ( $V_{s30} = 180 - 360$  m/s) describes ‘**stiff soils**’, and includes unconsolidated surface materials, such as sands, gravels, and some very stiff clays and silts.

The softest soils fall into **site class E** ( $V_{s30}$  less than 180 m/s), which commonly describes **soils** such as clays and silts which can be compressed by hand. These are generally very fine grained materials or loose porous sands which have been deposited after the last glaciation in underwater conditions, such as lakes, deltas (e.g. Fraser River Delta, BC) or pro-glacial lakes or seas (e.g. Champlain Sea deposits, ON and QC).

***Please note!***

It is important to recall that  $V_{s30}$  represents an average velocity over the top 30m of the ground. Therefore, soft soil overlying hard bedrock may fall into a site class B, C, or D depending on thicknesses, even though the two materials have distinctly different properties. It is also important to note that the 2005 and 2010 NBCCs specify that all sites containing more than 3 m of soft soil (with a plasticity index of greater than 20, a moisture content of greater than 40%, or an undrained shear strength of less than 25 kPa) must be classified as a site class E, even if the  $V_{s30}$  value indicates a higher site class. If shear wave velocity measurements indicate a low velocity ( $V_s$  less than 180 m/s) surface layer greater than 3 m in thickness, further tests should be done to check for these conditions.

A **site class F** also exists, but cannot be defined by shear wave velocities. It is a special category encompassing soft soils which are problematic (as defined in the NBCC, 2010):

- liquefiable soils, quick or highly sensitive clays and silts, and soils susceptible to collapse under seismic loading,
- highly organic clays (peats) greater than 3 m in thickness,
- highly plastic clays (plasticity index greater than 75), and greater than 8 m in thickness, or
- soft to medium stiff clays greater than 30 m in thickness.

In these cases, the determination of amplification is more complex than the other classes. This class can only be defined with site specific geotechnical testing, as described in the NBCC (NRC, 2010).

## **5.5 Site Classes and Amplification Factors**

The level of shaking felt during the ‘design earthquake’ (the probabilistic level of ground motion which modern structures are designed to resist) is predicted by models developed by the Canadian Hazards Information Service (CHIS) of the Geological Survey of Canada. Based on a study of historical and measured earthquakes, and knowledge of plate boundaries, these models predict the levels of shaking which may be felt across Canada at a 2% in 50 year probability of exceedance (for the 2010 NBCC). This probability level was determined to be most appropriate for structural design by the Canadian National Committee on Earthquake Engineering (CANCEE). These values are called spectral accelerations ( $S_a$ ) in units of [g], and are provided to describe an envelope at four different periods of shaking (0.2, 0.5, 1.0, and 2.0 seconds). The GSC’s on-line seismic hazard calculator offers the spectral acceleration values for any given site in Canada when the latitude and longitude are input to the interactive web-site:

(<http://www.earthquakescanada.nrcan.gc.ca/hazard-alea/interpolat/index-eng.php>). All  $S_a$  values output from the hazard calculator are given for ‘firm ground’ (site class C). These values must then be accordingly modified for the near surface conditions at the site based on the seismic site classification.

The NBCC provides look up tables containing the factors ( $F_a$ ,  $F_v$ ) which modify these spectral accelerations for a given site class and earthquake period (or frequency). Site class C is considered the ‘unity’ case, where we expect no amplification or deamplification of the given  $S_a$  for that location. Site classes A & B are assigned deamplification factors by the 2010 NBCC because less shaking would be expected on rock than at a site class C.

Site classes D and E are commonly given amplification factors since more shaking is expected at certain periods due to the presence of soft soil. However, at certain periods, a deamplification factor is assigned since the level of shaking is expected to be strong enough to cause the soil to 'damp' the ground motion. This is known to earthquake engineers as entering the 'non-linear range' of soil behaviour, where the soil begins to lose strength and to dampen ground motion.

## 5.6 Measuring Shear Wave Velocity

To measure shear wave velocity ( $V_s$ ) of near-surface soil and rock, shear wave travel times through the in-situ materials are measured on the order of milliseconds (ms), and  $V_s$  is calculated knowing the distance (metres or centimetres) through which the wave has traveled (e.g. Fig. 5-1). The equipment needed for conducting a shear wave survey consists of three main components; a seismic source to generate shear waves in the subsurface; geophones to measure ground vibration at specific locations; and a seismograph to digitally record the ground vibration over time.

There are several different types of seismic sources, including sledge hammers striking steel plates on the ground, weight drops, explosives, polarized shear wave sources, electrical 'sparker' sources, and controlled frequency vibrating sources. The choice of source type depends on many factors, including the type of seismic survey chosen, the ground conditions, the ambient seismic energy levels (background noise), and the required depth of investigation.

Geophones are very sensitive vibration detectors, which are typically planted at the ground surface, coupled to a borehole wall, or pushed into the ground using a seismic cone penetrometer. Modern seismographs are digital acquisition systems, capable of simultaneously recording data from an array of geophones. Seismic data are recorded for each receiver station as a function of time. Modern engineering seismographs are capable of recording 24, 48, or more channels of data (to record separate geophone responses) with record lengths from a fraction of a second to several seconds and at sample intervals as short as 62.5 microseconds.

## 5.7 Invasive vs. Non-invasive Shear Wave Methods

Shear wave surveys can be conducted non-invasively from the ground surface, or invasively by pushing a seismic cone penetrometer to 30m depth, or by drilling a borehole to 30 m depth and lowering instruments down it. In these Guidelines, we have broadly grouped survey types by 'non-invasive' or 'invasive' categories, and there are numerous survey options within each. Not all methods are suitable for all geological environments, and their limitations, and relative cost are briefly outlined in Table 5-1.

Non-invasive methods are generally the least expensive, as drilling/cone pushing equipment is not required on site. An array of geophones is planted at the ground surface and a source is used to generate shear waves, often a metal I-beam and sledge hammer for near surface investigations. These surveys include reflection and refraction methods using body waves, and modal analysis of surface waves using Rayleigh (surface) waves. These techniques are commonly used for seismic site assessments in industry, and are discussed in detail in Chapter 2, along with a few additional emerging technologies (landstreamer reflection surveying, and ambient noise techniques). It must be noted that surveys using surface waves for shear wave estimation require more complicated data processing techniques as well as a number of geotechnical assumptions. Therefore, these methods should be practiced by professionals with expertise in surface wave analysis.

Invasive methods are those which involve drilling, or pushing an instrumented geotechnical cone into soil. A borehole may be left uncased in competent rock, or cased with PVC (preferably) or metal in soil or friable rock. If casing is used, it is critical that it be well coupled to the formation with grout or cement to enable clear seismic signals to be received through the casing by the downhole tool. For downhole methods a receiver is lowered and clamped at known depth in a borehole (or a seismic cone is pushed

into soil to a known depth), and a shear wave source is generally placed at surface within a few metres of the borehole. The tool is commonly lowered at 0.5 or 1.0 m intervals and a seismic record of the surface source is made for each vertical location. Variations on these basic single downhole methods are also available. Crosshole seismic and crosshole tomography use two or more boreholes, separated by a few metres, where the source is placed in one hole and the receiver(s) is placed in the other. These types of surveys are reserved for cases where the very highest resolution is needed, as cost plays a factor in multiple borings. Acoustic logging involves deploying a specialized tool with a source and multiple receivers on the same instrument, but is limited to use in bedrock for best results. These techniques are discussed in detail in Chapter 3; presently vertical seismic profiling and seismic cone penetration are the most common invasive techniques used for site class assessment.

Under optimal conditions, invasive methods are generally considered the most accurate, as the receivers are passed through the materials being measured. Of these, the most accurate technique may be the seismic cone penetrometer (SCPT), as the tool is in constant contact with the soil, and the material around the cone has suffered less disturbance than with drilling (Hunter et al., 1991). Other information such as cone tip resistance and conductivities can also be provided with this method. However, a cased borehole, if well grouted (or an uncased boring in competent rock) can also provide high quality data, and other complementary geophysical logs can then be run in the same boring. Cost is a trade-off for invasive methods, since high costs can be realized for mobilizing the drilling equipment or pushing a seismic cone penetrometer. On the other hand, to a developer, the potential cost savings to accurately define the seismic site class (e.g. class B instead of class C) may be very well worth the expense.

Surface methods, while generally less costly than invasive methods, can result in a higher level of uncertainty as the waves must pass through a greater volume of material. They can, however, provide a very acceptable level of confidence when performed and analyzed by experienced geoprofessionals. If the techniques consist of reflection or refraction measurements, for example, optimal conditions may occur when soft materials overlie very hard materials, where stronger reflection/refraction amplitudes and good quality records commonly can be obtained. In this environment ( $V_s$  less than 200m/s), commercial MASW testing equipment is generally not able to generate low enough frequency waves to reach 30m. Where bedrock is shallow, the MASW technique also tends to underestimate the shear wave velocity of the bedrock. However, under conditions of shear wave velocity gradients or velocity reversals in the sediment column, the MASW or MMASW techniques may provide superior definition.

## **5.8 What to Expect: Reporting Guidelines**

As with all methods, the experience of the practitioner is a substantial factor in selecting the best type of survey for the site, both for optimizing the collection parameters, and for performing the interpretation. To demonstrate this, a survey report should include a minimum amount of information to reassure the client/authorities that the survey data is of good quality, and that interpretation was accurately performed. In each of the methods presented in Chapters 2, 3, and 4, a section on Recommended Guidelines for Reporting provides a summary of the types of information which should accompany a seismic site class evaluation, so that a third party reviewer has sufficient information to critique the results.

For review of a seismic site class survey report, a representative plot of the data (geophone response as wiggle traces or variable density logs, VDL) should be provided to give an indication of noise levels on site, and relative interpretability of the incoming shear wave (Figure 5-2; in text, see Chapter 3, Figure 3.2.1-9). A figure should also be provided showing the traveltimes interpretations which lead to the velocity calculations (Figure 5-3; in text, see Chapter 3, Figure 3.2.3-7). Certain methods with more complex processing routines require documentation of the data inversion (Figure 5-4; see Chapter 2, Figure 2.2.3-2). A final plot showing the interpreted velocity log versus depth is necessary, and it is helpful to display any geological information available at the site (Figures 5-5 and 5-6; in text, see Chapter 3, Figure 3.2.3-5; Figure 3.2.1-12).

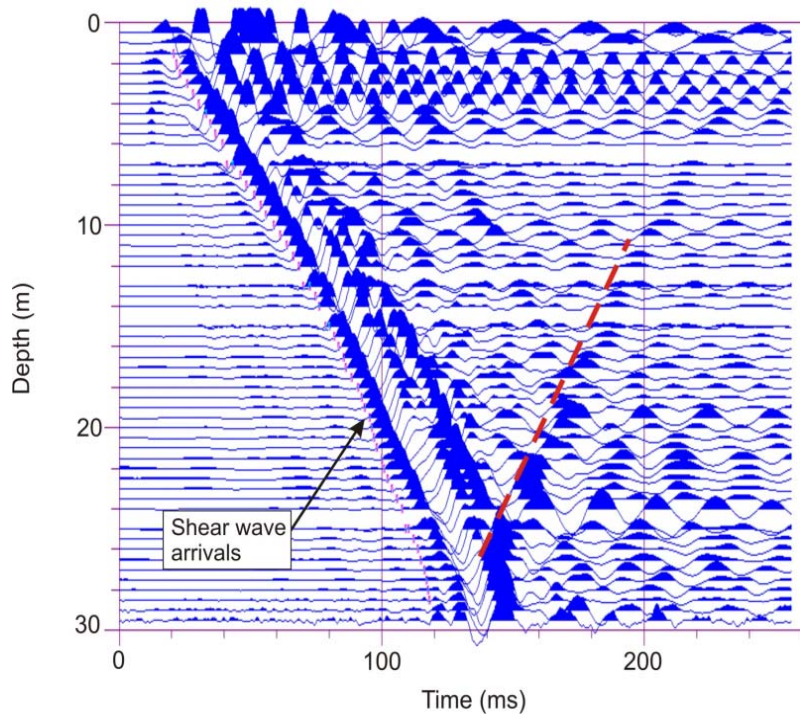


Figure 5-2. A plot of geophone response (as wiggle traces versus depth) gives an indication of noise levels on site, and relative interpretability of the incoming shear waves. This data sample shows clear and coherent shear wave arrivals all the way to the base of the borehole. Red dashed line shows the reflection from the bedrock surface (in text, see Chapter 3, Figure 3.2.1-9).

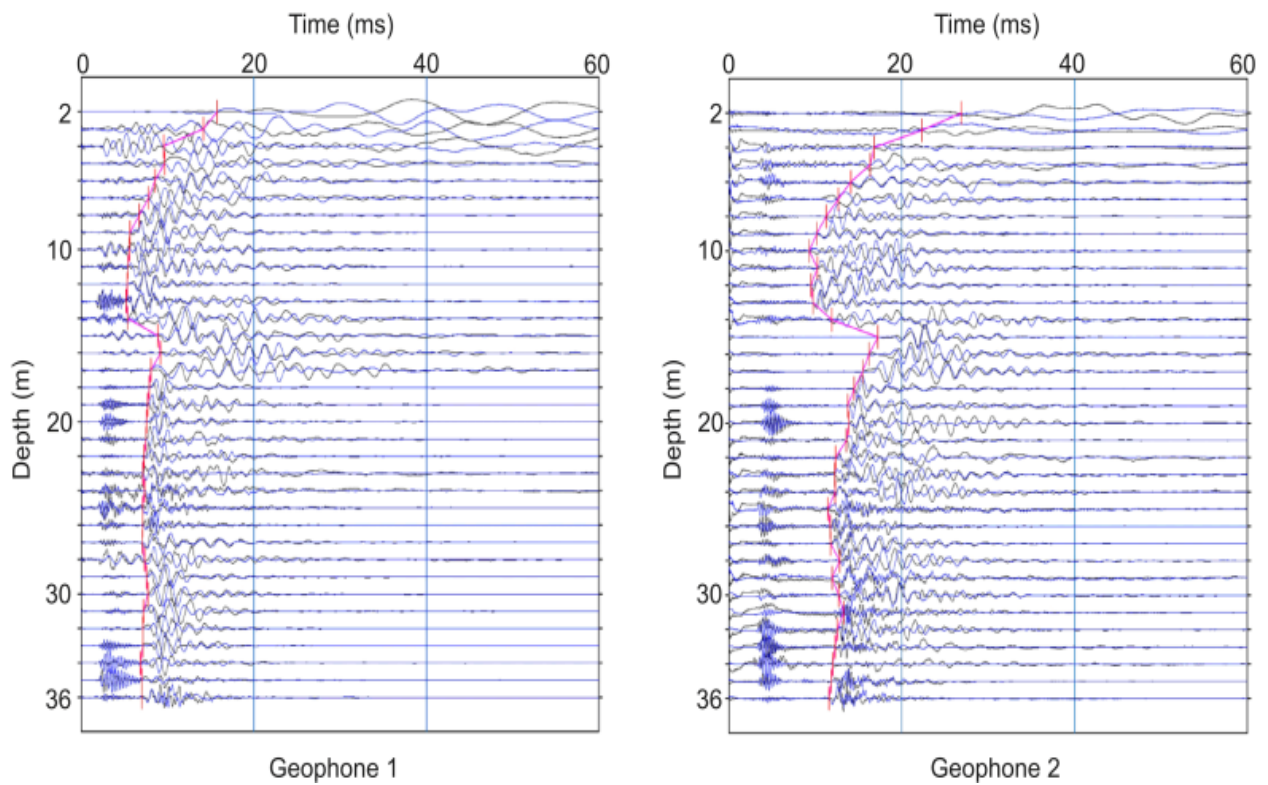


Figure 5-3. A figure showing the traveltime interpretations (red lines) which led to the velocity calculations (in text, see Chapter 3, Figure 3.2.3-7).

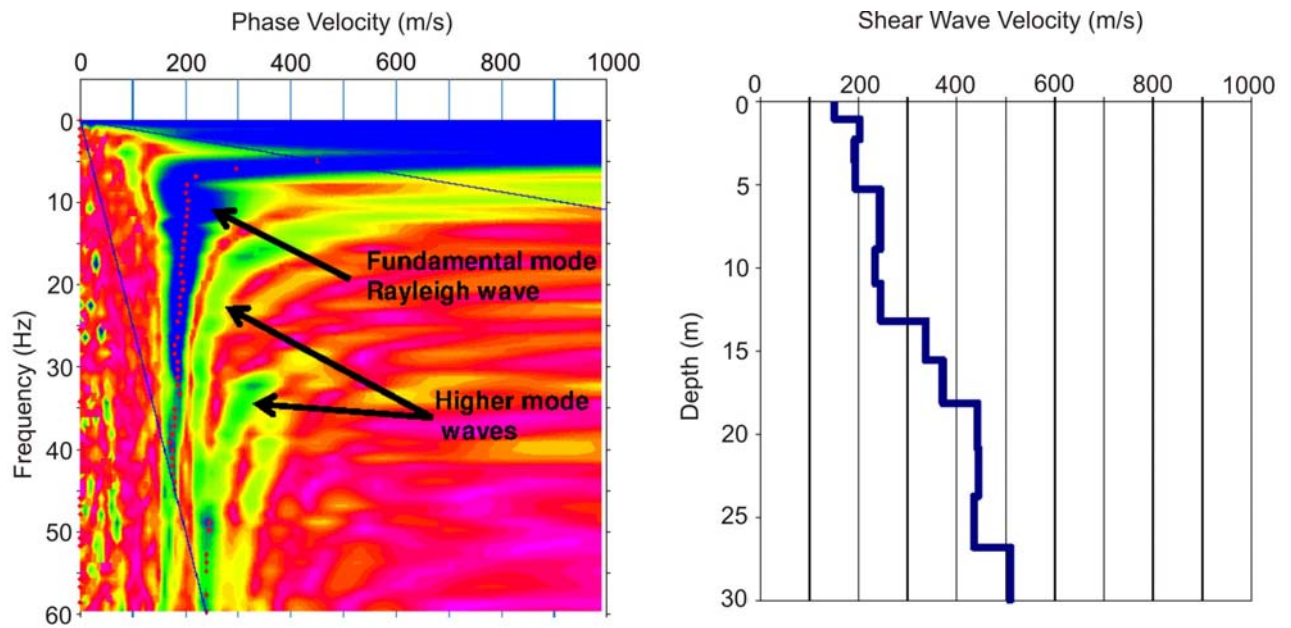


Figure 5-4.  $V_s$  estimation using surface wave techniques requires more complex processing routines (inversions). This requires an extra step of documentation of the data inversion (in text, see Chapter 2, Figure 2.2.3-2).

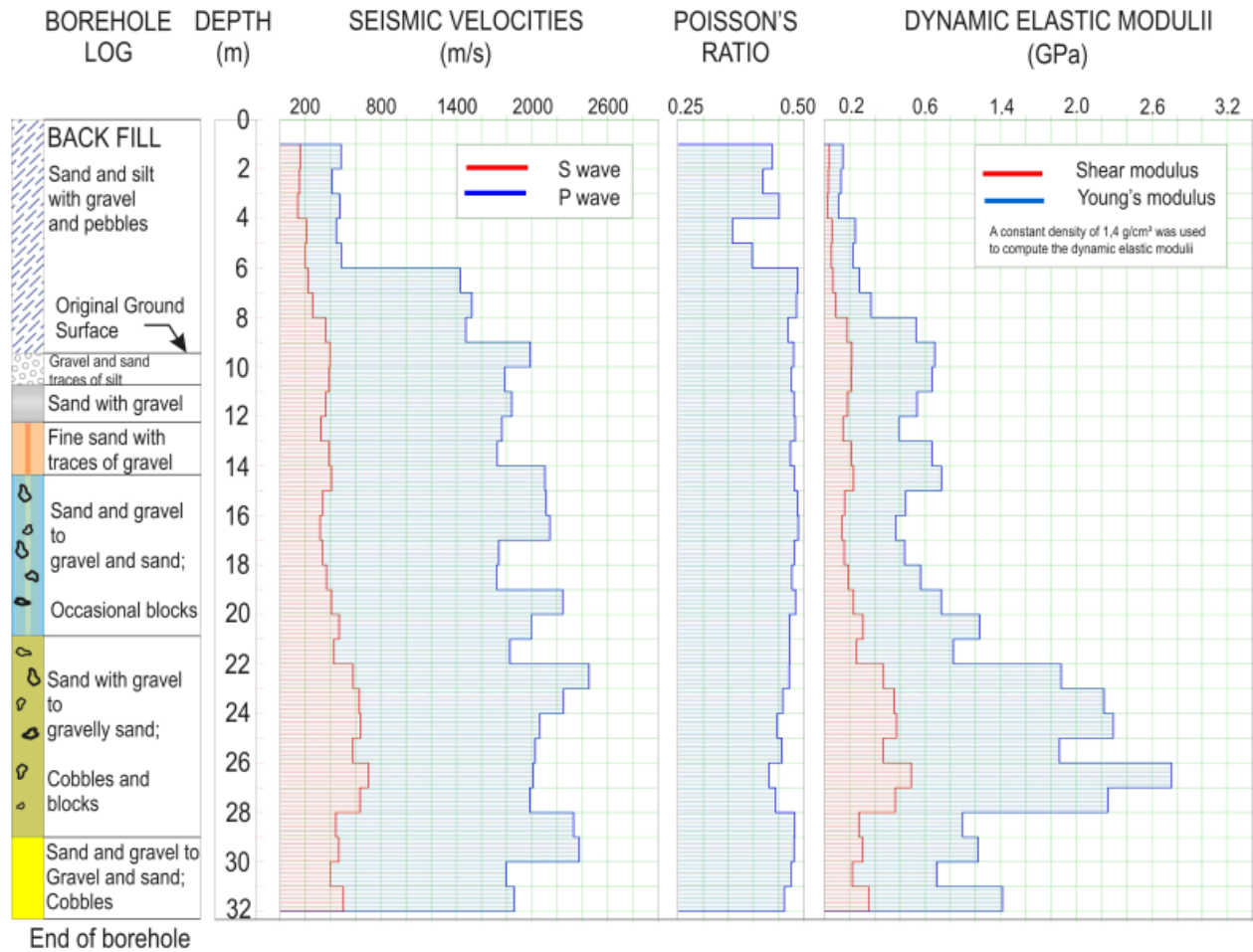


Figure 5-5. A final plot showing the interpreted velocity log versus depth, displayed with available geological information (in text, see Chapter 3, Figure 3.2.3-5).

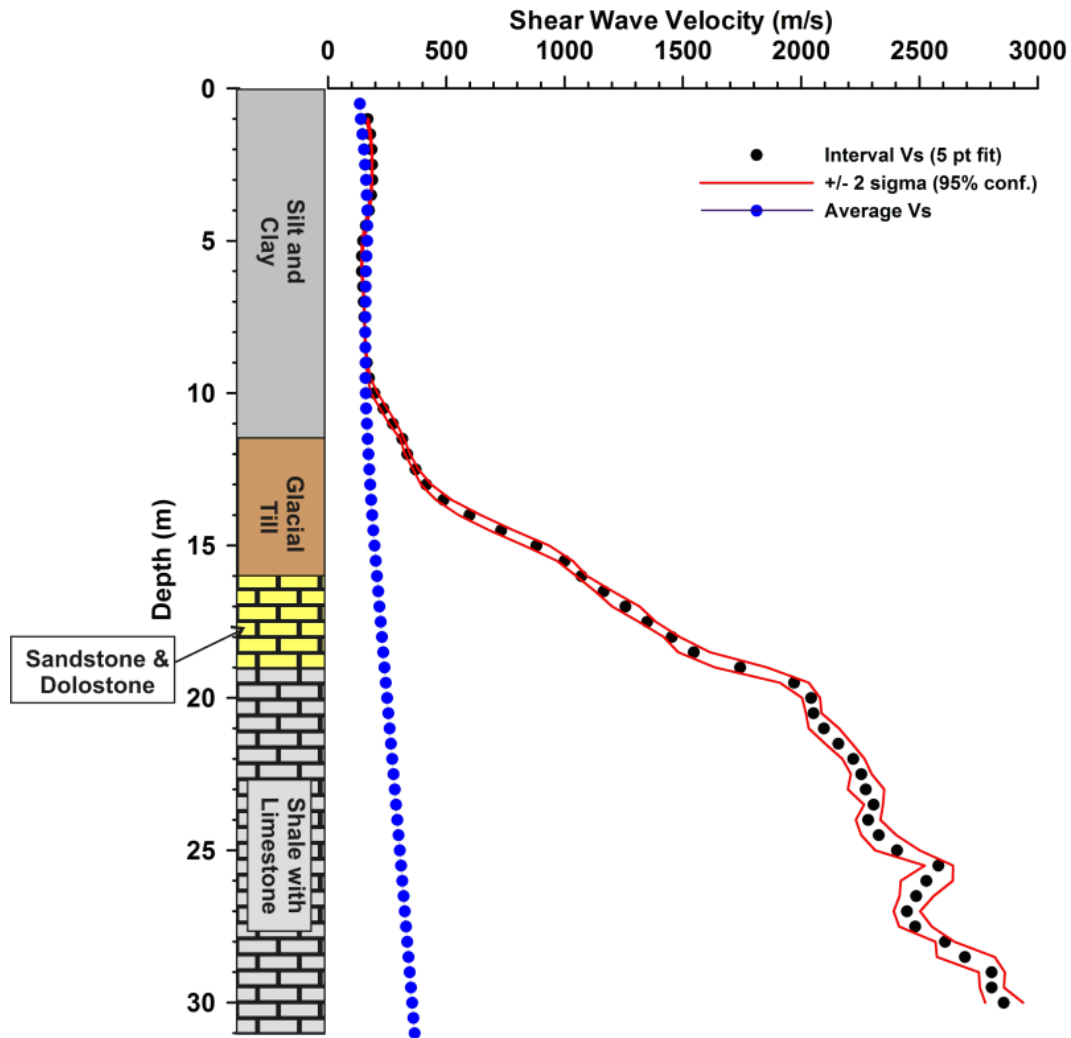


Figure 5-6. A final plot showing the interpreted shear wave velocity log versus depth, displayed with available geological information (in text, see Chapter 3, Figure 3.2.1-12).

## 5.9 When to Question or Request More Information

It is reasonable to feel concern when the reported velocity ranges seem unusually high or low, or inappropriate for the material described in the report. If a report provides a site class without any data to back it up, and with little or no description of the survey parameters or site conditions, it is suggested that the reviewer may request additional information. Images of the traveltime data can reveal signal-to-noise attributes of the site and provide a sense of the expected quality of the shear wave arrival interpretations. Description of steps taken in processing, especially in surface wave methods requiring modeling and assumptions, should also be provided.

Additional questions to examine during review include consideration of the size of the site, and whether or not sufficient work has been done to describe potential lateral variations of soil properties. Currently, there are no guidelines provided by regulatory bodies concerning minimal requirements to classify a large site; hence professional judgment is needed. As well, the survey report should include correlations of results with all previously available sub-surface geological and geotechnical information, including borings and complimentary geophysical surveys. Clients may have maps or old boring reports which can be provided as a guide to the consultant prior to the start of a survey.

**Table 5-1 – Non-technical Summary of Vs Methods for Seismic Site Assessment**

Method		Relative Cost to Client (\$,\$,\$,\$,\$)	Most Suitable Geological Env. for Vs <sub>30</sub> Investigation	Limitations/ Considerations
<b>Non-invasive Methods</b>	Refraction	\$	- soft soils over bedrock - bedrock at surface	- errors can result when hard layers overlie soft layers
	Reflection (planted array)	\$	- most conditions - soft soils over bedrock	- not suitable for very noisy ambient environments
	Reflection (Landstreamer & vibratory source)	\$\$\$	- most conditions	- need an even, competent surface; best for longer survey lines (e.g. along roads)
	Continuous surface wave (CSW)	\$	- most conditions - medium-soft to stiff soils overlying bedrock	- practical depth of investigation limited to approx 15m - not suitable for Vs <sub>30</sub> surveys where soft soil is very thick, or bedrock is very near surface
	Spectral analysis of surface waves (SASW)	\$	- most conditions - medium-soft to stiff soils overlying bedrock - need minimum of 60 m of open space for test	- data inversion process requires experienced interpreter - not suitable for Vs <sub>30</sub> surveys where soft soil is very thick, or bedrock is very near surface
	Multichannel analysis of surface wave (MASW)	\$	- most conditions - medium-soft to stiff soils overlying bedrock	- data inversion process requires experienced interpreter - not suitable for Vs <sub>30</sub> surveys where soft soil is very thick, or bedrock is very near surface
	Multimodal analysis of surface waves (MMASW)	\$\$	- most conditions	- data inversion process requires experienced interpreter - method currently proprietary in Canada
	Single station spectral ratios using ambient noise	\$	- most conditions - best results where soft soil overlies bedrock - can provide estimates of fundamental site resonance	- currently, method should not be used to assess seismic site class (topic of research)

Method		Relative Cost to Client (\$,\$\$,\$\$\$)	Most Suitable Geological Environment for $V_{s30}$ Investigation	Limitations/ Considerations
Non-invasive Methods	Spatially averaged coherency (SPAC) method ambient noise array	\$	- most conditions	- need flat topography beneath the array, and a flat-layered earth model - does not resolve fine layered structure, and bedrock velocity not well defined
	Frequency-wavenumber (f-k) ambient noise array	\$	- most conditions	
Invasive Methods	Seismic cone penetrometer (SCPT)	\$\$	- fine grained, soft soils	- cannot push cone into hard ground, but drilling out can extend depth range
	Vertical seismic profiling (VSP)	\$\$	- most conditions - borehole with casing required in soils	- casing must be solidly grouted to borehole wall
	Full waveform sonic logging	\$\$	- uncased boreholes in bedrock formations	- unsuitable for cased boreholes in soils and very soft rock
	Crosshole logging	\$\$\$	- most conditions	- vertical boreholes should be 5 m apart (ASTM standard), and grouted in soils and weathered bedrock
	Multichannel crosshole logging (tomography)	\$\$\$	- most conditions	- borehole orientation (dip and azimuth) must be accurately known

Table 5-1. Non-technical summary of methods for shear wave velocity measurements described in these Guidelines. For more complete detail on each method, please refer to the technical articles in Chapters 2.0 and 3.0.

## References

Hunter, J.A., Woeller, D.J. and Luternauer, J.L., 1991. Comparison of surface, borehole, and seismic cone penetrometer methods of determining the shallow shear wave velocity structure in the Fraser River Delta, British Columbia; in Current Research, Part A, Cordillera and Pacific Margin, Geological Survey of Canada, Paper 91-1A, p. 23-26.

Hunter, J.A., Burns, R.A., Good, R.L. and Pelletier, C. F., 1998. A compilation of shear wave velocities and borehole geophysics logs in unconsolidated sediments of the Fraser River Delta, British Columbia; Geological Survey of Canada, Open File 3622, 1 CD-ROM.  
<[ftp://ftp2.cits.mcan.gc.ca/pub/geott/ess\\_pubs/209/209974/of\\_3622.zip](ftp://ftp2.cits.mcan.gc.ca/pub/geott/ess_pubs/209/209974/of_3622.zip)> [accessed: Jan 2012]

Hunter, J.A., Crow, H.L., Brooks, G.R., Pyne, M., Motazedian, D., Lamontagne, M., Pugin, A. J.-M., Pullan, S.E., Cartwright, T., Douma, M., Burns, R.A., Good, R.L., Kaheshi-Banab, K., Caron, R., Kolaj, M., Folahan, I., Dixon, L., Dion, K., Duxbury, A., Landriault, A., Ter-Emmanuil, V., Jones, A., Plastow, G. and Muir, D., 2010. Seismic Site Classification and Site Period Mapping in the Ottawa Area Using Geophysical Methods; Geological Survey of Canada, Open File 6273, 1 DVD.  
<[ftp://ftp2.cits.mcan.gc.ca/pub/geott/ess\\_pubs/286/286323/of\\_6273.zip](ftp://ftp2.cits.mcan.gc.ca/pub/geott/ess_pubs/286/286323/of_6273.zip)> [accessed: Jan 2012]

National Research Council (NRC), 2010. National Building Code of Canada 2010, Volume 1, Division B, Part 4.

National Research Council (NRC), 2006. Commentary J, User's Guide – NBC 2005 Structural Commentaries (Part 4 of Division B), Canadian Commission on Buildings and Fire Codes, National Research Council of Canada.

## Chapter 6.0 Summary

*Jim Hunter & Heather Crow  
Geological Survey of Canada, Ottawa, ON*

The use of average shear wave velocities measured to 30 m depth ( $V_{s30}$ ) in soils and rock is the most versatile of the methods which can be used to assign a 2010 NBCC seismic site category. As shown in the technical articles, however, proficiency in near-surface  $V_s$  measurement methods requires experience in both collection and interpretation of the shear wave traveltimes; further clear directives do not exist in the NBCC for reporting the results. As a consequence, seismic site classification reports submitted across the country in the past few years have been inconsistent in method or format.

Table 6-1 provides a summary of shear wave measurement methods discussed in this report, and includes an assessment of the relative complexity of data collection and processing, and the most important limitations of the method. For detailed information and representative case studies, the article discussing the particular method should be consulted.

In addition, there are discretionary issues in the application of site classification, such as the number of boreholes/surveys required to classify a large site, and which is/are the most appropriate method(s) to use for site investigation if no prior knowledge of subsurface materials is available. The chapter on complementary geophysical techniques provides some guidance on common geophysical methods of subsurface site reconnaissance, which may be an aid for planning a seismic site classification survey(s).

This series of Guidelines was developed to provide technical support and representative case studies to geophysicists, geotechnical engineers, and those concerned with municipal building codes requiring seismic site classification following the 2010 NBCC. It is hoped that this report will help to better inform this community of professionals, ultimately resulting in improved performance of structures during seismic events within Canada.

It is possible that seismic site assessment in future building codes may include measurement of fundamental site periods (or frequencies), which are governed by the thickness of the soil and its stiffness (or shear wave velocity). For this reason, discussions describing the collection and analysis of site period measurements have been provided in the Guidelines. As the NBCC evolves in future, it is likely that the application of shear wave velocity measurements will be required in some capacity for the estimation of site effects. For this reason, it is anticipated that this guide may be updated in the future to accommodate changes in the NBCC.

### **Recommended citation:**

Hunter, J.A. and Crow, H.L., 2012. Chapter 6.0: Summary; *in* Shear Wave Velocity Measurement Guidelines for Canadian Seismic Site Characterization in Soil and Rock, (ed.) J.A. Hunter and H.L. Crow; Geological Survey of Canada, Open File 7078, p. 224-227.

**Table 6-1 – Technical Summary of Vs Methods for Seismic Site Assessment**

	<b>Method [Article]</b>	<b>Data Coll. Complex.</b>	<b>Data Proc. Complex.</b>	<b>Most Suitable Geological Env. for Vs<sub>30</sub> Investigations</b>	<b>Limitations/ Considerations</b>
<b>Non-invasive Methods</b>	Refraction [2.1.1]	Low	Low	-soft soils over bedrock - bedrock within a few metres of surface	- velocity reversals in near surface cannot be identified - 'hidden' layer effect could increase velocity-depth errors
	Reflection (single planted array) [2.1.2]	Low	Low	- most conditions	- not suitable in very noisy environments - requires reflecting horizon(s) characterized by velocity contrasts within ~30 m of surface
	Reflection (Landstreamer & vibratory source) [2.1.2]	High	High	- most conditions	- system designed for long survey lines along roads, not site investigations - signal scattered by coarse-grained materials (e.g. gravel, cobbles and boulders)
	Continuous surface wave (CSW) [2.2.1]	Low	Moderate/ High	- most conditions - medium-soft to stiff soils overlying bedrock	- practical depth of investigation limited to approx. 15 m
	Spectral analysis of surface waves (SASW) [2.2.2]	Low	Moderate/ High	- most conditions - need min. 60 m spread length for test - medium-soft to stiff soils overlying bedrock	- cannot distinguish higher modes from fundamental mode - data inversion process requires experienced interpreter
	Multichannel analysis of surface wave (MASW) [2.2.3]	Moderate	High	- most conditions - medium-soft to stiff soils overlying bedrock	- not suitable for Vs30 surveys where soil (Vs<200 m/s) is very thick or bedrock is very near surface - data inversion process requires experienced interpreter

	<b>Method [Article]</b>	<b>Data Coll. Complex.</b>	<b>Data Proc. Complex.</b>	<b>Most Suitable Geological Env. for Vs<sub>30</sub> Investigations</b>	<b>Limitations/ Considerations</b>
	Multimodal analysis of surface waves (MMASW) [2.2.4]	Moderate	Proprietary	- most conditions	- uses higher modes in Vs profile analysis - data inversion process requires experienced interpreter
<b>Non-invasive Methods</b>	Single station spectral ratios using ambient noise [2.3.1]	Low	Moderate	- can provide estimates of site resonance - best results in high Vs contrast settings (soil over bedrock)	- method cannot provide Vs or a seismic site class - shape of resonant peak influenced by subsurface topography (dipping impedance boundary)
	Spatially averaged coherency (SPAC) method ambient noise array [2.3.2]	Low	High	- most conditions	- need flat topography beneath the array, and a flat-layered earth model - does not resolve fine layered structure and bedrock velocity not well-defined (topic of current research)
	Frequency-wavenumber (f-k) ambient noise array [2.3.3]	Low	High	- most conditions	
<b>Invasive Methods</b>	Seismic cone penetrometer (SCPT) [3.1]	Moderate	Low	- fine grained, soft soils	- test depth is a function of the ground stiffness, cone capacity, and pushing capacity of system - drill out is possible to extend test depth range

	<b>Method [Article]</b>	<b>Data Coll. Complex.</b>	<b>Data Proc. Complex.</b>	<b>Most Suitable Geological Env. for Vs<sub>30</sub> Investigations</b>	<b>Limitations/ Considerations</b>
<b>Invasive Methods</b>	Vertical seismic profiling (VSP) [3.2.1]	Low	Low	- open boreholes in competent rock formations - cased boreholes in soils & weathered bedrock	- casing must be well coupled to formation - near surface p-wave interference with s-waves can lead to near-surface mispicks - sites with significant accumulations of organic material on surface beneath the seismic source are unfavourable
	Full waveform sonic logging [3.2.2]	Moderate	Moderate to High	- open boreholes in bedrock formations (Vs greater than 1500 m/s)	- unsuitable for unconsolidated materials (where casing velocity exceeds material velocity) - length of probe limits velocity measurements in top few metres of surface
	Crosshole logging [3.2.3]	Moderate	Low	-most conditions	- vertical boreholes should be less than 10 m apart and casing well grouted in unconsolidated materials - must be logged with a deviation tool if borings exceed 15 m depth - if considerable anisotropy exists (approximately 10%), this method yields velocities based on the vertical component of s-waves (SV), leading to an overestimation of the horizontally polarized shear waves (SH), as required for Vs <sub>30</sub> estimation
	Multichannel crosshole logging (tomography) [3.2.4]	Moderate	High	-most conditions	

Table 6-1. Technical summary of methods for shear wave velocity measurements described in these Guidelines. For more complete detail on each method, please refer to the technical articles in Chapters 2.0 and 3.0. Complx.=complexity, env.=environment.